

“Iron Complexes with Nitrogen Ligands for Catalytic Hydrogenation of Olefins”

Dissertation

zur Erlangung des Doktorgrades der Naturwissenschaften

Dr. rer. nat.

an der Fakultät für Chemie und Pharmazie
der Universität Regensburg



vorgelegt von

Matteo Villa

aus Busto Arsizio (Italienische Republik)

Regensburg 2017

The experimental part of this work was carried out between January 2014 and March 2017 at the University of Regensburg, Institute of Organic Chemistry under the supervision of Prof. Dr. Axel Jacobi von Wangelin.

The thesis was submitted: April 10th, 2017

Date of the defence: May 11th, 2017

Board of examiners:

Prof. Dr. Achim Göpferich (chairman)

Prof. Dr. Axel Jacobi von Wangelin (1st referee)

Prof. Dr. Olga García Mancheño (2nd referee)

Prof. Dr. Frank-Michael Matysik (examiner)

Table of Contents

1	Introduction	1
1.1	Iron-catalyzed hydrogenation	1
1.1.1	Heterogeneous Iron Catalysts	3
1.1.2	Homogeneous Iron Catalysts	7
1.1.3	Homogeneous Iron Catalysts with Non-Innocent Ligands	11
1.2	References	21
2	Iron-catalyzed olefin hydrogenation at 1 bar H ₂ with a FeCl ₃ -LiAlH ₄ catalyst	24
2.1	Introduction	25
2.2	Reaction conditions and substrate scope	26
2.3	Mechanistic studies	31
2.4	Conclusions	35
2.5	Experimental part	36
2.5.1	General	36
2.5.2	General hydrogenation procedures	37
2.5.4	Synthesis of starting material	38
2.5.5	Hydrogenation products	55
2.5.3	Mechanistic experimental details	71
2.5.6	[Li(thf) ₂ {Fe(tmeda)} ₂ (μ-AlH ₅)(μ-Al ₂ H ₉)] (4)	80
2.6	References	82
3	Alkene Hydrogenations by Soluble Iron Nanocluster Catalysts	85
3.1	Introduction	86
3.2	Results and Discussion	88
3.2	Conclusions	93
3.2	Experimental part	94
3.2.1	General	94
3.2.2	General procedures	96
3.2.3	General method for catalyst preparation	96

Table of Contents

3.2.4 General method for <i>in situ</i> catalyst preparation with $\text{LiN}(\text{SiMe}_3)_2$	96
3.2.5 General method for <i>in situ</i> catalyst preparation with various amines	96
3.2.6 General method for catalytic hydrogenation	96
3.2.7 General method for kinetic examination in catalytic hydrogenation	97
3.2.8 Synthesis of catalysts, reagents, and starting materials	98
3.2.9 Synthesis and characterization of $[\text{FeN}(\text{SiMe}_3)_2]_4(\text{toluene})$	118
3.2.10 Synthesis of $[\text{Fe}_6\{\text{N}(\text{SiMe}_3)_2\}_6\text{H}_5]$ and $[\text{Fe}_7\{\text{N}(\text{SiMe}_3)_2\}_7\text{H}_6]$:	122
3.3 References	126
4 Synthesis and Catalysis of Redox-active Bis(imino)acenaphthene (BIAN) Iron Complexes	129
4.1 Introduction	130
4.2 Results and Discussion	132
4.2.1 Synthesis	132
4.2.2 Characterizations	134
4.2.3 Catalytic studies	140
4.3 Conclusions	141
4.3 Experimental part	142
4.3.1 General	142
4.3.2 Electrochemistry	143
4.3.3 X-Ray Diffraction	144
4.3.4 General procedure for the synthesis $(\text{Ar}_2\text{BIAN})\text{FeCl}_2$ (2)	145
4.3.5 General procedure for the synthesis $[\text{Fe}(\text{Ar}_2\text{BIAN})_3][\text{BF}_4]_2$ (4)	146
4.3.6 General procedure for the synthesis $[\text{Zn}(\text{Ar}_2\text{BIAN})_3][\text{BF}_4]_2$ (5)	147
4.3.7 General procedure for catalytic hydrogenations of alkenes	147
4.3.8 Synthesis of starting materials	148
4.3.9 Hydrogenation products	149
4.4 References	178
5 Hydrogenations catalyzed by Redox-active Bis(imino)acenaphthene (BIAN) Iron Complexes	183

5.1 Introduction	184
5.2 Results and Discussion	185
5.3 Mechanistic experiments	192
5.4 Conclusions	194
5.5 Experimental part	195
5.4.1 General	195
5.4.2 General procedure for catalytic hydrogenations	196
5.4.3 Synthesis (dipp ₂ BIAN)FeCl ₂	196
5.4.4 Synthesis of starting material	197
5.4.5 Hydrogenation products	199
5.6 References	205
6 Synthesis of Reduced Bis(imino)acenaphthene (BIAN) Aluminium Complexes	207
6.1 Introduction	208
6.2 Results and Discussion	212
6.3 Conclusion	215
6.4 Experimental part	216
6.4.1 General	216
6.4.2 Synthesis of Aluminum-Complexes	217
6.5 References	220
7 Hydroaminations of Alkenes: A Radical, Revised, and Expanded Edition	221
7.1 References	226
8 Appendix	227
8.1 List of abbreviations	227
8.2 Summary	228
8.3 Zusammenfassung	232
8.4 Curriculum Vitae	236
8.5 Acknowledgements	238
8.6 Eidesstattliche Erklärung	239

1 Introduction

1.1 Iron-catalyzed hydrogenation

Catalysis represents a key technology for the industrial production of almost 80% of all chemical and pharmaceutical products.^[1] Among the different processes, metal-catalyzed hydrogenations emerged as one of the most important transformations for both small as well as for the large scale productions^[2], and as a matter of fact, the syntheses of many bulk and fine chemicals incorporate at least a hydrogenation step in the sequence. Taking a look at the pharmaceutical sphere, it is clear that in order to efficiently achieve such kind of transformation the catalyst needs to possess specific features like activity, chemoselectivity, and stereoselectivity. In the last couple of decades, a large number of homogeneous metal catalysts based on the noble metals, rhodium, iridium, palladium, platinum, and ruthenium, assisted by rational-designed and expensive ligands has been developed. These catalytic systems fulfill the previously mentioned properties and opened the pathway to the synthesis of fine chemicals inaccessible before. The relevance of these discoveries in the scientific field has been acknowledged with Nobel prizes at the beginning of this century.



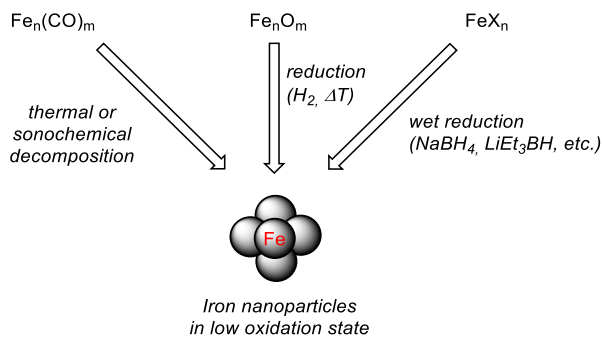
Figure 1-1 – William S. Knowles and Ryoji Noyori awarded with the Nobel Prize in chemistry in 2001 “for their work on chiral catalyzed hydrogenation reactions”.

Despite the high activity and chemoselectivity showed by these catalysts, their major drawback consists in the low natural abundance of the metals they are based on, resulting in increased operational costs. The price of palladium for example almost doubled during the past 10 years.^[3] Additionally, these metals are toxic, and their disposal is money and time-consuming. The sustainability and “green chemistry” principles, fully embraced nowadays by the scientific community expedite the development of new and more eco-friendly catalytic systems. One of the most promising candidates for the substitution of

these expensive and harmful metals is iron, being the 10th most abundant chemical element in the universe and exhibiting a clear safety profile. Interestingly, nitrogen fixation (Haber-Bosch) and carbon monoxide reduction (Fischer-Tropsch), two of the largest technical hydrogenations are catalyzed by heterogeneous iron species, but no competitive iron-catalyzed hydrogenations of fine chemical intermediates are employed yet. This field has acquired more and more attention in the last years and many Fe-based catalytic systems have been published so far.

1.1.1 Heterogeneous Iron Catalysts

In order to achieve robust iron-based catalytic systems, suitable for industrial applications, heterogeneous catalysts offer clear advantages, mainly the easy separation of the metal-free products' phase. Thanks to the recent availability of advanced synthetic and spectroscopic techniques, the synthesis and characterization of low valent iron nanoparticles have become easier.^[4] Fe-NPs, as hybrid catalysts, combine the high activity and high dispersion of the homogeneous catalytic systems with the native heterogeneous properties.



Scheme 1-1 – Classical approaches for nanoparticles production.

Different approaches have been developed for the synthesis of nanoparticles, thermal decomposition of iron carbonyls ($Fe(CO)_5$, $Fe_2(CO)_9$ and $Fe_3(CO)_{12}$) led to the formation of iron(0) particles. Different groups reported^[5] the efficient synthesis of Fe-NPs according to this methodology, usually surfactants, such as oleylamine or ionic liquids, were added to slow down the aggregation of the newly formed particles. Moores *et al.* reported in 2013^[6] a hydrogenation catalyst composed of iron(0) nanoparticles derived from decomposition of iron pentacarbonyl. These nanoparticles were supported on polystyrene beads thanks to polyethylene glycol linkers functionalized with amino groups, that served as stabilizers. Hydrogenation of primary and secondary alkenes, aldehydes and imines was achieved employing a flow set-up (Figure 1-2), this catalytic system also proved to be robust in the presence of water. Sonochemical treatment can be used as well to achieve iron carbonyls decomposition as reported by Stein *et al.* in 2011.^[7] Under these conditions, without heating, they efficiently produced iron(0) nanoparticles supported on chemically-derived graphene, this supported catalyst proved to be active in the hydrogenation of alkenes.

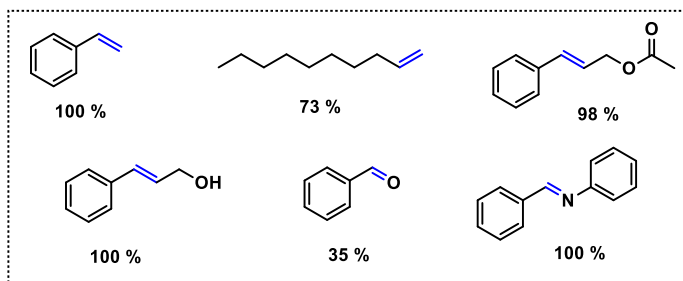


Figure 1-2 – Substrate scope reported by Moores *et al.*; Bonds in blue indicate the site of π -bond hydrogenation; Reaction conditions: 0.05 M substrate in EtOH, 100 °C, 40 bar H₂, 1 mL/min, 300 mg FeNP@PS-PEG-NH₂ (residence time 53 seconds).

Reduction of iron oxides represents a feasible approach for the synthesis of iron nanoparticles, Kang *et al.* described^[8] the thermal decomposition of iron(II) oleate to Fe₃O₄ and its subsequent reduction with H₂ at high temperature (700°C) yielding α -Fe-NPs. The high temperature required in these processes is the major drawback of this approach. Chaudret in 2013^[9] described the decomposition of Fe(hmds)₂ to monodisperse nanoparticles under milder conditions (150°C, 3 bar H₂). These NPs, with a diameter of 1.5 ± 0.2 nm, were then applied for the hydrogenation of primary and secondary alkenes and alkynes. Substrates without functional groups were almost quantitatively hydrogenated (Table 1-1), while ketones and aldehydes proved to be not suitable substrates for this catalytic system.

Table 1-1 – Hydrogenation of alkenes and alkynes with iron(0) nanoparticles reported by Chaudret *et al.*

$$\text{R}-\text{C}(\text{H})=\text{C}(\text{H})-\text{R}' \xrightarrow[10 \text{ bar H}_2, \text{ r.t., 20 h}]{\text{Fe-NPs (2.4 mol\%)}} \text{R}-\text{C}(\text{H})-\text{C}(\text{H})-\text{R}'$$

Entry	Substrate	Yield (%)
1		>99
2		87
3		89

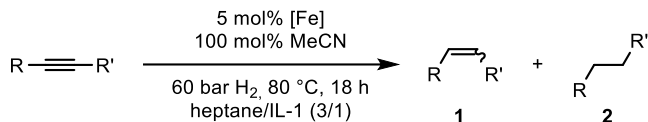
Wet reduction of iron salt proved in the last years to be the most applied approach for the synthesis of iron nanoparticles thanks to its easy operations and high versatility. A variety of reducing agents can be employed such as sodium borohydride, Super-Hydride, and Grignard reagents.^[10] Thomas *et al.*^[11] in 2013 described the formation of an active

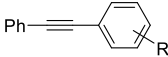
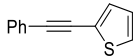
hydrogenation catalyst obtained *via* reduction of commercial iron(II) triflate with sodium triethylborohydride. The reductant, used in large excess (4 equivalents), serves also as a hydrogen source, and the scope comprehended few examples of tri-substituted olefins. De Vries in 2009 reported^[12] the reduction of cheap iron trichloride with three equivalents of EtMgCl resulting in Fe-NPs. These latter showed activity in the catalytic hydrogenation of alkenes and alkynes under mild reaction conditions. Few years later Welther *et al.* described^[13] the formation of iron nanoparticles applying a similar approach (FeCl₃ as iron precursor and Grignard reagents as reductants). The particles were extensively studied, and then applied in alkenes hydrogenation. Notably, chlorides, ethers, esters, primary and tertiary amides are tolerated by the system (Table 1-2).

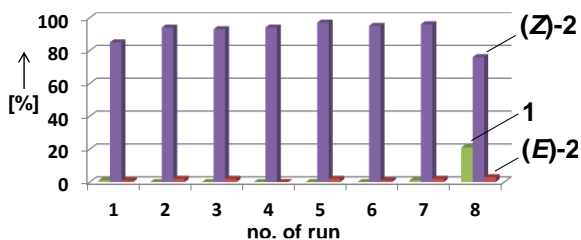
Table 1-2 - Functional group tolerance of iron-NPs described by Welther *et al.*

Entry	Substrate	Yield (%)
1		91
2		93
3		96
4		58

The implementation of ionic liquids led to a biphasic system in which the catalyst, dispersed in the IL phase, is stabilized, and can easily be separated by the products solubilized in the organic phase (heptane). Recycling of the catalyst by decantation is extremely effective, and its activity is conserved for more than 5 cycles (Figure 1-3). Gieshoff *et al.*^[14] expanded the application of this nanoparticles even further. Addition of acetonitrile effects the stereocontrol, coordinating to the particles surface it decreases the reactivity of the system, enabling the selective partial hydrogenation of alkynes to (*Z*)-alkenes (Table 1-3).

Table 1-3 - Partial hydrogenation of alkynes to (Z)-alkenes.

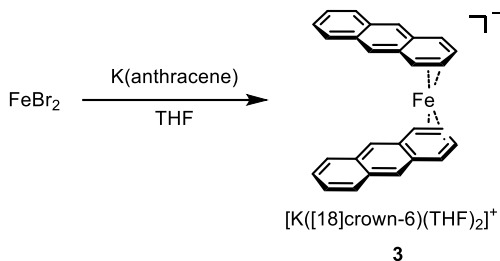
Entry	Alkyne	R	Yield alkene in %	Z/E
1		H	97	96 / 4
2		4- <i>t</i> -Bu	94	97 / 3
3		4-NH ₂	76	>99 / <1
4		4-Br	84	>99 / <1
5		4-Cl	89	>99 / <1
6		4-CO ₂ Me	53 (74)	>99 / <1
7		-	76	99 / 1
8	Ph—C≡C—R	Et	79	95 / 5
9		CO ₂ Me	13 (19)	96 / 4
10		SiMe ₃	19 (40)	92 / 8

**Figure 1-3** - Recycling of iron-nanoparticles catalyst.

1.1.2 Homogeneous Iron Catalysts

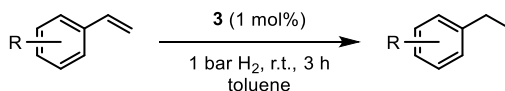
Homogeneous catalyzed hydrogenation has been dominated by noble metal based catalysts, nevertheless the great effort invested by different research groups in the last years yielded some interesting results. Additionally, compared to their heterogeneous counterpart, easier mechanistic investigations on homogeneous catalytic systems lead the way to a rational tuning of the catalysts.

Highly reduced iron species represent valid candidates as hydrogenation catalysts, ferrate stabilized by π -systems such as naphthalene or anthracene were firstly conveniently synthesized by the group of Ellis^[15] and Wolf^[16] by simple reduction of iron halide with a mixture of alkali metals (K) and the desired arene (Scheme 1-2). The result of this reductions are homogeneous iron complexes (**3**) with the metal atom in a negative formal oxidation state (-1). The easy substitution of the coordinated π -ligand with different arenes and dienes represent a good methodology for the synthesis of a collection of ferrates. The Jacobi von Wangelin group in collaboration with Wolf and co-workers tested these complexes in the hydrogenation of olefins.^[16-17] Simple alkenes were efficiently hydrogenated under mild conditions, unfortunately, the high reactivity of these complexes is translated in low tolerance for functional groups (Table 1-4).



Scheme 1-2 - Synthesis of ferrate according to Ellis *et al.*

Table 1-4 – Hydrogenation of styrenes catalyzed by complex **3**.



Entry	R	Yield (%)
1	H	89
2	4-F	100
3	4-NH ₂	0
4	4-COOMe	2
5	2-Cl	0

Phosphines represent one of the most investigated class of ligands employed in coordination chemistry. The application of transition metals complexes bearing organophosphorus moieties in the catalytic hydrogenation of unsaturated bonds allowed the achievement of astonishing results. Thanks to the profuse efforts carried on by different research groups in the last couple of decades, the library of well-defined iron-phosphine complexes increased exponentially. Among these, different ones showed interesting reactivity towards hydrogenation.

Multidentate phosphines are usually employed for these applications. Bianchini^[18] and Peters^[19] proved the activity of iron fragments coordinated to such ligands respectively for the partial hydrogenation of alkynes (**4**) and for the full hydrogenation of alkynes and alkenes (**5**, **6**). The key active intermediate for both of these catalytic systems is an iron-hydride species formed *in situ* and detected by NMR spectroscopy. This species after each turnover is regenerated by dihydrogen, this reactivation step was proposed by the authors after detection of $\text{LFeH}(\eta^2\text{-H}_2)$ (**7**) and $\text{LFe}(\text{H}_3)$ (**8**) species in the reaction mixture (Scheme 1-3).

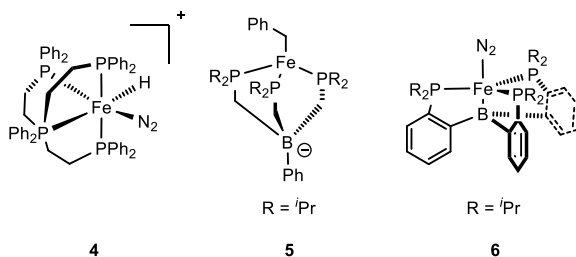
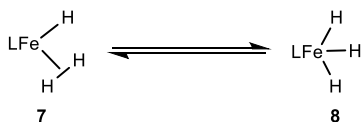
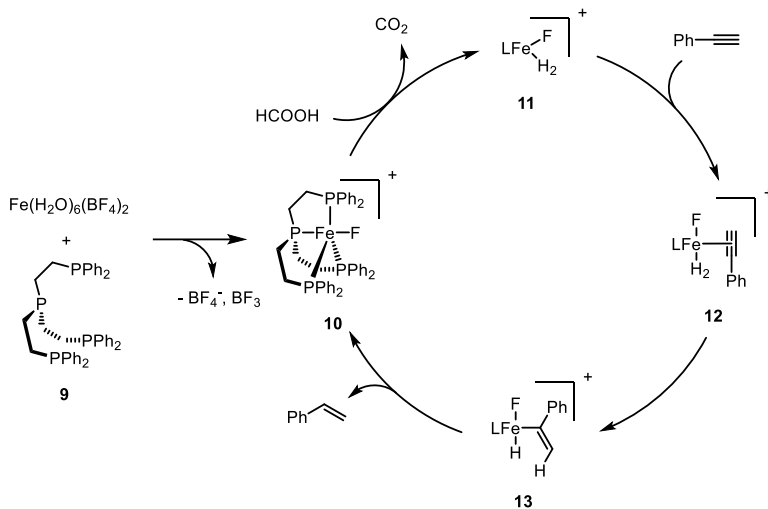


Figure 1-4 – Iron-phosphine complexes described by Bianchini *et al.* (**4**) and Peters *et al.* (**5**, **6**).



Scheme 1-3 – Equilibrium between Fe-H species detected by Peters *et al.*

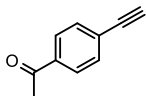
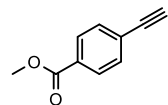
Similar tetradentate phosphines (**9**) have been employed in 2012 by Beller *et al.* for the partial hydrogenation of phenylacetylenes to styrenes.^[20] The catalyst was formed *in situ*, mixing $\text{Fe}(\text{H}_2\text{O})_6(\text{BF}_4)_2$ and the ligand. Formic acid was employed as hydrogen source and an iron fluoride intermediate (**10**) was proposed by the authors as active catalytic species (Scheme 1-4).



Scheme 1-4 – Catalytic cycle proposed by Beller *et al.*

Table 1-5 – Substrate scope reported by Beller *et al.*

Entry	Substrate	Catalyst (mol%)	Conv. (%)	Yield (%)
1		0.75	>99	>99
2		1	>99	>99
3		0.75	>99	>99
4		1.25	>99	98
5		0.75	>99	>99

6		1	>99	>99
7		2.5	>99	>99

The authors presented a broad scope for this catalytic system, the presence of reducible functional groups did not affect the chemoselectivity of the process. The same group applied this approach for the reduction of different substrates such as carbon dioxide^[21] and for the chemoselective carbonyl reduction of α,β -unsaturated aldehydes.^[22]

1.1.3 Homogeneous Iron Catalysts with Non-Innocent Ligands

As mentioned in the previous chapter the majority of homogeneous catalysts so far investigated and applied in hydrogenation are based on noble metals, while iron has been deeply investigated only in the last couple of decades. A reason for this delay could be found in the redox properties of these elements. Noble metals like palladium, platinum, rhodium, iridium and ruthenium easily undergo two-electron oxidative and reductive processes, thus are greatly favored for the development of the classical transition organometallic chemistry. Iron, on the other hand, can also engage even-numbered redox events but single electron transfer (SET) is always a competitive pathway and in many cases even preferred. This innate electronic structure represented a great limitation for the development of homogeneous iron-catalyzed processes. To overcome this problem different approaches are feasible but one approach has been shown to be very successful, namely the adoption of an organic molecule structure coordinated to the metal, which is able to cooperate with it during the redox processes: a non-innocent ligand. The importance of this ligands can be evaluated based on the number of reviews concerning this topic published in the last couple of years [23].

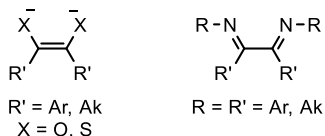
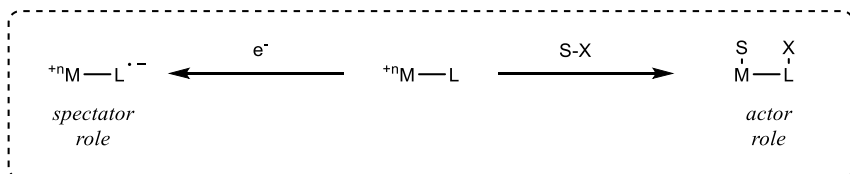


Figure 1-5 – Classical non-innocent ligand scaffolds.

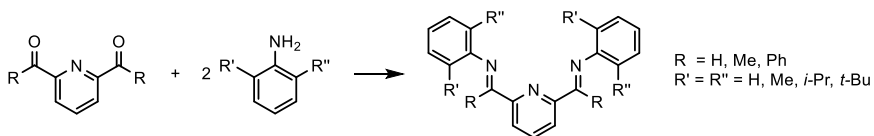
These ligands can be generically divided into two major classes based on their role in the catalytic pathway. The first one is composed by those ligands with a spectator role, they do not interact directly with the substrate, the catalytic activity is primarily metal-centered, however, they can act as electron reservoirs. The second class comprehends ligands which actively participate in the catalytic process forming and breaking bonds with the substrates, assuming an actor role.



Scheme 1-5 - Principal operation modes of non-innocent ligands.

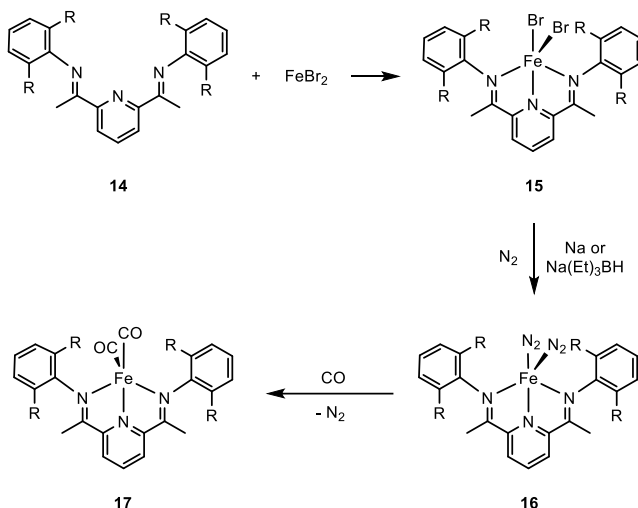
Among the first class of non-innocent ligands, one of the most noteworthy structural motifs is the bis(imino)pyridine (PDI) one. These (NNN)-pincer ligands and their non-

innocent behavior are known from many years, with their first synthesis being reported more than 40 years ago^[24], as a simple condensation between 2,6-pyridinecarboxaldehyde or 2,6-diacetylpyridine with the corresponding aniline (Scheme 1-6).



Scheme 1-6 - Classical synthesis of PDI ligands.

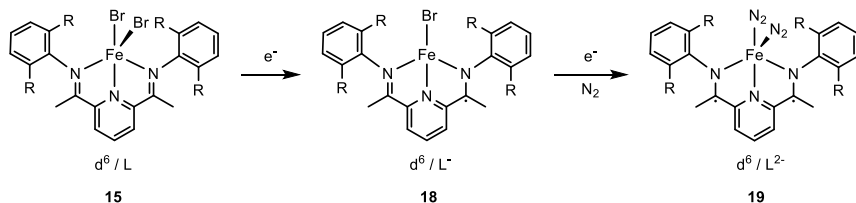
Only very recently they assumed a primary role in homogeneous iron-catalyzed transformations, a broad range of reactions such as polymerizations, hydrosilylation, and hydroboration were efficiently promoted by iron-PDI complexes.^[25] Regarding hydrogenations, seminal work was done by Chirik *et al.*. In a first report in 2004^[26], they reported the initial promising results, hydrogenation of mono- and di-substituted olefins was perfectly achieved within minutes. The active catalyst is formed by reduction of the pre-catalyst (PDI)FeBr₂ (**15**) with two equivalents of sodium or sodium triethylborohydride, the reduce complex is then trapped with nitrogen or carbon monoxide yielding square pyramidal active catalysts **16** and **17** (Scheme 1-7).



Scheme 1-7 - Synthesis of active (PDI)Fe species according to Chirik *et al.*

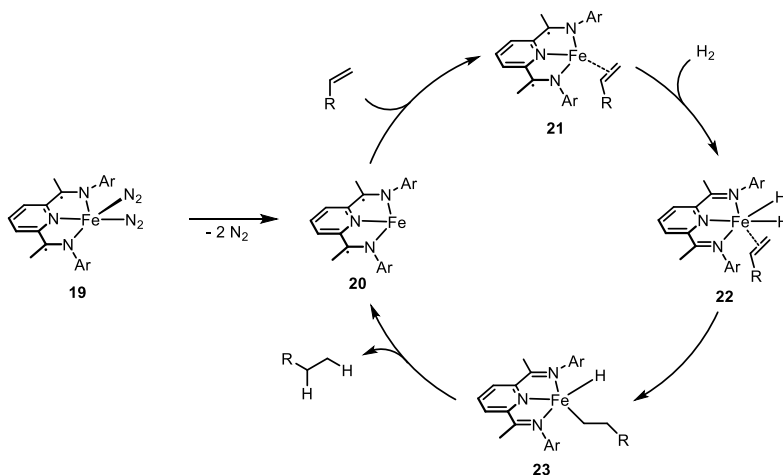
After a couple of years detailed structural, spectroscopic and computation studies were published by the same author^[27] and proved that the non-innocent behaviour of the ligand

is the key feature of this catalytic system. This example is the perfect case study for the explanation of the behaviour of redox active spectator ligands. Reduction of the initial iron precursor **15** occurs at the ligand and not at metal center (Scheme 1-8). The active catalyst is not an iron(0) species **16**, but is better described as an iron(II) species coordinated with a radical dianionic ligand, **19**.



Scheme 1-8 – Reduction of PDI-iron complexes.

The catalytic cycle proposed by Chirik for these catalysts is described in Scheme 1-9: initial decooordination of nitrogen molecules and coordination of the substrate leads to the formation of **21**, in the next step oxidative addition plays a crucial role and **21** is formally 2 electrons oxidized maintaining the iron center in formal oxidation state (+2)(**22**). Insertion of the substrate in the metal-hydrogen bond results in the formation of the iron-alkyl complex **23**, final reductive elimination forms the product and reduces the ligand back to the initial stage (**20**).



Scheme 1-9 - Catalytic cycle proposed by Chirik *et al.*

In 2005 the group Danopoulos *et al.*^[28] described the synthesis of iron pincer complexes in which the imino functionalities of the PDI ligand were substituted by *N*-heterocyclic carbenes (**25**). Inspired by this work and by the observation that addition of electron donating groups on the pyridine ring has an influence on the electronic properties of the metal^[29], Chirik *et al.* investigated these (CNC)Fe(N₂)₂ complexes for the hydrogenation of alkenes with outstanding results.^[30] Applying only 4 bars of hydrogens tri-substituted unfunctionalized olefins such as alpha-methyl stilbene, 2-methyl-2-butene, and 1-methylcyclohexene were quantitatively hydrogenated, even the tetra-substituted 2,3-dimethyl-1*H*-lindene was converted up to 60 % (Table 1-6, entry 5). Functionalized substrates, for example, acrylates, represented the limit of this catalytic system, with poor conversions with (CNC)Fe(N₂)₂ as the catalyst (Table 1-6, entry 1).

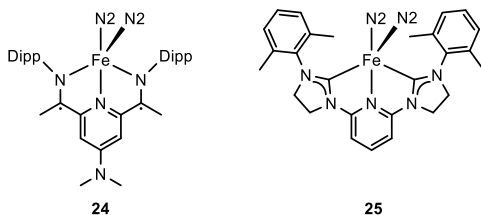
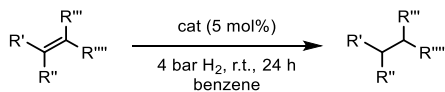


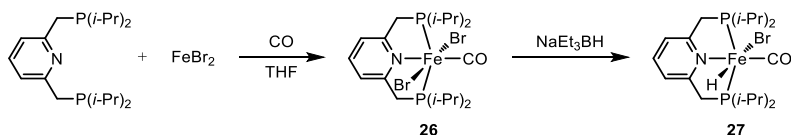
Figure 1-6 - Iron pincer complexes investigated by Chirik *et al.*

Table 1-6 - Hydrogenation results obtained with complexes **24** and **25**.



Entry	Substrate	Conversion (%) with 24	Conversion (%) with 25
1		>95	35
2		76	>95
3		15	>95
4		3	>95
5		3	68(48 h)

Not only PDI ligands showed to be efficient non-innocent ligands for iron-catalyzed hydrogenation reactions. Other pincer ligands afforded very interesting and reactive iron-based catalysts. One of the first publications describing a (PNP)Fe complex was from Milstein's laboratories.^[31] The core structure (**26**) was also in this case composed of a central pyridine ring, with two additional phosphine chelating groups bound to the aromatic ring in 2,2' position, using a methylene spacer to ensure the best coordination geometry. These complexes were first applied in the hydrogenation of carbon dioxide^[31a] and ketones^[31b] with very good results, the catalyst loading was lowered to 0.05 mol%, ensuring turnover numbers up to 2000, remarkable results in the field of iron catalysis (Table 1-7).

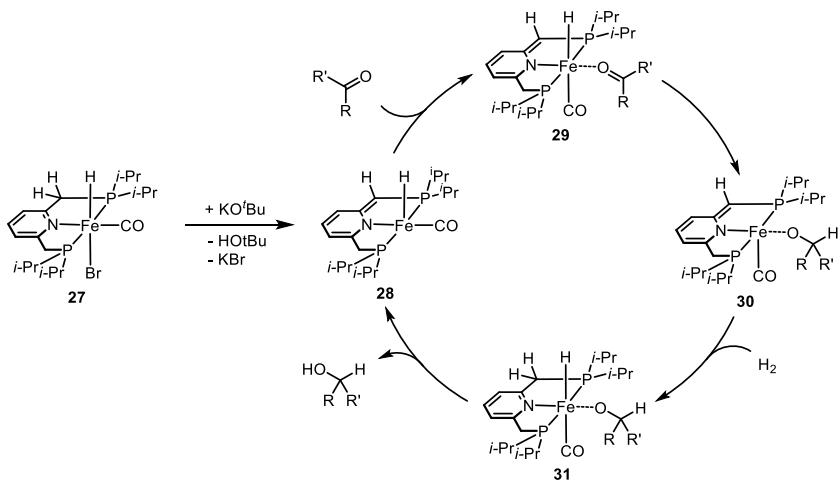


Scheme 1-10 - Synthesis of (PNP)-Fe complexes according to Milstein *et al.*

Table 1-7 - Hydrogenation of substituted ketones with **27**.

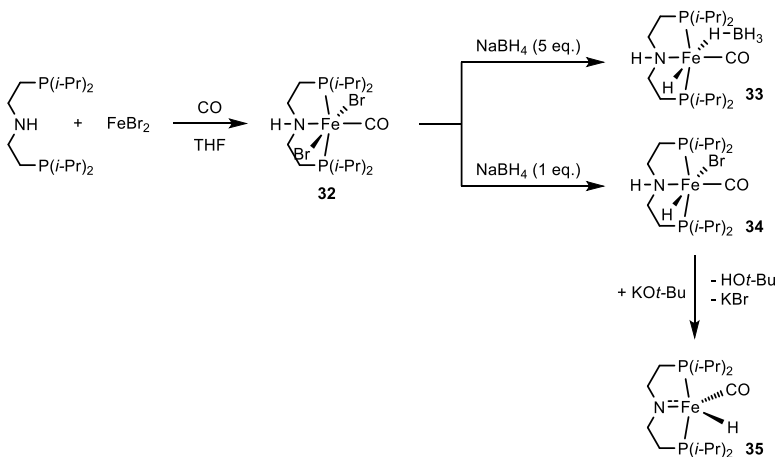
Entry	R	Yield (%)
1	H	94
2	Cl	86
3	Br	78
4	Me	72

The catalytic cycle proposed by the authors is showed in Scheme 1-11, the non-innocent ligand participate actively creating covalent bonds with the reagent, dihydrogen. The initial deprotonation of **27** results in the dearomatization of the pyridine ring, and thanks to the newly formed anionic nitrogen ligand the bromide can decoordinate from the metal center, with the oxidation state of iron in complex **28** still being (+2). The vacant site is occupied by the substrate, subsequent migration of the hydride leads to complex **30**. Rearomatization of the pyridine ring occurs in **31** after the activation of a dihydrogen molecule. Elimination of the product regenerates the initial catalyst **28**.



Scheme 1-11 - Catalytic cycle for hydrogenation of ketone proposed by Milstein *et al.*

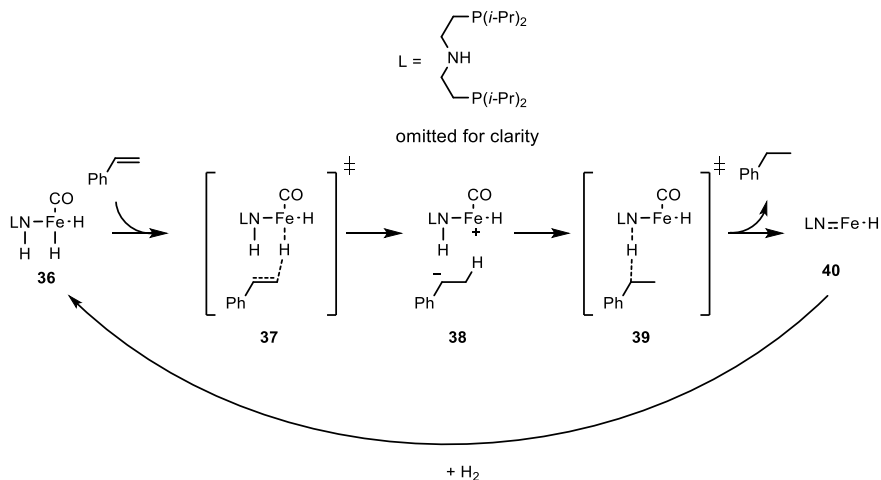
Following the same idea, different research groups developed similar ligands and complexes. In the time period of just a few months, Beller^[32], Guan^[33] and Jones^[34] independently reported the application of Fe-bis(phosphino)amine complexes (Scheme 1-12) as competent catalyst for the hydrogenation(**33**)/dehydrogenation(**35**) of different classes of molecules, such as esters, alcohols, and *N*-heterocycles.



Scheme 1-12 - Synthesis of Fe-bis(phosphino)amine complexes according to Guan *et al.*

From their reports it appears clear, that also in this case the ligand participates actively in the catalysis abstracting a proton from the substrate. As a proof of this concept, dehydrogenation attempts of tetraline with **35** failed while the more acidic tetrahydroquinoline showed good conversion.

In a follow-up paper^[35], the same authors increased the scope of this catalyst to the hydrogenation of primary and secondary olefins, but even more interestingly Xu *et al.* proved, thanks to experimental and theoretical evidences, the critical importance of the polarity of the substrate's C=C double bond for an efficient hydrogenation. Translating this information to the operative catalytic cycle the authors proposed a metal-ligand cooperative pathway via stepwise hydride transfer from the metal to the substrate (transition state **37**), followed by a proton transfer from the ligand (transition state **39**) (Scheme 1-13).



Scheme 1-13 - Mechanism proposed by Jones *et al.*

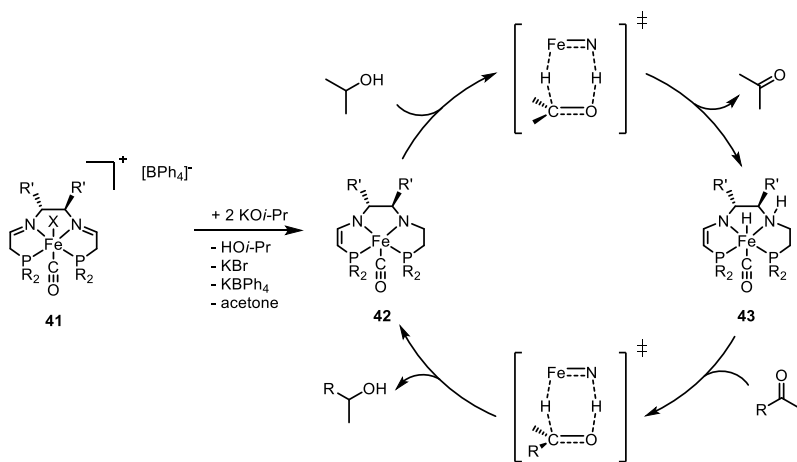
Slight modifications of this catalyst showed activity for other substrates families, Lange *et al.* in 2016^[36], exchanged the aliphatic groups on the phosphine moieties, obtaining a competent catalyst for the hydrogenation of nitriles to the corresponding primary amines. Despite the high hydrogen pressure needed, good to excellent yield were obtained, and a broad range of functional groups was tolerated.

The Langer group last year^[37] thoroughly explored the reactivity of Fe-bis(phosphino)complexes, and applied them to the hydrogenation of amides, yielding alcohols and amines. Investigating structural alterations on the PNP ligand they performed

a fine tuning of the scaffold, finally identifying in the one bearing less bulky ethyl-groups the best compromise between stability and activity of the catalyst.

Tetradentate PNNP ligand motifs have been thoroughly investigated by Morris *et al.* in the last decade^[38]. Different ligand structures were described by the group (Figure 1-7), chiral backbones were applied, leading this catalytic system to be one of the first iron-based catalyst reported for asymmetric transfer hydrogenation of ketones. Turnover frequencies of over 25000 h⁻¹ and excellent enantioselectivities were achieved.

Detailed kinetic^[39] and DFT^[40] studies proved the outer-sphere mechanism of this transformation (Scheme 1-14). A base, mandatory for the catalytic activity, initially deprotonate the neutral ligand in **41**, the resulting active complex **42**, then, dehydrogenates the sacrificial hydrogen source, usually isopropanol. The newly formed iron-hydride species **43** can subsequently reduce the substrate closing the catalytic cycle. As in the previously reported examples, this ligand has an actor role in this reaction, abstracting/donating a proton and keeping the metal center in +2 oxidation state.



Scheme 1-14 – Catalytic cycle proposed by Morris *et al.*

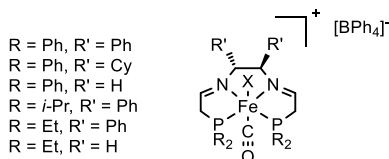
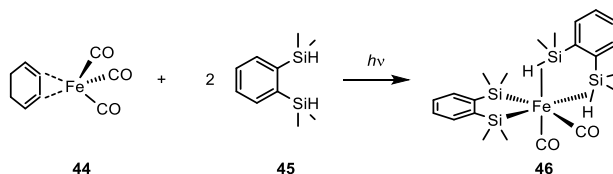


Figure 1-7 – Few examples of PNNP-iron complexes described by Morris *et al.*

Not only pincer ligands show non-innocent behavior, in 2013 Nagashima *et al.*^[41] reported an iron complex obtained irradiating with an high pressure mercury lamp of a mixture of one equivalent of $(\eta^4\text{-C}_6\text{H}_8)\text{Fe}(\text{CO})_3$ (**44**) with two equivalents of bis(dimethylsilyl)benzene (BDSB) (**45**). The resulting (**46**) is a distorted octahedral iron complex with two *cis*-CO ligands (Scheme 1-15). The exceptional hydrogenation activity of this complex is shown in Table 1-8, tri- and tetra-substituted olefins, extremely challenging substrates, were hydrogenated after six hours with only 1 bar of hydrogen.



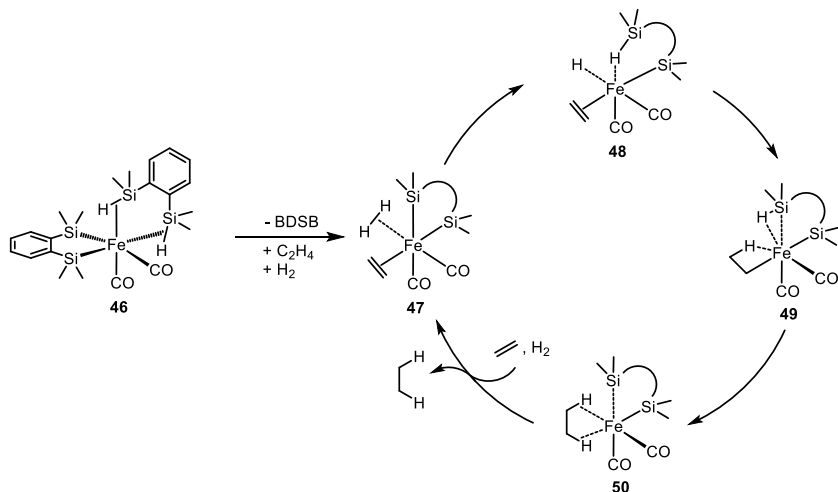
Scheme 1-15 - Synthesis of **46** according to Nagashima *et al.*

Table 1-8 - Hydrogenation of di-, tri- and tetra-substituted alkenes with **46**.

Entry	R	Yield (%)
1		99
2		99
3		59
4		20

Last year^[42] the same group reported interesting theoretical investigations about this complex that clarified its hydrogenation mechanism. The proposed cycle is shown in Scheme 1-16. Despite the different structure, this complex also owes its activity to the silyl ligand non-innocent behavior. After the initial decooordination of a bis(dimethylsilyl)benzene molecule, the resulting vacant sites are occupied by the substrate (simple ethene was employed for this study) and one molecule of dihydrogen (**47**). H₂ is then cooperatively cleaved by a silyl group of BDSB in conjunction with the metal center yielding **48**, the next step is an insertion of the substrate C=C double bond in the Fe-H bond, and finally hydrogen migration from the iron center to ethylene ligand

leads to the formation of the product and the regeneration of the initial iron complex, closing the catalytic cycle.



Scheme 1-16 - Catalytic cycle proposed by Nagashima *et al.*

Cyclopentadienones also belong to the non-innocent ligand family. Iron complexes containing this ligand motif, Knölker complexes (Figure 1-8), were firstly described by the homonym author almost two decades ago^[43] and subsequently have been successfully employed as catalysts for hydrogenation reactions.^[44] These systems have been deeply investigated, determining that a heterolytic cleavage of dihydrogen assisted by the cyclopentadienone ligand is the key step for the high activity of these complexes.

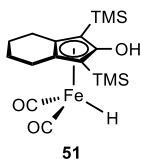


Figure 1-8 – First iron hydroxycyclopentadienyl complex reported by Knölker *et al.*

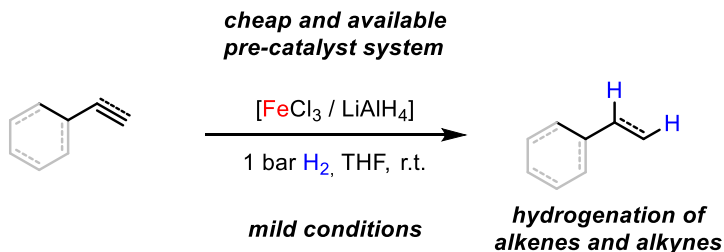
1.2 References

- [1] S. Enthaler, K. Junge, M. Beller, *Angew. Chem. Int. Ed.* **2008**, *47*, 3317-3321.
- [2] *The Handbook of Homogeneous Hydrogenation*, Wiley-VCH, Weinheim, **2007**.
- [3] http://www.monex.com/prods/palladium_chart.html.
- [4] D. Astruc, *Nanoparticles & Catalysis*, Wiley-VCH, Weinheim, **2008**.
- [5] a) H. Kura, M. Takahashi, T. Ogawa, *J. Phys. Chem. C* **2010**, *114*, 5835-5838; b) J. Krämer, E. Redel, R. Thomann, C. Janiak, *Organometallics* **2008**, *27*, 1976-1978.
- [6] R. Hudson, G. Hamasaka, T. Osako, Y. M. A. Yamada, C.-J. Li, Y. Uozumi, A. Moores, *Green Chem.* **2013**, *15*, 2141-2148.
- [7] M. Stein, J. Wieland, P. Steurer, F. Tölle, R. Mülhaupt, B. Breit, *Adv. Synth. Catal.* **2011**, *353*, 523-527.
- [8] Y. C. Han, H. G. Cha, C. W. Kim, Y. H. Kim, Y. S. Kang, *J. Phys. Chem. C* **2007**, *111*, 6275-6280.
- [9] V. Kelsen, B. Wendt, S. Werkmeister, K. Junge, M. Beller, B. Chaudret, *Chem. Commun* **2013**, *49*, 3416-3418.
- [10] a) C. Rangheard, C. de Julian Fernandez, P.-H. Phua, J. Hoorn, L. Lefort, J. G. de Vries, *Dalton Tran.* **2010**, *39*, 8464-8471; b) D. J. Frank, L. Guiet, A. Kaeslin, E. Murphy, S. P. Thomas, *RSC Adv.* **2013**, *3*, 25698-25701; c) A. J. MacNair, M.-M. Tran, J. E. Nelson, G. U. Sloan, A. Ironmonger, S. P. Thomas, *Org. Biomol. Chem.* **2014**, *12*, 5082-5088.
- [11] T. S. Carter, L. Guiet, D. J. Frank, J. West, S. P. Thomas, *Adv. Synth. Catal.* **2013**, *355*, 880-884.
- [12] P.-H. Phua, L. Lefort, J. A. F. Boogers, M. Tristany, J. G. de Vries, *Chem. Commun.* **2009**, 3747-3749.
- [13] A. Welther, M. Bauer, M. Mayer, A. Jacobi von Wangelin, *ChemCatChem* **2012**, *4*, 1088-1093.
- [14] T. N. Gieshoff, A. Welther, M. T. Kessler, M. H. G. Pechtl, A. Jacobi von Wangelin, *Chem. Commun* **2014**, *50*, 2261-2264.
- [15] W. W. Brennessel, R. E. Jilek, J. E. Ellis, *Angew. Chem. Int. Ed.* **2007**, *46*, 6132-6136.
- [16] D. Gaertner, A. Welther, B. R. Rad, R. Wolf, A. Jacobi Von Wangelin, *Angew. Chem. Int. Ed.* **2014**, *53*, 3722-3726.
- [17] P. Buschelberger, D. Gartner, E. Reyes-Rodriguez, F. Kreyenschmidt, K. Koszinowski, A. Jacobi von Wangelin, R. Wolf, *Chem. Eur. J.* **2016**.
- [18] a) C. Bianchini, M. Peruzzini, F. Zanobini, *J. Organomet. Chem.* **1988**, *354*, C19-C22; b) C. Bianchini, A. Meli, M. Peruzzini, F. Vizza, F. Zanobini, P. Frediani, *Organometallics* **1989**, *8*, 2080-2082; c) C. Bianchini, A. Meli, M. Peruzzini, P. Frediani, C. Bohanna, M. A. Esteruelas, L. A. Oro, *Organometallics* **1992**, *11*, 138-145.
- [19] a) E. J. Daida, J. C. Peters, *Inorg. Chem.* **2004**, *43*, 7474-7485; b) H. Fong, M.-E. Moret, Y. Lee, J. C. Peters, *Organometallics* **2013**, *32*, 3053-3062.
- [20] G. Wienhofer, F. A. Westerhaus, R. V. Jagadeesh, K. Junge, H. Junge, M. Beller, *Chem. Commun.* **2012**, *48*, 4827-4829.
- [21] C. Federsel, A. Boddien, R. Jackstell, R. Jennerjahn, P. J. Dyson, R. Scopelliti, G. Laurenczy, M. Beller, *Angew. Chem. Int. Ed.* **2010**, *49*, 9777-9780.

- [22] G. Wienhöfer, F. A. Westerhaus, K. Junge, M. Beller, *J. Organomet. Chem.* **2013**, *744*, 156-159.
- [23] a) L. A. Berben, B. de Bruin, A. F. Heyduk, *Chem. Commun.* **2015**, *51*, 1553-1554; b) S. Blanchard, E. Derat, M. Desage-El Murr, L. Fensterbank, M. Malacria, V. Mouries-Mansuy, *Eur. J. Inorg. Chem.* **2012**, *2012*, 376-389; c) A. Fuerstner, *ACS Cent. Sci.* **2016**, *2*, 778-789; d) W. Kaim, *Eur. J. Inorg. Chem.* **2012**, *2012*, 343-348; e) V. Lyaskovskyy, B. De Bruin, *ACS Catal.* **2012**, *2*, 270-279; f) P. J. Chirik, K. Wiegardt, *Science* **2010**, *327*, 794.
- [24] E. C. Alyea, P. H. Merrell, *Synth. React. Inorg. Met.-Org. Chem.* **1974**, *4*, 535-544.
- [25] a) S. K. Russell, E. Lobkovsky, P. J. Chirik, *J. Am. Chem. Soc.* **2011**, *133*, 8858-8861; b) A. M. Tondreau, C. C. H. Atienza, J. M. Darmon, C. Milsmann, H. M. Hoyt, K. J. Weller, S. A. Nye, K. M. Lewis, J. Boyer, J. G. P. Delis, E. Lobkovsky, P. J. Chirik, *Organometallics* **2012**, *31*, 4886-4893; c) J. H. Docherty, J. Peng, A. P. Dominey, S. P. Thomas, *Nat Chem* **2017**, advance online publication; d) A. M. Tondreau, E. Lobkovsky, P. J. Chirik, *Org. Lett.* **2008**, *10*, 2789-2792; e) K. T. Sylvester, P. J. Chirik, *J. Am. Chem. Soc.* **2009**, *131*, 8772-8774; f) B. L. Small, M. Brookhart, *J. Am. Chem. Soc.* **1998**, *120*, 7143-7144; g) B. L. Small, M. Brookhart, A. M. A. Bennett, *J. Am. Chem. Soc.* **1998**, *120*, 4049-4050; h) G. J. P. Britovsek, M. Bruce, V. C. Gibson, B. S. Kimberley, P. J. Maddox, S. Mastroianni, S. J. McTavish, C. Redshaw, G. A. Solan, S. Stroemberg, A. J. P. White, D. J. Williams, *J. Am. Chem. Soc.* **1999**, *121*, 8728-8740; i) G. J. P. Britovsek, V. C. Gibson, B. S. Kimberley, P. J. Maddox, S. J. McTavish, G. A. Solan, A. J. P. White, D. J. Williams, *Chem. Commun.* **1998**, 849-850; j) M. W. Bouwkamp, E. Lobkovsky, P. J. Chirik, *J. Am. Chem. Soc.* **2005**, *127*, 9660-9661.
- [26] S. C. Bart, E. Lobkovsky, P. J. Chirik, *J. Am. Chem. Soc.* **2004**, *126*, 13794-13807.
- [27] S. C. Bart, K. Chlopek, E. Bill, M. W. Bouwkamp, E. Lobkovsky, F. Neese, K. Wiegardt, P. J. Chirik, *J. Am. Chem. Soc.* **2006**, *128*, 13901-13912.
- [28] A. A. Danopoulos, J. A. Wright, W. B. Motherwell, *Chem. Commun.* **2005**, 784-786.
- [29] J. M. Darmon, Z. R. Turner, E. Lobkovsky, P. J. Chirik, *Organometallics* **2012**, *31*, 2275-2285.
- [30] R. P. Yu, J. M. Darmon, J. M. Hoyt, G. W. Margulieux, Z. R. Turner, P. J. Chirik, *ACS Catal.* **2012**, *2*, 1760-1764.
- [31] a) R. Langer, Y. Diskin-Posner, G. Leitus, L. J. Shimon, Y. Ben-David, D. Milstein, *Angew. Chem. Int. Ed.* **2011**, *50*, 9948-9952; b) R. Langer, G. Leitus, Y. Ben-David, D. Milstein, *Angew. Chem. Int. Ed.* **2011**, *50*, 2120-2124.
- [32] E. Alberico, P. Sponholz, C. Cordes, M. Nielsen, H. J. Drexler, W. Baumann, H. Junge, M. Beller, *Angew. Chem. Int. Ed.* **2013**, *52*, 14162-14166.
- [33] S. Chakraborty, H. Dai, P. Bhattacharya, N. T. Fairweather, M. S. Gibson, J. A. Krause, H. Guan, *J. Am. Chem. Soc.* **2014**, *136*, 7869-7872.
- [34] S. Chakraborty, W. W. Brennessel, W. D. Jones, *J. Am. Chem. Soc.* **2014**, *136*, 8564-8567.
- [35] R. Xu, S. Chakraborty, S. M. Bellows, H. Yuan, T. R. Cundari, W. D. Jones, *ACS Catal.* **2016**, *6*, 2127-2135.
- [36] S. Lange, S. Elangovan, C. Cordes, A. Spannenberg, H. Jiao, H. Junge, S. Bachmann, M. Scalone, C. Topf, K. Junge, M. Beller, *Catal. Sci. Technol.* **2016**, *6*, 4768-4772.

- [37] F. Schneck, M. Assmann, M. Balmer, K. Harms, R. Langer, *Organometallics* **2016**, *35*, 1931-1943.
- [38] a) P. O. Lagaditis, A. J. Lough, R. H. Morris, *Inorg. Chem.* **2010**, *49*, 10057-10066; b) N. Meyer, A. J. Lough, R. H. Morris, *Chem. Eur. J.* **2009**, *15*, 5605-5610; c) A. Mikhailine, A. J. Lough, R. H. Morris, *J. Am. Chem. Soc.* **2009**, *131*, 1394-1395; d) A. A. Mikhailine, R. H. Morris, *Inorg. Chem.* **2010**, *49*, 11039-11044; e) R. H. Morris, *Chem. Soc. Rev.* **2009**, *38*, 2282-2291; f) P. E. Sues, A. J. Lough, R. H. Morris, *Organometallics* **2011**, *30*, 4418-4431; g) C. Sui-Seng, F. Freutel, A. J. Lough, R. H. Morris, *Angew. Chem. Int. Ed.* **2008**, *47*, 940-943; h) C. Sui-Seng, F. N. Haque, A. Hadzovic, A.-M. Pütz, V. Reuss, N. Meyer, A. J. Lough, M. Zimmer-De Iuliis, R. H. Morris, *Inorg. Chem.* **2009**, *48*, 735-743; i) W. Zuo, A. J. Lough, Y. F. Li, R. H. Morris, *Science* **2013**, *342*, 1080.
- [39] A. A. Mikhailine, M. I. Maishan, A. J. Lough, R. H. Morris, *J. Am. Chem. Soc.* **2012**, *134*, 12266-12280.
- [40] D. E. Prokopchuk, R. H. Morris, *Organometallics* **2012**, *31*, 7375-7385.
- [41] Y. Sunada, H. Tsutsumi, K. Shigeta, R. Yoshida, T. Hashimoto, H. Nagashima, *Dalton Trans.* **2013**, *42*, 16687-16692.
- [42] A. Tahara, H. Tanaka, Y. Sunada, Y. Shiota, K. Yoshizawa, H. Nagashima, *J. Org. Chem.* **2016**, *81*, 10900-10911.
- [43] a) H.-J. Knölker, E. Baum, H. Goesmann, R. Klauss, *Angew. Chem. Int. Ed.* **1999**, *38*, 2064-2066; b) H.-J. Knölker, E. Baum, J. Heber, *Tetrahedron Lett.* **1995**, *36*, 7647-7650; c) H.-J. Knölker, J. Heber, *Synlett* **1993**, *1993*, 924-926; d) H.-J. Knölker, J. Heber, C. H. Mahler, *Synlett* **1992**, *1992*, 1002-1004.
- [44] a) A. Quintard, J. Rodriguez, *Angew. Chem. Int. Ed.* **2014**, *53*, 4044-4055; b) A. Berkessel, S. Reichau, A. von der Hoeh, N. Leconte, J.-M. Neudorfl, *Organometallics* **2011**, *30*, 3880-3887; c) A. von der Hoeh, A. Berkessel, *ChemCatChem* **2011**, *3*, 861-867; d) C. P. Casey, H. Guan, *J. Am. Chem. Soc.* **2007**, *129*, 5816-5817; e) A. Pagnoux-Ozherelyeva, N. Pannetier, M. D. Mbaye, S. Gaillard, J.-L. Renaud, *Angew. Chem. Int. Ed.* **2012**, *51*, 4976-4980; f) S. Fleischer, S. Zhou, K. Junge, M. Beller, *Angew. Chem. Int. Ed.* **2013**, *52*, 5120-5124; g) C. P. Casey, H. Guan, *J. Am. Chem. Soc.* **2009**, *131*, 2499-2507.

2 Iron-catalyzed olefin hydrogenation at 1 bar H₂ with a FeCl₃-LiAlH₄ catalyst^{i,ii}



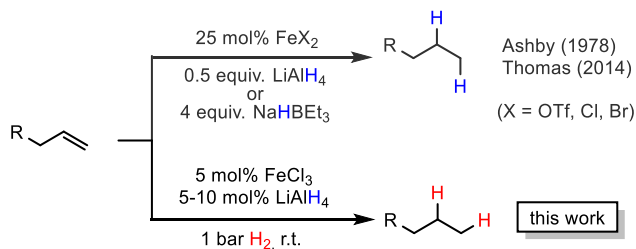
The scope and mechanism of a practical protocol for the iron-catalyzed hydrogenation of alkenes and alkynes at 1 bar H₂ pressure were studied. The catalyst is formed from cheap chemicals (5 mol% FeCl₃-LiAlH₄, THF). A homogeneous mechanism operates at early stages of the reaction while active nanoparticles form upon ageing of the catalyst solution.

ⁱReproduced from T. N. Gieshoff, M. Villa, A. Welther, M. Plois, U. Chakraborty, R. Wolf, A. Jacobi von Wangelin, *Green Chem* **2015**, *17*, 1408–1413 with permission from the Royal Society of Chemistry. Schemes, tables and text may differ from published version.

ⁱⁱAuthors contribution: Initial experiments were performed by A. Welther (Table 2-1, Table 2-2, Table 2-3 entries 1, 2, 3, 6, 10, 11), see A. Welther, *Dissertation*, University Regensburg, **2013**. Complex **4** (Scheme 2-3) was initially synthesized and analyzed by M. Plois and resynthesized by U. Chakraborty, see M. Plois, *Dissertation*, University Regensburg, **2012**. T. Gieshoff contributed equally in Table 2-3 and Table 2-4.

2.1 Introduction

Catalytic hydrogenations of olefins constitute one of the strongholds of transition metal catalysis within organic synthesis and technical processes.^[1] The majority of these methods involve noble metal catalysts based on Pd, Pt, Rh, Ir or toxic metals such as Ni or Co. Iron-catalyzed hydrogenations of olefins have only recently attracted great interest due to their expedient economic and environmental qualities.^[2] Homogeneous iron catalysts were mostly reported with phosphine and pyridyl-2,6-diimine ligands, sometimes requiring high pressures of H₂.^[3,4] Nanoparticle Fe catalysts could be prepared by reduction of iron salts with Grignard reagents in the absence of a suitable ligand or by decomposition of iron carbonyls.^[5] Fe-catalyzed reductions of olefins were recently reported with cheap ferrous salt pre-catalysts FeX₂ in the presence of an excess of lithium *N,N*-dimethylaminoborohydride (10 equiv.) or sodium triethylborohydride (4 equiv.) and required a high catalyst loading or the addition of tetra-dentate ligands.^[6] Reductions of alkenes and alkynes with LiAlH₄ in the presence of various transition metal halides (NiCl₂, TiCl₂, CoCl₂, FeCl₃) were already reported in the 1960s and postulated to involve metal hydride species that engage in formal hydrometalations of the olefin.^[7] Here, we wish to present a synthetic and mechanistic study on a hydrogenation protocol using catalytic amounts of a cheap Fe salt and catalytic amounts of lithium aluminiumhydride (LiAlH₄) as catalyst activator under an atmosphere of 1 bar H₂ as stoichiometric hydrogen source (Scheme 2-1).^[7e]



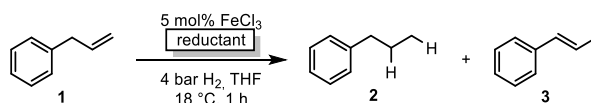
Scheme 2-1 - Iron-catalyzed reductions of olefins: Hydride vs. hydrogen methods.

This method allows the use of standard (ambient pressure) equipment. H₂ is an abundant raw material; LiAlH₄ is an easy-to-handle reductant with numerous applications.^[8]

2.2 Reaction conditions and substrate scope

Initial experiments with the model substrate allylbenzene (**1**) aimed at the identification of a suitable catalytic reductant which assists the formation of a low-valent iron catalyst (with dark brown color) from the commercial pre-catalyst FeCl₃ (Table 2-1).^[9] LiAlH₄ displayed excellent selectivity which exceeded that of earlier protocols with Grignard reagents.^[5] Isomerization of the terminal double bond into conjugation – which occurred in the related EtMgCl-mediated protocols (entries 2, 4) – was effectively suppressed.^[10] NaBH₄ was far less active even at elevated temperature and pressure (entries 6, 7). Interestingly, low ratios of LiAlH₄/FeCl₃ (1/1 to 2/1) fared optimal in the hydrogenation of **1** at 1 bar H₂. When employing a larger excess of LiAlH₄ (>2/1), the catalytic activity collapsed.^[7e] This stoichiometry differs from literature reports where large excess amounts of hydride reagents effected clean hydrogenations of olefins.^[6,7a-c] At 60°C, the FeCl₃/LiAlH₄ catalyst decomposed upon decolorization.

Table 2-1 - Selected optimization experiments.



Entry	Reductant (mol%)	Deviation from conditions ^a	2 in % ^c	3 in % ^c
1	-	-	<1	2
2	EtMgCl (30)	-	42	56
3	EtMgCl (30)	- ^b	16	<1
4	EtMgCl (30)	1 bar H ₂ , 20 h	60	36
5	Et ₂ Zn (20)	30 bar H ₂ , 80 °C, 12 h	4	1
6	NaBH ₄ (100)	50 bar H ₂ , 24 h	8	<1
7	NaBH ₄ (100)	MeOH/THF (1:1), 50 bar H ₂ , 50 °C, 20 h	45	38

8	LiAlH ₄ (10)	-	97	3
9	LiAlH₄ (10)	1 bar H₂, 20 h	98	1
10	LiAlH ₄ (30)	as entry 9, open to air ^d	95	3
11	LiAlH ₄ (10)	FeCl ₂	96	1
12	LiAlH ₄ (10)	Fe(acac) ₃	20	15

^a Conditions: 5 mol% FeCl₃ in THF (0.5 mL) under argon, addition of reductant at r.t., after 10 min addition of **1**, after 1 min exchange of Ar with 4 bar H₂; ^b prior storage of [FeCl₃/red.] catalyst mixture in THF under argon for 3 d at r.t.; ^c quantitative GC-FID vs. *n*-pentadecane as internal reference; ^d during catalyst preparation.

The catalyst system comprises of cheap and easy-to-handle reagents (FeCl₃ or FeCl₂, LiAlH₄, THF); the reaction operates under ambient conditions (1 bar H₂, 20°C), which make the general protocol practical for every-day use in standard synthesis laboratories. The optimized conditions were applied to functionalized allylbenzenes and styrenes (Table 2-2 and Table 2-3).^[9]

Allylbenzenes underwent only minimal olefin isomerization.^[10] Styrenes exhibited low propensity to undergo polymerization (entry 13, Table 2-3). The general protocol is compatible with several functional groups including F, Cl, Br, allyl and benzyl ethers, esters, carboxamides, pyridines and anilines. Clean hydrogenation was achieved with bulky, *ortho*-substituted, and electron-rich styrenes. For comparison, the FeCl₃/EtMgCl-derived catalyst effected undesired dehalogenation (Cl, Br)^[11] and allylether cleavage^[12], and showed no activity in the presence of carboxylates or cinnamates. Catalyst decomposition was effected by nitro groups, iodides, nitriles, ketones, and acidic protons (e.g. alkanols, pK_a~17), presumably by oxidation to catalytically inactive Fe(II) species (decolorization). Tri-substituted styrenes gave low conversions. In general, bulky and functionalized substrates were more reactive at elevated pressures (10 bar H₂).^[13]

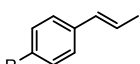
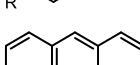
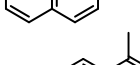
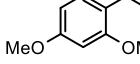
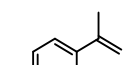
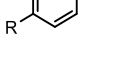
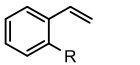

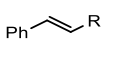
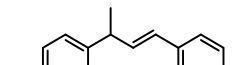

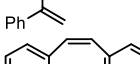
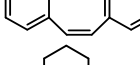
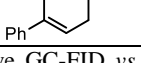
Table 2-2 - Hydrogenation of allylbenzenes at 1 bar H₂.

Entry	Allylbenzene	R	Yield in % ^a
1		H	93
2		Me	79 (92) ^b
3		OMe	84 (89) ^c
4		Me	95
5		OAc	93 (95) ^{c,d}
6		-	99
7		OMe	100
8		F	86

^a quantitative GC-FID vs. *n*-pentadecane as internal reference, conversion in % in parentheses if <95 %; ^b 7% 1-propen-1-ylbenzene (*E/Z* 9/1); ^c 24 h; ^d quantitative NMR (vs. CH₂Br₂)

Table 2-3 - Hydrogenation of styrene derivatives.

Entry	Styrene	R	Yield in % ^a
1		H	100
2		Me	98
3		OMe	98
4		Cl	93 ^b
5		Br	94 ^b
6		F	83 (91)
7		OBn	100 ^d
8		NH ₂	97 ^c
9		CO ₂ Me	97

10		H	98
11		OMe	84 (95)
12		-	100
13		-	86 (86) ^d
14		H	100 ^d
15		Cl	85 (89) ^f
16		Br	44 (56) ^f
17		Br	92 ^{c,f}
18		OMe	100 ^d
19		Cl	74 (86) ^b
20		OBn	100 ^d
21		Ph	100 ^d
22		Bn	100 ^{e,g}
23		CO ₂ Et	58 (68) ^{c,g}
24		-	48 (54)
25		-	83 ^c
26		-	33 (58) ^{c,g}
27		-	55 ^{e,g,h}
28		-	18 (18) ^c

^a quantitative GC-FID vs. *n*-pentadecane as internal reference, conversion in % in parentheses if <95 %; ^b <8 % ethylbenzene; ^c 20 h, 10 bar H₂; ^d 5 mol% LiAlH₄, 3 h; ^e 20 h; ^f <5 % cumene; ^g 5 mol% LiAlH₄; ^h unseparated mixture of mono- and dihydrogenated product isolated by column chromatography, NMR yield, 13% fully hydrogenated product, total conversion.

Hydrogenations of aliphatic alkenes (Table 2-4) were also catalyzed by FeCl₃-LiAlH₄ under similar conditions.^[9] Terminal olefins were only slowly isomerized (~10%).^[10]

Surprisingly, substrates containing moderately acidic protons (pK_a ~25)^[14] underwent hydrogenation with high selectivity (entries 10-13).^[15] Alkynes underwent Z-selective semi-hydrogenation,^[16] whereas complete hydrogenation to the alkanes was observed at longer reaction times or elevated pressures.

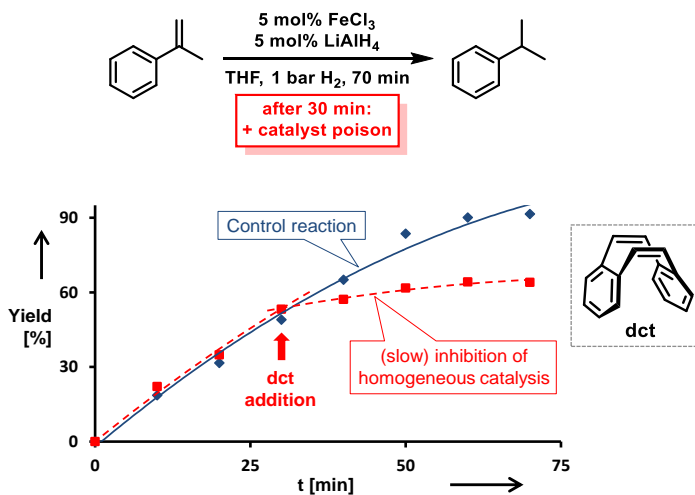
Table 2-4 - Hydrogenation of other alkenes and alkynes.

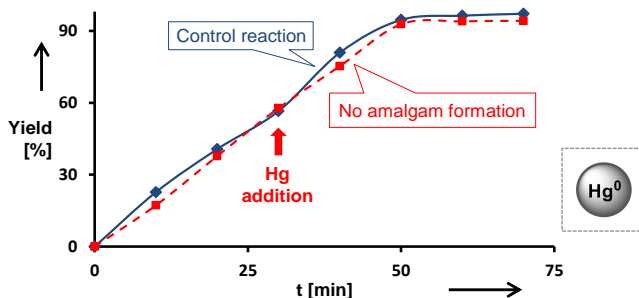
Entry	Substrate	Product	Yield in % ^a
1			82 ^b
2			89 ^{b,e,h}
3			82 (85) ^c
4			89 (89) ^d
5			65 (65) ^c
6			21 (44) ^b
7			100 ^d
8			64 (65) ^d
9			64 (65) ^d
10			96 ^{d,e}
11			96 ^{d,e}
12			38 (38) ^{d,e}
13			69 (69) ^{d,e,g}
14			100 ^c (R=H)
15			92 ^d (R = CO ₂ Me)
16			75 (80)

^a quantitative GC-FID vs. *n*-pentadecane as internal reference, conversion in % in parentheses if <95 %; ^b alkene isomers; ^c 20 h; ^d 10 bar H₂, 20 h; ^e 10 mol% LiAlH₄; ^f 60 °C; ^g 60 °C; ^h 7 h

2.3 Mechanistic studies

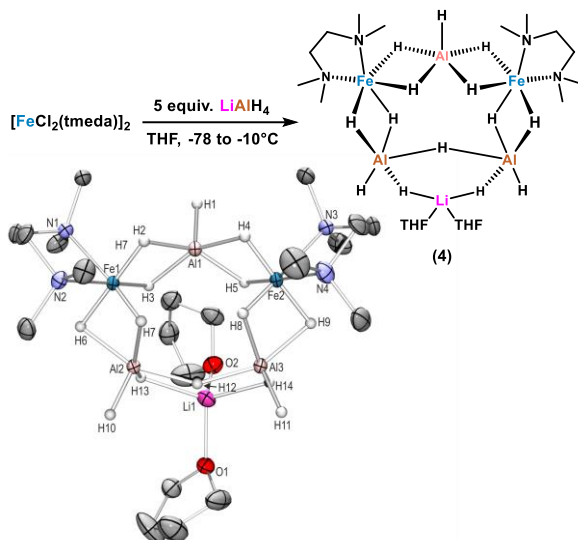
The distinction between homogeneous and heterogeneous catalysts is a challenging task.^[17] However, kinetic experiments with selective poisons can provide valuable information on the topicity of the catalyst species. We have performed two sets of poisoning experiments which appear to support a homogeneous mechanism. Dibenzo[*a,e*]cycloocta-tetraene (dct) is a selective ligand for homogeneous metal species due to its rigid tub-like structure and π -acceptor properties.^[18] Upon addition of 30 mol% dct (6 equiv. per [Fe]) to the hydrogenation of α -methylstyrene at 1 bar H₂ after 30 min, the catalyst activity was significantly inhibited (Scheme 2-2, top).^[9,19] A similar conclusion can be derived from a poisoning experiment with 3 equiv. Hg (60 equiv. Hg per [Fe]). A potential amalgam formation^[20] was not observed and no significant change of the catalyst activity was observed in comparison with the control reaction (Scheme 2-2, bottom).^[9] These results suggest the operation of a homogeneous catalyst species during the early stage of the catalytic hydrogenation.





Scheme 2-2 - Top: Poisoning experiment with 30 mol% dibenzo[*a,e*]cyclooctatetraene (dct, dashed curve) vs. control reaction (solid line). Bottom: Poisoning with 3 equiv. Hg (dashed) vs. control reaction (solid line).

Previous studies showed that the reaction of FeCl₃ with an excess of LiAlH₄ ultimately leads to the formation of iron metal and AlH₃ via the intermediate formation of a thermally unstable iron(II) compound with the composition Fe(AlH₄)₂.^[21,22] In an attempt to gain deeper insight into the catalyst species operating in homogeneous solution, we treated [FeCl₂(tmeda)]₂ (tmeda = *N,N,N',N'*-tetramethylethylenediamine) with LiAlH₄ at -70°C and obtained dark red crystals of the oligohydride compound [Li(thf)₂{Fe(tmeda)}₂(AlH₅)(Al₂H₉)] (**4**, Scheme 2-3).^[9] The hexa-metallic macrocyclic cage contains 14 bridging hydrido ligands and two Fe atoms with distorted octahedral coordination geometries. Unfortunately, the thermal instability prevented further spectroscopic characterization.

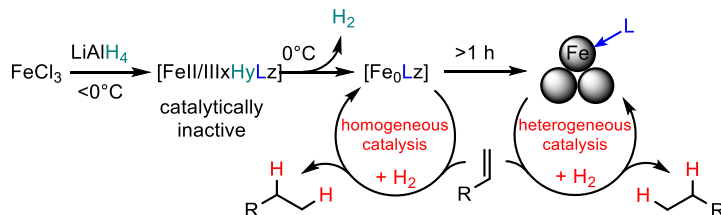


Scheme 2-3 - Synthesis of the soluble LiAlFe-oligohydride complex **4**.

However, complex **4** showed no activity in hydrogenations of styrenes (1-10 bar H₂, -10°C) and maintained its red color throughout the reaction. Above -10°C, the complex rapidly decomposed upon H₂ evolution to give a brown paramagnetic species which afforded good yields in hydrogenations at 20°C and 4 bar H₂. The crystallographic characterization of **4** documents that this or similar oligonuclear Fe(II) aluminohydride complexes may be intermediates en route to the formation of catalytically active low-valent iron species.^[23]

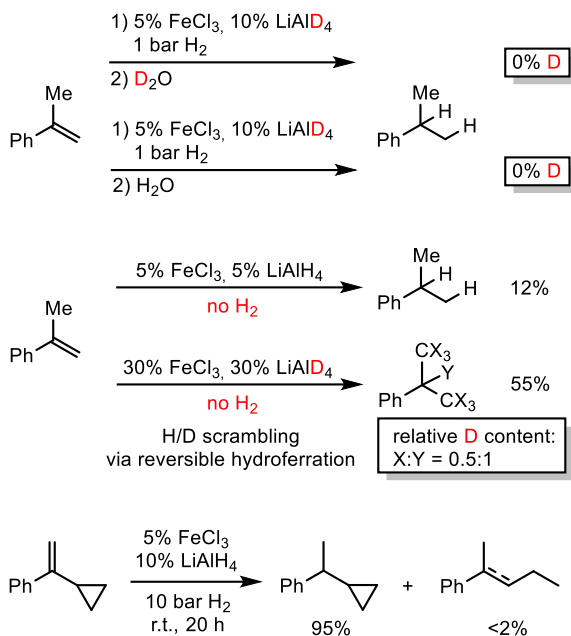
The initially homogeneous dark-brown catalyst species (possibly in the oxidation states 0 and/or +1)^[23] experience rapid ageing and particle formation after approximately 1 h under reductive conditions. Several methods of synthesis and characterization techniques of naked Fe(0) nanoparticles (prepared by reduction of ferric and ferrous halides) have been reported.^[5,7,23,24] DLS measurements (dynamic light scattering) of freshly prepared catalyst solutions (5 mol% FeCl₃/LiAlH₄, THF, r.t., 10 min, then 100 nm nanofiltration) documented the presence of poly-disperse particles of 250-1500 nm size after 30 min of ageing under anaerobic conditions in the absence of substrates. The aged species are much less catalytically active than their homogeneous counterparts. Catalyst solutions (FeCl₃/LiAlH₄ (1/1) in THF) stored at 0°C under argon for 6 h, 24 h, and 48 h afforded 42%, 12%, and 5% conversion of α -methylstyrene under standard conditions.

We postulate a homogeneous mechanism of soluble, low-valent iron catalyst in the initial stage of the hydrogenation reactions (Scheme 2-4). Such species are formed by reduction of FeCl₃ (or L_nFeCl₂) with LiAlH₄ at above 0°C and are typically characterized by the dark brown color. The absence of suitable ligands leads to the formation of Fe(0) nanoclusters^[5,22,24] which require higher H₂ pressures than the homogeneous species to maintain catalytic activity.



Scheme 2-4 - Proposed formation and catalysis of low-valent iron species.

Deuterium incorporation was observed at higher catalyst concentrations (30 mol% FeCl₃/LiAlD₄) in the absence of H₂ which gave ~55% hydrogenation product (Scheme 2-5, center).^[9] Such H₂-free conditions can effect H/D scrambling in the starting material and product (*via* reversible hydroferration) and the formation of radical intermediates (with participation of THF as H donor).^[9] However, the radical mechanism is very unlikely to operate under hydrogenation conditions in the presence of H₂ gas (Scheme 2-5):^[9] Reaction work-up with deuterium oxide (D₂O) and employment of lithium aluminium deuteride (LiAlD₄) showed no deuterium incorporation into the products, respectively (Scheme 2-5, top right). Further, the intermediacy of free C-radicals is unlikely: Employment of the radical probe 1-cyclopropyl-1-phenylethylene^[25] resulted in less than 2% ring opening (Scheme 5, bottom).^[9] The hydrogenation of various styrenes (1 bar H₂) was unaffected by the presence of 1 equiv. 1,1-diphenylethene. On the other hand, the addition of TEMPO (2,2,6,6-tetramethylpiperidinyloxy, 1 equiv.) inhibited conversion of α -methylstyrene (no TEMPO adduct detected), possibly by irreversible catalyst oxidation as indicated by the decolorization of the solution.



Scheme 2-5 - Mechanistic studies with deuterated reagents (top), in the absence of H₂ (center), and with radical probe (bottom).

2.4 Conclusions

In summary, we have studied the iron-catalyzed hydrogenation of various styrenes, alkenes, and alkynes under an atmosphere of 1 bar H₂. This method uses cheap and easy-to-handle reagents (FeCl₃, LiAlH₄, THF, H₂) which allow facile implementation in standard synthesis labs. Alkynes underwent Z-selective semi-hydrogenation. Sterically hindered and functionalized olefins showed higher conversions at elevated H₂ pressures. Mechanistic studies support the notion of a homogeneous catalyst species at the outset of the hydrogenation reactions (<1 h) while catalyst ageing results in the formation of particles which exhibited somewhat lower catalytic activity. The crystallographically characterized homogeneous Fe(II) oligohydride complex **4** can serve as starting point for further model catalyst preparations.

2.5 Experimental part

2.5.1 General

Chemicals and Solvents: Commercially available olefins were distilled under reduced pressure prior use. Solvents (THF, Et₂O, *n*-hexane) were distilled over sodium and benzophenone and stored over molecular sieves (4 Å). Lithium aluminium hydride and iron(III)chloride (98%, anhydrous) were stored and handled in a glovebox under argon (99.996%). Commercial lithium aluminium hydride was purified by extraction with diethyl ether and subsequent removal of the solvent under high vacuum. Solvents used for column chromatography were distilled under reduced pressure prior use (ethyl acetate).

Analytical Thin-Layer Chromatography: TLC was performed using aluminium plates with silica gel and fluorescent indicator (*Merck*, 60, F254). Thin layer chromatography plates were visualized by exposure to ultraviolet light (366 or 254 nm) or by immersion in a staining solution of molybdato-phosphoric acid in ethanol or potassium permanganate in water.

Column Chromatography: Flash column chromatography with silica gel 60 from *KMF* (0.040-0.063 mm). Mixtures of solvents used are noted in brackets.

High Pressure Reactor: Hydrogenation reactions were carried out in 160 and 300 mL high pressure reactors (*Parr*TM) in 4 mL glass vials. The reactors were loaded under argon, purged with H₂ (1 min), sealed and the internal pressure was adjusted. Hydrogen (99.9992%) was purchased from *Linde*.

¹H- und ¹³C-NMR-Spectroscopy: Nuclear magnetic resonance spectra were recorded on a *Bruker* Avance 300 (300 MHz) and *Bruker* Avance 400 (400 MHz). ¹H-NMR: The following abbreviations are used to indicate multiplicities: s = singlet; d = doublet; t = triplet, q = quartet; m = multiplet, dd = doublet of doublet, dt = doublet of triplet, dq = doublet of quartet, ddt = doublet of doublet of quartet. Chemical shift δ is given in ppm to tetramethylsilane.

Fourier-Transformations-Infrared-Spectroscopy (FT-IR): Spectra were recorded on a *Varian* Scimitar 1000 FT-IR with ATR-device. All spectra were recorded at room temperature. Wave number is given in cm⁻¹. Bands are marked as s = strong, m = medium, w = weak and b = broad.

Gas chromatography with FID (GC-FID): HP6890 GC-System with injector 7683B and *Agilent* 7820A System. Column: HP-5, 19091J-413 (30 m × 0.32 mm × 0.25 μm), carrier gas: N₂. GC-FID was used for reaction control and catalyst screening (Calibration with internal standard *n*-pentadecane and analytically pure samples).

Gas chromatography with mass-selective detector (GC-MS): *Agilent* 6890N Network GC-System, mass detector 5975 MS. Column: HP-5MS (30m × 0.25 mm × 0.25 μm, 5% phenylmethylsiloxane, carrier gas: H₂. Standard heating procedure: 50 °C (2 min), 25 °C/min -> 300 °C (5 min)

High resolution mass spectrometry (HRMS): The spectra were recorded by the Central Analytics Lab at the Department of Chemistry, University of Regensburg, on a MAT SSG 710 A from *Finnigan*

Dynamic Light Scattering: Dynamic light scattering experiments were performed with the help of a goniometer CGS-II from *ALV* (Germany). The goniometer is equipped with an ALV-7004/Fast Multiple Tau digital correlator and a vertical-polarized 22 mW HeNe-laser (wavelength = 623.8 nm). All measurements were done at a scattering angle of 90° after thermostating to 25 °C. The measurement time was 300 s. The obtained correlation functions were fitted with the software *TableCurve 2d v5.01* by a monomodal equation.

2.5.2 General hydrogenation procedures

General method for the hydrogenation with FeCl₃ (5mol%) and LiAlH₄ (10 mol%)

A 4 mL vial was charged with a freshly prepared solution of FeCl₃ in dry THF (0.50 mL, 0.05 M) and an aliquot of a vigorously stirred suspension of LiAlH₄ in dry THF (0.50 mL, 0.1 M) under argon atmosphere. After stirring for 30 min; the olefin (0.50 mmol) was added and the vial transferred to a high pressure reactor. The reactor was purged with H₂ (1 min), sealed, and the internal pressure adjusted to 1 bar H₂. After the designated reaction time, the vial was retrieved. The reaction was quenched with saturated aqueous NaHCO₃ (1 mL) and extracted with ethyl acetate (2 × 2 mL). The organic phases were dried (Na₂SO₄) and subjected to flash chromatography (SiO₂, pentane/ethyl acetate) or analyzed by quantitative GC-FID analysis vs. *n*-pentadecane as internal reference.

General method for the hydrogenation with FeCl₃ (5mol%) and LiAlH₄ (5 mol%)

A 25 mL flask was charged with a freshly prepared solution of FeCl₃ in dry THF (2 mL, 0.05 M) and an aliquot of a suspension of LiAlH₄ in dry THF (2 mL, 0.05 M) was added over 20 minutes at -78 °C under argon atmosphere via syringe pump. After stirring for additional 10 minutes, 1 mL of the catalyst suspension was added to a 4 mL vial with the olefin (0.50 mmol) and the vial was transferred to a high pressure reactor. The reactor was purged with H₂ (1 min), sealed, and the internal pressure adjusted to 1 bar H₂. After the designated reaction time, the vial was retrieved. The reaction was quenched with saturated aqueous NaHCO₃ (1 mL) and extracted with ethyl acetate (2 × 2 mL). The organic phases were dried (Na₂SO₄) and subjected to flash chromatography (SiO₂, pentane/ethyl acetate) or analyzed by quantitative GC-FID analysis vs. *n*-pentadecane as internal reference.

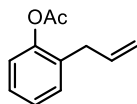
2.5.4 Synthesis of starting material

Preparation of allylbenzenes: Except for 2-allylphenyl acetate, allylbenzenes were prepared according to: M. Mayer, W. M. Czaplík and A. Jacobi von Wangelin, *Adv. Synth. Catal.* **2010**, 352, 2147. Analytical data were in full agreement with the literature reports.

Preparation of various styrenes, alkenes and alkynes: Non-commercial starting material was synthesized following the cited protocols.

2-Allylphenyl acetate

A 50 mL flask was charged with a solution of 2-allylphenol (1.4 mL, 10.6 mmol) in 15 mL CH₂Cl₂. Then, triethylamine (4.6 mL, 33 mmol) was added at 0 °C followed by the slow addition of the acetyl chloride (11.6 mmol). The reaction mixture was stirred at room temperature for 15 h, diluted with 20 mL of ethyl acetate and washed with saturated aqueous NH₄Cl (10 mL). The organic phases were dried (MgSO₄), concentrated, and subjected to silica gel flash chromatography (cyclohexane/ethyl acetate).



C₁₁H₁₂O₂

176.22 g/mol

Appearance

colorless oil

¹H-NMR

(300 MHz, CDCl₃) δ 7.33-7.11 (m, 4H), 7.03 (d, 8.0 Hz, 1H), 5.90 (dt, *J* = 16.5, 6.5 Hz, 1H), 5.21-4.93 (m, 1H), 3.30 (d, *J* = 6.5 Hz, 2H), 2.30 (s, 3H).

GC-MS

*t*_R = 5.82 min, (EI, 70 eV): *m/z* = 176 [M⁺].

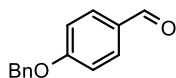
Analytical data were in full agreement with M. J. Gresser, S. M. Wales, P. A. Keller, *Tetrahedron* **2010**, 66, 6965-6976.

General procedure for styrene synthesis in a Wittig reaction

A 50 mL flask was charged with a suspension of methyltriphenylphosphonium bromide (6.94 mmol, 2.48 g) in THF (10 mL). Then, NaH-suspension in paraffine (60%, 6.94 mmol, 278 mg) was added in small portions. The reaction mixture was stirred at room temperature for 20 h followed by a dropwise addition of a solution of a ketone derivative (6.94 mmol) in THF (10 mL). The reaction mixture was stirred for 2 d at room temperature, quenched with H₂O (15 mL) and extracted with Et₂O (3 × 15 mL). The combined organic layers were dried (Na₂SO₄), concentrated and subjected to silica gel flash chromatography (*n*-pentane).

4-(Benzyloxy)benzaldehyde

Synthesis following the procedure by S. K. Das, G. Panda, *Tetrahedron* **2008**, *19*, 4162-4173.



C₁₄H₁₂O₂

212.24 g/mol

Appearance

colorless solid

Yield

1.72 g, 8.12 mmol (81%)

TLC

R_f = 0.20 (SiO₂, hexanes/ethyl acetate = 9/1)

¹H-NMR

(300 MHz, CDCl₃) δ 9.89 (s, 1H), 7.84 (d, *J* = 8.7 Hz, 2H), 7.48 – 7.33 (m, 5H), 7.08 (d, *J* = 8.7 Hz, 2H), 5.16 (s, 2H).

¹³C-NMR

(75 MHz, CDCl₃) δ 190.82, 163.72, 135.93, 132.02, 130.11, 128.75, 128.36, 127.51, 115.15, 70.28.

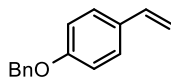
GC-MS

t_R = 9.96 min, (EI, 70 eV): *m/z* = 212 [M⁺], 152, 121, 91, 77, 65, 51.

Analytical data were in full agreement with T. Shintou, T. Mukaiyama, *J. Am. Chem. Soc.*, **2004**, *23*, 7359-7367.

1-(Benzyloxy)-4-vinylbenzene

Synthesis following the general procedure for styrene synthesis in a Wittig reaction.



C₁₅H₁₄O

210.27 g/mol

Appearance

colorless solid

Yield

1.25 g, 5.97 mmol (74%)

TLC

R_f = 0.28 (SiO₂, *n*-pentane)

¹H-NMR

(300 MHz, CDCl₃) δ 7.49 – 7.29 (m, 7H), 6.99 – 6.90 (m, 2H), 6.67 (dd, *J* = 17.6, 10.9 Hz, 1H), 5.63 (dd, *J* = 17.6, 0.9 Hz, 1H), 5.14 (dd, *J* = 10.9, 0.9 Hz, 1H), 5.08 (s, 2H).

¹³C-NMR

(75 MHz, CDCl₃) δ 158.57, 136.94, 136.21, 130.69, 128.63, 128.02, 127.50, 127.43, 114.88, 111.75, 70.03.

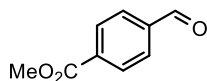
GC-MS

t_R = 9.40 min, (EI, 70 eV): *m/z* = 197 [M⁺], 183, 171, 156, 115, 102, 91, 75, 63, 51.

Analytical data were in full agreement with N. Kakusawa, K. Yamaguchi, J. Kouchichiro, *J. Organomet. Chem.* **2005**, *12*, 2956-2966.

Methyl-4-formylbenzoate

A 250 mL flask was charged with a solution of 4-formylbenzoic acid (15.0 mmol, 2.32 g) in dry methanol (75 mL). Trimethylsilylchloride (33.0 mmol, 4.20 mL) was added and the reaction mixture was stirred over night at room temperature. The product was isolated upon removal of the solvent under reduced pressure and silica gel flash chromatography (hexanes/ethyl acetate = 8/2).



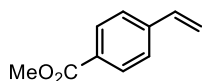
C₉H₈O₃
164.16 g/mol

Appearance	colorless solid
Yield	2.19 g, 13.3 mmol, 89%
TLC	R _f = 0.24 (SiO ₂ , hexanes/ethyl acetate = 8/2)
¹H-NMR	(400 MHz, CDCl ₃) δ 10.09 (s, 1H), 8.19 (d, <i>J</i> = 8.1 Hz, 2H), 7.94 (d, <i>J</i> = 8.3 Hz, 2H), 3.95 (s, 3H).
¹³C-NMR	(101 MHz, CDCl ₃) δ 191.7, 166.1, 139.2, 135.1, 130.2, 129.5, 52.6.
GC-MS	t _R = 7.13 min, (EI, 70 eV): m/z = 164 [M ⁺], 150, 133, 119, 105, 91, 77, 62, 51.

Analytical data were in full agreement with V. P. Baillargeon, J. K. Stille, *J. Am. Chem. Soc.* **1986**, *108*, 452–461.

Methyl-4-vinylbenzoate

Synthesis following the general procedure for styrene synthesis in a Wittig reaction.



C₁₀H₁₀O₂
162.19 g/mol

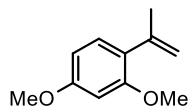
Appearance	colorless solid
Yield	234 mg, 1.44 mmol, 21%
TLC	R _f = 0.11 (SiO ₂ , <i>n</i> -pentane)
¹H-NMR	(400 MHz, CDCl ₃) δ 8.00 (d, <i>J</i> = 8.4 Hz, 2H), 7.46 (d, <i>J</i> = 8.4 Hz, 2H), 6.75 (dd, <i>J</i> = 17.6, 10.9 Hz, 1H), 5.86 (d, <i>J</i> = 17.6 Hz, 1H), 5.38 (d, <i>J</i> = 10.9 Hz, 1H), 3.91 (s, 3H).
¹³C-NMR	(101 MHz, CDCl ₃) δ 166.9, 141.9, 136.0, 129.9, 129.3, 126.1, 116.5, 52.1.

GC-MS $t_R = 6.51$ min, (EI, 70 eV): $m/z = 197$ [M⁺], 183, 171, 156, 115, 102, 91, 75, 63, 51.

Analytical data were in full agreement with A. Yokoyama, T. Maruyama, K. Tagami, H. Masu, K. Katagiri, I. Azumaya, T. Yokozawa, *Org. Lett.* **2008**, *10*, 3207–3210.

2,4-Dimethoxy- α -methylstyrene

Synthesis following the general procedure for styrene synthesis in a Wittig reaction.



C₁₁H₁₄O₂

178.23 g/mol

Appearance

pale yellow solid

Yield

570 mg, 3.20 mmol (64%)

¹H-NMR

(300 MHz, CDCl₃) δ 7.12 (m, 1H), 6.30 – 6.15 (m, 2H), 5.10 (m, 1H), 5.05 (m, 1H), 3.81 (s, 3H), 3.80 (s, 3H), 2.10 (s, 3H).

¹³C-NMR

(75 MHz, CDCl₃) δ 160.07, 157.69, 143.73, 129.72, 114.55, 103.95, 98.72, 55.41, 23.42.

GC-MS

$t_R = 7.23$ min, (EI, 70 eV): $m/z = 178$ [M⁺], 163, 148, 135, 120, 115, 105, 91, 77, 69, 63, 51.

HRMS

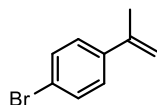
(EI, m/z): found 178.0996 [M⁺] (calculated 178.0994).

IR

(ATR-film) in [cm⁻¹] 2969 (w), 2955 (w), 2835 (w), 1737 (m), 1607 (s), 1578 (m), 1502 (s), 1463 (m), 1413 (w), 1371 (w), 1298 (m), 1257 (m), 1243 (m), 1206 (s), 1158 (s), 1102 (m), 1035 (s), 936 (w), 912 (w), 832 (m), 800 (m), 733 (m), 681 (w), 635 (m), 607 (w), 505 (m).

4-Bromo- α -methylstyrene

Synthesis following the general procedure for styrene synthesis in a Wittig reaction.



C₉H₉Br

197.08 g/mol

Appearance

colorless oil

Yield

1.06 g, 5.39 mmol, 77%

TLC

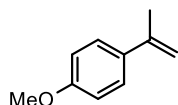
$R_f = 0.59$ (SiO₂, *n*-pentane)

¹H-NMR	(400 MHz, CDCl ₃) δ 7.50-7.35 (m, 2H), 7.42-7.29 (m, 2H), 5.36 (s, 1H), 5.10 (s, 1H), 2.12 (s, 3H).
¹³C-NMR	(101 MHz, CDCl ₃) δ 142.2, 140.1, 131.3, 127.2, 121.4, 113.1, 21.7.
GC-MS	<i>t</i> _R = 6.51 min, (EI, 70 eV): <i>m/z</i> = 197 [M ⁺], 183, 171, 156, 115, 102, 91, 75, 63, 51.

Analytical data were in full agreement with T. Taniguchi, A. Yajima, H. Ishibashi, *Adv. Synth. Catal.* **2011**, 353, 2643–2647.

4-Methoxy-*α*-methylstyrene

Synthesis following the general procedure for styrene synthesis in a Wittig reaction.



C₁₀H₁₂O

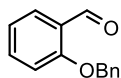
148.20 g/mol

Appearance	colorless liquid
Yield	1.04 g, 7.02 mmol (35%)
TLC	<i>R</i> _f = 0.25 (SiO ₂ , <i>n</i> -pentane)
¹H-NMR	(300 MHz, CDCl ₃) δ 7.42 (m, 2H), 6.87 (m, 2H), 5.29 (m, 1H), 4.99 (m, 1H), 3.82 (s, 3H), 2.13 (s, 3H).
¹³C-NMR	(75 MHz, CDCl ₃) δ 159.05, 142.56, 133.74, 126.60, 113.54, 110.68, 55.30, 21.94.
GC-MS	<i>t</i> _R = 6.39 min, (EI, 70 eV): <i>m/z</i> = 148 [M ⁺], 127, 133, 115, 105, 89, 77, 63, 51.

Analytical data were in full agreement with A. Fryszkowska, K. Fisher, J. M. Gardiner, G. M. Stephens, *J. Org. Chem.* **2008**, 73, 4295-4298.

2-(Benzyloxy)benzaldehyde

Synthesis following the procedure by S. K. Das, G. Panda, *Tetrahedron* **2008**, 19, 4162-4173.



C₁₄H₁₂O₂

212.24 g/mol

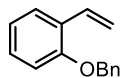
Appearance	yellowish liquid
Yield	943 mg, 4.40 mmol (44%)
TLC	<i>R</i> _f = 0.31 (SiO ₂ , hexanes/ethyl acetate = 9/1)

¹H-NMR	(300 MHz, CDCl ₃) δ 10.57 (s, 1H), 7.87 (dd, <i>J</i> = 8.0, 1.8 Hz, 1H), 7.58 – 7.50 (m, 1H), 7.48 – 7.31 (m, 5H), 7.09 – 7.01 (m, 2H), 5.20 (s, 2H).
¹³C-NMR	(75 MHz, CDCl ₃) δ 189.77, 161.05, 136.08, 135.94, 128.75, 128.46, 128.30, 127.31, 125.16, 121.02, 113.02, 70.45.
GC-MS	<i>t</i> _R = 9.74 min, (EI, 70 eV): <i>m/z</i> = 212 [M ⁺], 183, 121, 91, 77, 65, 51.

Analytical data were in full agreement with S. K. Das, G. Panda, *Tetrahedron*, **2008**, *19*, 4162-4173.

1-(Benzyloxy)-2-vinylbenzene

Synthesis following the general procedure for styrene synthesis in a Wittig reaction.



C₁₅H₁₄O

210.27 g/mol

Appearance	colorless oil
Yield	800 mg, 3.81 mmol (87%)
TLC	<i>R</i> _f = 0.21 (SiO ₂ , <i>n</i> -pentane)
¹H-NMR	(300 MHz, CDCl ₃) δ 7.54 (dd, <i>J</i> = 7.6, 1.7 Hz, 1H), 7.50 – 7.34 (m, 5H), 7.25 – 7.10 (m, 2H), 6.97 (m, 2H), 5.79 (dd, <i>J</i> = 17.8, 1.5 Hz, 1H), 5.28 (dd, <i>J</i> = 11.2, 1.5 Hz, 1H), 5.12 (s, 2H).
¹³C-NMR	(75 MHz, CDCl ₃) δ 155.88, 137.16, 131.65, 128.85, 128.59, 127.91, 127.33, 127.11, 126.53, 120.99, 114.49, 112.43, 70.27.
GC-MS	<i>t</i> _R = 9.13 min, (EI, 70 eV): <i>m/z</i> 210 [M ⁺], 193, 119, 91, 77, 65, 51.

Analytical data were in full agreement with M. Barbasiewicz, M. Bieniek, A. Michrowska, A. Szadkowska, A. Makal, K. Wozniak, K. Grella, *Adv. Synth. Catal.* **2007**, *349*, 193-203.

(1-cyclopropylvinyl)benzene

Synthesis following the general procedure for styrene synthesis in a Wittig reaction.

C₁₁H₁₂



144.22 g/mol

Appearance

colorless liquid

Yield

1.27 g, 8.8 mmol (80%)

TLC

$R_f = 0.53$ (SiO₂, hexanes)

¹H-NMR

(300 MHz, CDCl₃) $\delta = 7.67 - 7.57$ (m, 2H), 7.42 – 7.26 (m, 3H), 5.30 (d, $J=1.0$, 1H), 4.95 (t, $J=1.2$, 1H), 1.67 (tt, $J=8.3, 5.4, 1.2$, 1H), 0.92 – 0.79 (m, 2H), 0.61 (ddd, $J=6.4, 5.4, 4.1$, 2H).

¹³C-NMR

(75 MHz, CDCl₃) δ 149.47, 141.75, 128.28, 127.58, 126.25, 109.15, 77.58, 77.16, 77.16, 76.74, 15.78, 6.83.

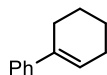
GC-MS

$t_R = 6.31$ min, (EI, 70 eV): $m/z = 144$ [M⁺], 129, 115, 103, 91, 77, 63, 51.

Analytical data were in full agreement with C. Chatalova-Sazepin, Q. Wang, G. M. Sammis, J. Zhu, *Angew. Chem. Int. Ed.* **2015**, *54*, 5443–5446.

1-Phenylcyclohexene

A solution of phenylmagnesiumbromide in THF (1 M, 50.0 mmol, 50.0 mL) was added dropwise to a solution of cyclohexanone (30.0 mmol, 3.20 mL) in THF (30 mL) at 0 °C. The reaction mixture was allowed to gain room temperature while stirring for 2 h. Then, the reaction mixture was cooled to 0 °C and quenched with aqueous HCl (5%, 25 mL) and extracted with Et₂O (3 × 15 mL). The combined organic layers were dried (MgSO₄), concentrated and dissolved in toluene (50 mL). After addition of a tip of a spatula *p*-toluenesulfonicacid the reaction mixture was heated under reflux for 12 h. The reaction mixture was concentrated and subjected to silica gel flash chromatography (*n*-pentane).



C₁₂H₁₄

158.24 g/mol

Appearance

colorless liquid

Yield

1.14 g, 7.22 mmol (24%)

TLC

$R_f = 0.36$ (SiO₂, *n*-pentane)

¹H-NMR

(300 MHz, CDCl₃) δ 7.49–7.38 (m, 2H), 7.34 (m, 2H), 7.27–7.19 (m, 1H), 6.15 (m, 1H), 2.44 (m, 2H), 2.30–2.14 (m, 2H), 1.90–1.75 (m, 2H), 1.75–1.61 (m, 2H).

¹³C-NMR

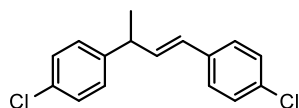
(101 MHz, CDCl₃) δ 142.8, 136.7, 128.3, 126.6, 125.0, 124.8, 27.5, 26.0, 23.2, 22.3.

GC-MS $t_R = 7.35$ min, (EI, 70 eV): $m/z = 158$ [M⁺], 143, 129, 113, 91, 77, 51.

Analytical data were in full agreement with M. A. Reichle, B. Breit, *Angew. Chem. Int. Ed.* **2012**, *51*, 5730–5734.

1,3-Bis-(4-chloro-phenyl)-1-butene

Synthesis following the procedure described by J. R. Cabrero-Antonino, A. Leyva-Pérez, A. Corma, *Adv. Synth. Catal.* **2010**, *352*, 1571–1576.



C₁₆H₁₄Cl₂

277.19 g/mol

Appearance

yellowish liquid

Yield

470 mg, 1.70 mmol, 34%

TLC

$R_f = 0.46$ (SiO₂, *n*-pentane)

¹H-NMR

(400 MHz, CDCl₃) δ 7.33–7.11 (m, 8H), 6.41–6.21 (m, 2H), 3.61 (m, 1H), 1.44 (d, $J = 7.0$ Hz, 3H).

¹³C-NMR

(101 MHz, CDCl₃) δ 145.5, 140.6, 131.7, 131.5, 129.7, 128.6, 128.4, 128.4, 39.7, 38.9, 33.2, 22.5.

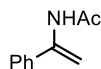
GC-MS

$t_R = 10.97$ min, (EI, 70 eV): $m/z = 276$ [M⁺], 241, 212, 191, 149, 125, 103, 91, 77, 65, 51.

Analytical data were in full agreement with J. R. Cabrero-Antonino, A. Leyva-Pérez, A. Corma, *Adv. Synth. Catal.* **2010**, *352*, 1571–1576.

N-(1-Phenylvinyl)acetamide

Synthesis following the procedure described by J. T. Reeves, Z. Tan, Z. S. Han, G. Li, Y. Zhang, Y. Xu, D. C. Reeves, N. C. Gonnella, S. Ma, H. Lee, B. Z. Lu, C. H. Senanayake, *Angew. Chem. Int. Ed.* **2012**, *51*, 1400–1404.



C₁₀H₁₁NO

161.20 g/mol

Appearance

colorless solid

Yield

235 mg, 1.48 mmol (15%)

¹H-NMR

(300 MHz, DMSO-*d*₆) δ 9.34 (s, 1H), 7.49 – 7.31 (m, 5H), 5.62 (s, 1H), 4.98 (s, 1H), 2.01 (s, 3H).

¹³C-NMR

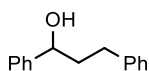
(75 MHz, DMSO-*d*₆) δ 169.04, 141.36, 140.94, 137.93, 128.18, 126.13, 101.78, 23.64.

GC-MS $t_R = 7.87$ min, (EI, 70 eV): $m/z = 161$ [M⁺], 146, 132, 119, 104, 77, 63, 51.

Analytical data were in full agreement with J. T. Reeves, Z. Tan, Z. S. Han, G. Li, Y. Zhang, Y. Xu, D. C. Reeves, N. C. Gonnella, S. Ma, H. Lee *et al.*, *Angew. Chem. Int. Ed.* **2012**, *51*, 1400–1404.

1,3-diphenylpropan-1-ol

A round-bottom flask was charged with benzaldehyde (35.0 mL, 3.61 g) in THF (40 mL) under inert atmosphere and cooled to 0 °C. A freshly prepared solution of benzyl magnesium bromide in THF (40 mmol; 0.5 M) was added dropwise. The solution was allowed to warm to room temperature and was stirred overnight. After 18 h an aqueous solution of hydrochloric acid (1 M, 100 mL) was added slowly. The crude product was extracted with diethyl ether Et₂O (3 × 50 mL) and the combined organic layers were dried over Na₂SO₄ and subjected to silica gel flash chromatography (hexanes/ethyl acetate 9/1).



C₁₅H₁₆O

212.29 g/mol

Appearance

yellowish oil

Yield

4.43 g, 20.9 mmol (60%)

TLC

$R_f = 0.14$ (SiO₂, hexanes/ethyl acetate = 9/1)

¹H-NMR

(300 MHz, CDCl₃) δ 7.48–7.33 (m, 7H), 7.27 (dd, $J = 7.7$, 1.4 Hz, 3H), 4.70 (dd, $J = 7.7$, 5.6 Hz, 1H), 2.88 (s, 1H), 2.76 (m, 2H), 2.31–1.95 (m, 2H).

¹³C-NMR

(75 MHz, CDCl₃) δ 144.70, 141.97, 128.61, 128.53, 127.71, 126.14, 125.99, 73.88, 40.56, 32.16.

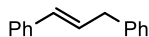
GC-MS

$t_R = 9.57$ min, (EI, 70 eV): $m/z = 212$ [M⁺], 194, 179, 165, 152, 133, 116, 107, 91, 79, 65, 51.

Analytical data were in full agreement with R. Martínez, D. J. Ramón, M. Yus, *Tetrahedron* **2006**, *62*, 8988–9001.

(*E*)-1,3-Diphenylpropene

A round-bottom flask was charged with 1,3-diphenylpropan-1-ol (7.50 mmol, 1.59 g) and a tip of a spatula of *p*-toluenesulfonic acid in toluene (50 mL). The solution was stirred under reflux for 20 h. After cooling to room temperature the reaction mixture was extracted with Et₂O (3 × 25 mL). The combined organic layers were washed with brine (25 mL), dried over Na₂SO₄ and subjected to silica gel flash chromatography (*n*-pentane).



C₁₅H₁₄

194.28 g/mol

Appearance

colorless oil

Yield

1.25 g, 6.44 mmol (86%)

TLC

R_f = 0.33 (SiO₂, *n*-pentane)

¹H-NMR

(300 MHz, CDCl₃) δ 7.47 – 7.27 (m, 10H), 6.53 (d, *J* = 15.9 Hz, 1H), 6.43 (dt, *J* = 15.9, 6.4 Hz, 1H), 3.62 (d, *J* = 6.3 Hz, 2H).

¹³C-NMR

(75 MHz, CDCl₃) δ 140.25, 137.55, 131.15, 129.32, 128.78, 128.60, 127.21, 126.29, 126.22, 39.45.

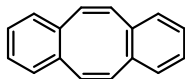
GC-MS

t_R = 9.01 min, (EI, 70 eV): *m/z* = 194 [M⁺], 179, 165, 152, 115, 103, 91, 78, 65, 51.

Analytical data were in full agreement with E. Alacid, C. Nájera, *Org. Lett.* **2008**, *10*, 5011–5014.

Dibenzo[*a,e*]cyclooctatetraene (dct)

Synthesis following the procedure described by G. Franck, M. Brill, G. Helmchen, *J. Org. Chem.* **2012**, *89*, 55–65.



C₁₆H₁₂

204.27 g/mol

Appearance

colorless solid

Yield

912 mg, 4.46 mmol (47%)

¹H-NMR

(300 MHz, CDCl₃): δ = 7.19–7.13 (m, 4H), 7.10–7.02 (m, 4H), 6.76 (s, 4H).

¹³C-NMR

(75 MHz, CDCl₃): δ = 137.1, 133.3, 129.1, 126.8.

GC-MS

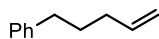
t_R = 9.35 min, (EI, 70 eV): *m/z* = 204 [M⁺].

Analytical data were in full agreement with G. Franck, M. Brill, G. Helmchen, *J. Org. Chem.* **2012**, *89*, 55–65.

Pent-4-en-1-ylbenzene

A flask was equipped with 2-phenylethylbromide (3.40 mmol, 629 mg) and dissolved in THF (4 mL) under inert atmosphere. A freshly prepared solution of allylmagnesiumchloride in THF (4 mL, 2 M) was added dropwise and the resulting

reaction mixture was stirred for 1 h under reflux. After cooling to room temperature, the reaction mixture was quenched with a saturated aqueous solution of NH₄Cl (10 mL) and extracted with CH₂Cl₂ (3 × 10 mL). The combined organic layers were dried over Na₂SO₄, concentrated and subjected to silica gel flash chromatography (hexanes/ethyl acetate = 98/2).



C₁₁H₁₄

146.23 g/mol

Appearance

colorless oil

Yield

348 mg, 2.38 mmol (70%)

¹H-NMR

(300 MHz, CDCl₃) δ 7.30 – 7.13 (m, 5H), 5.82 (ddt, *J* = 16.9, 10.2, 6.6 Hz, 1H), 5.06 – 4.93 (m, 2H), 2.65 – 2.57 (m, 2H), 2.12 – 2.04 (m, 2H), 1.77 – 1.65 (m, 2H).

¹³C-NMR

(75 MHz, CDCl₃) δ 141.42, 137.57, 127.42, 127.23, 124.64, 113.67, 34.28, 32.26, 29.59.

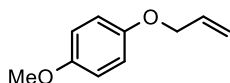
GC-MS

t_R = 5.77min, (EI, 70 eV): *m/z* = 146 [M⁺], 131, 117, 105, 92, 77, 65, 55, 51.

Analytical data were in full agreement with J. C. Anderson, R. H. Munday, *J. Org. Chem.* **2004**, *69*, 8971–8974.

1-(Allyloxy)-4-methoxybenzene

Synthesis following the procedure described by H. B. Mereyala, S. R. Gurralla, S. K. Mohan, *Tetrahedron*, **1999**, *55*, 11331-11342.



C₁₀H₁₂O₂

164.20 g/mol

Appearance

colorless liquid

Yield

1.41g, 8.59 mmol (86%)

TLC

R_f = 0.27 (SiO₂, PE/EE = 95/5)

¹H-NMR

(300 MHz, CDCl₃) δ 6.91 – 6.79 (m, 4H), 6.06 (ddt, *J* = 17.3, 10.6, 5.3 Hz, 1H), 5.41 (m, 1H), 5.28 (m, 1H), 4.49 (m, 2H), 3.77 (s, 3H).

¹³C-NMR

(75 MHz, CDCl₃) δ 153.89, 152.74, 133.62, 117.55, 115.71, 114.60, 69.51, 55.72.

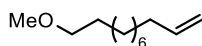
GC-MS

t_R = 6.88 min, (EI, 70 eV): *m/z* = 164 [M⁺], 123, 109, 95, 80, 63, 51.

Analytical data were in full agreement with A. B. Naidu, E. A. Jaseer and G.Sekar *J. Org. Chem.* **2009**, *74*, 3675–3679.

11-Methoxyundec-1-ene

A 100 mL flask was charged with NaH-suspension in paraffine (60%, 22.5 mmol, 0.90 g) in THF (30 mL) and cooled to 0 °C. After dropwise addition of 11-undec-1-enol (15 mmol, 2.55 g) the reaction mixture was allowed to gain room temperature while stirring for 2 h. Methyl iodide (15 mmol, 2.55 g) was added and the reaction mixture was heated under reflux for 3 h. Then, the reaction mixture was quenched with an aqueous saturated solution of NH₄Cl (5 mL) and H₂O (5 mL) and extracted with Et₂O (3 × 10 mL). The combined organic layers were dried (Na₂SO₄), concentrated and subjected to silica gel flash chromatography (hexanes/ethyl acetate = 98/2).



C₁₂H₂₄O

184.32 g/mol

Appearance

colorless liquid

Yield

2.48 g, 13.5 mmol, 90%

TLC

R_f = 0.36 (SiO₂, hexanes/ethyl acetate = 98/2)

¹H-NMR

(400 MHz, CDCl₃) δ 5.81 (ddt, *J* = 17.1, 10.2, 6.7 Hz, 1H), 4.99 (ddd, *J* = 17.1, 3.7, 1.6 Hz, 1H), 4.93 (ddt, *J* = 10.2, 2.3, 1.2 Hz, 1H), 3.36 (m, 2H), 3.33 (s, 3H), 2.08 – 1.99 (m, 2H), 1.61 – 1.51 (m, 2H), 1.36 – 1.24 (m, 11H).

¹³C-NMR

(101 MHz, CDCl₃) δ 139.25, 114.10, 72.99, 58.53, 33.81, 29.65, 29.54, 29.49, 29.43, 29.13, 28.94, 26.14.

GC-MS

t_R = 6.73 min, (EI, 70 eV): *m/z* = 184 [M⁺], 169, 152, 137, 124, 109, 95, 82, 67, 55.

HRMS

(CI, *m/z*): found 184.1829 [M⁺] (calculated 184.1827).

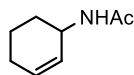
FT-IR

(ATR-film) in [cm⁻¹] 3077 (w), 2978 (w), 2924 (s), 2854 (s), 1641 (m), 1461 (m), 1387 (w), 1196 (w), 1119 (s), 992 (m), 908 (s), 722 (m), 635 (w).

N-(cyclohex-2-en-1-yl)acetamide

A mixture of 3-bromocyclohexene (9.3 mmol, 1.50 g) in CCl₄ (15 mL) and sodiumazide (30.9 mmol, 2.00 g) in H₂O (15 mL) was stirred at room temperature for 2 days. The aqueous phase was extracted with CH₂Cl₂ (2 × 25 mL) and ethyl acetate (1 × 25 mL). The

combined organic layers were dried (Na₂SO₄), concentrated and diluted in THF (6 mL). After the addition of triphenylphosphine (16.8 mmol, 4.40 g) the reaction mixture was stirred for 2 h. Then, aqueous NaOH (1 M, 40 mL) was added, the reaction mixture was stirred for 18 h, extracted with ethyl acetate (1 × 50 mL) and the organic layer was extracted with aqueous HCl (1 M, 3 × 15 mL). The combined aqueous layers were concentrated and suspended in CH₂Cl₂. After the addition of Et₃N (27.9 mmol, 3.87 mL), 4-(dimethylamino)-pyridine (0.9 mmol, 113.6 mg) and acetyl chloride (10.2 mmol, 0.73 mL) the reaction mixture was stirred at room temperature for 3 h. The reaction mixture was washed with aqueous saturated NaCl, dried (Na₂SO₄), concentrated and subjected to silica gel flash chromatography (hexanes/ethyl acetate = 1/4).



C₈H₁₃NO

139.19 g/mol

Appearance

colorless solid

Yield

643 mg, 4.60 mmol, 50%

TLC

R_f = 0.2 (SiO₂, hexanes/ethyl acetate = 1/4)

¹H-NMR

(400 MHz, CDCl₃) δ 5.95–5.77 (m, 1H), 5.74–5.32 (m, 2H), 4.46 (m, 1H), 1.99 (m, 2H), 1.96 (s, 3H), 1.93–1.81 (m, 1H), 1.71–1.58 (m, 2H), 1.58–1.42 (m, 1H)

¹³C-NMR

(101 MHz, CDCl₃) δ 169.2, 130.9, 127.7, 44.7, 29.5, 24.8, 23.5, 19.7.

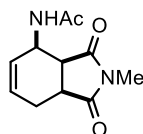
GC-MS

t_R = 6.68 min, (EI, 70 eV): m/z = 139 [M⁺], 111, 97, 79, 69, 60, 54.

Analytical data were in full agreement with Y. Leblanc, R. Zamboni, M. A. Bernstein, *J. Org. Chem.* **1991**, 56, 1971–1972.

N-Methyl-3-acetamido-1,2,3,6-tetrahydrophthalimide

Synthesis following the procedure described by R. Fichtler, J.-M. Neudörfel, A. Jacobi von Wangelin, *Org. Biomol. Chem.* **2011**, 9, 7224–7236.



C₁₁H₁₄N₂O₃

222.24 g/mol

Appearance

colorless solid

Yield

488 mg, 2.2 mmol (15%)

TLC

R_f = 0.13 (SiO₂, hexanes/ethyl acetate = 1/4)

¹H-NMR	(300 MHz, CDCl ₃) δ 7.27 (s, 1H), 5.86 (m, 1H), 5.72 (m, 1H), 4.81–4.61 (m, 1H), 3.19 (m, 2H), 2.94 (s, 3H), 2.71 (m, 1H), 2.21 (m, 1H), 2.08 (s, 3H).
¹³C-NMR	(75 MHz, CDCl ₃) δ 179.3, 179.2, 169.9, 132.9, 127.4, 45.2, 42.5, 38.8, 25.0, 24.1, 23.5.
GC-MS	<i>t</i> _R = 9.76 min, (EI, 70 eV): <i>m/z</i> = 222 [M ⁺], 204, 179, 165, 151, 136, 120, 105, 94, 79, 69, 58.

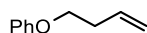
Analytical data were in full agreement with D. Strübing, H. Neumann, A. Jacobi von Wangelin, S. Klaus, S. Hübner, M. Beller, *Tetrahedron* **2006**, 62, 10962–10967.

General procedure for phenylalkenylether synthesis

A flask was charged with a phenol derivative (15.0 mmol) and triphenylphosphine (15.0 mmol, 3.93 g) under an inert atmosphere. After solvation in dry THF (25 mL) 3-buten-1-ol (15.0 mmol, 1.08 g) was added and the stirred solution was cooled by an external ice/water bath. Diisopropyl azodicarboxylate (16.5 mmol, 3.33 g) was added dropwise and the solution was allowed to come to room temperature and stirred for additional 18 h. After evaporation of the solvent under reduced pressure, the residue was purified by silica gel flash chromatography (hexanes).

(But-3-en-1-yloxy)benzene

Synthesis following the general procedure for phenylalkenylether synthesis.



C₁₀H₁₂O

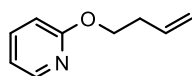
148.20 g/mol

Appearance	colorless liquid
Yield	1.14 g, 7.69 mmol (51%)
TLC	<i>R</i> _f = 0.26 (SiO ₂ , hexanes)
¹H-NMR	(300 MHz, CDCl ₃) δ 7.37 – 7.28 (m, 2H), 7.03 – 6.90 (m, 3H), 5.96 (m, 1H), 5.27 – 5.11 (m, 2H), 4.05 (t, <i>J</i> = 6.7 Hz, 2H), 2.59 (m, 2H).
¹³C-NMR	(75 MHz, CDCl ₃) δ 158.94, 134.56, 129.49, 120.73, 117.05, 114.61, 67.12, 33.74.
GC-MS	<i>t</i> _R = 5.93 min, (EI, 70 eV): <i>m/z</i> = 148 [M ⁺], 120, 107, 94, 77, 65, 55.

Analytical data were in full agreement with J. Niu, H. Zhou, Z. Li, J. Xu, S. Hu, *J. Org. Chem.* **2008**, 73, 7814–7817.

2-(but-3-en-1-yloxy)pyridine

Synthesis following the general procedure for phenylalkenylether synthesis.



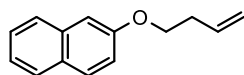
C₉H₁₁NO

198.26 g/mol

Appearance	yellowish liquid
Yield	949 mg, 6.36 mmol (42%)
TLC	R _f = 0.26 (SiO ₂ , hexanes/Et ₂ O = 30/1)
¹H-NMR	(300 MHz, CDCl ₃) δ 8.15 (m, 1H), 7.56 (m, 1H), 6.85 (m, 1H), 6.73 (m, 1H), 5.91 (m, 1H), 5.16 (m, 1H), 5.09 (m, 1H), 4.35 (m, 2H), 2.54 (m, 2H).
¹³C-NMR	(75 MHz, CDCl ₃) δ 163.77, 146.76, 138.64, 134.72, 116.84, 116.64, 111.19, 65.09, 33.47.
GC-MS	t _R = 5.70 min, (EI, 70 eV): m/z = 149 [M ⁺], 132, 120, 108, 95, 78, 67, 51.
HRMS	(APCI, m/z): found 150.0917 [M+H ⁺] (calculated 150.0913).
FT-IR	(ATR-film) in [cm ⁻¹] 3079 (w), 3018 (w), 2945 (w), 1595 (m), 1571 (m), 1468 (m), 1433 (m), 1312 (w), 1288 (m), 1272 (w), 1252 (w), 1143 (w), 1043 (w), 1020 (w), 989 (w), 912 (w), 779 (m), 548 (m), 533 (m), 495 (m).

2-(But-3-en-1-yloxy)naphthalene

Synthesis following the general procedure for phenylalkenylether synthesis.



C₁₄H₁₄O

198.26 g/mol

Appearance	yellowish liquid
Yield	2.50 g, 12.61 mmol (84%)
TLC	R _f = 0.32 (SiO ₂ , hexanes)
¹H-NMR	(300 MHz, CDCl ₃) δ 7.81 – 7.69 (m, 3H), 7.44 (ddd, J = 8.2, 6.9, 1.3 Hz, 1H), 7.34 (ddd, J = 8.1, 6.9, 1.3 Hz, 1H), 7.20 – 7.12 (m, 2H), 5.97 (ddt, J = 17.0, 10.2, 6.7 Hz, 1H), 5.22 (dq, J = 17.0, 1.6 Hz, 1H), 5.15 (ddd, J = 10.2, 3.0, 1.2 Hz, 1H), 4.15 (t, J = 6.7 Hz, 2H), 2.63 (m, 2H).

¹³C-NMR	(75 MHz, CDCl ₃) δ 156.88, 134.57, 134.50, 129.39, 128.97, 127.66, 126.74, 126.35, 123.58, 119.01, 117.12, 106.67, 67.21, 33.65.
GC-MS	<i>t</i> _R = 8.99 min, (EI, 70 eV): <i>m/z</i> = 198 [M ⁺], 183, 170, 157, 143, 126, 114, 101, 89, 77, 63, 53.

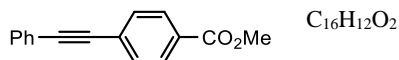
Analytical data were in full agreement with B. Branchi, C. Galli, P. Gentili, *Eur. J. Org. Chem.* **2002**, 2002, 2844–2854.

General procedure for alkyne synthesis by Sonogashira coupling

A 50 mL *Schlenk* tube with a screw cap was equipped with a stirring bar, charged with CuI (0.14 mmol, 27.0 mg), (0.04 mmol, 25.2 mg) Pd(Cl)₂(PPh₃)₂ and 3.59 mmol of the substituted iodo-benzene, evacuated three times and purged with nitrogen. Then 4 mL THF and 4 mL Et₃N were added. Phenylacetylene (3.59 mmol, 395 μL) was added slowly via syringe and the reaction mixture was stirred at room temperature for 15 h. Then, CH₂Cl₂ (25 mL) and aqueous HCl (25 mL, 1 M) were added and the reaction mixture was extracted with CH₂Cl₂ (2 × 25 mL). The combined organic layers were dried (Na₂SO₄) and the solvent removed by vacuum evaporation. The residue was then purified by silica gel flash chromatography (hexanes)

Methyl 4-(phenylethynyl)benzoate

Synthesis following the general procedure for alkyne synthesis by Sonogashira coupling.



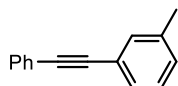
236.27 g/mol

Appearance	pale yellow solid
Yield	1.35 g, 5.71 mmol (82%)
TLC	<i>R</i> _f = 0.38 (SiO ₂ , hexanes/ethyl acetate = 9/1)
¹H-NMR	(300 MHz, CDCl ₃) δ 8.02 (m, 2H), 7.60 (m, 1H), 7.59 – 7.51 (m, 3H), 7.41 – 7.32 (m, 3H), 3.92 (s, 3H).
¹³C-NMR	(75 MHz, CDCl ₃) δ 166.57, 131.76, 131.53, 129.55, 129.47, 128.80, 128.47, 128.02, 122.71, 92.40, 88.67, 52.26.
GC-MS	<i>t</i> _R = 10.59 min, (EI, 70 eV): <i>m/z</i> = 236 [M ⁺], 205, 176, 151, 126, 102, 91, 76, 63, 51.

Analytical data were in full agreement with T. Schabel, C. Belger, B. Plietker, *Org. Lett.* **2013**, *15*, 2858–2861.

1-Methyl-3-(phenylethynyl)benzene

Synthesis following the general procedure for alkyne synthesis by Sonogashira coupling.



C₁₅H₁₂

192.26 g/mol

Appearance

colorless solid

Yield

1.76 g, 9.14 mmol (91%)

TLC

R_f = 0.55 (SiO₂, *n*-pentane)

¹H-NMR

(300 MHz, CDCl₃) δ 7.57 – 7.48 (m, 2H), 7.40 – 7.31 (m, 5H), 7.24 (t, *J* = 7.5 Hz, 1H), 7.15 (d, *J* = 7.6 Hz, 1H), 2.36 (s, 3H).

¹³C-NMR

(75 MHz, CDCl₃) δ 138.04, 132.20, 131.61, 129.19, 128.70, 128.35, 128.26, 128.19, 77.45, 77.03, 76.61, 21.27.

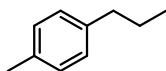
GC-MS

*t*_R = 9.23 min, (EI, 70 eV): *m/z* = 192 [M⁺], 176, 165, 152, 139, 126, 115, 95, 74, 63, 51.

Analytical data were in full agreement with H. Kim, P. H. Lee, *Adv. Synth. Catal.* **2009**, *351*, 2827–2832.

2.5.5 Hydrogenation products

1-Methyl-4-propylbenzene



C₁₀H₁₄

134.22 g/mol

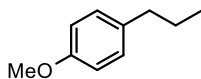
¹H-NMR (300 MHz, CDCl₃) δ 7.07 (s, 4H), 2.54 (m, 2H), 2.31 (s, 3H), 1.61 (m, 2H), 0.93 (m, 3H).

¹³C-NMR (75 MHz, CDCl₃) δ 139.55, 134.92, 128.83, 128.28, 37.51, 37.58, 24.65, 20.94, 13.80.

GC-MS *t*_R = 5.09 min, (EI, 70 eV): *m/z* = 134 [M⁺].

Analytical data were in full agreement with N. Sakai, K. Nagasawa, R. Ikeda, Y. Nakaike, T. Konakahara, *Tetrahedron Lett.* **2011**, 52, 3133-3136.

1-Methoxy-4-propylbenzene



C₁₀H₁₄O

150.22 g/mol

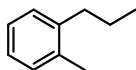
¹H-NMR (300 MHz, CDCl₃) δ 7.08 (d, *J* = 8.1 Hz, 2H), 6.81 (d, *J* = 8.2 Hz, 2H), 3.76 (s, 3H), 2.51 (t, *J* = 7.6 Hz, 2H), 1.71-1.46 (m, 2H), 0.92 (t, *J* = 7.3 Hz, 3H)

¹³C-NMR (75 MHz, CDCl₃) δ 157.58, 134.71, 129.24, 113.55, 55.12, 37.42, 37.09, 24.75, 13.71.

GC-MS *t*_R = 5.07 min, (EI, 70 eV): *m/z* = 150 [M⁺].

Analytical data were in full agreement with A. Dhakshinamoorthy, A. Sharmila, K. Pitchumani, *Chem. Eur. J.* **2010**, 16, 1128-1132.

1-Methyl-2-propylbenzene



C₁₀H₁₄

134.22 g/mol

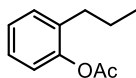
¹H-NMR (300 MHz, CDCl₃) δ 7.14-7.09 (m, 4H), 2.6-2.54 (m, 2H), 2.3 (s, 3H), 1.67-1.54 (m, 2H), 0.98 (t, 3H).

¹³C-NMR (75 MHz, CDCl₃) δ 140.86, 135.87, 130.03, 128.83, 125.76, 125.71, 35.39, 23.35, 19.28, 14.17.

GC-MS *t*_R = 5.18 min, (EI, 70 eV): *m/z* = 134 [M⁺].

Analytical data were in full agreement with X. Qian, L. N. Dawe, C. M. Kozak, *Dalton Trans.* **2011**, 40, 933-943.

2-Propylphenyl acetate



C₁₁H₁₄O₂

178.23 g/mol

¹H-NMR (300 MHz, CDCl₃) δ 7.18 (m, 3H), 7.00 (d, *J* = 7.5 Hz, 1H), 2.53–2.40 (t, 2H), 2.29 (s, 3H), 1.59 (m, 2H), 0.93 (t, *J* = 7.3 Hz, 3H).

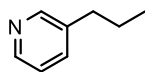
¹³C-NMR (75 MHz, CDCl₃) δ 169.64, 148.97, 134.27, 130.26, 126.89, 126.04, 122.22, 32.21, 23.10, 20.89, 14.00.

GC-MS *t*_R = 5.84 min, (EI, 70 eV): *m/z* = 178 [M⁺].

HRMS (EI, 70 eV): *m/z* = 178.009 +/- 5 ppm

FT-IR (ATR-film) in [cm⁻¹]: 3466 (w), (w), 3026 (w), 2958 (m), 2926 (m), 2866 (m), 1759 (s), 1636 (w), 1580 (w), 1487 (s), 1453 (s), 1367 (s), 1201 (s), 1179 (s), 1115 (s), 1036 (m), 1009 (m), 940 (m), 856 (w), 830 (m), 786 (m), 751 (s), 660 (m).

3-Propylpyridine



C₈H₁₁N

121.18 g/mol

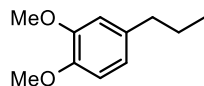
¹H-NMR (300 MHz, CDCl₃) δ 8.43 (d, *J* = 4.8 Hz, 2H), 7.49 (d, *J* = 7.5 Hz, 1H), 7.26-7.12 (m, 1H), 2.59 (t, *J* = 7.6 Hz, 2H), 1.78-1.32 (m, 2H), 0.95 (t, *J* = 7.3 Hz, 3H).

¹³C-NMR (75 MHz, CDCl₃) δ 149.87, 147.07, 137.69, 135.85, 123.34, 123.20, 34.99, 24.21, 23.98, 13.60.

GC-MS *t*_R = 4.20 min, (EI, 70 eV): *m/z* = 121 [M⁺].

Analytical data were in full agreement with A. Fischer, M. J. King, F. P. Robinson, *Can. J. Chem.* **1978**, 56, 3072-3077.

1,2-Dimethoxy-4-propylbenzene



C₁₁H₁₆O₂

180.24 g/mol

¹H-NMR

(300 MHz, CDCl₃) δ 6.83-6.64 (m, 3H), 3.87 (s, 3H), 3.85 (s, 3H), 2.53 (t, *J* = 7.8 Hz, 2H), 1.72-1.50 (m, 2H), 0.94 (t, *J* = 7.3 Hz, 3H).

¹³C-NMR

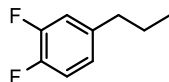
(75 MHz, CDCl₃) δ 148.72, 147.03, 135.36, 120.19, 111.79, 111.13, 55.81, 37.66, 24.77, 13.80.

GC-MS

*t*_R = 6.59 min, (EI, 70 eV): *m/z* = 180 [M⁺].

Analytical data were in full agreement with A. R. Katritzky, S. C. Jurczyk, M. Szajda, I. V. Shcherbakova, J. N. Lam, *Synthesis* **1994**, *1994*, 499-504.

1,2-Difluoro-4-propylbenzene



C₉H₁₀F₂

156.17 g/mol

¹H-NMR

(300 MHz, CDCl₃) δ 7.10-6.90 (m, 3H), 2.58 (m, 2H), 1.69-1.57 (m, 2H), 0.94 (m, 3H).

¹³C-NMR

(75 MHz, CDCl₃) δ 150.97, 147.71, 139.55, 124.13, 117.01, 116.75, 37.14, 24.35, 13.57.

GC-MS

*t*_R = 6.38 min, (EI, 70 eV): *m/z* = 156 [M⁺].

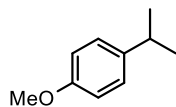
HRMS

(EI, 70 eV): *m/z* = 156.038 +/- 5 ppm

FT-IR

(ATR-film) in [cm⁻¹]: 3066 (w), 2920 (s), 2358 (w), 2326 (w), 1731 (w), 1604 (w), 1518 (s), 1487 (m), 1454 (m), 1376 (w), 1260 (s), 1220 (w), 1190 (w), 1116 (m), 1093 (m), 1020, 950 (w), 916 (w), 870 (m), 812 (s), 770 (m), 756(w).

1-Isopropyl-4-methoxybenzene



C₁₀H₁₄O

180.24 g/mol

¹H-NMR

(300 MHz, CDCl₃) δ 7.15 (m, 2H), 6.84 (m, 2H), 3.79 (s, 3H), 2.85 (hept, *J* = 6.9 Hz, 1H), 1.23 (d, *J* = 6.9 Hz, 6H).

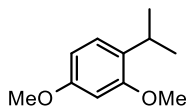
¹³C-NMR

(75 MHz, CDCl₃) δ 156.86, 141.06, 127.26, 113.77, 55.27, 33.28, 24.24.

GC-MS $t_R = 5.93$ min, (EI, 70 eV): $m/z = 150$ [M⁺], 120, 105, 91, 77, 65, 51.

Analytical data were in full agreement with Cahiez, G.; Foulgoc, L.; Moyeux, A. *Angew. Chem. Int. Ed.* **2009**, *48*, 2969–2972.

1-Isopropyl-2,4-dimethoxybenzene



C₁₁H₁₆O₂

180.25 g/mol

¹H-NMR (300 MHz, CDCl₃) δ 7.15 – 7.05 (m, 1H), 6.50 – 6.40 (m, 2H), 3.81 (s, 3H), 3.80 (s, 3H), 3.23 (hept, $J = 6.9$ Hz, 1H), 1.19 (d, $J = 6.9$ Hz, 6H).

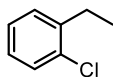
¹³C-NMR (75 MHz, CDCl₃) δ 158.67, 157.67, 129.52, 126.23, 103.81, 98.50, 55.33, 26.24, 22.89.

GC-MS $t_R = 7.11$ min, (EI, 70 eV): $m/z = 180$ [M⁺], 166, 150, 135, 121, 105, 91, 77, 65, 51.

HRMS (EI, m/z): found 180.1153 [M⁺] (calculated 180.1150).

FT-IR (ATR-film) in [cm⁻¹]: 2961 (m), 2870 (w), 2835 (w), 1612 (m), 1587 (m), 1504 (s), 1462 (m), 1446 (w), 1298 (m), 1257 (m), 1205 (s), 1151 (s), 1115 (s), 1096 (m), 1036 (s), 937 (w), 924 (w), 833 (m), 831 (m), 795 (m), 692 (w), 635 (w), 557 (w).

1-Chloro-2-ethylbenzene



C₈H₉Cl

140.61 g/mol

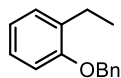
¹H-NMR (300 MHz, CDCl₃) δ 7.33 (d, $J = 7.7$ Hz, 2H), 7.25–7.07 (m, 2H), 2.76 (q, $J = 7.5$ Hz, 2H), 1.23 (t, $J = 7.5$ Hz, 3H).

¹³C-NMR (75 MHz, CDCl₃) δ 141.59, 133.77, 129.50, 129.33, 127.05, 126.79, 26.73, 14.03.

GC-MS $t_R = 4.77$ min, (EI, 70 eV): $m/z = 140$ [M⁺]

Analytical data were in full agreement with J. L. O'Connell, J. S. Simpson, P. G. Dumanski, G. W. Simpson, C. J. Easton, *Org. Biomol. Chem.* **2006**, *4*, 2716–2723.

1-Benzyloxy-2-ethylbenzene



C₁₅H₁₆O

212.29 g/mol

¹H-NMR

(300 MHz, CDCl₃) δ 7.51 – 7.30 (m, 5H), 7.19 (m, 2H), 6.98 – 6.88 (m, 2H), 5.11 (s, 2H), 2.74 (q, *J* = 7.5 Hz, 2H), 1.26 (t, *J* = 7.5 Hz, 3H).

¹³C-NMR

(75 MHz, CDCl₃) δ 156.49, 137.59, 133.03, 129.09, 128.55, 127.74, 127.09, 126.79, 120.77, 111.50, 69.77, 23.44, 14.26.

GC-MS

*t*_R = 8.86 min, (EI, 70 eV): *m/z* = 212 [M⁺], 122, 107, 91, 77, 65, 51.

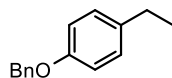
HRMS

(CI, *m/z*): found 212.1203 [M⁺] (calculated 212.1201).

FT-IR

(ATR-film) in [cm⁻¹] 3063 (w), 3035 (w), 2965 (m), 2928 (m), 2873 (w), 1601 (m), 1587 (m), 1491 (s), 1450 (s), 1379 (m), 1290 (w), 1236 (s), 1186 (w), 1125 (m), 1042 (m), 1020 (m), 851 (w), 747 (s), 733 (s), 694 (s), 624 (m), 462 (m).

1-Benzyloxy-4-ethylbenzene



C₁₅H₁₆O

212.29 g/mol

¹H-NMR

(300 MHz, CDCl₃) δ 7.51 – 7.30 (m, 5H), 7.18 – 7.11 (m, 2H), 6.97 – 6.89 (m, 2H), 5.07 (s, 2H), 2.62 (q, *J* = 7.6 Hz, 2H), 1.24 (t, *J* = 7.6 Hz, 3H).

¹³C-NMR

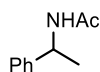
(75 MHz, CDCl₃) δ 156.89, 137.30, 136.72, 128.78, 128.60, 127.92, 127.52, 114.72, 70.08, 28.03, 15.93.

GC-MS

*t*_R = 9.17 min, (EI, 70 eV): *m/z* = 212 [M⁺], 122, 107, 91, 77, 65, 51.

Analytical data were in full agreement with C. Zhu, N. Yukimura, M. Yamane, *Organometallics* **2010**, *29*, 2098–2103.

***N*-(1-Phenylethyl)acetamide**



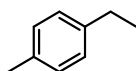
C₁₀H₁₃NO

163.22 g/mol

¹H-NMR	(300 MHz, CDCl ₃) δ 7.38 – 7.23 (m, 5H), 5.80 (s, 1H), 5.19 – 5.07 (m, 1H), 2.00 (s, 3H), 1.50 (d, J = 6.9 Hz, 3H).
¹³C-NMR	(75 MHz, CDCl ₃) δ 143.03, 128.73, 127.47, 126.23, 48.90, 23.47, 21.69.
GC-MS	<i>t</i> _R = 7.58 min, (EI, 70 eV): <i>m/z</i> = 163 [M ⁺], 148, 120, 106, 91, 77, 65, 51

Analytical data were in full agreement with B. V. Subba Reddy, N. Sivasankar Reddy, C. Madan, J. S. Yadav *Tetrahedron Lett.* **2010**, 51, 4827–4829.

1-Ethyl-4-methylbenzene



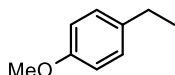
C₉H₁₂

120.19 g/mol

¹H-NMR	(300 MHz, CDCl ₃) δ 7.09 (s, 4H), 2.60 (q, J = 7.6 Hz, 2H), 2.31 (s, 3H), 1.21 (t, J = 7.6 Hz, 3H).
GC-MS	<i>t</i> _R = 4.36 min, (EI, 70 eV): <i>m/z</i> = 120 [M ⁺].

Analytical data were in full agreement with M. L. Kantam, R. Kishore, J. Yadav, M. Sudhakar, A. Venugopal, *Adv. Synth. Catal.* **2012**, 354, 663-669.

1-Ethyl-4-methoxybenzene



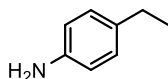
C₉H₁₂O

136.19 g/mol

¹H-NMR	(300 MHz, CDCl ₃) δ 7.1 (d, 2H), 6.82 (d, 2H), 3.77 (s, 3H), 2.58 (m, 2H), 1.20 (m, 3H).
¹³C-NMR	(75 MHz, CDCl ₃) 157.5, 136.4, 128.7, 115.38, 55.3, 28, 15.9.
GC-MS	<i>t</i> _R = 5.75 min, (EI, 70 eV): <i>m/z</i> = 136 [M ⁺].

Analytical data were in full agreement with B. Wang, H.-X. Sun, Z.-H. Sun, *Eur. J. Org. Chem.* **2009**, 22, 3688-3692.

4-Ethylaniline



C₈H₁₁N

121.18 g/mol

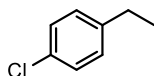
¹H-NMR (400 MHz, CDCl₃) δ 6.98 (d, 2H), 6.61 (d, 2H), 3.34 (bs, 2H), 2.53 (m, 2H), 1.19 (m, 3H).

¹³C-NMR (101 MHz, CDCl₃) δ 144.1, 134.5, 128.6, 115.4, 28, 16.

GC-MS *t*_R = 5.75 min, (EI, 70 eV): *m/z* = 121 [M⁺].

Analytical data were in full agreement with B. Wang, H.-X. Sun, G.-Q. Lin, Z.-H. Sun, *Adv. Synth. Catal.* **2009**, *351*, 415-422.

1-Ethyl-4-chlorobenzene



C₈H₉Cl

140.61 g/mol

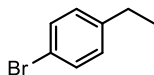
¹H-NMR (300 MHz, CDCl₃) δ 7.23 (d, *J* = 8.0 Hz, 2H), 7.10 (d, *J* = 8.0 Hz, 2H), 2.60 (q, *J* = 7.6 Hz, 2H), 1.23 (t, *J* = 7.6 Hz, 3H).

¹³C-NMR (75 MHz, CDCl₃) δ 142.63, 131.26, 129.22, 128.37, 28.28, 15.55.

GC-MS *t*_R = 4.92 min, (EI, 70 eV): *m/z* = 140 [M⁺], 125, 105, 89, 77, 63, 51.

Analytical data were in full agreement with M. E. Sloan, A. Staubitz, K. Lee, I. Manners, *Eur. J. Org. Chem.* **2011**, *4*, 672-675.

1-Ethyl-4-bromobenzene



C₈H₉Br

185.06 g/mol

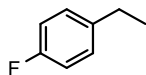
¹H-NMR (400 MHz, CDCl₃) δ 7.45–7.35 (m, 2H), 7.09–6.96 (m, 2H), 2.59 (q, *J* = 7.6 Hz, 2H), 1.20 (t, *J* = 7.6 Hz, 3H).

¹³C-NMR (101 MHz, CDCl₃) δ 143.2, 131.4, 129.7, 119.3, 28.4, 15.5.

GC-MS *t*_R = 5.76 min, (EI, 70 eV): *m/z* = 184 [M⁺], 169, 105, 89, 77, 63, 51.

Analytical data were in full agreement with T. Maegawa, T. Takahashi, M. Yoshimura, H. Suzuka, Y. Monguchi, H. Sajiki, *Adv. Synth. Catal.* **2009**, *351*, 2091–2095.

1-Ethyl-4-fluorobenzene



C₈H₉F

124.16 g/mol

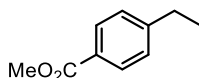
¹H-NMR (300 MHz, CDCl₃) δ 7.12-7.01 (m, 2H), 6.94-6.83 (m, 2H), 2.55 (q, *J* = 7.6 Hz, 2H), 1.15 (t, *J* = 7.6 Hz, 3H).

¹³C-NMR (75 MHz, CDCl₃) δ 162.75, 139.78, 129.18, 129.08, 115.15, 114.84, 28.11, 15.80.

GC-MS *t*_R = 3.54 min, (EI, 70 eV): *m/z* = 124 [M⁺].

Analytical data were in full agreement with E. C. Taylor, E. C. Bigham, D. K. Johnson, *J. Org. Chem.* **1977**, *42*, 362-363.

Methyl 4-ethylbenzoate



C₁₀H₁₂O₂

164.20 g/mol

¹H-NMR (400 MHz, CDCl₃) δ 7.96 (m, 2H), 7.27 (m, 2H), 3.90 (s, 3H), 2.71 (q, *J* = 7.6 Hz, 2H), 1.26 (t, *J* = 7.6 Hz, 3H).

¹³C-NMR (101 MHz, CDCl₃) δ 167.2, 149.8, 129.7, 127.9, 127.7, 52.0, 29.0, 15.2.

GC-MS *t*_R = 6.81 min, (EI, 70 eV): *m/z* = 164 [M⁺], 149, 133, 121, 105, 89, 77, 63, 51.

Analytical data were in full agreement with R. J. Rahaim, R. E. Maleczka, *Org. Lett.* **2011**, *13*, 584–587.

1-Cyclopropyl-1-phenylethane



C₁₁H₁₄

146.23 g/mol

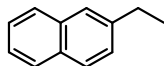
¹H-NMR (300 MHz, CDCl₃) δ 7.41 – 7.26 (m, 4H), 7.25 – 7.17 (m, 1H), 1.99 (dq, *J* = 9.2, 7.0 Hz, 1H), 1.35 (d, *J* = 7.0 Hz, 3H), 0.96 (qt, *J* = 9.2, 8.0, 5.0 Hz, 1H), 0.65 – 0.36 (m, 2H), 0.27 – 0.09 (m, 2H).

¹³C-NMR (75 MHz, CDCl₃) δ 147.38, 128.23, 127.00, 125.89, 44.67, 21.62, 18.56, 4.64, 4.34.

GC-MS *t*_R = 6.88 min, (EI, 70 eV): *m/z* = 146 [M⁺], 131, 117, 105, 91, 77, 65, 51.

Analytical data were in full agreement with R. T. Hrubiec, M. B. Smith, *J. Org. Chem.* **1984**, *49*, 385-388.

2-Ethynaphthalene



C₁₂H₁₂

156.22 g/mol

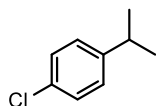
¹H-NMR (400 MHz, CDCl₃) δ 7.84–7.73 (m, 3H), 7.62 (s, 1H), 7.48–7.31 (m, 3H), 2.81 (q, *J* = 7.6 Hz, 2H), 1.33 (t, *J* = 7.6 Hz, 3H).

¹³C-NMR (101 MHz, CDCl₃) δ 141.8, 133.7, 132.0, 127.8, 127.6, 127.4, 127.1, 125.8, 125.6, 125.0, 77.4, 77.0, 76.7, 29.1, 15.5.

GC-MS *t*_R = 7.33 min, (EI, 70 eV): *m/z* = 156 [M⁺], 141, 128, 115, 102, 89, 77, 63, 51.

Analytical data were in full agreement with M. E. Sloan, A. Staubitz, K. Lee, I. Manners, *Eur. J. Org. Chem.* **2011**, *4*, 672–675.

1-Chloro-4-isopropylbenzene



C₉H₁₁Cl

154.64 g/mol

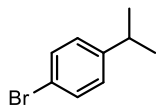
¹H-NMR (300 MHz, CDCl₃) δ 7.25 (m, 2H), 7.21–7.09 (m, 2H), 2.89 (m, 1H), 1.23 (d, *J* = 6.9 Hz, 6H).

¹³C-NMR (75 MHz, CDCl₃) δ 142.3, 131.3, 128.4, 127.8, 33.6, 23.9.

GC-MS *t*_R = 5.37 min, (EI, 70 eV): *m/z* = 154 [M⁺], 139, 125, 119, 105, 89, 77, 63, 51.

Analytical data were in full agreement with S. S. Kim, C. S. Kim, *J. Org. Chem.* **1999**, *64*, 9261–9264.

1-Bromo-4-isopropylbenzene



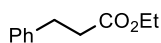
C₉H₁₁Br

199.09 g/mol

¹H-NMR	(400 MHz, CDCl ₃) δ 7.47–7.32 (m, 2H), 7.08 (m, 2H), 2.85 (sept, <i>J</i> = 6.9 Hz, 1H), 1.21 (d, <i>J</i> = 6.9 Hz, 6H).
¹³C-NMR	(101 MHz, CDCl ₃) δ 147.8, 131.3, 128.2, 119.3, 33.7, 30.9, 23.8.
GC-MS	<i>t</i> _R = 6.16 min, (EI, 70 eV): <i>m/z</i> = 198 [M ⁺], 185, 169, 158, 143, 119, 104, 91, 77, 63, 51.

Analytical data were in full agreement with M. A. Hall, J. Xi, C. Lor, S. Dai, R. Pearce, W. P. Dailey, R. G. Eckenhoff, *J. Med. Chem.* **2010**, *53*, 5667–5675.

Ethyl 3-phenylpropanoate



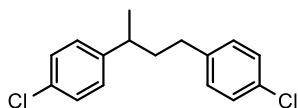
C₁₁H₁₄O₂

178.23 g/mol

¹H-NMR	(400 MHz, CDCl ₃) δ 7.33–7.26 (m, 2H), 7.24–7.16 (m, 3H), 4.13 (q, <i>J</i> = 7.1 Hz, 2H), 3.01–2.90 (m, 2H), 2.66–2.58 (m, 2H), 1.24 (t, <i>J</i> = 7.1 Hz, 3H).
¹³C-NMR	(101 MHz, CDCl ₃) δ 172.9, 140.6, 128.5, 128.3, 126.2, 60.4, 36.0, 31.0, 14.2.
GC-MS	<i>t</i> _R = 6.99 min, (EI, 70 eV): <i>m/z</i> = 178 [M ⁺], 133, 104, 91, 77, 65, 51.

Analytical data were in full agreement with M. Amatore, C. Gosmini, J. Périchon, *J. Org. Chem.* **2006**, *71*, 6130–6134.

1,3-Bis-(4-chlorophenyl)-butane



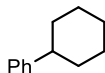
C₁₆H₁₆Cl₂

279.20 g/mol

¹H-NMR	(400 MHz, CDCl ₃) δ 7.34–6.97 (m, 8H), 2.79–2.61 (m, 1H), 2.55–2.39 (m, 2H), 1.95–1.82 (m, 2H), 1.25 (d, <i>J</i> = 6.9 Hz, 3H).
¹³C-NMR	(101 MHz, CDCl ₃) δ 145.5, 140.6, 131.7, 131.5, 129.7, 128.6, 128.4, 128.4, 39.7, 38.9, 33.2, 22.5.
GC-MS	<i>t</i> _R = 10.61 min, (EI, 70 eV): <i>m/z</i> = 279 [M ⁺], 191, 166, 139, 121, 103, 77, 51.
HRMS	(CI, <i>m/z</i>): found 278.0632 [M ⁺] (calculated 278.0629).

FT-IR (ATR-film) in [cm⁻¹] 3025 (w), 2960 (m), 2926 (m), 2859(w), 1894 (w), 1597 (w), 1491 (s), 1455 (m), 1408 (m), 1091 (s), 1013 (s), 825 (s), 531 (s), 489 (m).

Phenylcyclohexane



C₁₂H₁₆

160.26 g/mol

¹H-NMR (300 MHz, CDCl₃) δ 7.41–7.10 (m, 5H), 2.49 (m, 1H), 2.02–1.68 (m, 5H), 1.56–1.15 (m, 5H).

¹³C-NMR (75 MHz, CDCl₃) δ 148.1, 128.3, 126.9, 125.8, 44.7, 34.52, 27.0, 26.2.

GC-MS *t*_R = 6.88 min, (EI, 70 eV): *m/z* = 160 [M⁺], 131, 117, 104, 91, 78, 65, 51.

Analytical data were in full agreement with W. M. Czaplik, M. Mayer, A. Jacobi von Wangelin, *Angew. Chem. Int. Ed.* **2009**, *48*, 607–610.

1,3-Diphenylpropane



C₁₅H₁₆

196.29 g/mol

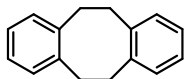
¹H-NMR (300 MHz, CDCl₃) δ 7.37 – 7.27 (m, 4H), 7.25 – 7.17 (m, 6H), 2.77 – 2.59 (m, 4H), 2.05 – 1.90 (m, 2H).

¹³C-NMR (75 MHz, CDCl₃) δ 142.33, 128.49, 128.35, 125.78, 35.48, 33.02.

GC-MS *t*_R = 8.65 min, (EI, 70 eV): *m/z* = 196 [M⁺], 179, 165, 152, 115, 105, 92, 79, 65, 51.

Analytical data were in full agreement with C.-T. Yang, Z.-Q. Zhang, Y.-C. Liu, L. Liu, *Angew. Chem. Int. Ed. Engl.* **2011**, *50*, 3904–3907.

Dibenzo-1,5-cyclooctadiene



C₁₆H₁₆

208.30 g/mol

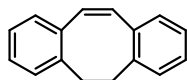
¹H-NMR (300 MHz, CDCl₃) δ 7.00 (m, 8H), 3.07 (s, 8H).

¹³C-NMR (75 MHz, CDCl₃) δ 140.62, 129.69, 126.12, 35.16.

GC-MS $t_R = 9.27$ min, (EI, 70 eV): $m/z = 208$ [M⁺], 193, 178, 165, 152, 128, 115, 104, 91, 78, 63, 51.

Analytical data were in full agreement with D. Guijarro, B. Mancheno, M. Yus, *Tetrahedron*. **1992**, 48, 4593-4600.

Dibenzo-1,3,5-cyclooctatriene



C₁₆H₁₄

206.29 g/mol

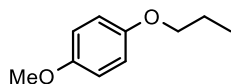
¹H-NMR (300 MHz, CDCl₃) δ 7.22 – 7.16 (m, 2H), 7.16 – 7.09 (m, 6H), 6.79 (s, 2H), 3.24 (s, 4H).

¹³C-NMR (101 MHz, CDCl₃) δ 139.85, 136.82, 131.51, 130.22, 129.97, 127.05, 125.55, 35.84.

GC-MS $t_R = 9.50$ min, (EI, 70 eV): $m/z = 206$ [M⁺], 191, 178, 165, 151, 139, 115, 106, 89, 77, 67, 51.

Analytical data were in full agreement with A. C. Cope, R. D. Smith, *J. Am. Chem. Soc.* **1955**, 77, 4596–4599.

1-Methoxy-4-*n*-propoxybenzene



C₁₀H₁₄O₂

166.22 g/mol

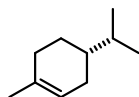
¹H-NMR (300 MHz, CDCl₃) δ 6.84 (s, 4H), 3.87 (t, $J = 6.6$ Hz, 2H), 3.77 (s, 3H), 1.87 – 1.70 (m, 2H), 1.03 (t, $J = 7.4$ Hz, 3H).

¹³C-NMR (75 MHz, CDCl₃) δ 153.65, 153.29, 115.43, 114.61, 70.17, 55.75, 22.70, 10.56.

GC-MS $t_R = 6.87$ min, (EI, 70 eV): $m/z = 166$ [M⁺], 124, 109, 95, 81, 64, 53.

Analytical data were in full agreement with A. B. Naidu, E. A. Jaseer, G. Sekar, *J. Org. Chem.* **2009**, 74, 3675–3679.

R)-4-Isopropyl-1-methyl-cyclohex-1-ene



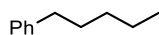
C₁₀H₁₈

138.25 g/mol

¹H-NMR	(300 MHz, CDCl ₃) δ 5.42 – 5.33 (m, 1H), 2.05 – 1.91 (m, 3H), 1.79 – 1.67 (m, 2H), 1.64 (s, 3H), 1.52 – 1.39 (m, 1H), 1.25 – 1.15 (m, 2H), 0.89 (d, <i>J</i> = 4.3 Hz, 3H), 0.87 (d, <i>J</i> = 4.3 Hz, 3H).
¹³C-NMR	(75 MHz, CDCl ₃) δ 133.97, 121.03, 40.01, 32.30, 30.83, 28.97, 26.49, 23.50, 20.02, 19.70.
GC-MS	<i>t</i> _R = 4.81 min, (EI, 70 eV): <i>m/z</i> = 138 [M ⁺], 123, 95, 79, 67, 55.

Analytical data were in full agreement with D. F. Schneider, M. S. Viljoen, *Tetrahedron* **2002**, 58, 5307-5315.

n-Pentylbenzene



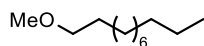
C₁₁H₁₆

148.25 g/mol

¹H-NMR	(300 MHz, CDCl ₃) δ 7.31 – 7.13 (m, 5H), 2.64 – 2.56 (m, 2H), 1.62 (m, 2H), 1.38 – 1.26 (m, 4H), 0.89 (t, <i>J</i> = 6.9 Hz, 3H).
¹³C-NMR	(75 MHz, CDCl ₃) δ 141.93, 127.37, 127.18, 124.51, 34.93, 30.50, 30.20, 21.53, 13.01.
GC-MS	<i>t</i> _R = 5.81 min, (EI, 70 eV): <i>m/z</i> = 148 [M ⁺], 133, 105, 91, 78, 65.

Analytical data were in full agreement with L. Ackermann, A. R. Kapdi, C. Schulzke, *Org. Lett.* **2010**, 12, 2298–2301.

1-Methoxyundecane



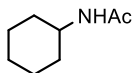
C₁₂H₂₆O

186.33 g/mol

¹H-NMR	(400 MHz, CDCl ₃) δ 3.36 (t, <i>J</i> = 6.7 Hz, 2H), 3.32 (s, 3H), 1.61–1.50 (m, 2H), 1.39–1.18 (m, 16H), 0.87 (t, <i>J</i> = 6.9 Hz, 3H).
¹³C-NMR	(101 MHz, CDCl ₃) δ 73.0, 58.5, 31.9, 29.7, 29.6, 29.5, 29.4, 26.2, 22.7, 14.1.
GC-MS	<i>t</i> _R = 6.76 min, (EI, 70 eV): <i>m/z</i> = 186 [M ⁺], 154, 126, 111, 97, 83, 69, 56.
HRMS	(CI, <i>m/z</i>): found 186.1987 [M ⁺] (calculated 186.1984).

FT-IR (ATR-film) in [cm⁻¹] 2923 (s), 2853 (s), 1745 (w), 1459 (m), 1379 (w), 1238 (w), 1195 (w), 1118 (s), 965 (w), 722 (w).

N-Cyclohexylacetamide



C₈H₁₅NO

141.21 g/mol

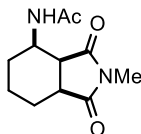
¹H-NMR (400 MHz, CDCl₃) δ 5.32 (s, 1H), 3.87–3.65 (m, 1H), 1.95 (s, 3H), 1.94–1.87 (m, 2H), 1.75–1.66 (m, 2H), 1.66–1.55 (m, 1H), 1.43–1.29 (m, 2H), 1.23–1.04 (m, 3H).

¹³C-NMR (101 MHz, CDCl₃) δ 169.0, 48.2, 33.3, 25.6, 24.9, 23.6.

GC-MS *t*_R = 6.71 min, (EI, 70 eV): *m/z* = 141 [M⁺], 112, 82, 60.

Analytical data were in full agreement with R. Pelagalli, I. Chiarotto, M. Feroci, S. Vecchio, *Green Chem.* **2012**, *14*, 2251-2255.

N-Methyl-3-(acetamido)-hexahydrophthalimide



C₁₁H₁₆N₂O₃

224.26 g/mol

¹H-NMR (400 MHz, CDCl₃) δ 7.16 (s, 1H), 4.31 (ddt, *J* = 12.7, 9.0, 5.3 Hz, 1H), 3.10–2.99 (m, 2H), 2.98 (s, 3H), 2.09–2.02 (m, 1H), 2.01 (s, 3H), 2.00–1.93 (m, 1H), 1.68–1.50 (m, 2H), 1.40 (m, 1H), 1.15 (m, 1H).

¹³C-NMR (101 MHz, CDCl₃) δ 179.2, 179.2, 169.5, 44.9, 42.3, 41.3, 27.6, 24.7, 24.6, 23.5, 20.5.

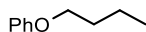
GC-MS *t*_R = 9.81 min, (EI, 70 eV): *m/z* = 224 [M⁺], 207, 181, 165, 153, 138, 126, 112, 96, 80, 70, 60, 51.

HRMS (CI, *m/z*): found 225.1234 [M+H⁺] (calculated 225.1234).

FT-IR (ATR-film) in [cm⁻¹] 3324 (m), 2957 (w), 2924 (w), 2861 (w), 1769 (m), 1703 (s), 1647 (s), 1539 (s), 1460 (w), 1431 (s), 1378 (s), 1306 (m), 1271 (s), 1197 (w), 1162 (w), 1113 (m), 1050 (m), 982 (m), 952 (m), 910 (m), 762 (m), 682 (S), 596 (s), 543 (s), 454 (m).

Melting Point 128 °C

n-Butoxybenzene



C₁₀H₁₄O

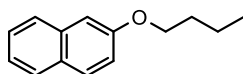
150.22 g/mol

¹H-NMR (300 MHz, CDCl₃) δ 7.34 – 7.26 (m, 2H), 6.99 – 6.87 (m, 3H), 3.97 (t, *J* = 6.5 Hz, 2H), 1.85 – 1.70 (m, 2H), 1.62 – 1.41 (m, 2H), 0.98 (t, *J* = 7.4 Hz, 3H).

¹³C-NMR (75 MHz, CDCl₃) δ 159.13, 129.43, 120.46, 114.49, 67.56, 31.38, 19.29, 13.90.

GC-MS *t*_R = 6.00 min, (EI, 70 eV): *m/z* = 150 [M⁺], 94, 77. 65. 51. Analytical data were in full agreement with J. Niu, H. Zhou, Z. Li, J. Xu, S. Hu, *J. Org. Chem.* **2008**, *73*, 7814–7817.

2-(*n*-Butoxy)naphthalene



C₁₄H₁₆O

200.28 g/mol

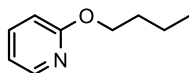
¹H-NMR (300 MHz, CDCl₃) δ 7.80 – 7.70 (m, 3H), 7.44 (ddd, *J* = 8.2, 7.0, 1.3 Hz, 1H), 7.33 (ddd, *J* = 8.1, 6.9, 1.2 Hz, 1H), 7.19 – 7.10 (m, 2H), 4.09 (t, *J* = 6.5 Hz, 2H), 1.93 – 1.77 (m, 2H), 1.63 – 1.47 (m, 2H), 1.02 (t, *J* = 7.4 Hz, 3H).

¹³C-NMR (75 MHz, CDCl₃) δ 157.13, 134.63, 129.32, 128.88, 127.65, 126.71, 126.30, 123.47, 119.06, 106.52, 67.71, 31.34, 19.36, 13.93.

GC-MS *t*_R = 9.01 min, (EI, 70 eV): *m/z* = 200 [M⁺], 144, 127, 115, 89, 57.

Analytical data were in full agreement with C. Cazorla, E. Pfordt, M.-C. Duclos, E. Metay, M. Lemaire, *Green Chem* **2011**, *13*, 2482–2488.

2-(*n*-Butoxy)pyridine



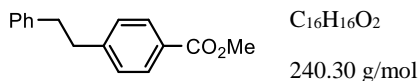
C₉H₁₃NO

151.21 g/mol

¹H-NMR	(300 MHz, CDCl ₃) δ 8.14 (ddd, <i>J</i> = 5.1, 2.0, 0.9 Hz, 1H), 7.55 (ddd, <i>J</i> = 8.4, 7.1, 2.0 Hz, 1H), 6.83 (ddd, <i>J</i> = 7.1, 5.1, 0.9 Hz, 1H), 6.76 – 6.66 (m, 1H), 4.27 (t, <i>J</i> = 6.7 Hz, 2H), 1.81 – 1.69 (m, 2H), 1.48 (m, 2H), 0.97 (t, <i>J</i> = 7.4 Hz, 3H).
¹³C-NMR	(75 MHz, CDCl ₃) δ 164.08, 146.89, 138.48, 116.45, 111.08, 65.70, 31.17, 19.29, 13.91.
GC-MS	<i>t</i> _R = 5.82 min, (EI, 70 eV): <i>m/z</i> = 151 [M ⁺], 121, 108, 95, 78, 67, 51.

Analytical data were in full agreement with D. Chambers, Richard, M. Parsons, G. Sandford, J. Skinner, Christopher, J. Atherton, Malcolm, S. Moilliet, John, *J. Chem. Soc., Perkin Trans. 1* **1999**, 803–810.

Methyl 4-phenylethylbenzoate



¹H-NMR	(300 MHz, CDCl ₃) δ 7.99 (d, <i>J</i> = 8.1 Hz, 2H), 7.32 – 7.27 (m, 2H), 7.27 – 7.21 (m, 3H), 7.21 – 7.15 (m, 2H), 3.92 (s, 3H), 3.07 – 2.90 (m, 4H).
¹³C-NMR	(75 MHz, CDCl ₃) δ 167.17, 147.22, 141.19, 129.74, 128.60, 128.50, 128.45, 127.97, 126.14, 52.03, 37.94, 37.50.
GC-MS	<i>t</i> _R = 10.13 min, (EI, 70 eV): <i>m/z</i> = 240 [M ⁺], 209, 178, 165, 149, 118, 105, 91, 78, 65, 50.

Analytical data were in full agreement with P. J. Rushworth, D. G. Hulcoop, D. J. Fox, *J. Org. Chem.* **2013**, 78, 9517–9521.

(Z)-1-Methyl-3-styrylbenzene



¹H-NMR	(400 MHz, CDCl ₃) δ 7.29 – 6.98 (m, 9H), 6.58 (s, 2H), 2.27 (s, 3H).
¹³C-NMR	(101 MHz, CDCl ₃) δ 137.91, 137.47, 137.33, 129.31, 129.01, 128.84, 128.47, 128.39, 127.98, 127.18, 126.00, 123.54, 21.47.

GC-MS $t_R = 8.37$ min, (EI, 70 eV): $m/z = 194$ [M⁺], 179, 165, 152, 128, 115, 105, 91, 83, 65, 50.

Analytical data were in full agreement with F. Alonso, P. Riente, M. Yus, *Eur. J. Org. Chem.* **2009**, 2009, 6034–6042.

2.5.3 Mechanistic experimental details

Kinetic Experiments

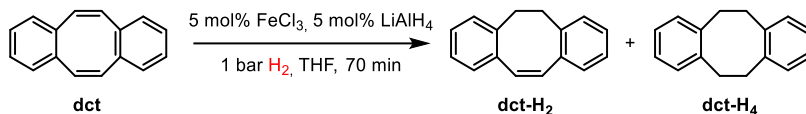
Kinetic studies were performed in a rubber septum sealed *Schlenk* tube under a dihydrogen atmosphere. Catalyst preparation according to the general method for the hydrogenation with FeCl₃ (5 mol%) and LiAlH₄ (5 mol%). Samples were taken via syringe (50 μL) and quenched with an aqueous solution of sodium hydrogen carbonate. After extraction with ethyl acetate and filtration over a pad of silica, the samples were analyzed by GC-FID. Selected catalyst poisons (dct, Hg) were added after 30 minutes via syringe (dct as a solution in 100 μL THF).

Table 2-5 - Hydrogenation of α -methylstyrene with selective catalyst poisons.

Entry	Time / min	Yield in % no additive	Yield in % + dct (30 mol%)	Yield in % + Hg (300 mol%)
1	0	0	0	0
2	10	23	22	17
3	20	41	35	38
4	30	57	53	58
5	40	81	57	75
6	50	95	62	93
7	60	96	64	94
8	70	97	64	94

^a quantitative GC-FID vs. *n*-pentadecane as internal reference

Table 2-6 - Dct consumption in the hydrogenation of α -methylstyrene with 30 mol% dct.



Entry	Time / min	dct	dct-H ₂	dct-H ₄
1	30	100	0	0
2	40	58	40	2
3	50	36	59	5
4	60	28	65	7
5	70	27	66	7

^a determined by relative peak areas of GC-FID

Deuteration experiments

For deuterium exchange experiments the reaction mixture after hydrogenation of α -methylstyrene at 1 bar H₂ in 3 h was quenched with D₂O, extracted with Et₂O (2 × 1 mL), filtered over a pad of silica and analyzed by GC-FID, ¹H and ²H-NMR to check for D-incorporation.

In a second experiment, LiAlD₄ was used instead of LiAlH₄. The reaction mixture after hydrogenation of α -methylstyrene at 1 bar H₂ in 3 h was quenched with H₂O, extracted with Et₂O (2 × 1 mL), filtered over a pad of silica and analyzed by GC-FID, ¹H-NMR to check for D-incorporation.

In both experiments no incorporation of D has been detected.

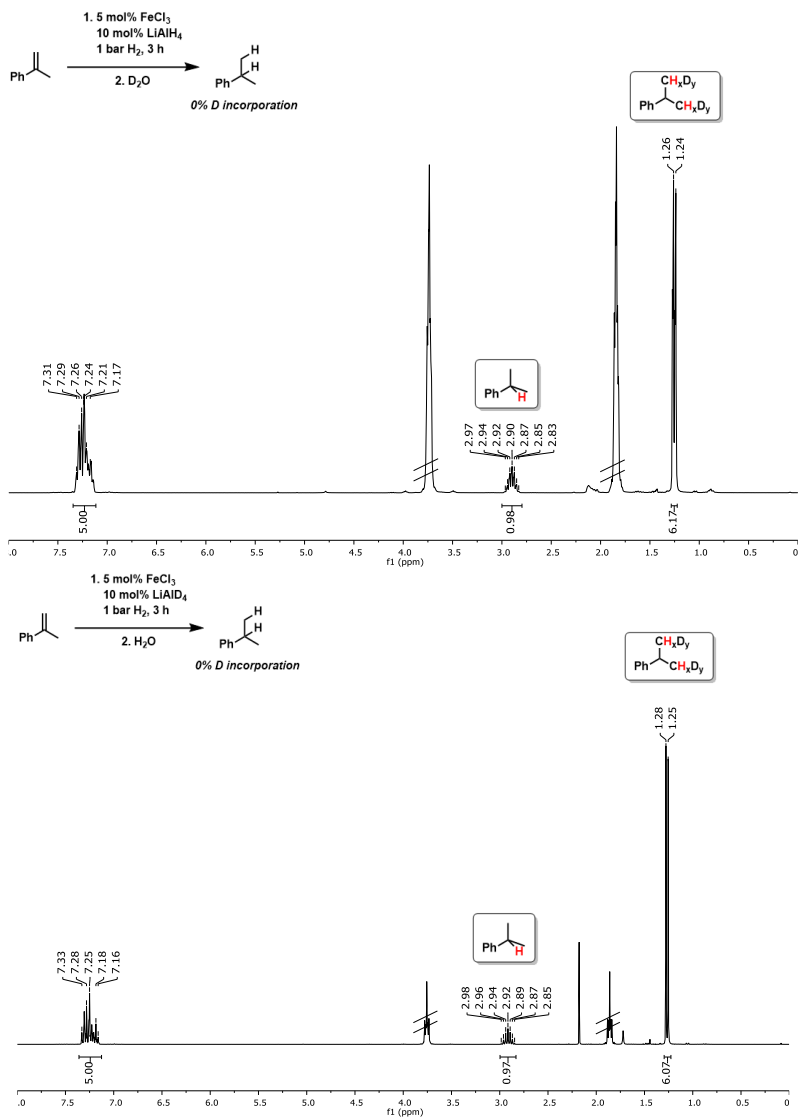


Figure 2-1 - ¹H-NMR spectrum after hydrogenation of α -methylstyrene with 5 mol% FeCl₃ and 10 mol% LiAlH₄ and quench with D₂O (top) and after hydrogenation of α -methylstyrene with 5 mol% FeCl₃ and 10 mol% LiAlD₄ and quench with H₂O (bottom).

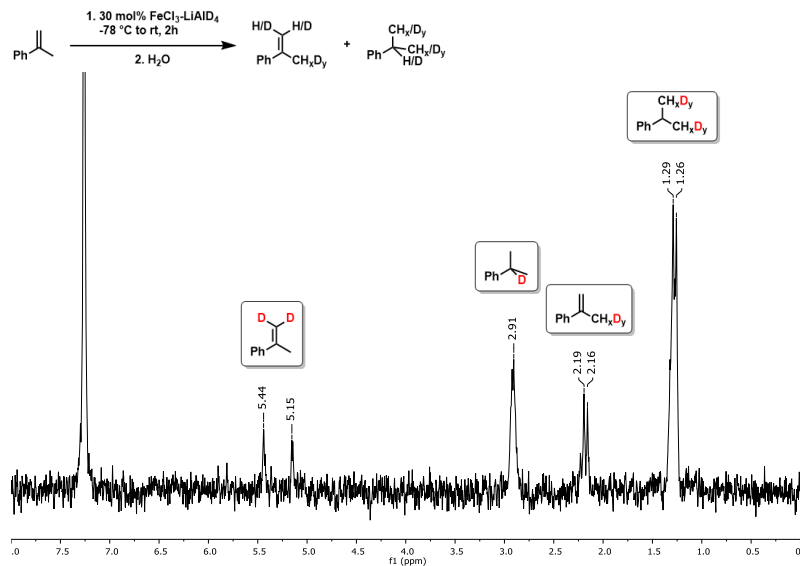
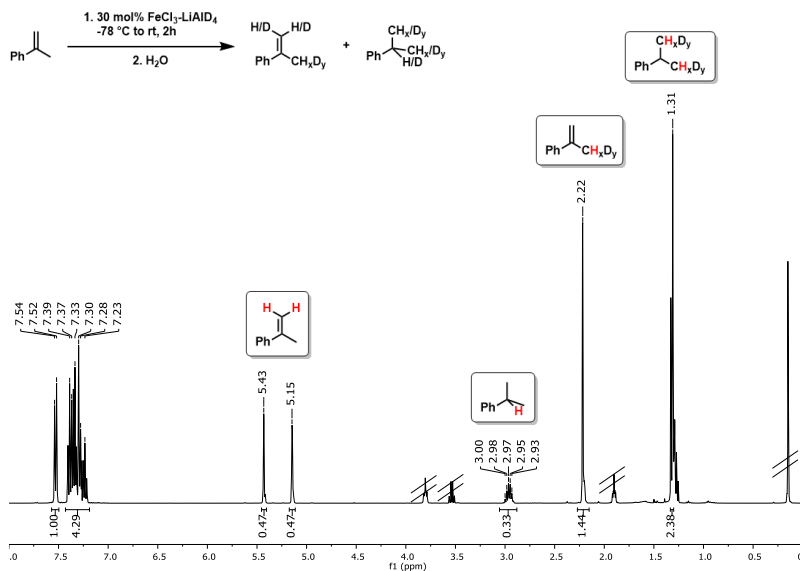


Figure 2-2 - ¹H-NMR (top) and ²H-NMR (bottom) of crude reaction mixture after extraction. Substrate addition 20 min after catalyst preparation. ~55% product yield.

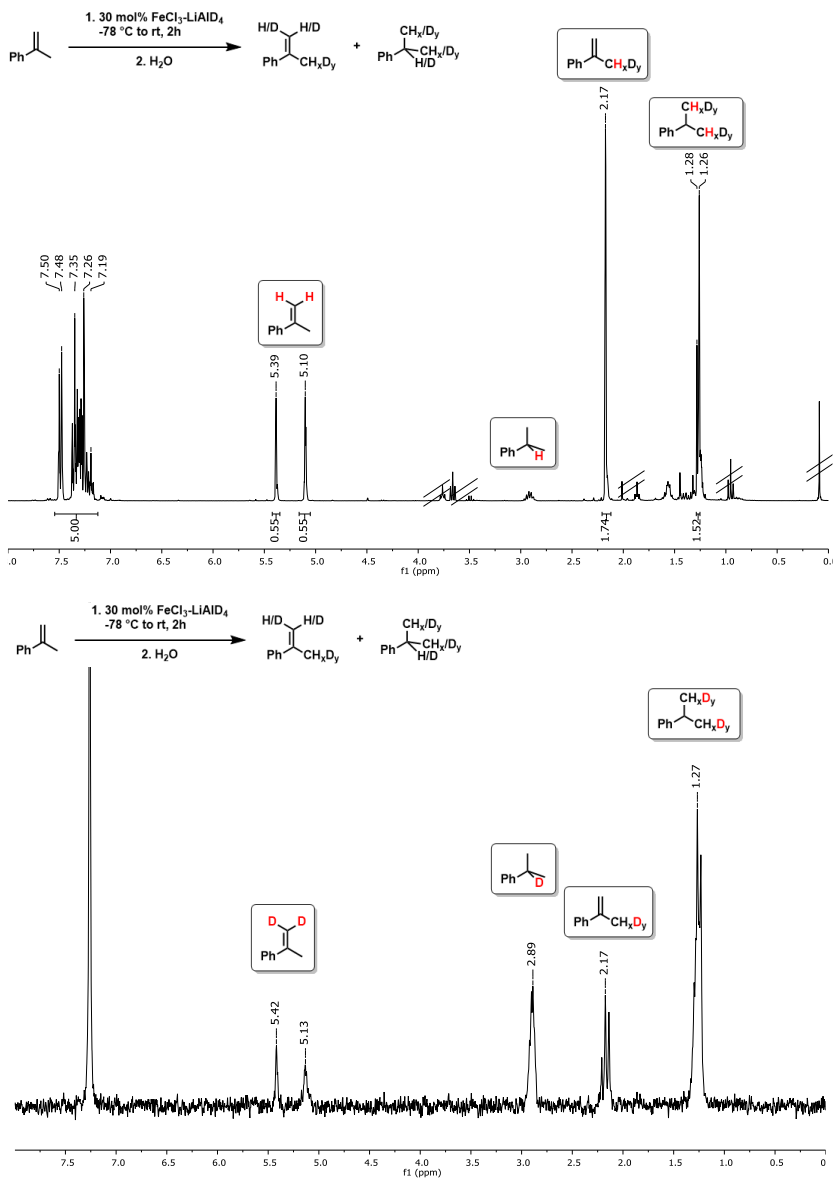


Figure 2-3 - ¹H-NMR (top) and ²H-NMR (bottom) of crude reaction mixture after extraction. Substrate addition **prior** catalyst preparation. ~54% product yield.

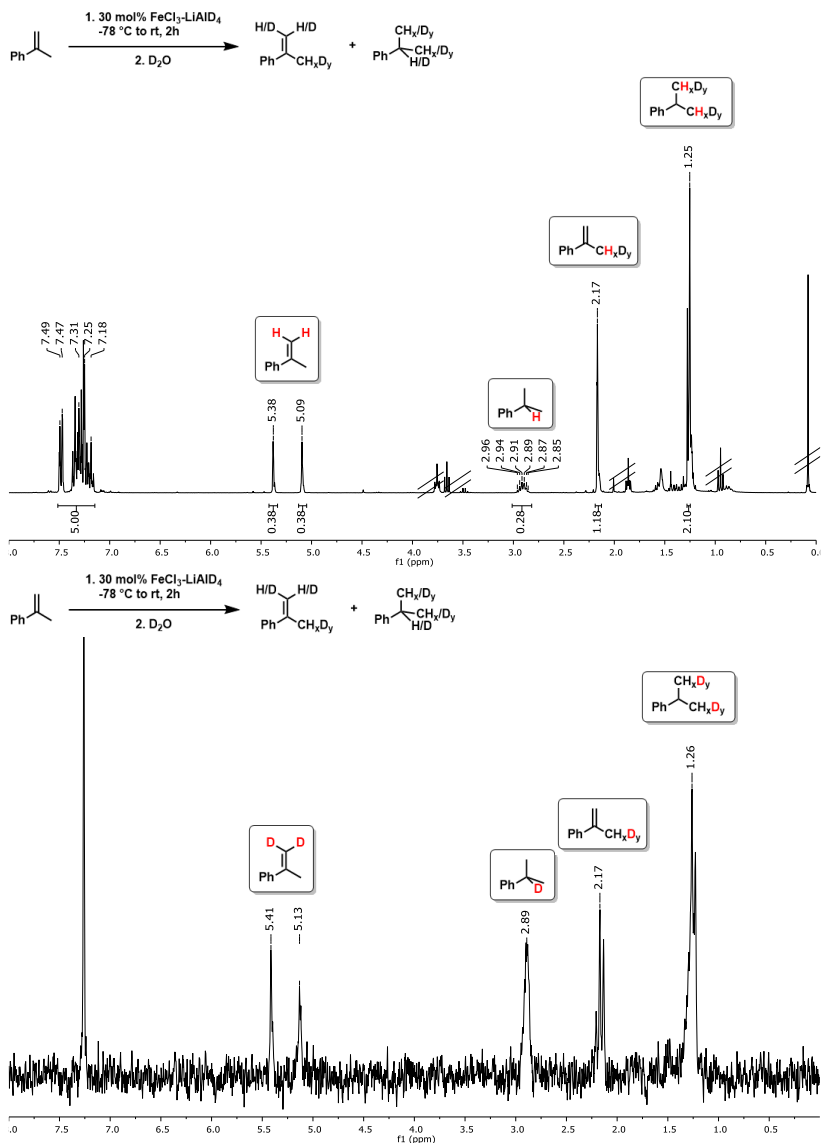
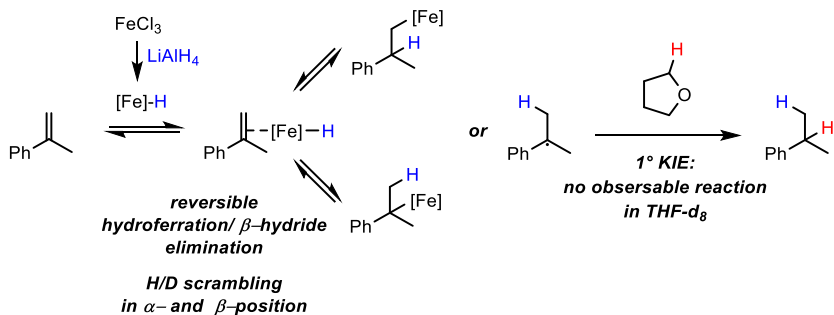


Figure 2-4 - ¹H-NMR (top) and ²H-NMR (bottom) of crude reaction mixture after extraction and D₂O quench. Substrate addition prior catalyst preparation. ~61% product yield.

A) H₂-free reaction:

-slower

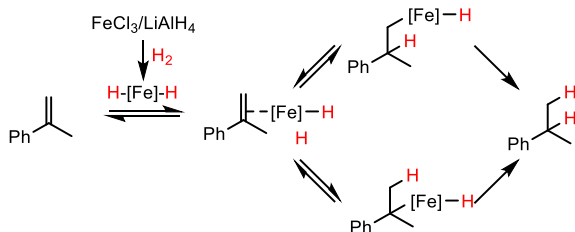
-radical intermediates?



B) Hydrogenation reaction:

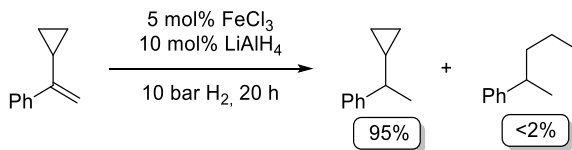
-faster

-no radical intermediates



Scheme 2-6 - Mechanistic proposal of H₂ free reaction (A) and under dihydrogen atmosphere (B).

The observation of H/D scrambling in the olefin and product with D incorporation into the α- and β-positions suggests reversible hydroferration/β-hydride elimination at the Fe center. The very slow reaction in THF-d₈ under H₂-free conditions support the notion of a radical H/D-abstraction which is governed by a primary kinetic isotope effect (1° KIE). The operation of a radical mechanism is slower than the hydrogenation mechanism, especially at high H₂ pressures. See radical clock experiment at 10 bar H₂ below.



Scheme 2-7 - Radical clock experiment.

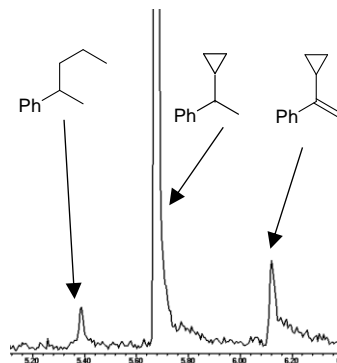


Figure 2-5 - GC-MS spectrum of the reaction mixture of the hydrogenation of α -cyclopropylstyrene after work-up.

DLS measurement

The pre-catalyst was synthesized as described in the general procedure of hydrogenation reactions with FeCl₃/LiAlH₄ = 1/1 but in the absence of any unsaturated substrate. After stirring for additional 10 minutes, the mixture was diluted with anhydrous THF to achieve a final concentration $c[\text{Fe}] = 1.25 \text{ mM}$. The mixture was filtered through a 100 nm PTFE filter (sample B). The samples were measured after ageing at room temperature for 30 minutes.

Mean particle sizes:

Sample A:

$d = 297 \text{ nm} (\pm 30)$

Sample B (after filtration through 100 nm filter, three independent experiments):

$d = 334 \text{ nm} (\pm 30)$

$d = 1490 \text{ nm} (\pm 400)$

$d = 244 \text{ nm} (\pm 80)$ at higher dilution with $c[\text{Fe}] = 0.25 \text{ mM}$

2.5.6 [Li(thf)₂{Fe(tmeda)}₂(μ-AlH₅)(μ-Al₂H₉) (4)

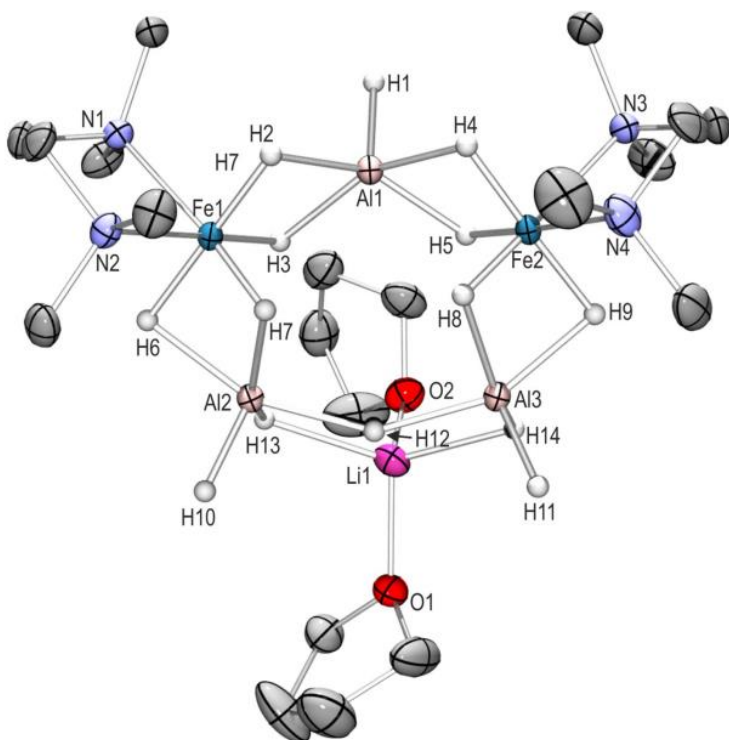
All manipulations were carried out under an inert atmosphere of purified argon, using standard *Schlenk* or glovebox techniques. Solvents (THF, *n*-hexane) were dried by refluxing over sodium and distilled under argon prior to use. Commercial lithium aluminium hydride was purified by extraction with diethyl ether and subsequent removal of the solvent under high vacuum. [FeCl₂(tmeda)]₂ was prepared according to: S. C. Davies, D. L. Hughes, G. J. Leigh, J. R. Sanders, J. S. de Souza, *J. Chem. Soc., Dalton Trans.* **1997**, 1981.

Synthesis of **4**: [FeCl₂(tmeda)]₂ (2.490 g, 5.12 mmol, 1.0 equiv.) was dissolved in THF (120 mL). The cooled (−78 °C) solution was added to a suspension of LiAlH₄ (0.912 g, 23.38 mmol) in 120 ml THF, which was also cooled at −78 °C with a dry ice acetone bath. A deep red suspension formed that was stirred for 30 min at −78 °C. Subsequently, the cold solution was filtered through a P4 frit. The filtrate was layered with pre-cooled (−20 °C) *n*-hexane. Storage at −78 °C gave a deep red crystalline solid. The mother liquor was removed with a cannula. Dark red crystals of **4** were obtained by dissolving the remaining solid in cold toluene (50 mL) at −78 °C and layering this solution with pre-cooled *n*-hexane. A suitable crystal was selected, transferred to paratone oil that was cooled under a stream of cooled N₂ gas, and mounted on a glass fibre in the cooled nitrogen stream of the diffractometer for the X-ray structure determination. The further spectroscopic characterization of the compound was prevented by its high thermal instability. Decomposition to a dark brown residue was observed at temperatures above −10 °C in the solid state as well as in solution. The crystallographic data of **4** were collected on a Bruker APEXII diffractometer equipped with a rotating anode (Mo-Kα radiation, λ = 0.71073 Å). A red plate with the dimensions 0.19 × 0.11 × 0.05 mm^{−3}. The structures were solved using direct methods and refined against *F*² using the program suite SHELXTL-97.23.

a) *SHELXTL-Plus*, REL. 4.1; Siemens Analytical X-RAY Instruments Inc.: Madison, WI, **1990**; b) Sheldrick, G. M. *SHELXL 97*, Program for the Refinement of Structures, University of Göttingen, **1997**; c) Sheldrick, G.M., *Acta Cryst.*, 2008, **A64**, 112.

The positions of the hydrogen atoms bound to aluminium and iron were located on the Fourier difference map and refined freely. All other hydrogen atoms were placed on calculated positions and refined using a riding model. Crystal Data for C₂₀H₆₂Al₃Fe₂LiN₄O₂ (M = 590.32 g mol^{−1}): orthorhombic, space group *Pca*2₁, *a* = 15.4965(7) Å, *b* = 16.8579(7) Å, *c* = 12.6159(6) Å, *V* = 3295.8(3) Å³, *Z* = 4, *T* = 153(1) K, μ(Mo Kα) = 0.981 mm^{−1}, *D*_{calc} = 1.190 g mm^{−3}, 30041 reflections measured (6.86 ≤ θ ≤ 27.10), 5799 unique (*R*_{int} = 0.0617, *R*_{sigma} = 0.0489) which were used in all calculations. The final *R*₁ was 0.0329 (*I* > 2σ(*I*)) and *wR*₂ was 0.1674 (all data). The crystallographic information file (CIF) has been deposited at the **CCDC**, 12 Union Road,

Cambridge, CB21EZ, U.K., and can be obtained on request free of charge, by quoting the publication citation and deposition number **1034372**.



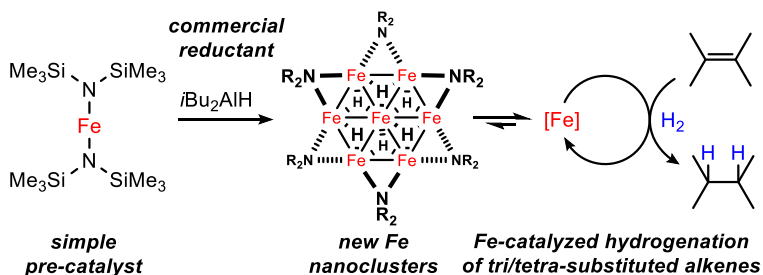
2.6 References

- [1] a) *Catalytic Hydrogenation*; L. Cerveny (ed.); Elsevier: Amsterdam, **1986**. b) *The Handbook of Homogeneous Hydrogenation*; J. G. de Vries and C. J. Elsevier (eds.); Wiley-VCH: Weinheim, **2007**; c) S. Nishimura, *Handbook of Heterogeneous Catalytic Hydrogenation for Organic Synthesis*; Wiley: New York, **2001**.
- [2] a) K. Junge, K. Schröder and M. Beller, *Chem. Commun.* **2011**, 47, 4849; b) B. A. F. Le Bailly and S. P. Thomas, *RSC Adv.* **2011**, 1, 1435.
- [3] a) E. J. Daida and J. C. Peters, *Inorg. Chem.* **2004**, 43, 7474; b) C. Bianchini, A. Meli, M. Peruzzini, P. Frediani, C. Bohanna, M. A. Esteruelas and L. A. Oro, *Organometallics* **1992**, 11, 138.
- [4] a) R. P. Yu, J. M. Darmon, J. M. Hoyt, G. W. Margulieux, Z. R. Turner and P. J. Chirik, *ACS Catal.* **2012**, 2, 1760; b) R. J. Trovitch, E. Lobkovsky, E. Bill and P. J. Chirik, *Organometallics* **2008**, 27, 1470; c) S. C. Bart, E. Lobkovsky and P. J. Chirik, *J. Am. Chem. Soc.* **2004**, 126, 13794; d) T. S. Carter, L. Guiet, D. J. Frank, J. West and S. P. Thomas, *Adv. Synth. Catal.* **2013**, 355, 880.
- [5] a) P. H. Phua, L. Lefort, J. A. F. Boogers, M. Tristany and J. G. de Vries, *Chem. Commun.* **2009**, 45, 3747; b) M. Stein, J. Wieland, P. Steurer, F. Tölle, R. Mülhaupt and B. Breit, *Adv. Synth. Catal.* **2011**, 353, 523; c) A. Welther, M. Bauer, M. Mayer and A. Jacobi von Wangelin, *ChemCatChem* **2012**, 4, 1088; d) R. Hudson, A. Rivière, C. M. Cirtiu, K. L. Luska and A. Moores, *Chem. Commun.* **2012**, 48, 3360; e) A. Welther and A. Jacobi von Wangelin, *Curr. Org. Chem.* **2013**, 17, 326; f) R. Hudson, G. Hamasaka, T. Osako Y. M. A. Yamada, C. J. Li, Y. Uozumi and A. Moores, *Green Chem.* **2013**, 15, 2141.
- [6] a) B. A. F. Le Bailly, M. D. Greenhalgh and S. P. Thomas, *Chem. Commun.* **2012**, 48, 1580; b) D. J. Frank, L. Guiet, A. Käslin, E. Murphy and S. P. Thomas, *RSC Adv.* **2013**, 3, 25698.
- [7] LiAlH₄ as hydride source in metal-catalyzed reductions: a) G. Dozzi, S. Cucinella, A. Mazzei, *J. Organomet. Chem.* **1979**, 164, 1; b) E. C. Ashby and J. J. Lin, *J. Org. Chem.* **1978**, 43, 2567; c) E. C. Ashby and J. J. Lin, *Tetrahedron Lett.* **1977**, 51, 4481. For early reports of H₂ evolution from iron hydride species and catalytic olefin hydrogenations, see: d) Y. Takegami, T. Ueno and T. Fujii, *Kogyo Kagaku Zasshi (J. Chem. Soc. Jpn., Ind. Chem. Sec.)* **1964**, 67, 1009; e) Y. Takegami, T. Ueno and T. Fujii, *Bull. Chem. Soc. Jpn.* **1965**, 38, 1279.
- [8] a) Technical production and use of H₂: H.-J. Arpe, *Industrial Organic Chemistry*; Wiley-VCH: Weinheim **2010**; b) selected applications of LiAlH₄: S. Yaragorla, *Synlett* **2008**, 19, 3073.
- [9] Please see chapter 0 for detailed experimental and analytical data.
- [10] Olefin isomerization with iron carbonyls: a) J. V. Crivello, S. Kong, *J. Org. Chem.* **1998**, 63, 6745; b) M. R. Reddy, M. Periasamy, *J. Organomet. Chem.* **1995**, 491, 263; c) P. A. Tooley, L. W. Arndt, M. Y. Darensbourg, *J. Am. Chem. Soc.* **1985**,

- 107, 2422; d) R. Jennerjahn, R. Jackstell, I. Piras, R. Franke, H. Jiao, M. Bauer and M. Beller, *ChemSusChem* **2012**, *5*, 734; e) naked Fe(0) species: M. Mayer, A. Welther and A. Jacobi von Wangelin, *ChemCatChem* **2011**, *3*, 1567. Allylbenzenes were prepared according to: f) M. Mayer, W. M. Czaplik and A. Jacobi von Wangelin, *Adv. Synth. Catal.* **2010**, *352*, 2147.
- [11] a) F. Alonso, I. P. Beletskaya and M. Yus, *Chem. Rev.* **2002**, *102*, 4009; b) W. M. Czaplik, S. Grupe, M. Mayer and A. Jacobi von Wangelin, *Chem. Commun.* **2010**, *46*, 6350.
- [12] D. Gärtner, H. Konnerth and A. Jacobi von Wangelin, *Catal. Sci. Technol.* **2013**, *3*, 2541.
- [13] a) α -Methylstyrene was hydrogenated at 4 bar H₂ in the presence of various functionalized additives (1 equiv.). No decrease of hydrogenation selectivity was observed when adding PhCl, PhBr, PhCO₂Me, PhNH₂, PhCONH₂, and 1,1-diphenylethylene, respectively. With PhNO₂, PhCN, PhI, and MeCN, no conversion of α -methylstyrene was observed, respectively, neither was the additive significantly consumed (<5%). b) At 1-2 bar H₂, much lower tolerance of functional groups was observed. We assume that the presence of functionalized substrates or polar moieties enhances catalyst ageing and formation of a heterogeneous species which appeared to somewhat less active. It should also be noted that sporadic cases of somewhat lower reproducibilities of reactions at 1 bar H₂ pressure were observed with substrates bearing polar functional groups.
- [14] *N*-Methylacetamide (AcNHMe), pK_a 25.9. F. G. Bordwell, J. A. Harrelson and T.-Y. Lynch, *J. Org. Chem.* **1990**, *55*, 3337.
- [15] *N*-Acetylaminocyclohexenes were prepared according to: a) D. Strübing, H. Neumann, A. Jacobi von Wangelin, S. Klaus, S. Hübner and M. Beller, *Tetrahedron* **2006**, *62*, 10962; b) S. Hübner, H. Neumann, A. Jacobi von Wangelin, S. Klaus, D. Strübing, H. Klein, M. Beller, *Synthesis* **2005**, *2084*; c) S. Klaus, S. Hübner, H. Neumann, D. Strübing, A. Jacobi von Wangelin, D. Gördes and M. Beller, *Adv. Synth. Catal.* **2004**, *346*, 970; d) A. Jacobi von Wangelin, H. Neumann, D. Gördes, A. Spannenberg and M. Beller, *Org. Lett.* **2001**, *3*, 2895.
- [16] Fe-catalyzed *Z*-selective semihydrogenation of alkynes: a) S. Enthaler, M. Haberberger and E. Irran, *Chem. Asian J.*, 2011, **6**, 1613; b) L. Ilies, T. Yoshida and E. Nakamura, *J. Am. Chem. Soc.* **2012**, *134*, 16951; c) C. Belger and B. Plietker, *Chem. Commun.* **2012**, *48*, 5419; d) T. N. Gieshoff, A. Welther, M. T. Kessler, M. H. G. Prechtel and A. Jacobi von Wangelin, *Chem. Commun.* **2014**, *50*, 2261.
- [17] a) J. A. Widegren and R. G. Finke, *J. Mol. Catal. A* **2003**, *198*, 317; b) D. Astruc, F. Lu and J. Ruiz Aranzaes, *Angew. Chem. Int. Ed.* **2005**, *44*, 7852; c) R. H. Crabtree, *Chem. Rev.* **2012**, *112*, 1536.
- [18] a) D. R. Anton and R. H. Crabtree, *Organometallics* **1983**, *2*, 855; b) G. Franck, M. Brill and G. Helmchen, *J. Org. Chem.* **2012**, *89*, 55; c) J. F. Sonnenberg and R. H. Morris, *Catal. Sci. Technol.* **2014**, *4*, 3426.

- [19] The observation of a partial inhibition by dct results from a superposition of an effective catalyst inhibition by the presence of dct and (a slower) hydrogenation of dct as substrate itself (see entry 27 in Table 2-3).
- [20] Iron forms only metastable alloys with mercury (amalgam). The maximum concentration of Fe(0) in Hg was reported to be 2-3 wt.%. a) S. Mørup, S. Linderoth, J. Jacobsen and M. Holmblad, *Hyperfine Interact.* **1991**, 69, 489; b) S. Linderoth and S. Mørup *J. Phys. Condens. Matter* **1992**, 4, 8627.
- [21] a) G. W. Schaeffer, J. S. Roscoe and A. C. Stewart, *J. Am. Chem. Soc.* **1956**, 78, 729; b) H. Neumaier, D. Bückel and G. Ziegelmaier, *Z. Anorg. Allg. Chem.* **1966**, 345, 46; c) M. E. Kost and A. L. Golovanova, *Izv. Akad. Nauk SSSR, Ser. Khim.* **1957**, 5, 991.
- [22] The stable low-spin iron(II) aluminohydride complex [(Me³tacn)₂Fe₂(μ-AlH₆)⁺] has recently been reported (tacn = 1,4,7-triazacyclononane): M. Oishi, T. Endo, M. Oshima and H. Suzuki, *Inorg. Chem.* **2014**, 53, 5100.
- [23] a) A. Fürstner, R. Martin, H. Krause, G. Seidel, R. Goddard and C. W. Lehmann, *J. Am. Chem. Soc.* **2008**, 130, 8773; b) A. Hedström, E. Lindstedt and P.-O. Norrby, *J. Organomet. Chem.* **2013**, 748, 51.
- [24] a) C. Rangheard, C. de Julian Fernandez, P.-H. Phua, J. Hoorn, L. Lefort and J. G. de Vries, *Dalton Trans.* **2010**, 39, 8464; b) R. Schoch, W. Desens, T. Werner and M. Bauer, *Chem. Eur. J.* **2013**, 19, 15816; c) V. Kelsen, B. Wendt, S. Werkmeister, K. Junge, M. Beller and B. Chaudret, *Chem. Commun.* **2013**, 49, 3416.
- [25] a) D. Griller and K. U. Ingold, *Acc. Chem. Res.* **1980**, 13, 317; b) M. Newcomb, *Tetrahedron* **1993**, 49, 1151.

3 Alkene Hydrogenations by Soluble Iron Nanocluster Catalysts^{i,ii}



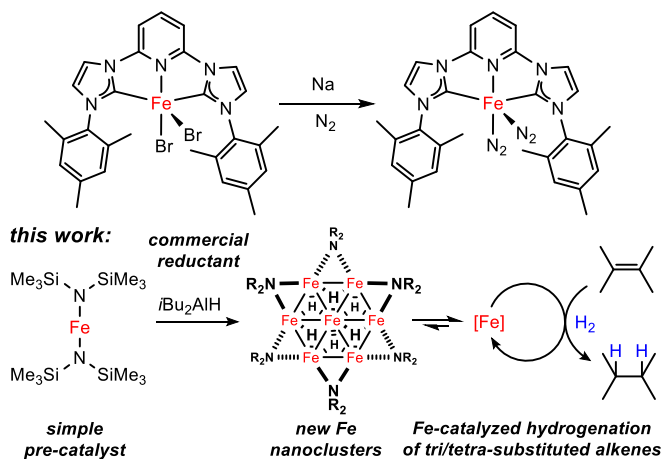
The replacement of noble metal technologies and the realization of new reactivities with earth abundant metals is at the heart of sustainable synthesis. Alkene hydrogenations have so far been most effectively performed by noble metal catalysts. This study reports an iron-catalyzed hydrogenation protocol for tri- and tetra-substituted alkenes of unprecedented activity and scope under mild conditions (1-4 bar H₂, 20°C). Instructive snapshots at the interface of homogeneous and heterogeneous iron catalysis were recorded by the isolation of novel Fe nanocluster architectures that act as catalyst reservoirs and soluble seeds of particle growth.

ⁱ Reproduced from T. N. Gieshoff, U. Chakraborty, M. Villa, A. Jacobi von Wangelin, *Angew. Chem. Int. Ed.* **2017**, *56*, 3585-3589, with permission from Wiley-VCH. Schemes, tables and text may differ from published version.

ⁱⁱ Authors contribution: Initial optimization experiments (Table 3-1, Table 3-2, Scheme 3-2), the major part of the substrate scope (Scheme 3-3) and the poisoning experiments (Scheme 3-4) were performed by T. Gieshoff, see T. Gieshoff, *Dissertation*, University Regensburg, **2016**. Fe₄, Fe₆ and Fe₇ clusters (Scheme 3-5) were initially synthesized and analyzed by T. Gieshoff and U. Chakraborty, see T. Gieshoff *Dissertation*, University Regensburg, **2016**.

3.1 Introduction

Catalytic hydrogenations of unsaturated C=C bond systems are pivotal to modern chemical transformations and mostly performed with nickel or platinum group catalysts.^[1] While some of the largest technical processes are iron-catalyzed hydrogenations (Haber-Bosch, Fischer-Tropsch), the potential of iron as abundant, non-toxic, and cheap transition metal catalyst for C=C hydrogenations has only very recently been tapped.^[2] Significant progress in the design of molecular Fe catalysts was made by the introduction of tridentate bis(imino)pyridine ligands (PDI) by Budzelaar *et al.*^[3] and Chirik *et al.*^[4] The (PDI)Fe(N₂)₂ pre-catalysts cleanly hydrogenate mono- and di-substituted alkenes under mild conditions and exceed the productivity of some precious metal catalysts.^[4] Further improved activities were observed with the related bis(carbene)-pyridine iron(0) complexes (Scheme 3-1, top).^[4] On the other hand, ill-defined or nanoparticulate Fe catalysts were prepared by decompositions of iron carbonyls or by reductions of iron salts with organometallic or hydride reagents but exhibited only moderate hydrogenation activities.^[5] While providing an operationally simple access to Fe-based hydrogenation catalysts, the latter approaches provided limited mechanistic insight, often involved precipitation of heterogeneous species especially in the absence of suitable ligands, and generally displayed high catalyst sensitivity and limited scope. From our recent studies into the development of low-valent iron catalysts for hydrogenations,^[6] we reasoned that an effective yet operationally simple protocol would fulfill the following criteria: i) the active catalyst is prepared *in situ* by the reduction of iron(II) precursors with commercial reductants; ii) the catalyst contains bulky ligands that are cheap, easily available, coordinate iron in various low oxidation states, and prevent unwanted aggregation to larger, catalytically inactive particles; iii) the ligands create a lipophilic periphery that enhances solubilization under the non-polar conditions of alkene hydrogenations; iv) the catalytic hydrogenation operates under mild conditions without sophisticated additives in common organic solvents. With these framework conditions, we investigated combinations of iron(II) bis(1,1,1,3,3,3-hexamethyl-disilazan-2-ide), Fe(hmds)₂,^[7] and various reductants. Documented herein are the benefits of using this simple catalytic system that presents tangible advances over the current state-of-the-art that could not have been predicted: Clean hydrogenations of challenging alkenes (e.g. tetra-substituted) proceed under very mild conditions. A most user-friendly protocol can be adopted by simple mixing of the ferrous salt, reductant, and ligand. The isolation of novel soluble Fe nanocluster topologies provides new insight into reductive catalyst formation and cluster aggregation (Scheme 3-1, bottom).



Scheme 3-1 - Soluble Fe catalysts for hydrogenations of alkenes.

3.2 Results and Discussion

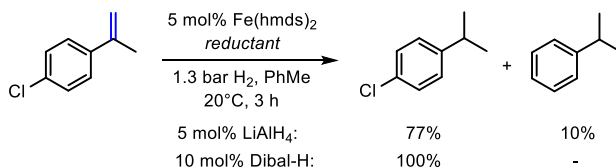
There are several reports of the coordination chemistry of Fe(hmnds)₂ in the presence of various ligands but only very few applications to catalytic reactions have been demonstrated.^[8] The displacement of hmnds ligands from Fe(hmnds)₂ by formal hydride donors has not received significant attention despite its relevance to the preparation of simple hydridoiron species^[9] and hydrogenase model compounds^[10]. In the context of alkene hydrogenations, Chaudret *et al.* prepared catalytically active Fe nanoparticles by thermal decomposition of Fe(hmnds)₂ at 150°C in the presence of H₂.^[11] We studied the generation of active hydrogenation catalysts from Fe(hmnds)₂ and various simple and commercial hydride donors and reductants under mild conditions (Table 3-1). Ethylmagnesium chloride or zinc afforded poor hydrogenation catalysts (entries 1, 2). Similar low activity was observed when following Chaudret's protocol of thermal decomposition of Fe(hmnds)₂ to nanoparticles (entry 3).^[11] Extremely high hydrogenation activity was achieved in the presence of aluminium hydrides and organoaluminium reagents (entries 6-9).^[12] The most active catalyst was formed with *di*iso-butylaluminium hydride (Dibal-H) which afforded quantitative conversion of 1-phenyl-1-cyclohexene at 1.3 bar H₂ and 20°C after 30 min. The operationally most convenient *in situ* catalyst formation from FeCl₂, HN(SiMe₃)₂, and *n*-butyllithium gave nearly identical yields (entry 10). Complete inhibition was observed in the absence of Dibal-H or the amido ligand N(TMS)₂, respectively (entries 11, 12). Further tests of the catalyst mixtures revealed high chemo-selectivity and robustness when employing Dibal-H (Scheme 2, Table 2). This catalyst could be stored in solution for several days or dried in vacuum without significant loss of activity (entries 1-4, Table 3-2, turnover frequency (TOF) recorded after 7 min reaction at ~20% conversion).

Table 3-1 - Selected optimization experiments.

Entry	Reductant (mol%)	Conditions	Yield [%] ^a
1	EtMgCl (10)	5 bar H ₂ , 40°C, 18 h	5 (9)
2	Zn (10)	as entry 1	<1 (1)
3	-	5 bar H ₂ , 150°C, 18 h	1 (1)
4	NaBH ₄ (5)	as entry 1	99 (99)
5	NaBH ₄ (5)	1.3 bar H ₂ , 20°C, 3 h	1 (2)
6	LiAlH ₄ (5)	as entry 4	99 (99)
7	Me ₃ Al (10)	1.3 bar H ₂ , 20°C, 0.5 h	90 (98)
8	<i>i</i> Bu ₃ Al (10)	as entry 7	93 (99)
9	<i>i</i>Bu₂AlH (10)	as entry 7	100 (100)

10	<i>i</i> Bu ₂ AlH (10)	FeCl ₂ , HN(TMS) ₂ , <i>n</i> -BuLi ^c	98 (99)
11	-	as entry 7	<1 (1)
12	<i>i</i> Bu ₂ AlH (10)	as entry 7, FeCl ₂ ^b	<1 (1)

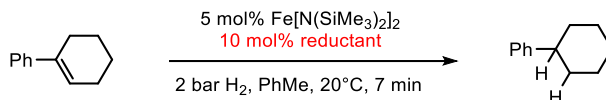
Conditions: 0.2 mmol alkene, 0.5 M in toluene, 5 mol% Fe[N(SiMe₃)₂]₂, reductant, H₂. ^a Yields determined by quantitative GC-FID vs. internal *n*-pentadecane. ^b 5 mol% FeCl₂ instead of Fe(hmde)₂. ^c 5 mol% FeCl₂, 10 mol% HN(SiMe₃)₂, 10 mol% *n*-butyllithium (1.6 M in PhMe) instead of Fe(hmde)₂.



Scheme 3-2 - Chemoselectivity of the Fe(hmde)₂/Dibal-H catalyst.

The optimized set of conditions was applied to the hydrogenation of various alkenes (Scheme 3-3). Mono-, di-, and tri-substituted alkenes were cleanly reacted under 2 bar H₂ pressure at room temperature.

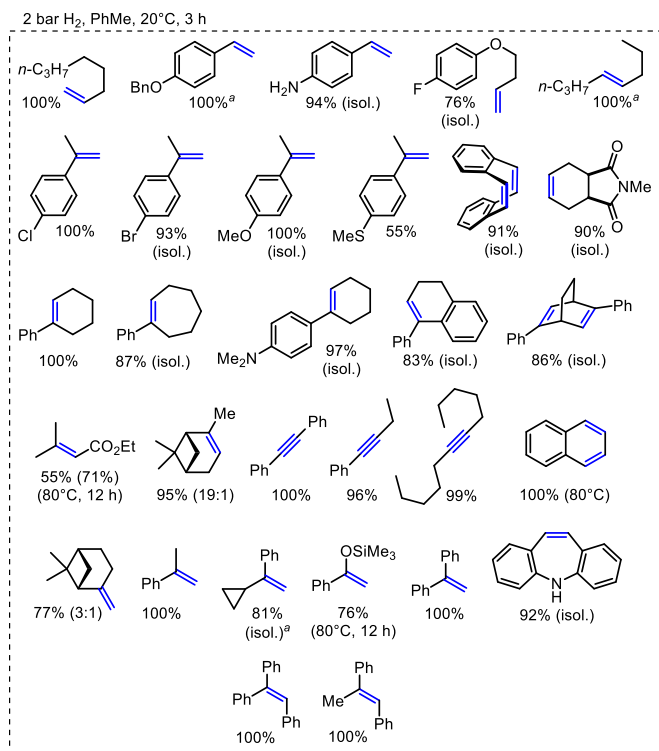
Table 3-2 - Robustness of the Fe(hmde)₂/Dibal-H catalyst.

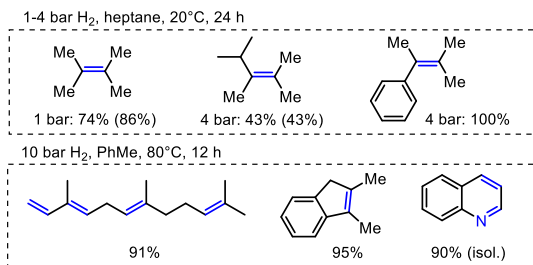


Entry	Reductant	Catalyst treatment	TOF [h ⁻¹]
1	Dibal-H	freshly prepared	41
2	Dibal-H	storage for 5 d in solution	37
3	Dibal-H	solvent removal, then dissolution	30
4	Dibal-H	solvent removal, storage for 5 d, then dissolution	27
5	Me ₃ Al	freshly prepared	13
6	Me ₃ Al	storage for 1 d in solution	<1
7	Dibal-H	from FeCl ₂ ·1.5thf, HN(TMS) ₂ , <i>n</i> -BuLi	27

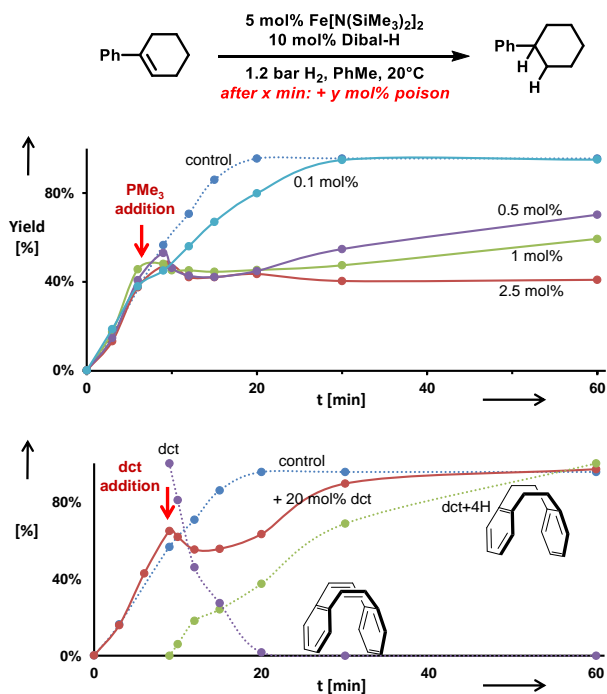
The mild conditions tolerated fluoride, chloride, bromide, silylenol ether, amine, imide, ester, thioether, and benzyl-ether functions. The hydrogenations of some challenging substrates required elevated temperature and/or pressure. Remarkably mild conditions enabled the hydrogenation of tetra-substituted alkenes (1-4 bar H₂, 20°C).^[4] The harsher

conditions required for complete hydrogenation of 1,2-dimethylindene might be a consequence of the low isomerization activity of the $\text{Fe}(\text{hmds})_2/\text{Dibal-H}$ catalyst.^[13] Notably, no ring-opening of α -cyclopropyl styrene was observed.^[14] With reduced catalyst loadings of 0.5 mol% $\text{Fe}(\text{hmds})_2$ and 1 mol% Dibal-H, turnover frequencies (TOF in h^{-1}) of 660 and 280 were recorded in the hydrogenations of 1-octene and α -methylstyrene, respectively (2 bar H_2 , PhMe, 20 °C, 5 min). Under the same conditions, conversion of 1-phenyl-1-cyclohexene required 3 mol% catalyst loading which resulted in a TOF of 60 h^{-1} . Alkynes were cleanly reacted to alkanes under identical conditions (Scheme 3-3). Kinetic poisoning studies were performed to ascertain the topology of the operating catalyst species.^[15] The addition of “sub-catalytic” amounts of trimethylphosphine (PMe_3) led to catalyst inhibition already at a catalyst/poison ratio of 10/1 (Scheme 3-4, top).^[16] Contrary to this, the selective homogeneous catalyst poison dibenzo-[a,e]cyclooctatetraene^[17] (dct, 4 equiv. per Fe) showed no significant inhibition but was merely a competing substrate for hydrogenation (Scheme 3-4, bottom). We thus postulate the operation of a heterotopic mechanism by polynuclear low-valent Fe catalysts.



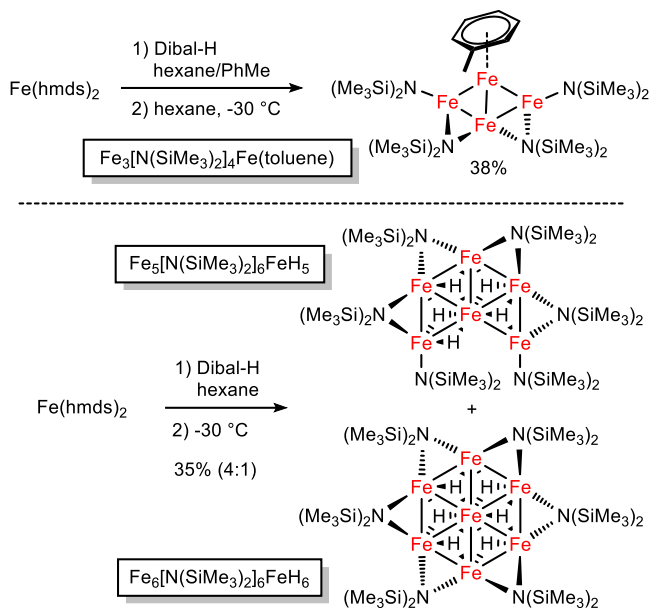


Scheme 3-3 - Substrate scope of iron-catalyzed hydrogenations of alkenes and alkynes. Bonds in blue indicate the site of complete π -bond hydrogenation. Standard conditions: 0.2 mmol alkene/alkyne, 0.5 M in toluene, 5 mol% Fe[N(SiMe₃)₂]₂, 10 mol% Dibal-H, 2 bar H₂, 20 °C, 3 h. If not otherwise noted, yields were determined by quantitative GC-FID vs. *n*-pentadecane. Conversions are given in parentheses if <90%; ^a 0.5 mol% Fe[N(SiMe₃)₂]₂, 1 mol% Dibal-H.

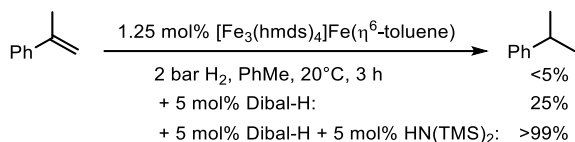


Scheme 3-4 - Poisoning studies with trimethylphosphine (PMe₃, top) and dibenzo[*a,e*]cyclooctatetraene (dct, bottom).

In an effort to identify potential catalytically active species, we investigated the reaction of $\text{Fe}[\text{N}(\text{SiMe}_3)_2]_2$ with Dibal-H under the conditions of the hydrogenation reactions (toluene or hexane, 20°C). The reaction of $\text{Fe}[\text{N}(\text{SiMe}_3)_2]_2$ and Dibal-H in a toluene/hexane mixture underwent rapid colour change from green to brown-black. Filtration, removal of the solvents, and crystallization from *n*-hexane afforded the dark crystalline Fe_4 nanocluster $\text{Fe}_3(\text{hmds})_4\text{Fe}(\text{toluene})$ in 38% yield (Scheme 3-5, Figure 1).^[18] Single crystal structure analysis showed a planar Fe_4 core which is peripherally decorated with four hmds ligands of which two hmds adopt a bridging μ^2 -coordination mode. One Fe atom bears an η^6 -toluene. The para-magnetic complex had a melting point of 123 °C and exhibited an effective magnetic moment $\mu_{\text{eff}} = 2.0 \mu_{\text{B}}$ (in C_6D_6). Two structurally related nanoclusters were isolated by slow solvent evaporation from the reaction of $\text{Fe}[\text{N}(\text{SiMe}_3)_2]_2$ and Dibal-H in *n*-hexane. Crystal structure analysis established the dark-red oligohydroidoiron clusters $\text{Fe}_5(\text{hmds})_6\text{FeH}_5$ and $\text{Fe}_6(\text{hmds})_6\text{FeH}_6$ (35% yield, 4/1, Scheme 3-5, Figure 3-1). The Fe_6 cluster is a truncated derivative of the Fe_7 cluster and bears one μ^2 -H and four μ^3 -H atoms coordinated to iron. The highly symmetrical Fe_7 cluster, a low-valent “Fe wheel”, contains six peripheral μ^2 -hmds ligands and six μ^3 -H ligands.^[19] The composition of the cluster mixture was further verified by X-ray analysis, elemental analysis, and LIFDI-MS (m/z 1301.2287, 1358.1793). The Fe_4 , Fe_6 and Fe_7 nanocluster architectures contain multiple iron centers in low oxidation states (formally Fe^0 , Fe^{I} , Fe^{II}) and constitute a distinct class of metallic cluster complexes^[20] that adopt rare planar Fe_n geometries and are void of the common carbonyl, nitrido, oxo and carbido ligands.^[21] Generally, discrete metallic clusters with direct interactions between the redox centers are considered as materials for optical, magnetic, and catalytic applications.^[22] Detailed studies of spectroscopic and coordination properties of the Fe nanoclusters are beyond the scope of this catalytic method development but will be reported soon. Preliminary studies proved that the Fe_4 nanocluster is a competent hydrogenation pre-catalyst in the presence of Dibal-H and $\text{HN}(\text{TMS})_2$ (Scheme 3-6).



Scheme 3-5 -Synthesis of novel planar Fe₄, Fe₆, and Fe₇ nanoclusters.



Scheme 3-6 - Catalytic hydrogenation with the isolated Fe₄ nanocluster.

3.2 Conclusions

In summary, we have developed an iron-catalyzed hydrogenation protocol that displays unprecedented activity for challenging tri- and tetra-substituted alkenes under very mild reaction conditions. The catalyst is prepared by reaction of $\text{Fe}[\text{N}(\text{SiMe}_3)_2]_2$ with diisobutyl-aluminium hydride or by a most user-friendly *in situ* method from FeCl_2 . The isolation of novel low-valent nanoclusters with planar Fe₄, Fe₆, and Fe₇ geometries under such conditions provides new insight into the interface of homogeneous/heterogeneous catalysis and the growth of metallic nanoparticle materials. Further studies of the spectroscopic and chemical properties of these and related planar $[(\text{amido})\text{Fe}]_n$ nanoclusters are currently being executed.

3.2 Experimental part

3.2.1 General

Chemicals and Solvents: Commercially available olefins were distilled under reduced pressure prior use. Solvents (THF, Et₂O, *n*-hexane, toluene) were distilled over sodium and benzophenone and stored over molecular sieves (4 Å). LiN(SiMe₃)₂ (*SigmaAldrich*, 97%) was sublimated and stored under argon. HN(SiMe₃)₂, HNEt₂, HN(*i*-Pr)₂, HNPhMe and 2,2,6,6-tetramethylpiperidine were distilled over CaH₂ and stored under argon prior use. HNPh₂ was recrystallized in *n*-pentane. Solvents used for column chromatography were distilled under reduced pressure prior use (ethyl acetate). DiBAIH (1 M in toluene), AlMe₃ (2 M in toluene), Al(^{*i*}Bu)₃ were used as received from *SigmaAldrich* or diluted before use.

Analytical Thin-Layer Chromatography: TLC was performed using aluminium plates with silica gel and fluorescent indicator (*Merck*, 60, F254). Thin layer chromatography plates were visualized by exposure to ultraviolet light (366 or 254 nm) or by immersion in a staining solution of molybdato-phosphoric acid in ethanol or potassium permanganate in water.

Column Chromatography: Flash column chromatography with silica gel 60 from *KMF* (0.040-0.063 mm). Mixtures of solvents used are noted in brackets.

High Pressure Reactor: Hydrogenation reactions were carried out in 160 and 300 mL high pressure reactors (*Parr*TM) in 4 mL glass vials. The reactors were loaded under argon, purged with H₂ (1 min), sealed and the internal pressure was adjusted. Hydrogen (99.9992%) was purchased from *Linde*.

¹H- und ¹³C-NMR-Spectroscopy: Nuclear magnetic resonance spectra were recorded on a *Bruker Avance 300* (300 MHz) and *Bruker Avance 400* (400 MHz). ¹H-NMR: The following abbreviations are used to indicate multiplicities: s = singlet; d = doublet; t = triplet, q = quartet; m = multiplet, dd = doublet of doublet, dt = doublet of triplet, dq = doublet of quartet, ddt = doublet of doublet of quartet. Chemical shift δ is given in ppm to tetramethylsilane.

Fourier-Transformations-Infrared-Spectroscopy (FT-IR): Spectra were recorded on a *Varian Scimitar 1000* FT-IR with ATR-device. All spectra were recorded at room temperature. Wave number is given in cm⁻¹. Bands are marked as s = strong, m = medium, w = weak and b = broad.

Gas chromatography with FID (GC-FID): HP6890 GC-System with injector 7683B and *Agilent 7820A* System. Column: HP-5, 19091J-413 (30 m × 0.32 mm × 0.25 μm),

carrier gas: N₂. GC-FID was used for reaction control and catalyst screening (Calibration with internal standard *n*-pentadecane and analytically pure samples).

Gas chromatography with mass-selective detector (GC-MS): *Agilent 6890N Network GC-System*, mass detector 5975 MS. Column: HP-5MS (30 m × 0.25 mm × 0.25 μm, 5% phenylmethylsiloxane, carrier gas: H₂. Standard heating procedure: 50 °C (2 min), 25 °C/min → 300 °C (5 min)

Chiral gas chromatography with FID (chiral GC-FID): *Fisons GC 8000*. Column: CP-Chirasil-Dex CB (25 m × 0.25 mm ID, 0.25 μm film), carrier gas: Ar. Injection 0.1 μL. Inlet: 200 °C, Detector: 200 °C, Column 50-200 °C with 3 to 10 °C per minute.

Headspace gas chromatography with TCD (HS-GC-TCD): *Infinicon 3000 Micro GC*. Column: 5 Å molecular sieves, carrier gas: argon. Standard heating procedure: 120 °C (3 min). Headspace GC-TCD was used for quantification of H₂, CH₄ and C₂H₆ in the reduction of FeX₂ salts (X = N(SiMe₃)₂, Cl) with aluminium organyls (DiBAIH, Al(^{*i*}Bu)₃, AlMe₃). Calibrations of examined gases were conducted by hydrolyzation of LiAlH₄ (H₂), MeMgCl (CH₄) and EtMgCl (C₂H₆).

Headspace gas chromatography with mass-selective detector (HS-GC-MS): *Agilent 7890 B GC-system*, mass detector *AccuTOF GCX* from *Jeol*. Column: HP 5 (30 m × 0.25 mm × 0.25 μm) from *Agilent*, carrier gas: helium. Standard heating procedure: 22.2 °C (2 min), 1 °C/min (17.8 min) → 40 °C (3 min) with a flow of 0.6 mL/min. Split 50:1. Injection: 1 μL at 120 °C.

High resolution mass spectrometry (HRMS): The spectra were recorded by the Central Analytics Lab at the Department of Chemistry, University of Regensburg, on a MAT SSG 710 A from *Finnigan*.

Gas-uptake reaction monitoring: Gas-uptake was monitored with a *Man On the Moon X201* kinetic system to maintain a constant reaction pressure. The system was purged with hydrogen prior use. Reservoir pressure was set to about 9 bar H₂. Calibration of the reservoir pressure drop in relation to H₂ consumption was performed by quantitative hydrogenation of various amounts of α -methylstyrene with a Pd/C catalyst in 1 mL of THF.

3.2.2 General procedures

3.2.3 General method for catalyst preparation

In an argon-filled glovebox a flame-dried flask was charged with a solution of $\text{Fe}[\text{N}(\text{SiMe}_3)_2]_2$ in toluene (50 mM, 1 mL, 50 μmol). A solution of DiBAIH in toluene (100 mM, 1 mL, 100 μmol) was added via syringe. The solution turned black immediately and was stirred at room temperature for 5 minutes prior to use.

3.2.4 General method for *in situ* catalyst preparation with $\text{LiN}(\text{SiMe}_3)_2$

In an argon-filled glovebox a flame-dried flask was charged with $\text{LiN}(\text{SiMe}_3)_2$ (16.7 mg; 100 μmol) and suspended in toluene (1 mL). $\text{FeCl}_2(\text{thf})_{1.5}$ (11.7 mg, 50 μmol) was added and the resulting suspension was stirred at room temperature. After 60 minutes a solution of DiBAIH in toluene (100 mM, 1 mL, 100 μmol) was added via syringe. The solution turned black immediately and was stirred at room temperature for 5 minutes prior to use.

3.2.5 General method for *in situ* catalyst preparation with various amines

In an argon-filled glovebox a flame-dried flask was charged with an amine (110 μmol) and toluene (0.8 mL). A solution of *n*-BuLi in toluene (50 mM, 0.2 mL, 100 μmol) was added at room temperature. After 30 minutes of stirring, $\text{FeCl}_2(\text{thf})_{1.5}$ (11.7 mg, 50 μmol) was added and the resulting suspension was stirred for 60 minutes. After that, a solution of DiBAIH in toluene (100 mM, 1 mL, 100 μmol) was added via syringe. The solution turned black immediately and was stirred at room temperature for 5 minutes prior to use.

3.2.6 General method for catalytic hydrogenation

In an argon-filled glovebox a flame-dried 4 mL reaction vial was charged with the substrate (0.2 mmol) and *n*-pentadecane as internal reference for GC-FID quantification (0.2 mmol). After addition of freshly prepared catalyst suspension (400 μL ; 5 mol% [Fe]), the reaction vial was transferred to a high pressure reactor which was sealed and removed from the glovebox. The reactor was purged with H_2 (3×3 bar) and the reaction pressure and temperature were set. After the indicated reaction time, the vial was retrieved and hydrolyzed with a saturated aqueous solution of sodium hydrogen carbonate (0.5 mL). The reaction mixture was extracted with ethyl acetate (1×0.5 mL) and analyzed by GC-FID and GC-MS.

For product isolation, 0.5 to 1 mmol of the starting material was used. After quenching, the product was extracted with ethyl acetate (3×3 mL), washed with brine (10 mL), dried over sodium sulfate and filtered over a pad of silica. Removal of the solvent at reduced pressure afforded the product in high purity.

3.2.7 General method for kinetic examination in catalytic hydrogenation

A flame-dried 10 mL 2-neck flask was connected to a *Man on the Moon X201* gas-uptake system and kept at 23 °C with the help of a water bath. After purging with H₂, the system was set to a reaction pressure of 1.9 bar. Freshly prepared catalyst mixture (1 mL) was added via syringe and stirred for 2 minutes. Monitoring of the hydrogen uptake started with the addition of the substrate (0.5 mmol).

Optimization experiments

Stability of the catalyst

The catalyst stability was determined by comparison of the hydrogenation rate of 1-phenylcyclohexene after several catalyst treatments. Turnover frequencies were calculated upon the yield after 7 minutes.

Table 3-S1 - Comparison of TOF after various catalyst pretreatments.

Entry	Reductant	Catalyst pretreatment	TOF ^a / h ⁻¹
1	DiBAIH	freshly prepared	41
2	DiBAIH	storage for 5 d in solution	37
3	DiBAIH	removal of solvent and resolution	30
4	DiBAIH	removal of solvent, storage for 5 d under argon and resolution	27
5	AlMe ₃	freshly prepared	13
6	AlMe ₃	storage for 20 h in solution	<1
7	DiBAIH	<i>in situ</i> synthesis of Fe[N(SiMe ₃) ₂] ₂	27

^a determined with yield after 7 minutes.

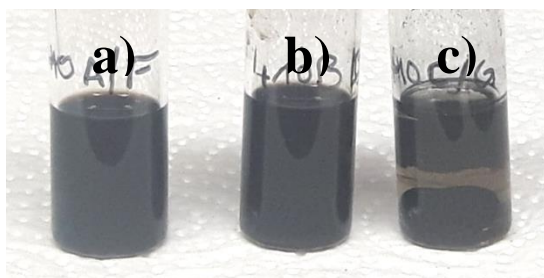


Figure 3-S1 - Catalyst in solution after 20 h storage under argon; a) $\text{Fe}[\text{N}(\text{SiMe}_3)_2]_2\text{-DiBAIH}$; b) $\text{FeCl}_2(\text{thf})_{1.5}\text{-LiN}(\text{SiMe}_3)_2\text{-DiBAIH}$; c) $\text{Fe}[\text{N}(\text{SiMe}_3)_2]_2\text{-AlMe}_3$.

3.2.8 Synthesis of catalysts, reagents, and starting materials

General procedure for styrene synthesis in a Wittig reaction

A 50 mL flask was charged with a suspension of methyltriphenylphosphonium bromide (1 equiv.) in THF (0.7 M). Then, NaH-suspension in paraffine (60%, 1 equiv.) was added in small portions. The reaction mixture was stirred at room temperature for 20 h followed by a dropwise addition of a solution of a ketone/aldehyde derivative (1 equiv.) in THF (0.7 M). The reaction mixture was stirred for 2 d at room temperature, quenched with H_2O (15 mL) and extracted with Et_2O (3×15 mL). The combined organic layers were dried (Na_2SO_4), concentrated and subjected to silica gel flash chromatography (*n*-pentane).

Synthesis of $\{\text{Fe}[\text{N}(\text{SiMe}_3)_2]_2\}$

Synthesis according to R. A. Andersen, K. Faegri, J. C. Green, A. Haaland, M. F. Lappert, W. P. Leung, K. Rypdal, *Inorg. Chem.* **1988**, 27, 1782–1786 with slight modifications.

A flame-dried *Schlenk*-flask under argon was charged with $\text{LiN}(\text{SiMe}_3)_2$ (6.37 g, 2.2 equiv., 38.1 mmol) in diethyl ether (60 mL). At 0 °C FeCl_2 (2.24 g, 1.0 equiv., 17.1 mmol, 97%) was added in portions. The resulting reaction mixture was allowed to warm to room temperature and stirred for 24 h. The solid residue was suspended in *n*-hexane (25 mL) filtered over a glass frit and washed with *n*-hexane (5×3 mL). After removing the solvent under reduced pressure, the crude product was purified by distillation under reduced pressure (90 °C, 10^{-3} mbar) to obtain a dark green oil which crystallizes upon standing at room temperature.



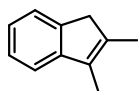
753.24 g/mol

Yield 4.71 g, 12.5 mmol (73%)
¹H-NMR (400 MHz, C₆D₆) δ = 64.10 (bs).

Analytical data were in full agreement with R. A. Andersen, K. Faegri, J. C. Green, A. Haaland, M. F. Lappert, W. P. Leung, K. Rypdal, *Inorg. Chem.* **1988**, 27, 1782–1786.

2,3-Dimethyl-1H-indene

Synthesis following the procedure described by M. V. Troutman, D. H. Appella, S. L. Buchwald, *J. Am. Chem. Soc.* **1999**, 121, 4916–4917.

C₁₁H₁₂

144.22 g/mol

Appearance colorless liquid

Yield 1.49 g, 10.3 mmol (69%)

TLC *R*_f = 0.66 (SiO₂, *n*-pentane)

¹H-NMR (300 MHz, CDCl₃) δ 7.37 (m, 1H), 7.31 – 7.21 (m, 2H), 7.12 (m, 1H), 3.31 – 3.21 (m, 2H), 2.07 (m, 3H), 2.04 (m, 3H).

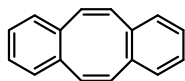
¹³C-NMR (75 MHz, CDCl₃) δ 126.05, 123.55, 122.97, 117.91, 42.46, 13.95, 10.17.

GC-MS *t*_R = 6.77 min, (EI, 70 eV): *m/z* = 144 [M⁺], 129, 115, 89, 77, 63, 51.

Analytical data were in full agreement with M. G. Schrems, E. Neumann, A. Pfaltz, *Angew. Chem. Int. Ed.* **2007**, 46, 8274–8276.

Dibenzo[*a,e*]cyclooctatetraene (dct)

Synthesis following the procedure described by G. Franck, M. Brill, G. Helmchen, *J. Org. Chem.* **2012**, 89, 55-65.

C₁₆H₁₂

204.27 g/mol

Appearance colorless solid

Yield 912 mg, 4.46 mmol (47%)

TLC *R*_f = 0.46 (SiO₂, hexanes)

¹H-NMR (300 MHz, CDCl₃): δ 7.19–7.13 (m, 4H), 7.10–7.02 (m, 4H), 6.76 (s, 4H).

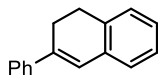
¹³C-NMR (75 MHz, CDCl₃): δ 137.1, 133.3, 129.1, 126.8.

GC-MS *t*_R = 9.35 min, (EI, 70 eV): *m/z* = 204 [M⁺].

Analytical data were in full agreement with G. Franck, M. Brill, G. Helmchen, *J. Org. Chem.* **2012**, *89*, 55-65.

4-Phenyl-1,2-dihydronaphthalene

Synthesis was performed by Schachtner, Josef, *Dissertation* **2016**, Regensburg.



C₁₆H₁₄

206.29 g/mol

Appearance colorless liquid

Yield 912 mg, 4.46 mmol (47%)

TLC *R*_f = 0.41 (SiO₂, hexanes)

¹H-NMR (300 MHz, CDCl₃) δ 7.43 – 7.27 (m, 5H), 7.24 – 7.05 (m, 3H), 7.01 (dd, *J* = 7.4, 1.6 Hz, 1H), 6.09 (t, *J* = 4.7 Hz, 1H), 2.86 (m, 2H), 2.42 (ddd, *J* = 9.1, 7.2, 4.7 Hz, 2H).

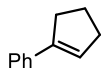
¹³C-NMR (75 MHz, CDCl₃) δ 128.9, 128.3, 127.8, 127.7, 127.2, 126.3, 125.6, 28.4, 23.7.

GC-MS *t*_R = 9.37 min, (EI, 70 eV): *m/z* = 206 [M]⁺, 178, 165, 152, 128, 102, 78, 51.

Analytical data were in full agreement with P. Peach, D. J. Cross, J. A. Kenny, I. Houson, L. Campbell, T. Walsgrove, M. Wills, *Tetrahedron*, **2006**, *62*, 1864-1876.

1-Phenyl-1-cyclopentene

Synthesis was performed by Schachtner, Josef, *Dissertation* **2016**, Regensburg.



C₁₁H₁₂

144.22 g/mol

Appearance colorless liquid

Yield 1.99 g, 13.8 mmol (69%)

TLC *R*_f = 0.66 (SiO₂, hexanes)

¹H-NMR (300 MHz, CDCl₃) δ 7.48 – 7.42 (m, 2H), 7.36 – 7.27 (m, 2H), 7.25 – 7.18 (m, 1H), 6.19 (m, 1H), 2.82 – 2.61 (m, 2H), 2.54 (m, 2H), 2.15 – 1.93 (m, 2H).

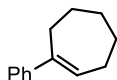
$^{13}\text{C-NMR}$ (75 MHz, CDCl_3) δ 128.29, 128.27, 127.60, 126.82, 126.12, 125.91, 125.54, 66.45, 33.37, 33.18, 28.91, 28.08, 23.37, 19.35.

GC-MS $t_R = 6.94$ min, (EI, 70 eV): $m/z = 144$ $[\text{M}]^+$, 129, 115, 103, 91, 77, 63, 51.

Analytical data were in full agreement with W. Su, S. Urgaonkar, P. A. McLaughlin, J. G. Verkade, *J. Am. Chem. Soc.* **2004**, 126, 16433–16439.

1-Phenyl-1-cycloheptene

Synthesis was performed by Schachtner, Josef, *Dissertation* **2016**, Regensburg.



$\text{C}_{13}\text{H}_{16}$

172.27 g/mol

Appearance

colorless liquid

Yield

2.89 g, 16.8 mmol (84%)

TLC

$R_f = 0.69$ (SiO_2 , hexanes)

$^1\text{H-NMR}$

(300 MHz, CDCl_3) δ 7.42 – 7.16 (m, 5H), 6.13 (m, 1H), 2.75 – 2.52 (m, 2H), 2.43 – 2.25 (m, 2H), 1.94 – 1.80 (m, 2H), 1.74 – 1.50 (m, 4H).

$^{13}\text{C-NMR}$

(75 MHz, CDCl_3) δ 144.99, 130.45, 128.13, 126.26, 125.67, 32.86, 32.82, 28.92, 26.98, 26.85.

GC-MS

$t_R = 7.97$ min, (EI, 70 eV): $m/z = 172$ $[\text{M}^+]$, 157, 144, 129, 115, 104, 91, 77, 63, 51.

Analytical data were in full agreement with G. Baddeley, J. Chadwick, H. T. Taylor, *J. Chem. Soc.* **1956**, 451.

(1-cyclopropylvinyl)benzene

Synthesis following the general procedure for styrene synthesis in a Wittig reaction.



$\text{C}_{11}\text{H}_{12}$

144.22 g/mol

Appearance

colorless liquid

Yield

1.27 g, 8.8 mmol (80%)

TLC

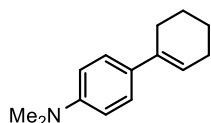
$R_f = 0.53$ (SiO_2 , hexanes)

¹H-NMR	(300 MHz, CDCl ₃) δ 7.67 – 7.57 (m, 2H), 7.42 – 7.26 (m, 3H), 5.30 (m, 1H), 4.95 (m, 1H), 1.67 (ttd, <i>J</i> =8.3, 5.4, 1.2, 1H), 0.92 – 0.79 (m, 2H), 0.61 (ddd, <i>J</i> =6.4, 5.4, 4.1, 2H).
¹³C-NMR	(75 MHz, CDCl ₃) δ 149.47, 141.75, 128.28, 127.58, 126.25, 109.15, 77.58, 77.16, 77.16, 76.74, 15.78, 6.83.
GC-MS	<i>t</i> _R = 6.31 min, (EI, 70 eV): <i>m/z</i> = 144 [M ⁺], 129, 115, 103, 91, 77, 63, 51.

Analytical data were in full agreement with C. Chatalova-Sazepin, Q. Wang, G. M. Sammis, J. Zhu, *Angew. Chem. Int. Ed.* **2015**, *54*, 5443–5446.

4-(Cyclohex-1-enyl)-*N,N*-dimethylaniline

Synthesis was performed by Schachtner, Josef, *Dissertation* **2016**, Regensburg.



C₁₄H₁₉N

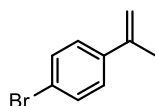
201.31 g/mol

Appearance	colorless liquid
Yield	1.65 g, 8.20 mmol (82%)
TLC	<i>R</i> _f = 0.82 (SiO ₂ , hexanes)
¹H-NMR	(300 MHz, CDCl ₃) δ 7.41 – 7.19 (m, 2H), 6.76 (ddd, <i>J</i> = 13.1, 6.8, 2.8 Hz, 2H), 6.06 – 6.00 (m, 1H), 2.96 (m, 6H), 2.35 – 2.49 (m, 2H), 2.27 – 2.14 (m, 2H), 1.87 – 1.73 (m, 2H), 1.61 – 1.72 (m, 2H).
¹³C-NMR	(75 MHz, CDCl ₃) δ 149.4, 136.0, 129.1, 125.6, 121.7, 116.7, 112.7, 112.6, 40.8, 40.7, 27.4, 25.9, 23.2, 22.4.
GC-MS	<i>t</i> _R = 9.59 min, (EI, 70 eV): <i>m/z</i> = 202 [M ⁺], 180, 157, 129, 101, 77, 51.

Analytical data were in full agreement with K. Ishiuka, H. Seike, T. Hatakeyama, M. Nakamura, *J. Am. Chem. Soc.* **2010**, *132*, 13117–13119.

4-Bromo-*α*-methylstyrene

Synthesis following the general procedure for styrene synthesis in a Wittig reaction.



C₉H₉Br

197.08 g/mol

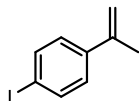
Appearance	colorless oil
-------------------	---------------

Yield	1.06 g, 5.39 mmol (77%)
TLC	$R_f = 0.59$ (SiO ₂ , <i>n</i> -pentane)
¹H-NMR	(400 MHz, CDCl ₃) δ 7.50-7.35 (m, 2H), 7.42-7.29 (m, 2H), 5.36 (s, 1H), 5.10 (s, 1H), 2.12 (s, 3H).
¹³C-NMR	(101 MHz, CDCl ₃) δ 142.2, 140.1, 131.3, 127.2, 121.4, 113.1, 21.7.
GC-MS	$t_R = 6.51$ min, (EI, 70 eV): $m/z = 197$ [M ⁺], 183, 171, 156, 115, 102, 91, 75, 63, 51.

Analytical data were in full agreement with T. Taniguchi, A. Yajima, H. Ishibashi, *Adv. Synth. Catal.* **2011**, 353, 2643–2647.

4-Iodo- α -methylstyrene

Synthesis following the general procedure for styrene synthesis in a Wittig reaction.



C₉H₉I

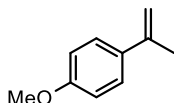
244.08 g/mol

Appearance	colorless solid
Yield	1.21 g, 4.96 mmol (71%)
TLC	$R_f = 0.84$ (SiO ₂ , <i>n</i> -pentane)
¹H-NMR	(300 MHz, CDCl ₃) δ 7.70 – 7.59 (m, 2H), 7.24 – 7.15 (m, 2H), 5.40 – 5.33 (m, 1H), 5.12 – 5.07 (m, 1H), 2.14 – 2.09 (m, 3H).
¹³C-NMR	(75 MHz, CDCl ₃) δ 142.28, 140.70, 137.27, 134.97, 127.41, 113.15, 92.88, 21.62.
GC-MS	$t_R = 7.14$ min, (EI, 70 eV): $m/z = 244$ [M ⁺], 127, 115, 102, 91, 75, 63, 50.

Analytical data were in full agreement with G. B. Bachman, C. L. Carlson, M. Robinson, *J. Am. Chem. Soc.* **1951**, 73, 1964–1965.

4-Methoxy- α -methylstyrene

Synthesis following the general procedure for styrene synthesis in a Wittig reaction.



C₁₀H₁₂O

148.20 g/mol

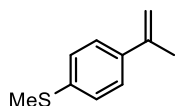
Appearance	colorless liquid
-------------------	------------------

Yield	1.04 g, 7.02 mmol (35%)
TLC	$R_f = 0.25$ (SiO ₂ , <i>n</i> -pentane)
¹H-NMR	(300 MHz, CDCl ₃) δ 7.42 (m, 2H), 6.87 (m, 2H), 5.29 (m, 1H), 4.99 (m, 1H), 3.82 (s, 3H), 2.13 (s, 3H).
¹³C-NMR	(75 MHz, CDCl ₃) δ 159.05, 142.56, 133.74, 126.60, 113.54, 110.68, 55.30, 21.94.
GC-MS	$t_R = 6.39$ min, (EI, 70 eV): $m/z = 148$ [M ⁺], 127, 133, 115, 105, 89, 77, 63, 51.

Analytical data were in full agreement with A. Fryszkowska, K. Fisher, J. M. Gardiner, G. M. Stephens, *J. Org. Chem.* **2008**, 73, 4295-4298.

Methyl(4-(prop-1-en-2-yl)phenyl)sulfane

Synthesis following the general procedure for styrene synthesis in a Wittig reaction.



C₁₀H₁₂S

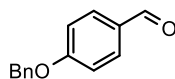
164.27 g/mol

Appearance	colorless solid
Yield	1.09 g, 6.63 mmol (33%)
TLC	$R_f = 0.44$ (SiO ₂ , <i>n</i> -pentane)
¹H-NMR	(300 MHz, CDCl ₃) δ 7.45 – 7.35 (m, 2H), 7.25 – 7.18 (m, 2H), 5.36 (dq, $J=1.6, 0.8$, 1H), 5.06 (dq, $J=1.5, 1.5$, 1H), 2.49 (s, 3H), 2.14 (dd, $J=1.5, 0.8$, 3H).
¹³C-NMR	(75 MHz, CDCl ₃) δ 142.51, 138.01, 137.49, 126.37, 125.90, 111.96, 21.75, 15.91.
GC-MS	$t_R = 7.38$ min, (EI, 70 eV): $m/z = 164$ [M ⁺], 149, 134, 115, 102, 91, 77, 69, 51.

Analytical data were in full agreement with G. Fraenkel, J. M. Geckle, *J. Am. Chem. Soc.* **1980**, 102, 2869–2880.

4-(Benzyloxy)benzaldehyde

Synthesis following the procedure by S. K. Das, G. Panda, *Tetrahedron* **2008**, 19, 4162-4173.



C₁₄H₁₂O₂

212.24 g/mol

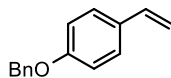
Appearance	colorless solid
-------------------	-----------------

Yield	1.72 g, 8.12 mmol (81%)
TLC	$R_f = 0.20$ (SiO ₂ , hexanes/ethyl acetate = 9/1)
¹H-NMR	(300 MHz, CDCl ₃) δ 9.89 (s, 1H), 7.84 (d, $J = 8.7$ Hz, 2H), 7.48 – 7.33 (m, 5H), 7.08 (d, $J = 8.7$ Hz, 2H), 5.16 (s, 2H).
¹³C-NMR	(75 MHz, CDCl ₃) δ 190.82, 163.72, 135.93, 132.02, 130.11, 128.75, 128.36, 127.51, 115.15, 70.28.
GC-MS	$t_R = 9.96$ min, (EI, 70 eV): $m/z = 212$ [M ⁺], 152, 121, 91, 77, 65, 51.

Analytical data were in full agreement with T. Shintou, T. Mukaiyama, *J. Am. Chem. Soc.*, **2004**, *23*, 7359-7367.

1-(Benzyloxy)-4-vinylbenzene

Synthesis following the general procedure for styrene synthesis in a Wittig reaction.



C₁₅H₁₄O

210.27 g/mol

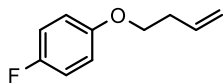
Appearance	colorless solid
Yield	1.25 g, 5.97 mmol (74%)
TLC	$R_f = 0.28$ (SiO ₂ , <i>n</i> -pentane)
¹H-NMR	(300 MHz, CDCl ₃) δ 7.49 – 7.29 (m, 7H), 6.99 – 6.90 (m, 2H), 6.67 (dd, $J = 17.6, 10.9$ Hz, 1H), 5.63 (dd, $J = 17.6, 0.9$ Hz, 1H), 5.14 (dd, $J = 10.9, 0.9$ Hz, 1H), 5.08 (s, 2H).
¹³C-NMR	(75 MHz, CDCl ₃) δ 158.57, 136.94, 136.21, 130.69, 128.63, 128.02, 127.50, 127.43, 114.88, 111.75, 70.03.
GC-MS	$t_R = 9.40$ min, (EI, 70 eV): $m/z = 197$ [M ⁺], 183, 171, 156, 115, 102, 91, 75, 63, 51.

Analytical data were in full agreement with N. Kakusawa, K. Yamaguchi, J. Kouchichiro, *J. Organomet. Chem.* **2005**, *12*, 2956-2966.

1-(but-3-en-1-yloxy)-4-fluorobenzene

Synthesis following the procedure by J. A. Murphy, F. Schoenebeck, N. J. Findlay, D. W. Thomson, S. Zhou, J. Garnier; *J. Am. Chem. Soc.* **2009**, *131*, 6475-6479.

C₁₀H₁₁FO



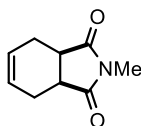
166.20 g/mol

Appearance

colorless liquid

Yield

1.89 g, 11.38 mmol (76%)

TLC $R_f = 0.80$ (SiO₂, hexanes/ethyl acetate = 99/1)**¹H-NMR**(300 MHz, CDCl₃) δ 7.03 – 6.91 (m, 2H), 6.88 – 6.78 (m, 2H), 5.90 (ddt, $J = 17.0, 10.2, 6.7$ Hz, 1H), 5.14 (qdd, $J = 3.0, 2.6, 1.4$ Hz, 2H), 3.97 (t, $J = 6.7$ Hz, 2H), 2.53 (qt, $J = 6.7, 1.3$ Hz, 2H).**¹³C-NMR**(75 MHz, CDCl₃) δ 158.81, 155.66, 155.00, 134.37, 117.11, 115.92, 115.62, 115.59, 115.49, 67.86, 33.67.**GC-MS** $t_R = 5.96$ min, (EI, 70 eV): $m/z = 166$ [M⁺], 138, 125, 112, 95, 83, 75, 55.**HRMS**(EI, m/z): found 166.0798 [M⁺] (calculated 166.0794).**FT-IR**(ATR-film) in [cm⁻¹] 2872 (w), 1642 (w), 1504 (s), 1472 (m), 1431 (w), 1388 (w), 1294 (w), 1247 (m), 1202 (s), 1096 (m), 1036 (m), 988 (m), 916 (s), 825 (s), 744 (s), 513 (s).**N-Methyl-1,2,3,6-tetrahydrophthalimide**Synthesis was performed by Schachtner, Josef, *Dissertation* **2016**, Regensburg.C₉H₁₁NO₂

165.19 g/mol

Appearance

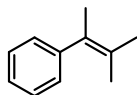
colorless solid

Yield

5.7 g, 34.5 mmol (70%)

TLC $R_f = 0.42$ (SiO₂, hexanes/ethyl acetate 2/1)**¹H-NMR**(400 MHz, CDCl₃): δ 5.92-5.85 (m, 2H), 3.12-3.05 (m, 2H), 2.96 (s, 3H), 2.64-2.58 (m, 2H), 2.27-2.19 (m, 2H).**GC-MS** $t_R = 7.58$ min (EI, 70 eV): $m/z = 165$ [M⁺], 150, 136, 107, 80, 65, 57, 51.Analytical data were in full agreement with E. Schefczik, *Chem. Ber.* **1965**, 98, 1270–1281.**(3-methylbut-2-en-2-yl)benzene**

Synthesis following the procedure by W. Adam, M. A. Arnold, M. Grüne, W. M. Nau, U. Pischel, C. R. Saha-Möller, *Organic Letters* **2002**, *4*, 537-540.



$C_{11}H_{14}$

146,23 g/mol

Appearance

colorless liquid

Yield

850 mg, 5.8 mmol (39%)

1H -NMR

(300 MHz, $CDCl_3$) δ 7.36 – 7.13 (m, 5H), 1.99 (s, 3H), 1.84 (s, 3H), 1.62 (s, 3H).

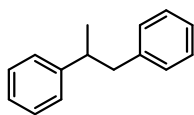
^{13}C -NMR

(75 MHz, $CDCl_3$) δ 145.35, 130.00, 128.44, 127.94, 127.23, 125.73, 22.11, 20.85, 20.59.

GC-MS

t_R = 5,62 min. (EI, 70 eV): m/z = 146 [M^+], 131, 115, 103, 91, 77, 65, 51.

Analytical data were in full agreement with W. Adam, M. A. Arnold, M. Grüne, W. M. Nau, U. Pischel, C. R. Saha-Möller, *Org. Lett.* **2002**, *4*, 537-540.

Hydrogenation products**Propane-1,2-diylidibenzene**C₁₅H₁₆

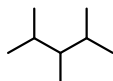
196,29 g/mol

¹H-NMR (300 MHz, CDCl₃) δ 7.44 – 7.10 (m, 10H), 3.17 – 2.95 (m, 2H), 2.91 – 2.78 (m, 1H), 1.31 (d, *J* = 6.8 Hz, 3H).

¹³C-NMR (75 MHz, CDCl₃) δ 147.05, 140.88, 129.23, 128.37, 128.17, 127.11, 126.09, 125.91, 45.13, 41.96, 21.23.

GC-MS *t_R* = 8,24 min, (EI, 70 eV): *m/z* = 196 [M⁺], 178, 165, 152, 139, 128, 115, 105, 91, 77, 65, 51.

Analytical data were in full agreement with C. Metallinos, J. Zaifman, L. Van Belle, L. Dodge, M. Pilkington, *Organometallics* **2009**, 28, 4534-4543.

2,3,4-trimethylpentaneC₈H₁₈

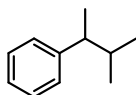
114,23 g/mol

¹H-NMR (300 MHz, CDCl₃) δ 1.73 – 1.54 (m, 2H), 1.00 – 0.92 (m, 1H), 0.87 (d, *J* = 6.8 Hz, 6H), 0.79 (d, *J* = 6.7 Hz, 6H), 0.73 (d, *J* = 6.8 Hz, 3H).

¹³C-NMR (75 MHz, CDCl₃) δ 45.12, 29.65, 21.73, 18.31, 10.81.

GC-MS *t_R* = 2,24 min, (EI, 70 eV): *m/z* = 114 [M⁺], 83, 71, 55.

Analytical data were in full agreement with the data available on vendor website (Sigma-Aldrich product number 257508, CAS Number 565-75-3)

(3-methylbutan-2-yl)benzeneC₁₁H₁₆

148,28 g/mol

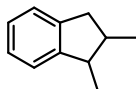
¹H-NMR (300 MHz, CDCl₃) δ 7.35 – 7.14 (m, 5H), 2.42 (m, 1H), 1.77 (m, 1H), 1.24 (d, *J* = 7.0 Hz, 3H), 0.94 (d, *J* = 6.7 Hz, 3H), 0.76 (d, *J* = 6.7 Hz, 3H).

¹³C-NMR (75 MHz, CDCl₃) δ 147.10, 128.02, 127.65, 125.68, 46.88, 34.45, 21.20, 20.20, 18.78.

GC-MS $t_R = 5,41$ min, (EI, 70 eV): $m/z = 148$ [M^+], 131, 115, 105, 77, 65, 51.

Analytical data were in full agreement with V. Jurčík, S. P. Nolan, C. S. J. Cazin, *Chemistry – A European Journal* **2009**, 15, 2509-2511.

1,2-dimethyl-2,3-dihydro-1H-indene



$C_{11}H_{14}$

146.23 g/mol

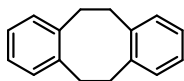
1H -NMR (400 MHz, $CDCl_3$) δ 7.23 – 7.10 (m, 4H), 3.17 (m, 1H), 3.04 – 2.92 (m, 1H), 2.63 – 2.53 (m, 2H), 1.15 (d, $J = 7.2$ Hz, 3H), 0.99 (d, $J = 6.8$ Hz, 3H).

^{13}C -NMR (75 MHz, $CDCl_3$) δ 148.81, 142.95, 126.10, 126.04, 124.48, 123.59, 42.39, 39.39, 37.84, 15.20, 14.67.

GC-MS $t_R = 6.03$ min, (EI, 70 eV): $m/z = 146$ [M^+], 131, 115, 103, 91, 77, 63, 51.

Analytical data were in full agreement with R. P. Yu, J. M. Darmon, J. M. Hoyt, G. W. Margulieux, Z. R. Turner, P. J. Chirik, *ACS Catal.* **2012**, 2, 1760–1764.

5,6,11,12-tetrahydridibenzo[*a,e*][8]annulene



$C_{16}H_{16}$

208.30 g/mol

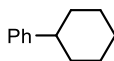
1H -NMR (300 MHz, $CDCl_3$) δ 7.06 – 6.93 (m, 8H), 3.07 (s, 8H).

^{13}C -NMR (75 MHz, $CDCl_3$) δ 140.60, 129.67, 126.10, 35.16.

GC-MS $t_R = 9.45$ min, (EI, 70 eV): $m/z = 208$ [M^+], 193, 178, 165, 115, 104, 91, 78, 63, 51.

Analytical data were in full agreement with D. Guijarro, B. Mancheño, M. Yus, *Tetrahedron* **1992**, 48, 4593–4600.

Phenylcyclohexane



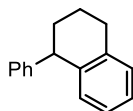
$C_{12}H_{16}$

160.26 g/mol

¹H-NMR	(300 MHz, CDCl ₃) δ 7.34 – 7.25 (m, 2H), 7.24 – 7.14 (m, 3H), 2.60 – 2.39 (m, 1H), 2.00 – 1.79 (m, 4H), 1.80 – 1.73 (m, 1H), 1.51 – 1.19 (m, 5H).
¹³C-NMR	(75 MHz, CDCl ₃) δ 148.1, 128.3, 126.5, 125.8, 44.7, 34.52, 27.0, 26.2.
GC-MS	<i>t</i> _R = 7.30 min, (EI, 70 eV): <i>m/z</i> = 160 [M ⁺], 143, 129, 115, 102, 91, 77, 63, 51.

Analytical data were in full agreement with W. M. Czaplik, M. Mayer, A. Jacobi von Wangelin, *Angew. Chem. Int. Ed.* **2009**, *48*, 607–610.

1-Phenyl-1,2,3,4-tetrahydronaphthalene



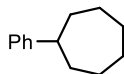
C₁₆H₁₆

208.30 g/mol

¹H-NMR	(300 MHz, CDCl ₃) δ 7.37 – 7.10 (m, 7H), 7.09 – 7.01 (m, 1H), 6.86 (d, <i>J</i> = 7.8 Hz, 1H), 4.14 (t, <i>J</i> = 6.6 Hz, 1H), 3.04 – 2.76 (m, 2H), 2.31 – 2.10 (m, 1H), 2.03 – 1.68 (m, 3H).
¹³C-NMR	(75 MHz, CDCl ₃) δ 147.55, 139.40, 137.61, 130.21, 128.99, 128.88, 128.25, 125.96, 125.92, 125.66, 45.65, 33.30, 29.82, 21.00.
GC-MS	<i>t</i> _R = 9.33 min, (EI, 70 eV): <i>m/z</i> = 208 [M ⁺], 179, 165, 152, 130, 115, 104, 91, 78, 63, 51.

Analytical data were in full agreement with S. T. Bright, J. M. Coxon, P. J. Steel, *J. Org. Chem.* **1990**, *55*, 1338–1344.

Phenylcycloheptane



C₁₃H₁₈

174.29 g/mol

¹H-NMR	(300 MHz, CDCl ₃) δ 7.35 – 7.11 (m, 5H), 2.76 – 2.56 (m, 1H), 2.00 – 1.75 (m, 4H), 1.74 – 1.49 (m, 8H).
¹³C-NMR	(75 MHz, CDCl ₃) δ 150.05, 128.31, 126.70, 125.52, 47.10, 36.86, 27.99, 27.27.
GC-MS	<i>t</i> _R = 7.80 min, (EI, 70 eV): <i>m/z</i> = 174 [M ⁺], 117, 104, 91, 78, 65, 55.

Analytical data were in full agreement with S. Kawamura, K. Ishizuka, H. Takaya, M. Nakamura, *Chem. Commun.* **2010**, 46, 6054–6056.

1,1-Diphenylethane



C₁₄H₁₄

182.27 g/mol

¹H-NMR (300 MHz, CDCl₃) δ 7.35 – 7.11 (m, 10H), 4.15 (q, *J* = 7.1, 1H), 1.63 (d, *J* = 7.2, 3H).

GC-MS *t*_R = 7.97 min, (EI, 70 eV): *m/z* = 182 [M⁺], 167, 152, 139, 128, 115, 103, 89, 77, 63, 51.

Analytical data were in full agreement with F. Schoenebeck, J. A. Murphy, S.-z. Zhou, Y. Uenoyama, Y. Miclo, T. Tuttle, *J. Am. Chem. Soc.* **2007**, 129, 13368–13369.

1-Cyclopropyl-1-phenylethane



C₁₁H₁₄

146.23 g/mol

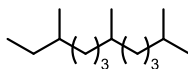
¹H-NMR (300 MHz, CDCl₃) δ 7.41 – 7.26 (m, 4H), 7.25 – 7.17 (m, 1H), 1.99 (dq, *J* = 9.2, 7.0 Hz, 1H), 1.35 (d, *J* = 7.0 Hz, 3H), 0.96 (qt, *J* = 9.2, 8.0, 5.0 Hz, 1H), 0.65 – 0.36 (m, 2H), 0.27 – 0.09 (m, 2H).

¹³C-NMR (75 MHz, CDCl₃) δ 147.38, 128.23, 127.00, 125.89, 44.67, 21.62, 18.56, 4.64, 4.34.

GC-MS *t*_R = 5.87 min, (EI, 70 eV): *m/z* = 146 [M⁺], 131, 117, 105, 91, 77, 65, 51.

Analytical data were in full agreement with T. N. Gieshoff, M. Villa, A. Welther, M. Plois, U. Chakraborty, R. Wolf, A. Jacobi von Wangelin, *Green Chem* **2015**, 17, 1408–1413.

2,6,10-Trimethyldodecane



C₁₅H₃₂

212.42 g/mol

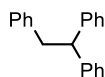
¹H-NMR (300 MHz, CDCl₃) δ 1.77 – 1.44 (m, 4H), 1.42 – 0.98 (m, 14H), 0.93 – 0.75 (m, 14H).

$^{13}\text{C-NMR}$ (75 MHz, CDCl_3) δ 42.41, 39.43, 39.39, 37.88, 37.48, 37.43, 37.41, 37.32, 37.01, 36.97, 35.76, 35.64, 34.47, 34.44, 34.42, 33.07, 32.83, 32.80, 30.56, 29.59, 29.49, 28.47, 28.00, 25.31, 24.84, 24.53, 22.78, 22.74, 22.64, 19.76, 19.70, 19.28, 19.22, 16.22, 11.46, 11.43.

GC-MS $t_{\text{R}} = 7.18$ min, (EI, 70 eV): $m/z = 212$ [M^+], 183, 127, 113, 85, 71, 57.

Analytical data were in full agreement with D. K. Dalling, R. J. Pugmire, D. M. Grant, W. E. Hull, *Magn. Reson. Chem.* **1986**, *24*, 191–198.

Ethane-1,1,2-triyltribenzene



$\text{C}_{20}\text{H}_{18}$

258.36 g/mol

$^1\text{H-NMR}$ (300 MHz, CDCl_3) δ 7.30 - 6.95 (m, 15H), 4.24 (t, $J = 7.8$ Hz, 1H), 3.37 (d, $J = 7.8$ Hz, 2H).

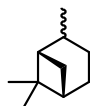
$^{13}\text{C-NMR}$ (75 MHz, CDCl_3) δ 144.45, 140.26, 129.08, 128.34, 128.05, 126.19, 125.88, 53.11, 42.11.

GC-MS $t_{\text{R}} = 10.67$ min, (EI, 70 eV): $m/z = 258$ [M^+], 167, 152, 139, 128, 115, 102, 91, 77, 65, 51.

Analytical data were in full agreement with T. C. Fessard, H. Motoyoshi, E. M. Carreira, *Angew. Chem. Int. Ed.* **2007**, *46*, 2078–2081.

Pinane

Mixture of diastereomers.



$\text{C}_{10}\text{H}_{18}$

138.25 g/mol

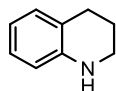
$^1\text{H-NMR}$ mixture of isomers

$^{13}\text{C-NMR}$ (75 MHz, CDCl_3) δ 67.98, 65.88, 48.07, 47.62, 41.35, 40.88, 39.49, 38.82, 35.95, 33.96, 29.35, 28.30, 26.84, 26.54, 25.63, 24.61, 23.93, 23.83, 23.22, 23.04, 22.90, 21.61, 20.09, 15.29.

GC-MS $t_{\text{R}} = 4.67$ min, (EI, 70 eV): $m/z = 138$ [M^+], 123, 95, 81, 67, 55.

Analytical data were in full agreement with A. Stolle, B. Ondruschka, W. Bonrath, T. Netscher, M. Findeisen, M. M. Hoffmann, *Chemistry* **2008**, *14*, 6805–6814.

1,2,3,4-Tetrahydroquinoline



$C_9H_{11}N$

133.19 g/mol

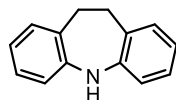
1H -NMR (300 MHz, $CDCl_3$) δ 7.03 – 6.92 (m, 2H), 6.62 (td, $J = 7.4, 1.2$ Hz, 1H), 6.50 (d, $J = 7.8$ Hz, 1H), 3.98 (s, 1H), 3.37 – 3.25 (m, 2H), 2.78 (t, $J = 6.4$ Hz, 2H), 2.03 – 1.88 (m, 2H).

^{13}C -NMR (75 MHz, $CDCl_3$) δ 144.82, 129.56, 126.76, 121.48, 116.97, 114.23, 42.03, 27.02, 22.22.

GC-MS $t_R = 7.17$ min, (EI, 70 eV): $m/z = 133$ [M^+], 118, 104, 91, 77, 63, 51.

Analytical data were in full agreement with M. Ortiz-Marciales, L. D. Rivera, M. de Jesus, S. Espinosa, J. A. Benjamin, O. E. Casanova, I. G. Figueroa, S. Rodriguez, W. Correa, *J. Org. Chem.* **2005**, *70*, 10132–10134.

10,11-Dihydro-5H-dibenzo[b,f]azepine



$C_{14}H_{13}N$

195.27 g/mol

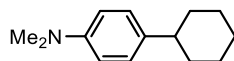
1H -NMR (300 MHz, $CDCl_3$) δ 7.18 – 7.04 (m, 4H), 6.89 – 6.66 (m, 4H), 6.02 (s, 1H), 3.12 (s, 4H).

^{13}C -NMR (75 MHz, $CDCl_3$) δ 141.38, 129.62, 127.57, 125.76, 118.38, 116.86, 33.87.

GC-MS $t_R = 10.16$ min, (EI, 70 eV): $m/z = 195$ [M^+], 180, 167, 152, 118, 97, 89, 77, 63, 51.

Analytical data were in full agreement with J. A. Profitt, H. H. Ong, *J. Org. Chem.* **1979**, *44*, 3972–3974.

4-Cyclohexyl-*N,N*-dimethylaniline



$C_{14}H_{21}N$

203.33 g/mol

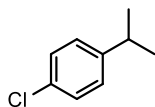
¹H-NMR (300 MHz, CDCl₃) δ 7.15 – 7.07 (m, 2H), 6.77 – 6.72 (m, 2H), 2.93 (s, 6H), 2.52 – 2.38 (m, 1H), 1.94 – 1.80 (m, 4H), 1.78 – 1.70 (m, 1H), 1.48 – 1.34 (m, 4H), 1.34 – 1.25 (m, 1H).

¹³C-NMR (75 MHz, CDCl₃) δ 127.34, 113.11, 43.53, 41.06, 34.75, 27.05, 26.26.

GC-MS *t_R* = 9.30 min, (EI, 70 eV): *m/z* = 203, 160, 146, 134, 118, 103, 91, 77, 65, 55.

Analytical data were in full agreement with Z. Li, H.-M. Sun, Q. Shen, *Org. Biomol. Chem.* **2016**, *14*, 3314–3321.

1-Chloro-4-isopropylbenzene



C₉H₁₁Cl

154.64 g/mol

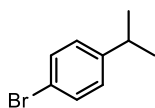
¹H-NMR (300 MHz, CDCl₃) δ 7.25 (m, 2H), 7.21–7.09 (m, 2H), 2.89 (m, 1H), 1.23 (d, *J* = 6.9 Hz, 6H).

¹³C-NMR (75 MHz, CDCl₃) δ 142.3, 131.3, 128.4, 127.8, 33.6, 23.9.

GC-MS *t_R* = 5.37 min, (EI, 70 eV): *m/z* = 154 [M⁺], 139, 125, 119, 105, 89, 77, 63, 51.

Analytical data were in full agreement with S. S. Kim, C. S. Kim, *J. Org. Chem.* **1999**, *64*, 9261–9264.

1-Bromo-4-isopropylbenzene



C₉H₁₁Br

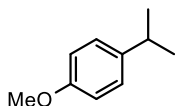
199.09 g/mol

¹H-NMR (300 MHz, CDCl₃) δ 7.47 – 7.36 (m, 2H), 7.15 – 7.04 (m, 2H), 2.87 (hept, *J* = 6.9 Hz, 1H), 1.23 (d, *J* = 6.9 Hz, 6H).

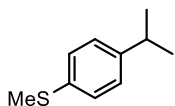
¹³C-NMR (101 MHz, CDCl₃) δ 147.8, 131.3, 128.2, 119.3, 33.7, 30.9, 23.8.

GC-MS *t_R* = 6.16 min, (EI, 70 eV): *m/z* = 198 [M⁺], 185, 169, 158, 143, 119, 104, 91, 77, 63, 51.

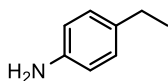
Analytical data were in full agreement with M. A. Hall, J. Xi, C. Lor, S. Dai, R. Pearce, W. P. Dailey, R. G. Eckenhoff, *J. Med. Chem.* **2010**, *53*, 5667–5675.

1-Isopropyl-4-methoxybenzeneC₁₀H₁₄O

180.24 g/mol

¹H-NMR(300 MHz, CDCl₃) δ 7.15 (m, 2H), 6.84 (m, 2H), 3.79 (s, 3H), 2.95 – 2.78 (m, 1H), 1.23 (d, *J* = 6.9 Hz, 6H).**¹³C-NMR**(75 MHz, CDCl₃) δ 156.86, 141.06, 127.26, 113.77, 55.27, 33.28, 24.24.**GC-MS***t_R* = 5.93 min, (EI, 70 eV): *m/z* = 150 [M⁺], 120, 105, 91, 77, 65, 51.Analytical data were in full agreement with Cahiez, G.; Foulgoc, L.; Moyeux, A. *Angew. Chem. Int. Ed.* **2009**, *48*, 2969–2972.**Methyl(4-(prop-2-yl)phenyl)sulfane**C₁₀H₁₄S

166.28 g/mol

¹H-NMR(300 MHz, CDCl₃) δ 7.26 – 7.19 (m, 2H), 7.19 – 7.13 (m, 2H), 2.88 (m, 1H), 2.48 (s, 3H), 1.24 (d, *J* = 6.9 Hz, 6H).**¹³C-NMR**(75 MHz, CDCl₃) δ 146.11, 135.05, 127.20, 127.01, 77.47, 77.04, 76.62, 33.65, 24.00, 16.42.**GC-MS***t_R* = 7.20 min, (EI, 70 eV): *m/z* = 166 [M⁺], 151, 136, 104, 91, 77, 51.Analytical data were in full agreement with X.-m. Wu, J.-m. Lou, G.-b. Yan, *Synlett* **2016**, *27*, 2269–2273.**4-Ethylaniline**C₈H₁₁N

121.18 g/mol

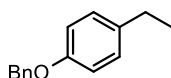
¹H-NMR(300 MHz, CDCl₃) δ 7.01 (d, *J* = 8.5 Hz, 2H), 6.68 (d, *J* = 8.3 Hz, 2H), 3.78 (s, 2H), 2.56 (q, *J* = 7.6 Hz, 2H), 1.20 (t, *J* = 7.6 Hz, 3H).

$^{13}\text{C-NMR}$ (101 MHz, CDCl_3) δ 143.23, 134.98, 128.64, 115.64, 28.03, 15.98.

GC-MS $t_R = 6.11$ min, (EI, 70 eV): $m/z = 121$ [M^+], 106, 93, 77, 65, 51.

Analytical data were in full agreement with B. Wang, H.-X. Sun, G.-Q. Lin, Z.-H. Sun, *Adv. Synth. Catal.* **2009**, 351, 415-422.

1-Benzoyloxy-4-ethylbenzene



$\text{C}_{15}\text{H}_{16}\text{O}$

212.29 g/mol

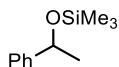
$^1\text{H-NMR}$ (300 MHz, CDCl_3) δ 7.51 – 7.30 (m, 5H), 7.18 – 7.11 (m, 2H), 6.97 – 6.89 (m, 2H), 5.07 (s, 2H), 2.62 (q, $J = 7.6$ Hz, 2H), 1.24 (t, $J = 7.6$ Hz, 3H).

$^{13}\text{C-NMR}$ (75 MHz, CDCl_3) δ 156.89, 137.30, 136.72, 128.78, 128.60, 127.92, 127.52, 114.72, 70.08, 28.03, 15.93.

GC-MS $t_R = 9.17$ min, (EI, 70 eV): $m/z = 212$ [M^+], 122, 107, 91, 77, 65, 51.

Analytical data were in full agreement with C. Zhu, N. Yukimura, M. Yamane, *Organometallics* **2010**, 29, 2098–2103.

Trimethyl-(1-phenylethoxy)silane



$\text{C}_{11}\text{H}_{18}\text{OSi}$

194.35 g/mol

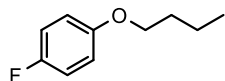
$^1\text{H-NMR}$ (300 MHz, CDCl_3) δ 7.36 – 7.18 (m, 5H), 4.86 (q, $J = 6.4$ Hz, 1H), 1.43 (d, $J = 6.4$ Hz, 3H), 0.07 (s, 9H).

$^{13}\text{C-NMR}$ (75 MHz, CDCl_3) δ 146.33, 128.02, 126.73, 125.24, 70.48, 26.78, 0.00.

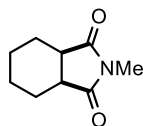
GC-MS $t_R = 5.74$ min, (EI, 70 eV): $m/z = 179$ [M-CH_3], 105, 75, 51.

Analytical data were in full agreement with Y. Onishi, Y. Nishimoto, M. Yasuda, A. Baba, *Org. Lett.* **2011**, 13, 2762–2765.

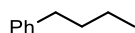
4-Fluorobenzyl-*n*-butylether

C₁₀H₁₃FO

168.21 g/mol

¹H-NMR(300 MHz, CDCl₃) δ 7.02 – 6.91 (m, 2H), 6.87 – 6.78 (m, 2H), 3.92 (t, *J* = 6.5 Hz, 2H), 1.75 (m, 2H), 1.56 – 1.41 (m, 2H), 0.97 (t, *J* = 7.4 Hz, 3H).**¹³C-NMR**(75 MHz, CDCl₃) δ 158.68, 155.53, 155.28, 115.87, 115.56, 115.44, 115.33, 77.46, 77.24, 77.04, 76.62, 68.31, 31.35, 19.24, 13.87.**GC-MS***t*_R = 6.04 min, (EI, 70 eV): *m/z* = 168 [M⁺], 112, 95, 83, 75, 57, 50.**HRMS**(EI, *m/z*): found 168.0954 [M⁺] (calculated 168.0950).**FT-IR**(ATR-film) in [cm⁻¹] 2961 (m), 2937 (m), 2874 (w), 1504 (s), 1472 (m), 1390 (w), 1292 (w), 1247 (m), 1206 (s), 1096 (w), 1069 (w), 1028 (w), 974 (w), 825 (s), 755 (s), 723 (m), 512 (m).**2-Methylhexahydro-1*H*-isoindole-1,3(2*H*)-dione**C₉H₁₃NO₂

167.21 g/mol

¹H-NMR(300 MHz, CDCl₃) δ 2.97 (s, 3H), 2.85 (td, *J* = 4.5, 2.2 Hz, 2H), 1.98 – 1.80 (m, 2H), 1.80 – 1.68 (m, 2H), 1.53 – 1.35 (m, 4H).**¹³C-NMR**(75 MHz, CDCl₃) δ 179.95, 77.46, 77.04, 76.62, 39.77, 24.67, 23.71, 21.61.**GC-MS***t*_R = 7.77 min, (EI, 70 eV): *m/z* = 167 [M⁺], 138, 113, 82, 67, 54.Analytical data were in full agreement with B. Bailey, R. D. Haworth, J. McKenna, *J. Chem. Soc.* **1954**, 967.***n*-Butylbenzene**C₁₀H₁₄

134.22 g/mol

¹H-NMR	(300 MHz, CDCl ₃) δ 7.38 – 7.27 (m, 2H), 7.20 (m, 3H), 2.68 – 2.57 (m, 2H), 1.71 – 1.54 (m, 2H), 1.37 (dq, <i>J</i> = 14.5, 7.3 Hz, 2H), 0.94 (t, <i>J</i> = 7.3 Hz, 3H).
¹³C-NMR	(75 MHz, CDCl ₃) δ 142.95, 128.44, 128.24, 125.57, 35.71, 33.73, 22.42, 14.01.
GC-MS	<i>t</i> _R = 5.09 min, (EI, 70 eV); <i>m/z</i> = 134 [M ⁺], 128, 115, 105, 92, 77, 65, 51.

Analytical data were in full agreement with L. Ackermann, A. R. Kapdi, C. Schulzke, *Org. Lett.* **2010**, *12*, 2298–2301.

2,5-diphenylbicyclo[2.2.2]octane



C₂₀H₂₂

262.40 g/mol

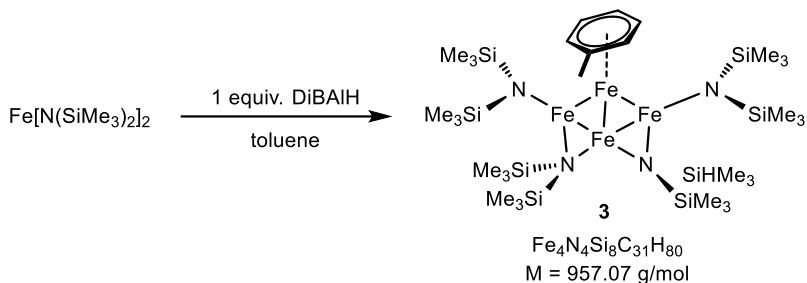
¹H-NMR	Complex mixture
¹³C-NMR	(75 MHz, CDCl ₃) δ 146.52, 146.38, 146.06, 145.67, 128.28, 128.25, 128.23, 128.18, 127.85, 127.82, 127.53, 125.72, 125.70, 125.62, 42.51, 41.95, 41.25, 40.76, 34.25, 33.68, 32.13, 32.01, 31.43, 27.90, 27.09, 26.64, 26.52, 20.58, 19.73.
GC-MS	<i>t</i> _R = 11.25, 11.48, 11.54, (EI, 70 eV); <i>m/z</i> = 262 [M ⁺], 158, 143, 129, 115, 104, 91, 78, 65, 51

3.2.9 Synthesis and characterization of [FeN(SiMe₃)₂]₄(toluene)

General

Chemicals and Solvents: Solvents (THF, Et₂O, *n*-hexane, toluene) were distilled over sodium and benzophenone and stored over molecular sieves (4 Å). All manipulations were performed under purified argon inside a glovebox or using *Schlenk* techniques. Fe[N(SiMe₃)₂]₂ was synthesized as previously described. DiBAIH was used as received from *SigmaAldrich* (1 M in toluene).

¹H- und ¹³C-NMR-Spectroscopy: Nuclear magnetic resonance spectra were recorded on a *Bruker Avance 300* (300 MHz) and *Bruker Avance 400* (400 MHz). ¹H-NMR: The following abbreviations are used to indicate multiplicities: s = singlet; d = doublet; t = triplet, q = quartet; m = multiplet, dd = doublet of doublet, dt = doublet of triplet, dq = doublet of quartet, ddt = doublet of doublet of quartet. Chemical shift δ is given in ppm to tetramethylsilane.



Scheme 3-S1 - Synthesis of [Fe₄]-cluster **[FeN(SiMe₃)₂]₄(toluene)**

A 10 mL flame-dried *Schlenk* flask was charged with Fe[N(SiMe₃)₂]₂ (190 mg, 0.50 mmol) in a mixture of *n*-hexane/toluene (4 mL, 3/1). A solution of DiBAIH in toluene (0.50 mmol, 1 M, 0.50 mL) was added at room temperature via syringe with immediate color change from green to brown-black. The reaction mixture was stirred at room temperature for 30 minutes, filtered through a P4 frit after which the solvent was removed completely under reduced pressure. The dark brown oily residue was powdered by 3 cycles freeze-pump-thaw and crystallized in *n*-hexane (0.3 mL) at -30 °C. After 24 h, a dark crystalline compound was obtained in 38% yield (46 mg, 0.048 mmol).

¹H-NMR (400 MHz, C₆D₆) δ 52.84 (bs), -1.83 (bs), -5.31 (bs), -12.06 (bs), -20.57 (bs), -22.73 (bs); effective magnetic moment (C₆D₆): μ_{eff} = 2.0 μ_B; melting point = 123 °C; elemental analysis calcd for Fe₄N₄Si₈C₃₁H₈₀ (957.07): C 38.90, H 8.43, N 5.85; found: C 38.05, H 8.19, N 5.87.

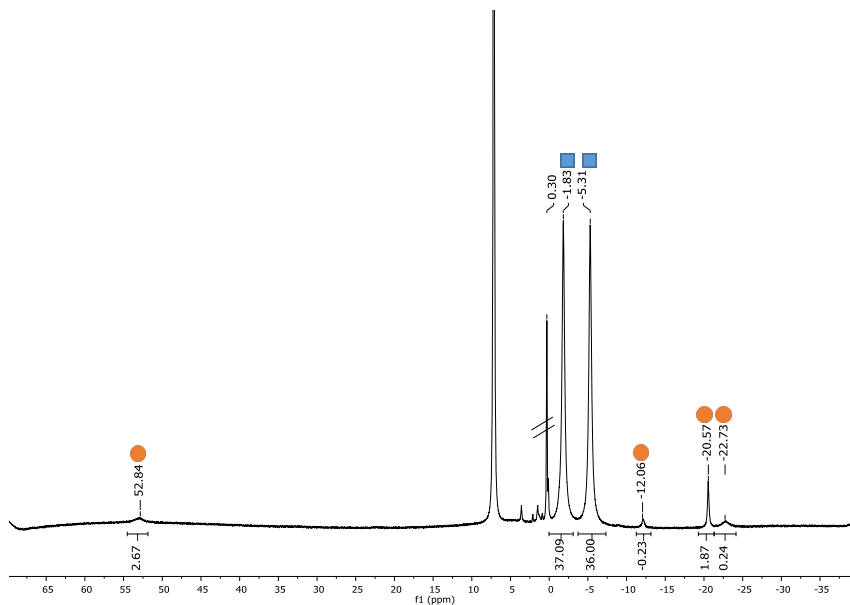


Figure3-S2 - $^1\text{H-NMR}$ of $[\text{FeN}(\text{SiMe}_3)_2]_4(\text{toluene})$ in C_6D_6 . Peak assignments: SiMe_3 (■), toluene (●).

For X-Ray structure determination, a suitable crystal ($0.19 \times 0.16 \times 0.11$) mm^3 was selected and mounted on a MITIGEN holder with inert oil on a SuperNova, Single source at offset, Atlas diffractometer. The crystal was kept at $T = 123.00(10)$ K during data collection. Using **Olex2** (Dolomanov *et al.*, 2009)¹, the structure was solved in the space group $\text{P}2_1/c$ (# 14) by Direct Methods using the **ShelXT** (Sheldrick, 2015)² structure solution program and refined by Least Squares using version 2014/7 of **ShelXL** (Sheldrick, 2015)³. All non-hydrogen atoms were refined anisotropically. Hydrogen atom positions were calculated geometrically and refined using the riding model. Data were measured using w scans scans of 1.0° per frame for 6.0 s using CuK α radiation (micro-focus sealed X-ray tube, n/a kV, n/a mA). The total number of runs and images was based on the strategy

¹ O.V. Dolomanov and L.J. Bourhis and R.J. Gildea and J.A.K. Howard and H. Puschmann, Olex2: A complete structure solution, refinement and analysis program, *J. Appl. Cryst.*, (2009), **42**, 339-341.

² Sheldrick, G.M., Crystal structure refinement with ShelXL, *Acta Cryst.*, (2015), **C27**, 3-8.

³ Sheldrick, G.M., ShelXT-Integrated space-group and crystal-structure determination, *Acta Cryst.*, (2015), **A71**, 3-8.

calculation from the program CrysAlisPro (Agilent). The maximum resolution achieved was $Q = 76.438$ $^{\circ}$

Cell parameters were retrieved using the CrysAlisPro (Agilent) software and refined using CrysAlisPro (Agilent) on 23809 reflections, 55 % of the observed reflections. Data reduction was performed using the CrysAlisPro (Agilent) software which corrects for Lorentz polarisation. The final completeness is 99.90 out to 76.438 in θ . The absorption coefficient μ of this material is 11.172 at this wavelength ($\lambda = 1.54184$) and the minimum and maximum transmissions are 0.70913 and 1.00000 .

Crystal Data. $C_{31}H_{80}Fe_4N_4Si_8$, $M_r = 957.11$, monoclinic, $P2_1/c$ (No. 14), $a = 18.59832(16)$ Å, $b = 14.75827(12)$ Å, $c = 18.28580(17)$ Å, $\beta = 96.4495(8)^{\circ}$, $\alpha = \gamma = 90^{\circ}$, $V = 4987.31(7)$ Å³, $T = 123.00(10)$ K, $Z = 4$, $Z' = 1$, $\mu(\text{CuK}\alpha) = 11.172$, 43076 reflections measured, 10425 unique ($R_{int} = 0.0307$) which were used in all calculations. The final wR_2 was 0.0650 (all data) and R_I was 0.0262 ($I > 2(I)$).

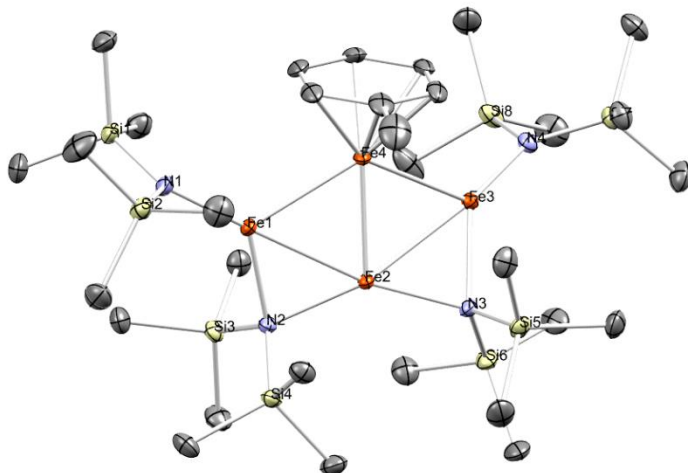


Figure 3-S3 - X-Ray structure of $[\text{FeN}(\text{SiMe}_3)_2]_4(\text{toluene})$ visualized with software *Mercury*. Hydrogen atoms are omitted for clarity.

3.2.10 Synthesis of $[\text{Fe}_6\{\text{N}(\text{SiMe}_3)_2\}_6\text{H}_5]$ and $[\text{Fe}_7\{\text{N}(\text{SiMe}_3)_2\}_7\text{H}_6]$:

A light green solution of $\text{Fe}\{\text{N}(\text{SiMe}_3)_2\}_2$ (190 mg, 0.50 mmol) in *n*-hexane (2 mL) was treated with 0.5 mL of 1(M) DiBAIH solution (0.50 mmol) in *n*-hexane at ambient temperature. The color of the solution immediately turned to dark red-brown and it was stirred for three hour. The solution was evaporated completely to a dark red-brown sticky solid, which was treated with 0.5 mL of *n*-hexane and the obtained suspension was stored at room temperature overnight. The dark brown solid was isolated by filtration through glass pipette embedded with glass-filter. Dark red-brown single crystals were obtained by slow evaporation of the *n*-hexane solution at room temperature. Composition of the product to $[\text{Fe}_6\{\text{N}(\text{SiMe}_3)_2\}_6\text{H}_5]$ and $[\text{Fe}_7\{\text{N}(\text{SiMe}_3)_2\}_7\text{H}_6]$ in 4 : 1 ratio was verified by X-ray analysis, elemental analysis and LIFDI-MS. Yield: 37 mg (0.028 mmol, 35 %). Elemental analysis calculated for $\text{C}_{36}\text{H}_{113.2}\text{Fe}_{6.2}\text{N}_6\text{Si}_{12}$: C 32.91, H 8.69, N 6.40; found: C 33.4, H 8.51, N 6.3. $^1\text{H NMR}$ (C_6D_6 , 400.13 MHz, 300K): -16.34 (SiMe_3), -3.29 (SiMe_3), 29.72 (SiMe_3).

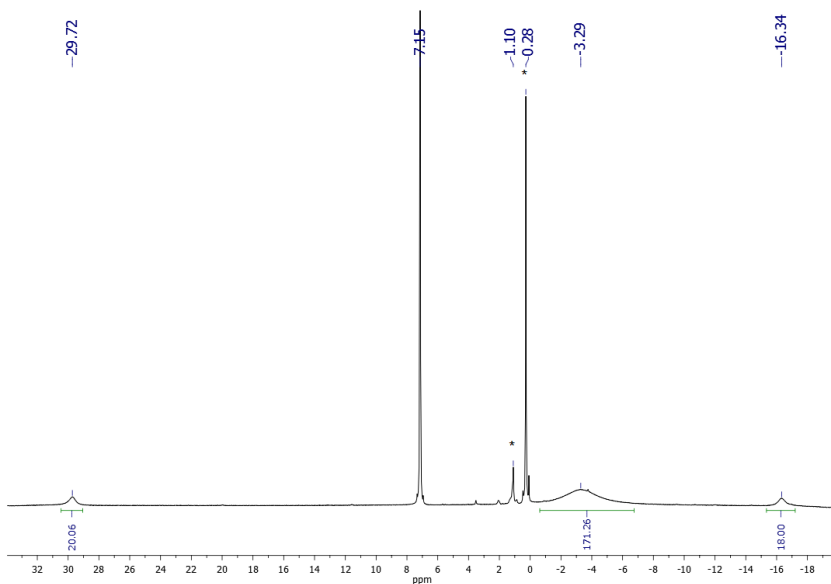


Figure 3-S4 - $^1\text{H NMR}$ spectrum of Fe6/Fe7 cluster mixture (C_6D_6 , 400.13 MHz, 300K).

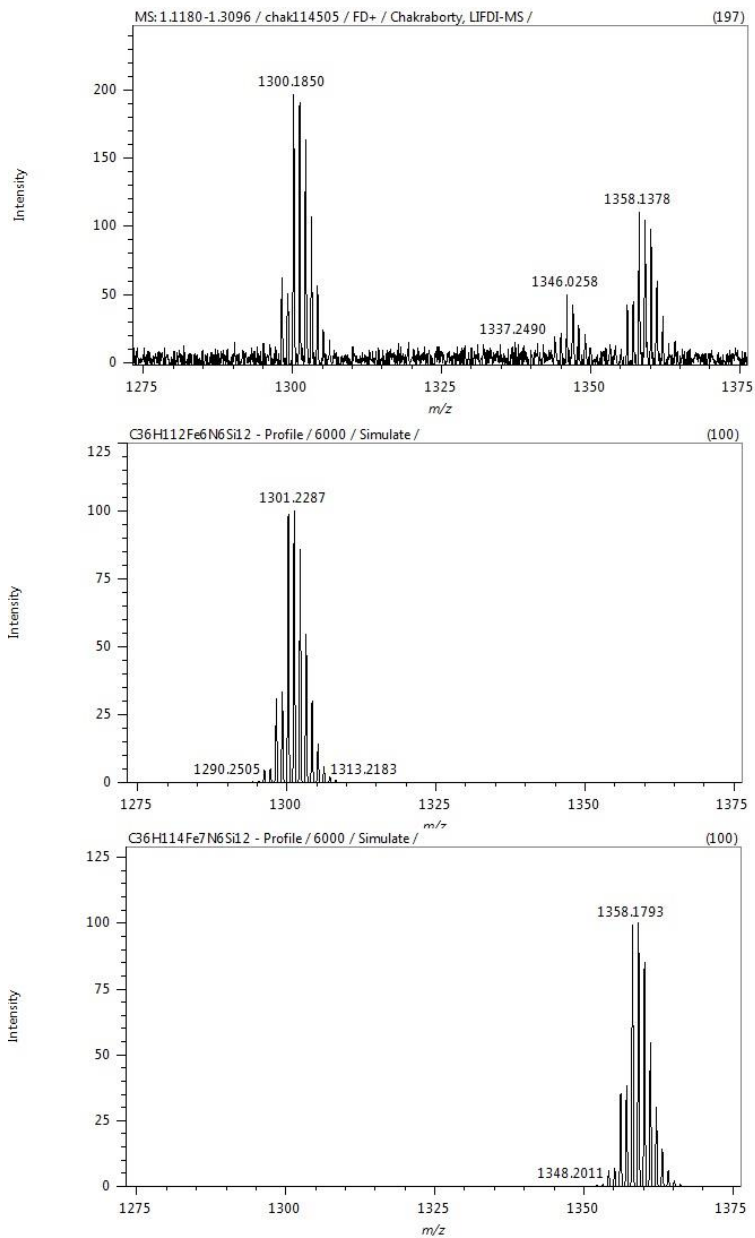


Figure 3-S5 - LIFDI-MS spectrum of Fe6/Fe7 cluster mixture in toluene.

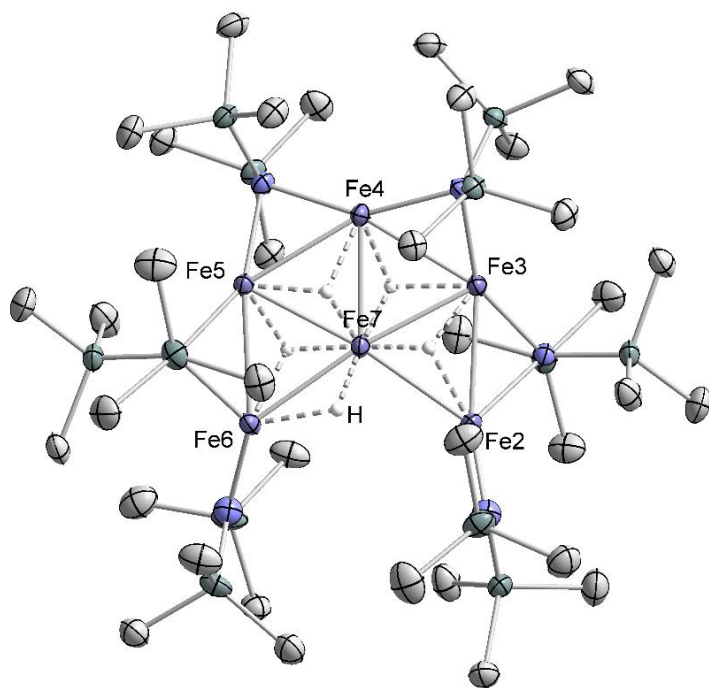


Figure 3-S6 - Diamond plot of the Fe₆ Cluster.

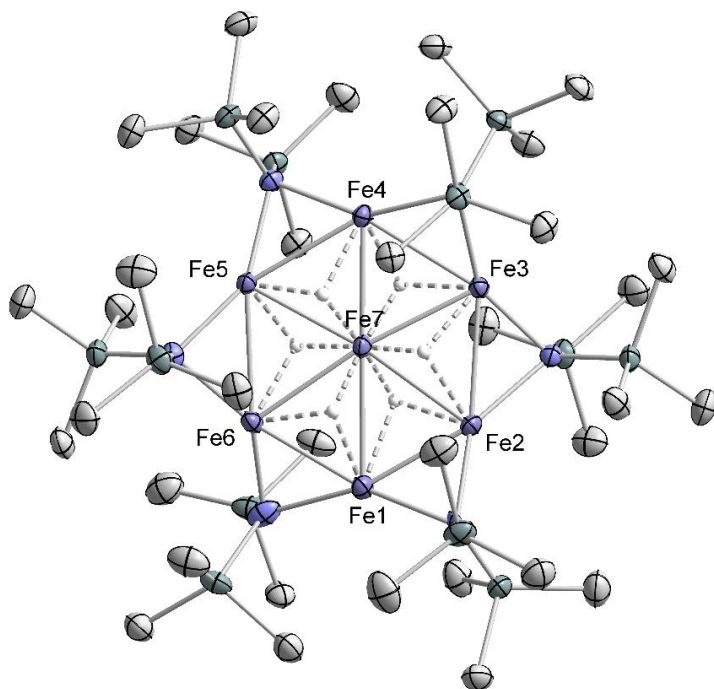


Figure 3-S7 - Diamond plot of the Fe₇ Cluster.

3.3 References

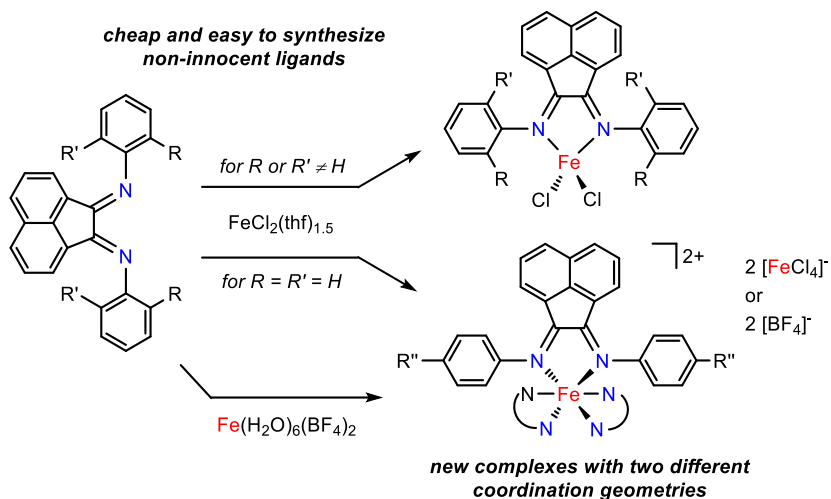
- [1] a) *The Handbook of Homogeneous Hydrogenation* (Eds.: J. G. de Vries, C. J. Elsevier), Wiley-VCH: Weinheim, **2007**; b) S. Nishimura, *Handbook of Heterogeneous Catalytic Hydrogenation for Organic Synthesis*; Wiley, New York, **2001**.
- [2] a) *Catalysis without Precious Metals* (Ed.: R. M. Bullock), Wiley-VCH, Weinheim, **2010**; b) P. J. Chirik, *Acc. Chem. Res.* **2015**, *48*, 1687; c) K. Junge, K. Schröder, M. Beller, *Chem. Commun.* **2011**, *47*, 4849; d) B. A. F. Le Bailly, S. P. Thomas, *RSC Adv.* **2011**, *1*, 1435.
- [3] Q. Knijnenburg, A. D. Horton, H. van der Heijden, A. W. Gal, P. H. M. Budzelaar, patent WO2003042131 A1 20030522, **2003**.
- [4] a) S. C. Bart, E. Lobkovsky, P. J. Chirik, *J. Am. Chem. Soc.* **2004**, *126*, 13794; b) R. J. Trovitch, E. Lobkovsky, E. Bill, P. J. Chirik, *Organometallics* **2008**, *27*, 1470; c) J. M. Hoyt, M. Shevlin, G. W. Margulieux, S. W. Krska, M. T. Tudge, P. J. Chirik, *Organometallics* **2014**, *33*, 5781; d) R. P. Yu, J. M. Darmon, J. M. Hoyt, G. W. Margulieux, Z. R. Turner, P. J. Chirik, *ACS Catal.* **2012**, *2*, 1760.
- [5] a) P. H. Phua, L. Lefort, J. A. F. Boogers, M. Tristany, J. G. de Vries, *Chem. Commun.* **2009**, 3747; b) C. Rangheard, C. de Julian Fernandez, P.-H. Phua, J. Hoorn, L. Lefort, J. G. de Vries, *Dalton Trans.* **2010**, *39*, 8464; c) M. Stein, J. Wieland, P. Steurer, F. Tölle, R. Mülhaupt, B. Breit, *Adv. Synth. Catal.* **2011**, *353*, 523; d) R. Hudson, A. Rivière, C. M. Cirtiu, K. L. Luska, A. Moores, *Chem. Commun.* **2012**, *48*, 3360; e) A. Welther, A. Jacobi von Wangelin, *Curr. Org. Chem.* **2013**, *17*, 326; f) T. S. Carter, L. Guiet, D. J. Frank, J. West, S. P. Thomas, *Adv. Synth. Catal.* **2013**, *355*, 880; g) D. J. Frank, L. Guiet, A. Kaslin, E. Murphy, S. P. Thomas, *RSC Adv.* **2013**, *3*, 25698; h) R. Hudson, G. Hamasaka, T. Osako, Y. M. A. Yamada, C.-J. Li, Y. Uozumi, A. Moores, *Green Chem.* **2013**, *15*, 2141; i) A. J. MacNair, M.-M. Tran, J. E. Nelson, G. U. Sloan, A. Ironmonger, S. P. Thomas, *Org. Biomol. Chem.* **2014**, *12*, 5082.
- [6] a) D. Gärtner, A. Welther, B. R. Rad, R. Wolf, A. Jacobi von Wangelin, *Angew. Chem. Int. Ed.* **2014**, *53*, 3722; b) T. N. Gieshoff, M. Villa, A. Welther, M. Plois, U. Chakraborty, R. Wolf, A. Jacobi von Wangelin, *Green Chem.* **2015**, *17*, 1408; c) A. Welther, M. Bauer, M. Mayer, A. Jacobi von Wangelin, *ChemCatChem* **2012**, *4*, 1088.
- [7] R. A. Andersen, K. Faegri, J. C. Green, A. Haaland, M. F. Lappert, W.-P. Leung, *Inorg. Chem.* **1988**, *27*, 1782.
- [8] Selected recent examples: a) M. I. Lipschutz, T. Chantarojsiri, Y. Dong, T. D. Tilley, *J. Am. Chem. Soc.* **2015**, *137*, 6366; b) L. C. H. Maddock, T. Cadenbach, A. R. Kennedy, I. Borilovic, G. Aromí, E. Hevia, *Inorg. Chem.* **2015**, *54*, 9201; c) T. Hatakeyama, R. Imayoshi, Y. Yoshimoto, S. K. Ghorai, M. Jin, H. Takaya, K. Norisuye, Y. Sohrin, M. Nakamura, *J. Am. Chem. Soc.* **2012**, *134*, 20262; d) J. Yang,

- T. D. Tilley, *Angew. Chem. Int. Ed.* **2010**, *49*, 10186; e) J. Yang, M. Fasulo, T. D. Tilley, *New J. Chem.* **2010**, *34*, 2528.
- [9] H. Nakazawa, M. Itazaki, *Top. Organomet. Chem.* **2011**, *33*, 27.
- [10] a) W. Lubitz, H. Ogata, O. Rüdiger, E. Reijerse, *Chem. Rev.* **2014**, *114*, 4081; b) S. Tschierlei, S. Ott, R. Lomoth, *Energy Environ. Sci.* **2011**, *4*, 2340; c) P. Du, R. Eisenberg, *Energy Environ. Sci.* **2012**, *5*, 6012.
- [11] V. Kelsen, B. Wendt, S. Werkmeister, K. Junge, M. Beller, B. Chaudret, *Chem. Commun.* **2013**, *49*, 3416.
- [12] Ziegler-type Fe/Al catalysts in hydrogenations: a) M. F. Sloan, A. S. Matlack, D. S. Breslow, *J. Am. Chem. Soc.* **1963**, *85*, 4014; b) Y. Takegami, T. Ueno, T. Fujii, *Bull. Chem. Soc. Jpn.* **1965**, *38*, 1279; c) N. F. Noskova, A. Zh. Kazimova, K. K. Kambarova, S. R. Savelev, N. L. Melamud, *Zh. Org. Khim.* **1992**, *28*, 1352.
- [13] a) Isomerization of allylbenzene (to β -methylstyrene) and 1-octene (to 2-,3-,4-octenes) with 5 mol% Fe(hmds)₂/10 mol% Dibal-H proceeded sluggishly under otherwise identical conditions (no H₂). b) M. Mayer, A. Welther, A. Jacobi von Wangelin, *ChemCatChem* **2011**, *3*, 1567.
- [14] M. Newcomb, in: *Encyclopedia of Radicals in Chemistry, Biology and Materials* (Eds.: C. Chatgililoglu, A. Studer), Wiley, Chichester, **2012**.
- [15] a) J. A. Widegren, R. G. Finke, *J. Mol. Catal. A* **2003**, *198*, 317; b) D. Astruc, F. Lu, J. Ruiz Aranzaes, *Angew. Chem. Int. Ed.* **2005**, *44*, 7852; c) R. H. Crabtree, *Chem. Rev.* **2012**, *112*, 1536.
- [16] a) K.-N. T. Tseng, J. W. Kampf, N. K. Szymczak, *ACS Catal.* **2015**, *5*, 411; b) Y. Li, S. Yu, X. Wu, J. Xiao, W. Shen, Z. Dong, J. Gao, *J. Am. Chem. Soc.* **2014**, *136*, 4031; c) E. Alberico, P. Sponholz, C. Cordes, M. Nielsen, H.-J. Drexler, W. Baumann, H. Junge, M. Beller, *Angew. Chem. Int. Ed.* **2013**, *52*, 14162.
- [17] a) D. R. Anton, R. H. Crabtree, *Organometallics* **1983**, *2*, 855; b) G. Franck, M. Brill, G. Helmchen, *J. Org. Chem.* **2012**, *89*, 55; c) J. F. Sonnenberg, R. H. Morris, *Catal. Sci. Technol.* **2014**, *4*, 3426; d) D. Gärtner, A. L. Stein, S. Grupe, J. Arp, A. Jacobi von Wangelin, *Angew. Chem. Int. Ed.* **2015**, *54*, 10545.
- [18] a) A structurally similar tetraborane motif: A. Maier, M. Hofmann, H. Pritzkow, W. Siebert, *Angew. Chem. Int. Ed.* **2002**, *41*, 1529. b) A related synthesis of an (η^6 -toluene)Fe(I) diamide complex: T. Janes, J. M. Rawson, D. Song, *Dalton Trans.* **2013**, *42*, 10640.
- [19] Y. Lee, K. J. Anderton, F. T. Sloane, D. M. Ermert, K. A. Abboud, R. García-Serres, L. J. Murray, *J. Am. Chem. Soc.* **2015**, *137*, 10610; b)
- [20] Non-planar nitrido/imido/amido Fe clusters: a) R. Hernández Sánchez, T. A. Betley, *J. Am. Chem. Soc.* **2015**, *137*, 13949; b) D. A. Iovan, T. A. Betley, *J. Am. Chem. Soc.* **2016**, *138*, 1983; c) R. Hernández Sánchez, A. K. Bartholomew, T. M. Powers, G. Ménard, T. A. Betley, *J. Am. Chem. Soc.* **2016**, *138*, 2235; d) R. Hernández Sánchez, S.-L. Zheng, T. A. Betley, *J. Am. Chem. Soc.* **2015**, *137*, 11126; e) R. Hernández Sánchez, A. M. Willis, S.-L. Zheng, T. A. Betley, *Angew. Chem. Int. Ed.*

- 2015**, 54, 12009; f) T. M. Powers, T. A. Betley, *J. Am. Chem. Soc.* **2013**, 135, 12289; g) E. T. Hennessy, T. A. Betley, *Science* **2013**, 340, 591; h) Q. Zhao, T. A. Betley, *Angew. Chem. Int. Ed.* **2011**, 50, 709; i) E. R. King, E. T. Hennessy, T. A. Betley, *J. Am. Chem. Soc.* **2011**, 133, 4917; j) „Kochi-type“ $[\text{Fe}_8\text{Me}_{12}]$ double decker: S. B. Muñoz, S. L. Daifuku, W. W. Brennessel, M. L. Neidig, *J. Am. Chem. Soc.* **2016**, 138, 7492; k) Related Co_6 and Co_7 clusters: Y. Ohki, Y. Shimizu, R. Araake, M. Tada, W. M. C. Sameera, J.-I. Ito, H. Nishiyama, *Angew. Chem. Int. Ed.* **2016**, 55, 15821.
- [21] a) M. Akita, in: *Comprehensive Organometallic Chemistry III* (Eds.: R. H. Crabtree, D. M. P. Mingos), Vol. 6, 1st ed., Elsevier, Amsterdam, **2007**, 259; b) K. H. Whitmire, *Adv. Organomet. Chem.* **1998**, 42, 1. Anionic $(\text{CO})_x\text{Fe}_3$ triangles or non-planar $(\text{CO})_x\text{Fe}_4$ envelopes with bridging amido/imido/nitrido ligands: c) P. Zanello, F. Laschi, A. Cinquantini, R. Della Pergola, L. Garlaschelli, M. Cucco, F. Demartin, T. R. Spalding, *Inorg. Chim. Acta* **1994**, 226, 1; d) R. D. Pergola, C. Bandini, F. Demartin, E. Diana, L. Garlaschelli, P. L. Stanghellini, P. Zanello, *Dalton Trans.* **1996**, 747; e) H. Bantel, P. Suter, H. Vahrenkamp, *Organometallics* **1995**, 14, 4424.
- [22] a) *Metal Clusters in Chemistry* (Eds.: P. Braunstein, L. A. Oro, P. R. Raithby), Wiley-VCH, Weinheim, **1999**; b) D. Gatteschi, R. Sessoli, J. Villain, *Molecular Nanomagnets*, Oxford University Press, Oxford, **2006**; c) E. de Smit, B. M. Weckhuysen, *Chem. Soc. Rev.* **2008**, 37, 2758.

4 Synthesis and Catalysis of Redox-active

Bis(imino)acenaphthene (BIAN) Iron Complexes^{i,ii}



Reactions of various substituted bis(imino)acenaphthenes (R-BIAN) with $\text{FeCl}_2(\text{thf})_{1.5}$ afforded the tetrahedral complexes $(\text{R-BIAN})\text{FeCl}_2$ (**2**) from bulky α -diimines and the octahedral complexes $[\text{Fe}(\text{R-BIAN})_3][\text{FeCl}_4]_2$ (**3**) from less bulky ligands. The driving force of the formation of complexes **3** is the high ligand-field stabilization of the low-spin Fe(II). The two sets of complexes exhibit distinct CT band intensities and redox activities. $(\text{R-BIAN})\text{FeCl}_2$ complexes showed reversible ligand-centered reductions at -0.9 V (vs. FcH/FcH^+); further reduction led to decomposition. Irreversible oxidations were observed at 0.2 and 0.4 V associated with a reduction at -0.4 V as well as a ligand-centered redox event at 1.0 V. First applications of the Fe(BIAN) complexes to hydrogenations of alkenes documented good catalytic activity under mild conditions.

ⁱReproduced from Matteo Villa, Dominique Miesel, Alexander Hildebrandt, Fabio Ragaini, Dieter Schaarschmidt, Axel Jacobi von Wangelin; *ChemCatChem* **2017**, DOI: 10.1002/cctc.201700144, with permission from Wiley-VCH. Schemes, tables and text may differ from the published article.

ⁱⁱAuthors contribution: Electrochemical characterizations were performed in collaboration with Dominique Miesel and Alexander Hildebrandt.

4.1 Introduction

The past years have witnessed an increasing interest in the synthesis of well-defined iron complexes and catalysts.^[1] These developments have mainly been driven by sustainability criteria (low price, low toxicity) and a lack of available complexes and mechanistic insight.^[2] Besides iron nanoparticles and various precursors forming such particles under the reaction conditions,^[3] a broad range of well-defined iron complexes have been applied in various catalytic transformations. Very recently, non-innocent, redox-active ligands have complemented the earlier examples of phosphine^[4] and *N*-heterocyclic carbene complexes^[5] and have tremendously enriched the landscape of coordination chemistry and catalytic applications.^[6] One of the most prominent classes of redox-active ligands are diimines of which several classes of complexes and catalysts have been reported. α -Diimine iron complexes with the simplest ligands of this class, 1,4-diazabutadiene (DAB), have been studied since the 1970s.^[7] Bis(imino)pyridine (PDI) ligands were successfully applied by Brookhart *et al.* and Gibson *et al.* to olefin polymerizations.^[8] The key characteristic of PDI ligands is their ability to reversibly exchange electrons with the coordinated metal. Elementary steps within the catalytic cycle involving the transfer of electrons between the metal complex and the substrate are facilitated by such ligand participation as uncommon oxidation states at the metal atom can be avoided. Although bis(imino)acenaphthenes (BIANs) have been known for more than 50 years, they have received much less attention as redox-active ligands in coordination chemistry and catalysis.^{[9],[10]}

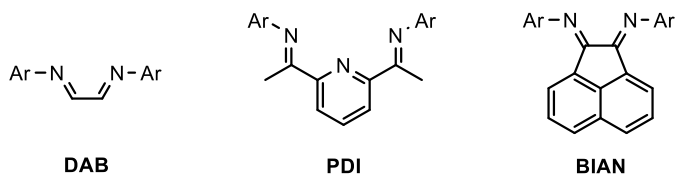


Figure 4-1 - Generic structures of important diimine ligands: bis(imino)pyridine (PDI), 1,4-diazabutadiene (DAB), bis(imino)acenaphthene (BIAN).

The rigidity of the acenaphthene backbone forces these molecules to adopt an *s-cis* conformation which facilitates the formation of stable metal complexes. The stereoelectronic properties of BIANs can easily be tuned by the incorporation of substituted primary amines during imine formation. Such ligands have been reported to efficiently coordinate almost all main-group elements^[10] and transition metals.^[11] BIANs have been extensively studied in olefin polymerizations^[12] and have been shown to be active in many other catalytic transformations.^[13] Surprisingly, only very few examples of iron complexes with BIAN ligands have been published.^[14] Most of these reports involve modification of the general ligand structure by a pendant donor arm with the aim

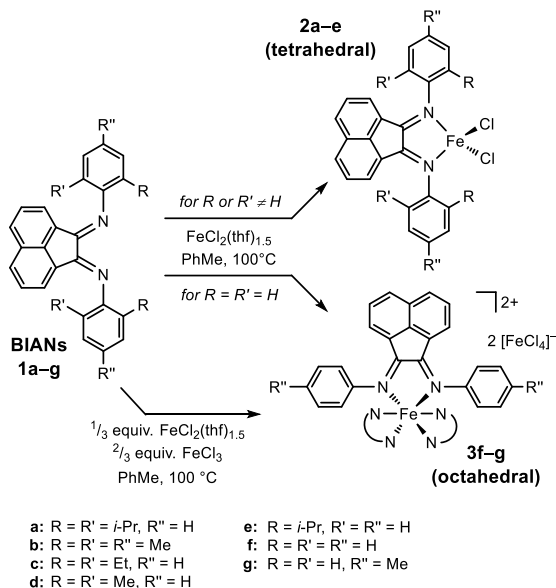
of mimicking the PDI behavior.^[15] Recently, Fe complexes with sterically hindered dipp_2BIAN ($\text{dipp}=\text{Ar}=2,6\text{-diisopropylphenyl}$, see figure 4-1) and mes_2BIAN ($\text{mes}=\text{Ar}=\text{mesityl}$, see figure 4-1) have been successfully applied as pre-catalysts to hydrosilylations of carbonyl compounds^[16] and olefins.^[17] These studies documented only moderate activity of the complexes and involved no full electrochemical characterization of the complexes despite the strongly reducing reaction conditions and the postulation of an active catalyst species in lower oxidation states.

In an effort to enhance the knowledge of well-defined Fe complexes of the BIAN ligand family (**1**), we herein report the synthesis of several high-spin ($(\text{R-BIAN})\text{FeCl}_2$, **2**) and low-spin complexes ($[\text{Fe}(\text{R-BIAN})_3][\text{FeCl}_4]_2$, **3**, and $[\text{Fe}(\text{R-BIAN})_3][\text{BF}_4]_2$, **4**) and document their structural, optoelectronic, and electrochemical properties.

4.2 Results and Discussion

4.2.1 Synthesis

The reaction of equimolar amounts of $\text{FeCl}_2(\text{thf})_{1.5}$ with bis(imino)acenaphthenes (**1a–g**) in toluene at $100\text{ }^\circ\text{C}$ resulted in the formation of isolable iron complexes for all cases studied. However, the nature of the *N*-aryl substituents of the BIANs had a crucial role on the composition of resultant $\text{Fe}(\text{BIAN})$ complexes. BIANs containing at least one *ortho*-substituent in the *N*-aryl groups gave tetrahedral 1:1 complexes **2**; the less bulky phenyl- and 4-tolyl-BIAN derivatives gave the octahedral 1:3 complexes **3** (Scheme 4-1). Both series of complexes could clearly be distinguished by mass spectrometry (**2**: $[\text{M}]^+$; **3**: $[\text{M}]^{2+}$) and UV/Vis spectroscopy (*vide infra*). Complexes **2** and **3** were green solids forming green solutions in acetonitrile. They are soluble in polar organic solvents, such as tetrahydrofuran or dichloromethane, and to a lesser extent in toluene, but are insoluble in hydrocarbons. In general, the 1:3 complexes exhibited higher solubility. The tetrahedral iron complexes **2** were sensitive toward oxidation^[18] and hydrolysis. The addition of water to an acetonitrile solution of **2a** (Ar = *dipp*) instantly caused a color change from green to yellow consistent with the formation of the free BIAN ligand **1a**. In contrast, the octahedral complexes **3** were less sensitive: exposure of solutions thereof to aerobic conditions did not result in visible changes of the appearances over a couple of hours.

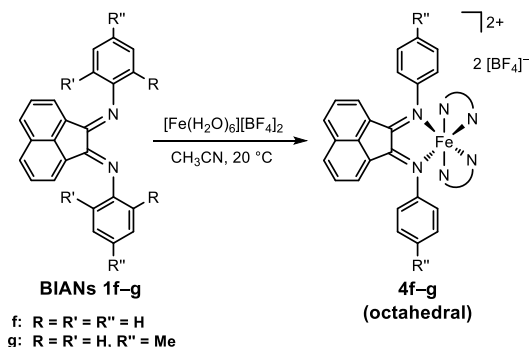


Scheme 4-1 - Ligands **1a–g** and synthesis of $\text{Fe}(\text{BIAN})$ complexes **2a–e**, **3f–g**.

The conclusion whether tetrahedral (**2**) or octahedral (**3**) complexes were formed could also be drawn from the presence of unreacted BIAN or by-products thereof in the crude reaction mixture. Purification of the crude mixtures by washing with toluene gave slightly green filtrates for complexes **2** and orange-to-red filtrates for **3**. The synthesis of the $[\text{Fe}(\text{R-BIAN})_3][\text{FeCl}_4]_2$ complexes **3** from $\text{FeCl}_2(\text{thf})_{1.5}$ is stoichiometrically unbalanced regarding chloride anions and electrons. Assuming strict exclusion of air during the preparation, the oxidation of Fe(II) to Fe(III) must be accompanied by reduction of BIAN which is also documented by the color of the toluene filtrates of **3**. The synthesis of derivative **3f** was also performed from $\text{FeCl}_2(\text{thf})_{1.5}$, FeCl_3 and **1f** in a 1:2:3 ratio, which increased the yield of the Fe complex from 75% to 87% and gave a more accurate elemental analysis.

The number of transition metal complexes in which the metal is coordinated by three BIAN ligands is quite limited^{[14c],[19]} and most of these examples are best described with at least one ligand being reduced to a radical anion. To our knowledge, $[\text{Cr}((3,5\text{-Xyl})_2\text{BIAN})_3][\text{PF}_6]_3$ ^[19d] and $[\text{Fe}(\text{H}_2\text{BIAN})_3][\text{FeBr}_3(\text{thf})_2]$ ^[14c] are the only exclusions. The latter example shows obviously some similarities to compounds **3**; in both cases equimolar amounts of an Fe(II) salt and a BIAN were reacted. However, the ferrate anions in **3** contain Fe(III), which might be caused by the use of iron dichloride instead of iron dibromide, the application of toluene instead of THF or the different electrochemical behavior of **1f** and **1g** and H_2BIAN .

The presence of the paramagnetic and redox-active counterion $[\text{FeCl}_4]^-$ in complexes **3f-g** resulted in difficult characterizations by NMR and cyclic voltammetry (CV). Therefore, complexes **4f-g** were prepared from $[\text{Fe}(\text{H}_2\text{O})_6][\text{BF}_4]_2$ in acetonitrile (Scheme 4-2).

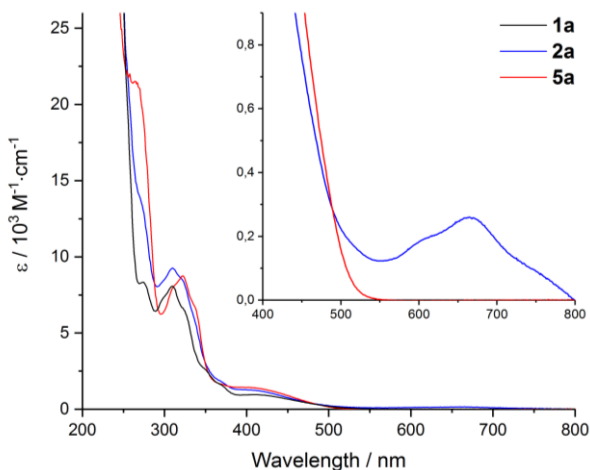


Scheme 4-2 - Synthesis of Fe(BIAN) complexes **4f** and **4g**.

4.2.2 Characterizations

For comparison of spectroscopic data of the ligand-derived complexes, selected Zn complexes (**5a,f,g**) were synthesized by reaction of $[\text{Zn}(\text{H}_2\text{O})_6][\text{BF}_4]_2$ with **1f,g** in acetonitrile and, according to a literature procedure, by reaction of ZnCl_2 with **1a** in glacial acetic acid.^[20]

UV/Vis spectra of the Fe and Zn complexes and the free ligands were recorded in acetonitrile solution at room temperature. The free R-BIANs **1a–g** exhibited intense absorptions in the UV region and a broad absorption at around 400 nm which are commonly assigned to $\pi\text{-}\pi^*$ transitions of the aryl substituents and the acenaphthene backbone and to an intra-ligand charge transfer, respectively.^[21] These bands are slightly shifted in the Fe and Zn complexes (Figure 4-2, Table 4-S1). Additionally, all Fe complexes exhibited charge transfer (CT) absorptions in the range of 550 and 800 nm. The intensity of these absorptions strongly depends on the coordination geometry and serves as an excellent probe to distinguish tetrahedral (molar absorptivity $150\text{--}500 \text{ M}^{-1}\cdot\text{cm}^{-1}$) and octahedral ($6200\text{--}14100 \text{ M}^{-1}\cdot\text{cm}^{-1}$) Fe(BIAN) complexes. Complex **2a** exhibited two weak absorptions (ligand field bands) in the near infrared at 1435 and 1830 nm with extinction coefficients of 8 and $16 \text{ M}^{-1}\cdot\text{cm}^{-1}$, respectively, which is in good agreement with other tetrahedral Fe(II) complexes in a N_2Cl_2 environment (Figure 4-S6).^[22]



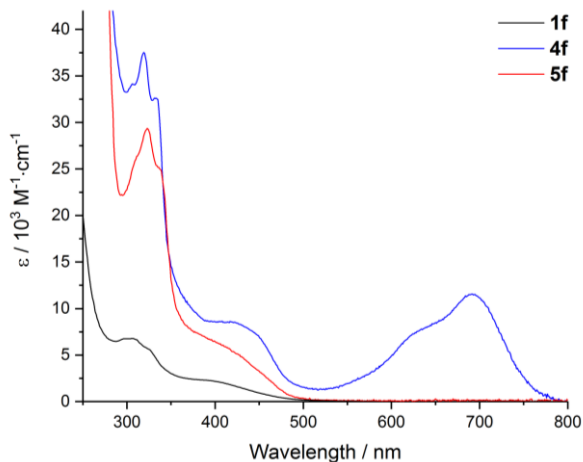


Figure 4-2 - Top: UV/Vis spectra of **1a** (black), **2a** (Fe, blue), and **5a** (Zn, red) in acetonitrile at 10^{-4} M (inset: **2a** at 10^{-3} M). Bottom: UV/Vis spectra of **1f** (black), **4f** (Fe, blue), and **5f** (Zn, red) in acetonitrile at 10^{-5} – 10^{-4} M.

Selected Fe and Zn complexes were analyzed by single crystal X-ray diffraction. The molecular structures and important bond lengths (Å) and bond angles (°) are given in Figures 4-3, 4-4 (**2b,c**) and 4-S10,4-S11,4-S12, 4-S13, 4-S14 and 4-S15 (**3f,g**, **4g**, **5a,f**). The crystal and structure refinement data are summarized in Tables 4-S3,4-S4,4-S5 and 4-S6.

The asymmetric units of **2b** and **5f** contain only half of the molecule as the Fe compound and the Zn cation lie at a site of crystallographic C_2 symmetry. Contrary, for **3g** and **5a** two independent molecules were found in the asymmetric units. The metal ions are coordinated in a distorted tetrahedral N_2Cl_2 or distorted octahedral N_6 geometry. The distortion is caused by the rigidity of the planar BIAN ligands which results in $N-M-N'$ bond angles (N, N' of the same BIAN moiety) between 77 and 82° depending on the $M-N$ distance. For the Zn and the tetrahedral Fe complexes, $M-N$ bond lengths between 2.11 and 2.18 Å were found. These separations are 1.99 – 2.00 Å in the octahedral complexes **3f,g** and **4g** which clearly indicates the low-spin state of Fe(II). The Fe–Cl separation in the counterions of **3f** and **3g** is typical for $[FeCl_4]^-$.^[23] The acenaphthene backbone is essentially planar; the N -aryl substituents are orthogonal to this plane. The bond lengths of the $N=C-C=N$ moiety are indicative of a C–C single bond and two C=N double bonds, which is in full agreement with the formulation of a neutral 1,2-diimine ligand.^{[24],[25]} It is noteworthy that the octahedral Fe complexes **3** and **4** contain slightly shortened C–C bonds whereas the C=N bonds are slightly longer. This deviation does not necessarily indicate a partial reduction of the BIAN ligands but could be a consequence of an

increased metal-to-ligand backbonding. Comparison of Zn complex **5a** with the corresponding Fe(II) complex^[16] and Co(II) complex^[26] shows that they form an isomorphous family. The complexes **2b,c** and **3g** exhibit in the solid-state parallel displaced $\pi \cdots \pi$ interactions between the *N*-aryl substituents, the acenaphthene backbone and co-crystallized toluene molecules. Graphical representations along with geometrical data can be found in the ESI.

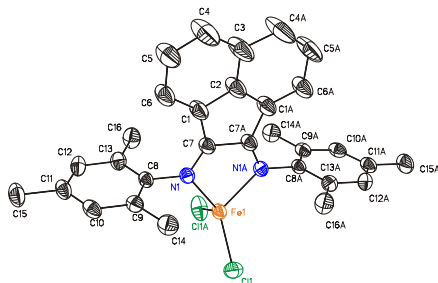


Figure 4-3 - ORTEP diagram (50% probability level) of the molecular structure of **2b** with the atom-numbering scheme. All H atoms and one molecule n-pentane are omitted for clarity. Symmetry code: A: $-x, y, -z+0.5$. Selected bond lengths (\AA), angles ($^\circ$): C7–C7A 1.521(5), C7–N1 1.274(3), C8–N1 1.444(3), Fe1–Cl1 2.2217(7), Fe1–N1 2.1368(19); C7–N1–C8 119.09(19), C7–N1–Fe1 112.92(16), C8–N1–Fe1 112.92(16), N1–Fe1–Cl1 113.65(6), N1–Fe1–Cl1A 113.86(5), N1–Fe1–N1A 78.64(10), Cl1–Fe1–Cl1A 117.24(5).

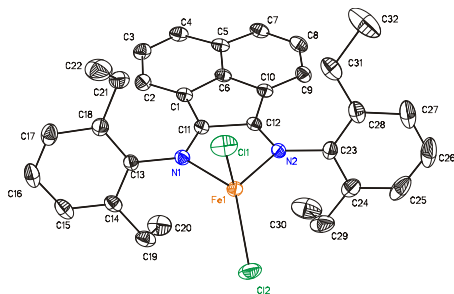


Figure 4-4 - ORTEP diagram (50% probability level) of the molecular structure of **2c** with the atom-numbering scheme. All H atoms and one molecule toluene are omitted for clarity. Selected bond lengths (\AA), angles ($^\circ$): C11–C12 1.510(2), C11–N1 1.284(2), C12–N2 1.281(2), C13–N1 1.4350(19), C23–N2 1.4378(19), Fe1–Cl1 2.2283(5), Fe1–Cl2 2.2182(5), Fe1–N1 2.1422(13), Fe1–N2 2.1251(12); C11–N1–C13 119.69(13), C11–N1–Fe1 111.83(10), C13–N1–Fe1 127.60(9), C12–N2–C23 120.82(13), C12–N2–Fe1 112.78(10), C23–N2–Fe1 125.92(10), N1–Fe1–N2 78.41(5), N1–Fe1–Cl1 104.18(4),

N1–Fe1–Cl2 122.51(4), N2–Fe1–Cl1 112.62(4), N2–Fe1–Cl2 113.81(4), Cl1–Fe1–Cl2 118.635(18).

The presence of the octahedral Fe complexes in a low-spin state explains the different reactivity of FeCl₂ and ZnCl₂ toward BIANs bearing only H atoms in the 2- and 6-positions of the *N*-aryl substituents. The thermodynamic driving force of the formation of Fe(BIAN)₃ complexes is most likely due to a significant gain in ligand field stabilization. Consequently, the reaction of ZnCl₂ with **1g** gave the tetrahedral 1:1 complex.^[21c]

¹H and ¹³C{¹H} NMR spectra were recorded of the octahedral Fe and Zn complexes **4f,g** and **5f,g**. Unlike in the free BIAN ligands **1f,g**, two sets of resonances were observed for the *ortho/ortho'* and *meta/meta'* positions of the aryl substituents, which are also significantly broader than the remaining resonances of the acenaphthene backbone. This clearly indicates that free rotation of the *N*-aryl substituents is hindered in Fe and Zn complexes. The longer M–N distances of **5f,g** indicate a smaller rotation barrier and thus give broader ¹H resonances of the *ortho* and *meta* protons in comparison with the respective Fe complexes. The ¹³C{¹H} NMR spectra confirmed the presence of (up to) 13 different carbon atoms in the aromatic region. The solution magnetic moments of **2a–e** were determined by the Evans NMR method. Measurements in thf-d₈ gave magnetic moments between 4.9 and 5.3 μ_B, which indicates the presence of high-spin Fe(II) centers.

The redox chemistry of bis(imino)acenaphthenes has extensively been studied in the past. The cyclic voltammograms (CVs) are strongly dependent on the electronic nature of the *N*-aryl substituents; however, the common features are two separate reductions to the monoanionic and dianionic forms and oxidation of the terminal *N*-aryl substituents.^{[21b],[25]} A 4e⁻-reduction of **1a** was achieved by Fedushkin *et al.* by reaction with sodium metal in diethyl ether. The solid-state structures showed that the first two electrons reduce the acenaphthene diimine to the acenaphthylene diamine, and the following two reductions occurred at the naphthalene moiety.^[27] CVs were recorded for the tetrahedral complexes **2a,c** and **5a** and the octahedral complexes **4f,g** and **5f,g** in acetonitrile using [N(*n*-Bu)₄][PF₆] as electrolyte (Tables 4-1, 4-S2 and Figures 4-5, 4-S16 to 4-S25). The electrochemical features of compounds **2** were very similar and will therefore be discussed on the example of **2a** (Table 4-1). Fe complex **2a** showed a reversible reduction at –0.91 V which is also present in the Zn complex **5a** at slightly more negative potential (Figure 4-5). This corresponds to the reduction of the neutral BIAN to the radical anion state. Upon further decrease of potential, additional cathodic waves were observed (e.g. BIAN reduction to dianion, reduction of Fe(II)). However, the following redox events gave complex CVs which were indicative of rapid decomposition of the analyte. An increased potential range to +1.5 V afforded irreversible oxidations at 0.20, 0.42 and 0.99 V and an irreversible reduction at –0.36 V. The reduction event also occurred when the potential was raised to +0.7 V (Figure 4-5, bottom, dashed line). A comparison with the respective

Zn compound showed that solely the oxidation at 0.99 V is ligand-centered (Figure 4-5, bottom).

Table 4-1 - Cyclic voltammetry data of **2a,c,d** and **5a**.

	$E_1^o (\Delta E_p) / \text{mV}$	E_{pa1} / mV	E_{pa2} / mV	E_{pa3} / mV	E_{pc} / mV
2a	-910 (87)	195	420	990	-360
2c	-920 (78)	185	410	1015	-385
2d	-925 (76)	160	380	n.d.	-355
5a	-995 (88)	-	-	1010	-

n.d.: not determined. E_{pa} : anodic peak potential. E_{pc} : cathodic peak potential.

The difference between E_1^o of **2a,c,d** and **5a** of 70–85 mV documented that the BIAN ligand in the Fe complexes is slightly less electron-rich than in the Zn complex. A more pronounced metal-to-ligand back bonding in the Zn complex or a stronger π -donation of the BIAN ligands toward Fe would in principle be in agreement with the observation. Though, the inspection of the C–C and C=N bond lengths of the N=C–C=N moiety, which are affected by both interactions, showed no significant differences (*vide supra*). It is instructive to note that Krüger and co-workers recorded a CV of the octahedral Fe(II) complex of **1f** with *N,N'*-dimethyl-2,11-diaza[3.3](2,6)pyridinophane that showed reversible BIAN reduction to the radical anion (-1.01 V) and dianion (-1.52 V) and reversible Fe(II)→Fe(III) oxidation (+0.73 V vs. FcH/FcH⁺).^[14d] The striking difference to the behavior of the tetrahedral complexes may result from the degree of anion coordination to the metal. The reduction of the BIAN ligands facilitates the cleavage of coordinated chloride anions forming highly reactive tri- or di-coordinated metal species in solution. Due to the relatively low concentration of the analyte, a stabilization of these species by dimerization is rather unlikely^[28] and consequently, rapid decomposition of the reduced metal complexes is to be expected. This may explain why for singly reduced **2a,c,d** and **5a** an irreversible electrochemical behavior is observed upon further decrease of the applied potential. However, it should not be concealed that free bis(imino)acenaphthenes very often do not show reversible redox events in CVs.^{[21b],[25]}

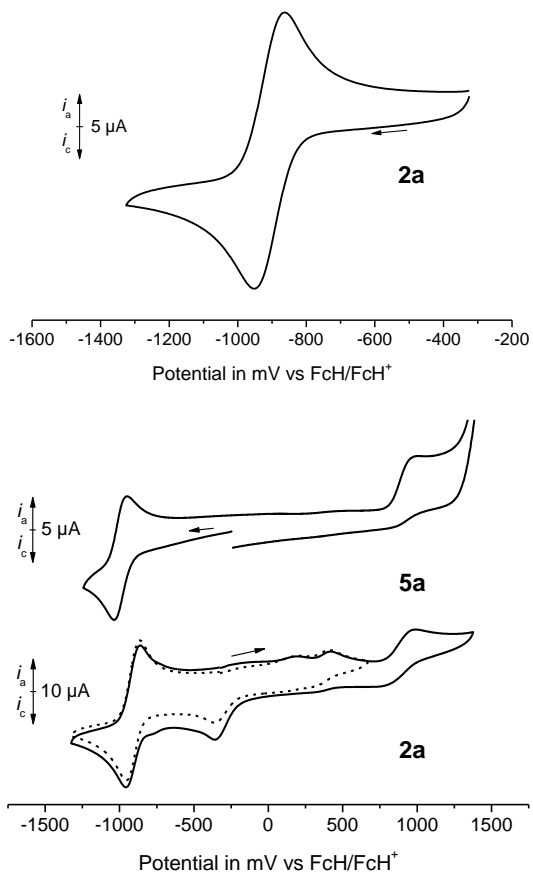
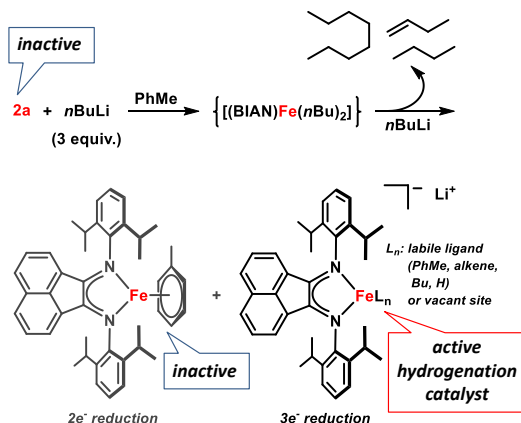


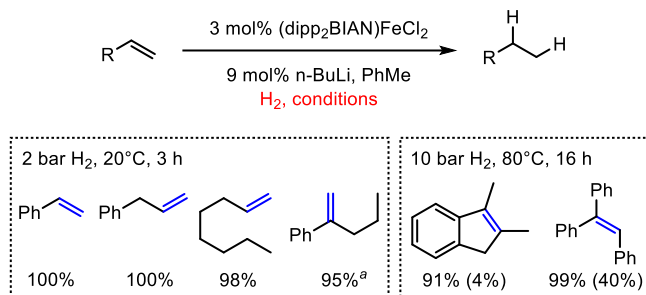
Figure 4-5 - Cyclic voltammograms (scan rate 200 mV·s⁻¹) of **2a** (10^{-3} M (solid line: -1.3 to 1.4 V, dashed line: -1.3 to 0.7 V)) and **5a** ($0.5 \cdot 10^{-3}$ M).

4.2.3 Catalytic studies

We have then applied the tetrahedral complexes of type **2** to the hydrogenation of alkenes.^{[29],[30]} Good catalytic activities were only observed when the complexes were activated by addition of a strong reductant. Treatment of **2a** with 3 equiv. *n*-butyllithium (*n*-BuLi) afforded the active hydrogenation catalyst.^[31] The observation of octane (67%), octenes (28%), and hexadecane (5%) formation from the reaction of **2a** with 3 equiv. *n*-octyllithium in toluene which corresponds to a reduction of the metal complex by at least two electrons. However, the reduction of **2a** with *n*-BuLi on a preparative scale (150 mg **2a**) afforded a mixture of species. The major component (~70 %) could be separated by extraction of the dried residue with hexane and was identified as (dipp)₂BIAN)Fe(η⁶-C₇H₈), which had previously been prepared by Findlater and co-workers.^[16] This formal two-electron reduction species was inactive in the hydrogenation of α -methylstyrene (1.9 bar H₂, 20 °C, 3 h). In contrast, the minor component of the reduction of **2a** with *n*-BuLi which was obtained from extraction with toluene and washing with hexane showed identical catalytic activity to the *in situ* generated catalyst mixture. In accordance with recent literature, we postulate a three-electron reduction of the (BIAN)FeCl₂ complex to a low-valent (BIAN)Fe species which possibly contains the BIAN ligand in the radical anion or dianion state (Scheme 4-3).^{[16],[17],[32]} Attempts to disclose the chemical identity of this fraction have not yet been successful. Application of the **2a**/BuLi catalyst solution to the hydrogenation of various alkenes resulted in excellent yields of the corresponding alkane products (Scheme 4-4). Similar reactions with catalytic FeCl₂(thf)_{1.5} gave much lower yields.^[33] It is important to note that clean hydrogenations of tri- and tetra-substituted alkenes were achieved at elevated H₂ pressure and temperature.



Scheme 4-3 - Reductive activation of the pre-catalyst **2a**.



Scheme 4-4 - Catalytic hydrogenations of alkenes (yields of reactions with 3 mol% FeCl₂(thf)_{1.5} in parentheses); ^a traces of isomerized product.

4.3 Conclusions

A series of Fe complexes of the general composition (R-BIAN)FeCl₂ (**2**) and [Fe(R-BIAN)₃][FeCl₄]₂ (**3**) was prepared by reaction of FeCl₂(thf)_{1.5} with various bis(imino)acenaphthenes (BIANs). The presence of *N*-aryl substituents in 2- or 6-position governs the formation of tetrahedral or octahedral complexes. The low-spin configuration of Fe(II) in the octahedral complexes **3** suggests that a gain in ligand-field stabilization is the thermodynamic driving force of this pathway. UV/Vis spectroscopy allowed the unambiguous distinction between complexes of type **2** and **3** as the latter exhibited much stronger CT absorptions in the visible region. This interpretation is in full accordance with the results obtained from mass spectrometry and X-ray diffraction. The electrochemical properties of complexes **2** and [Fe(BIAN)₃][BF₄]₂ (**4**) were determined by cyclic voltammetry. All compounds showed reversible BIAN-centered 1e⁻-reductions in the potential range of -0.7 to -1.2 V vs FcH/FcH⁺, whereby the BIAN ligand in **2** is reduced to a radical anion. A further decrease of the potential leads to irreversible reductions. For (BIAN)FeCl₂, a ligand-related irreversible oxidation at 1.0 V was identified along with two Fe-centered irreversible oxidations at 0.2 and 0.4 V associated with a reduction at -0.4 V.

(i) The facile synthetic access to iron BIAN complexes, (ii) their stereoelectronic modulation by variation of the *N*-aryl substituents, stoichiometry, and counterion, and (iii) the non-innocent character of the BIAN ligands are a prime motivation to apply such complexes as catalysts to redox reactions. Initial catalytic studies in hydrogenations of olefins documented the excellent activity of (dipp₂BIAN)FeCl₂ (**2a**). Our group is currently investigating further avenues toward new iron-catalyzed reduction, hydrofunctionalization and dehydrogenation protocols with these complexes.

4.3 Experimental part

4.3.1 General

Chemicals and Solvents: All experiments involving air- and moisture-sensitive compounds were performed under an atmosphere of dry argon or nitrogen using standard Schlenk and glovebox techniques. Solvents (THF, toluene) were distilled over sodium and benzophenone and stored over molecular sieves (4 Å). Anhydrous acetonitrile was purchased from and Carl Roth. All starting materials were obtained from commercial suppliers and used without further purification unless otherwise noted. **1**^[34] and **5a**^[35] were synthesized according to literature procedures. FeCl₂(thf)_{1.5} has been prepared by heating FeCl₂ to reflux in tetrahydrofuran overnight and subsequently removing the solvent by filtration. Commercially available reductant (*n*-BuLi) were used as received from Sigma-Aldrich or diluted before use. Commercially available olefins were distilled under reduced pressure prior use.

High Pressure Reactor: Hydrogenation reactions were carried out in 160 and 300 mL high pressure reactors (*Parr*TM) in 4 mL glass vials. The reactors were loaded under argon, purged with H₂ (1 min), sealed and the internal pressure was adjusted. Hydrogen (99.9992%) was purchased from *Linde*.

¹H- und ¹³C-NMR-Spectroscopy: Nuclear magnetic resonance spectra were recorded on a *Bruker* Avance 300 (300 MHz) and *Bruker* Avance 400 (400 MHz). ¹H-NMR: The following abbreviations are used to indicate multiplicities: s = singlet; d = doublet; t = triplet, q = quartet; m = multiplet, dd = doublet of doublet, dt = doublet of triplet, dq = doublet of quartet, ddt = doublet of doublet of quartet. Chemical shift δ is given in ppm to tetramethylsilane.

IR spectroscopy: IR absorption spectra were measured with a Varian 670-IR FT-IR spectrometer using ATR technique on a Gladi ATR Base Optic Assembly with a 2.2×3.0 mm ATR diamond crystal sampling area

Elemental Analyses (CHN): Elemental analyses (CHN) were performed with a Vario micro cube elemental analyzer.

Mass Spectrometry: Mass spectra were recorded on an Agilent Q-TOF 6540 UHD in electrospray ionization (ESI) mode and on a Joel AccuTOF GCX in liquid injection field desorption ionization (LIFDI) mode

UV/Vis Spectroscopy: UV/Vis analyses were performed on a Varian Cary 50 UV/Vis spectrophotometer using screw-capped Hellma quartz SUPRASIL cuvettes (10×10 mm).

Gas chromatography with FID (GC-FID): HP6890 GC-System with injector 7683B and *Agilent 7820A* System. Column: HP-5, 19091J-413 (30 m × 0.32 mm × 0.25 μm), carrier gas: N₂. GC-FID was used for reaction control and catalyst screening (Calibration with internal standard *n*-pentadecane and analytically pure samples).

Gas chromatography with mass-selective detector (GC-MS): *Agilent 6890N* Network GC-System, mass detector 5975 MS. Column: HP-5MS (30m × 0.25 mm × 0.25 μm, 5% phenylmethylsiloxane, carrier gas: H₂. Standard heating procedure: 50 °C (2 min), 25 °C/min -> 300 °C (5 min)

4.3.2 Electrochemistry

Electrochemical measurements were carried out using 0.25–1.0 mmol·L⁻¹ solutions of the analytes and [N(*n*-Bu)₄][PF₆] (0.1 mol·L⁻¹) as supporting electrolyte in acetonitrile. The studies were performed with two different apparatus. This involved an Autolab PGSTAT101 potentiostat using a Pt disc working electrode, a Pt counter electrode and an Ag wire as pseudo-reference electrode. Secondly, a Radiometer Volta-lab PGZ 100 electrochemical workstation using a Pt disc working electrode, a Pt counter electrode and an Ag/Ag⁺ (0.01 mol·L⁻¹ AgNO₃) reference electrode was applied. The reference electrode consists of a silver wire which was inserted into a Luggin capillary with a Vycor tip filled with a solution of 0.01 mol·L⁻¹ AgNO₃ and 0.1 mol·L⁻¹ [N(*n*-Bu)₄][PF₆] in acetonitrile, whereas this Luggin capillary was inserted into a second Luggin capillary with a Vycor tip filled with a solution of 0.1 mol·L⁻¹ [N(*n*-Bu)₄][PF₆] in acetonitrile.^[36] The working electrodes were pretreated by polishing on a Buehler microcloth subsequently with 1 μm and 1/4 μm diamond paste. Ferrocene (FcH) was employed as internal standard; the redox potentials are given against the ferrocene/ferrocenium redox couple.^[37]

The electrochemistry of the octahedral complexes **4** is exemplified with the discussion of **4g** (Figure 4-S21,4-S22). Table 4-S2 contains the respective electrochemical data. When recording the CV between -1.6 and 0 V vs FcH/FcH⁺, two reversible redox processes at $E^{\circ'} = -0.75$ and -1.24 V were observed. The electron-donating *para*-methyl substituents in **4g** gave a cathodic shift of both events in comparison with **4f** (-0.70 and -1.19 V). Both reversible redox steps correspond to a 1e⁻-reduction of the corresponding BIANs.^[38] For metal complexes containing two or more BIAN ligands very often 1e⁻-redox processes are observed^[39] resulting in the formation of compounds in which formerly identical redox-active moieties have different oxidation states.^[40]

With a wider cathodic scan window (-2.0 to 0 V; Figure 4-S21, bottom) an irreversible reduction of **4g** at -1.85 V accompanied with an irreversible oxidation at -0.35 V was

observed. Further widening of the potential range (-2.0 to +1.5 V; Figure 4-S22) revealed two additional irreversible oxidations which appear to be associated with the decomposition of **4g** as they were absent prior to the irreversible reduction. While it is well known for BIAN complexes that the ligand can be reduced in two consecutive steps^{[21b],[25]} this did not hold true for the Fe complexes **4** under our conditions. It seems that after 1e⁻-reduction of every BIAN ligand coordinated to Fe, decomposition of the complex occurred. The corresponding Zn complex **5g** exhibited three BIAN-centered reversible reductions (Figure 4-S23, up) prior to an irreversible reduction at one BIAN which induces decomposition. The fact that the BIAN-reduction steps of the Zn complex **5g** proceed in a much narrower potential window ($E^{o'} = -0.97, -1.08, -1.36$ V) than the corresponding Fe complex **4g** supports the notion of a less pronounced electronic coupling between appropriate ligand orbitals through the Zn atom which is most likely due to the lack of non-populated d-orbitals in Zn²⁺. A similar trend was observed by Tomson and Anstey at the example of $[M((3,5\text{-Xyl})_2\text{BIAN})_3]$ (M = Al, Ga, Cr) whereby ligand-centered redox processes occurred in case of the chromium complex in a much broader potential window than in case of aluminium and gallium.^[39c]

4.3.3 X-Ray Diffraction

Single crystals were obtained by slow diffusion of pentane into a solution of **2b**, **3f,g** or **5f** in dichloromethane, slow diffusion of diethyl ether into a solution of **4g** in acetonitrile or **5a** in dichloromethane or by recrystallization from toluene (**2c**). Data were collected with an Agilent Technologies SuperNova Atlas CCD diffractometer with microfocus Cu K_α radiation ($\lambda = 1.54184$ Å) and a SuperNova Eos CCD diffractometer with microfocus Mo K_α radiation ($\lambda = 0.71073$ Å). The structures were solved by direct methods and refined by full-matrix least-squares procedures on F^2 .^[41] All non-hydrogen atoms were refined anisotropically, and a riding model was employed in the treatment of the hydrogen atom positions. Geometrical and displacement restraints were applied to the structures where necessary. The selected crystals of **3g** and **5a** were non-merohedral twins. The respective twin law was determined with the CrysAlisPro software, and the structures were refined with the corresponding HKLF5 files. PLATON SQUEEZE was used for the refinement of **4g**.^[42]

The crystal and structure refinement data are given in Tables 4-S3 and 4-S6. CCDC 1510919 (**2b**), 1510920 (**2c**), 1510921 (**3f**), 1510922 (**3g**), 1510923 (**4g**), 1510924 (**5a**), and 1510925 (**5f**) contain the supplementary crystallographic data for this paper. The data can be obtained free of charge from The Cambridge Crystallographic Data Centre via www.ccdc.cam.ac.uk/structures.

4.3.4 General procedure for the synthesis (Ar₂BIAN)FeCl₂ (2)

In a Schlenk flask FeCl₂(thf)_{1.5} (1 mmol, 1 equiv.) and the BIAN ligand (1.1 mmol, 1.1 equiv.) were suspended in toluene (20 mL). The mixture was heated to 100 °C and stirred for 16 h during which the formation of a precipitate was observed. After cooling to r.t. the suspension was concentrated in vacuo and filtered. The solid residue was washed with toluene (3×5 mL) and dried to afford the desired complex.

(dipp₂BIAN)FeCl₂ (2a)

Green solid, 86 % yield. mp >240 °C (decomp); **Anal. calcd (%)** for C₃₆H₄₀Cl₂FeN₂: C, 68.91; H, 6.43; N, 4.46. Found: C, 68.84; H, 6.19; N, 4.33; **IR**: $\tilde{\nu}$ = 2957, 2926, 2866, 1647, 1614, 1597, 1577, 1463, 1433, 1417, 1286, 836, 802, 783, 760 cm⁻¹; **LIFDI-MS** (*m/z*) calcd for C₃₆H₄₀Cl₂FeN₂: 626.1914, found: 626.1756 [*M*]⁺; μ_{eff} (thf-d₈, 300 K): 4.9(2) μ_{B} .

(mes₂BIAN)FeCl₂ (2b)

Green solid, 86 % yield.^[43] mp >250 °C (decomp); **Anal. calcd (%)** for C₃₀H₂₈Cl₂FeN₂: C, 66.32; H, 5.19; N, 5.16. Found: C, 66.06; H, 5.26; N, 5.02; **IR**: $\tilde{\nu}$ = 3020, 2908, 2856, 1660, 1627, 1604, 1586, 1481, 1418, 1290, 1243, 857, 834, 780, 731, 695 cm⁻¹; **LIFDI-MS** (*m/z*) calcd for C₃₀H₂₈Cl₂FeN₂: 542.0979, found: 542.1978 [*M*]⁺; μ_{eff} (thf-d₈, 300 K): 4.9(3) μ_{B} .

(bis(2,6-diethylphenyl)BIAN)FeCl₂ (2c)

Green solid, 85 % yield. mp >240 °C (decomp); **Anal. calcd (%)** for C₃₂H₃₂Cl₂FeN₂ × ½ C₇H₈: C, 69.06; H, 5.88; N, 4.54. Found: C, 69.07; H, 5.81; N, 4.40; **IR**: $\tilde{\nu}$ = 2964, 2930, 2868, 1654, 1619, 1598, 1580, 1442, 1417, 1290, 833, 805, 779, 756, 727, 692 cm⁻¹; **LIFDI-MS** (*m/z*) calcd for C₃₀H₂₈Cl₂FeN₂: 570.1292, found: 570.1184 [*M*]⁺; μ_{eff} (thf-d₈, 300 K): 5.2(3) μ_{B} .

(bis(2,6-dimethylphenyl)BIAN)FeCl₂ (2d)

Green solid, 89 % yield. mp >250 °C (decomp); **Anal. calcd (%)** for C₂₈H₂₄Cl₂FeN₂: C, 65.27; H, 4.70; N, 5.44. Found: C, 65.45; H, 4.77; N, 5.18; **IR**: $\tilde{\nu}$ = 3023, 2979, 2919, 2856, 1659, 1631, 1605, 1585, 1470, 1441, 1419, 1293, 1225, 832, 776, 745 cm⁻¹; **LIFDI-MS** (*m/z*) calcd for C₂₈H₂₄Cl₂FeN₂: 514.0666, found: 514.1618 [*M*]⁺; μ_{eff} (thf-d₈, 300 K): 5.0(3) μ_{B} .

(bis(2-isopropylphenyl)BIAN)FeCl₂ (2e)

Green solid, 93 % yield. mp >310 °C (decomp); **Anal. calcd (%)** for C₃₀H₂₈Cl₂FeN₂: C, 66.32; H, 5.19; N, 5.16. Found: C, 65.89; H, 5.23; N, 4.88; **IR**: $\tilde{\nu}$ = 3069, 3026, 2959,

2926, 2867, 1652, 1598, 1482, 1443, 1418, 1281, 832, 779, 757, 744 cm^{-1} ; **LIFDI-MS** (m/z) calcd for $\text{C}_{30}\text{H}_{28}\text{Cl}_2\text{FeN}_2$: 542.0979, found: 542.1975 [M]⁺; μ_{eff} (thf-d₈, 300 K): 5.3(3) μ_{B} .

[Fe(Ph₂BIAN)₃][FeCl₄]₂ (**3f**)

In a Schlenk flask FeCl₂(thf)_{1.5} (0.2 mmol, 1 equiv.), FeCl₃ (0.4 mmol, 2 equiv.) and Ph₂BIAN (0.6 mmol, 3 equiv.) were suspended in toluene (12 mL). The mixture was heated to 100 °C and stirred for 16 h during which the formation of a green precipitate was observed. After cooling to room temperature the suspension was concentrated in vacuo and filtered. The solid residue was washed with toluene (3×5 mL) and dried to afford the desired green complex in 87 % yield (251 mg). mp >250 °C (decomp); **Anal. calcd (%)** for $\text{C}_{72}\text{H}_{48}\text{Cl}_8\text{Fe}_3\text{N}_6$: C, 59.71; H, 3.34; N, 5.80. Found: C, 60.19; H, 3.49; N, 5.51; **IR**: $\tilde{\nu}$ = 3058, 1656, 1625, 1601, 1586, 1483, 1417, 1299, 826, 766, 701, 639 cm^{-1} ; **ESI-MS** (m/z) calcd for $\text{C}_{72}\text{H}_{48}\text{FeN}_6$: 526.1639, found: 526.1645 [M]²⁺.

4.3.5 General procedure for the synthesis [Fe(Ar₂BIAN)₃][BF₄]₂ (**4**)

In a Schlenk flask [Fe(H₂O)₆][BF₄]₂ (1.0 mmol, 1 equiv.) and BIAN (3.3 mmol, 3.3 equiv.) were dissolved in acetonitrile (40 mL). After stirring for 20 hours at room temperature the green solution was filtered. The filtrate was evaporated to dryness and the solid residue was washed with thf/toluene (1:1, 4×10 mL) and toluene (3×5 mL). The solid was dried to afford the desired complex.

[Fe(Ph₂BIAN)₃][BF₄]₂ (**4f**)

Deep green solid, 92 % yield. mp >240 °C (decomp); **Anal. calcd (%)** for $\text{C}_{72}\text{H}_{48}\text{B}_2\text{F}_8\text{FeN}_6$: C, 70.50; H, 3.94; N, 6.85. Found: C, 70.92; H, 4.05; N, 6.66; **IR**: $\tilde{\nu}$ = 3061, 1651, 1623, 1599, 1583, 1485, 1418, 1300, 1118, 1051, 830, 764, 701, 637 cm^{-1} ; **ESI-MS** (m/z) calcd for $\text{C}_{72}\text{H}_{48}\text{FeN}_6$: 526.1639, found: 526.1653 [M]²⁺; **¹H NMR** (400 MHz, CD₃CN) δ = 8.65 (m, 6H), 8.48 (d, J = 8.3 Hz, 6H), 7.76 (m, 6H), 7.53 (t, J = 7.8 Hz, 6H), 6.98 (d, J = 7.3 Hz, 6H), 5.98 (t, J = 7.4 Hz, 6H), 4.80 (br, 6H), 3.99 ppm (d, J = 6.1 Hz, 6H); **¹³C{¹H} NMR** (101 MHz, CD₃CN) δ = 164.97, 144.50, 140.72, 137.99, 134.83, 134.36, 133.28, 130.94, 125.56, 124.35, 123.67 ppm.

[Fe((4-Tol)₂BIAN)₃][BF₄]₂ (**4g**)

Deep green solid, 93 % yield. mp >270 °C (decomp); **Anal. calcd (%)** for $\text{C}_{78}\text{H}_{60}\text{B}_2\text{F}_8\text{FeN}_6$: C, 71.47; H, 4.61; N, 6.41. Found: C, 71.01; H, 4.86; N, 6.90; **IR**: $\tilde{\nu}$ = 2922, 2858, 1656, 1624, 1588, 1503, 1418, 1300, 1123, 1050, 832, 815, 779, 634 cm^{-1} ; **ESI-MS** (m/z) calcd for $\text{C}_{78}\text{H}_{60}\text{FeN}_6$: 568.2109, found: 568.2126 [M]²⁺; **¹H NMR** (400 MHz, CD₃CN) δ = 8.35 (d, J = 8.3 Hz, 6H), 7.60 (d, J = 7.5 Hz, 6H), 7.56 (dd, J =

8.3, 7.3 Hz, 6H), 7.04 (d, $J = 6.7$ Hz, 6H), 6.81 (d, $J = 7.3$ Hz, 6H), 5.95 (d, $J = 7.2$ Hz, 6H), 4.59 (d, $J = 7.7$ Hz, 6H), 2.91 ppm (s, 18H); $^{13}\text{C}\{^1\text{H}\}$ NMR (101 MHz, CD_3CN) $\delta = 165.48, 151.82, 145.37, 144.59, 140.30, 133.70, 133.61, 130.19, 130.07, 129.34, 127.54, 125.20, 124.68, 19.94$ ppm.

4.3.6 General procedure for the synthesis $[\text{Zn}(\text{Ar}_2\text{BIAN})_3][\text{BF}_4]_2$ (5)

In a Schlenk flask $[\text{Zn}(\text{H}_2\text{O})_6][\text{BF}_4]_2$ (1.0 mmol, 1 equiv.) and Ar-BIAN (3.3 mmol, 3.3 equiv.) were dissolved in acetonitrile (40 mL). After stirring for 20 hours at room temperature the solution was evaporated to dryness. The solid residue was washed with thf/toluene (1:1, 3×15 mL) and toluene (3×10 mL). The solid was dried to afford the desired complex.

$[\text{Zn}(\text{Ph}_2\text{BIAN})_3][\text{BF}_4]_2$ (5f)

Yellow solid, 91 % yield. mp >250 °C (decomp); **Anal. calcd** (%) for $\text{C}_{72}\text{H}_{48}\text{B}_2\text{F}_8\text{N}_6\text{Zn}$: C, 69.96; H, 3.91; N, 6.80. Found: C, 69.66; H, 4.02; N, 6.55; **IR**: $\tilde{\nu} = 3059, 1666, 1629, 1585, 1484, 1449, 1436, 1419, 1284, 1250, 1227, 1119, 1050, 831, 763, 699$ cm^{-1} ; **ESI-MS** (m/z) calcd for $\text{C}_{72}\text{H}_{48}\text{N}_6\text{Zn}$: 530.1610, found: 530.1605 $[\text{M}]^{2+}$; ^1H NMR (400 MHz, CD_3CN) $\delta = 8.34$ (d, $J = 8.3$ Hz, 6H), 7.62 (dd, $J = 8.3, 7.4$ Hz, 6H), 7.46 (m, 6H), 7.27–7.42 (m, 6H), 7.10–7.22 (m, 6H), 6.92–7.05 (m, 6H), 6.81 (d, $J = 7.4$ Hz, 6H), 5.22 ppm (d, $J = 5.6$ Hz, 6H); $^{13}\text{C}\{^1\text{H}\}$ NMR (101 MHz, CD_3CN) $\delta = 165.36, 146.48, 146.46, 134.44, 132.30, 131.67, 130.12, 129.37, 128.19, 125.51, 121.02, 120.85$ ppm.

$[\text{Zn}((4\text{-Tol})_2\text{BIAN})_3][\text{BF}_4]_2$ (5g)

Yellow solid, 93 % yield. mp >270 °C (decomp); **Anal. calcd** (%) for $\text{C}_{78}\text{H}_{60}\text{B}_2\text{F}_8\text{N}_6\text{Zn}$: C, 70.95; H, 4.58; N, 6.37. Found: 70.56; H, 4.77; 6.45; **IR**: $\tilde{\nu} = 2924, 2862, 1663, 1632, 1586, 1503, 1421, 1283, 1249, 1119, 1052, 832, 819, 776$ cm^{-1} ; **ESI-MS** (m/z) calcd for $\text{C}_{78}\text{H}_{60}\text{N}_6\text{Zn}$: 572.2080, found: 572.2079 $[\text{M}]^{2+}$; ^1H NMR (400 MHz, CD_3CN) $\delta = 8.32$ (d, $J = 8.3$ Hz, 6H), 7.62 (dd, $J = 8.3, 7.3$ Hz, 6H), 6.66–7.29 (m, 18H), 6.85 (d, $J = 7.3$ Hz, 6H), 5.17 (br, 6H), 2.36 ppm (s, 18H); $^{13}\text{C}\{^1\text{H}\}$ NMR (101 MHz, CD_3CN) $\delta = 165.14, 146.17, 143.97, 139.63, 134.16, 132.25, 131.85, 129.98, 128.02, 125.73, 120.83, 21.05$ ppm.

4.3.7 General procedure for catalytic hydrogenations of alkenes

A 4 mL vial was charged with a freshly prepared solution of $(\text{dipp})_2\text{BIAN}\text{FeCl}_2$ (**2a**) in toluene (2.50 mL, 0.003 M) and an aliquot of a solution of *n*-BuLi in toluene (45 μL , 0.5 M) was added under an argon atmosphere. The alkene (0.25 mmol) was added and the vial transferred to a high pressure reactor. The reactor was purged with H_2 (1 min), sealed, and the internal temperature and pressure adjusted. After the desired reaction time, the autoclave was purged and the vial was retrieved. The reaction was quenched with

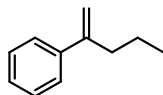
saturated aqueous NaHCO_3 (0.5 mL) and extracted with ethyl acetate (1 mL). The organic phases were filtered through a plug of silica (ethyl acetate as eluent) and analyzed by quantitative GC-FID analysis vs. *n*-pentadecane as internal reference.

4.3.8 Synthesis of starting materials

Styrene, ethylbenzene, alpha-methylstyrene, cumene, allylbenzene, propylbenzene, 1-octene, octane and 1,1,2-triphenylethylene were obtained from commercial suppliers, non-commercial starting materials were synthesized following the cited protocols.

2-Phenyl-1-pentene

Synthesis following the procedure by M. W. Justik, G. F. Koser, *Tetrahedron Lett.* **2004**, 45, 6159–6163.



$\text{C}_{11}\text{H}_{14}$
164.2 g/mol

Appearance

colorless liquid

Yield

1.21 g, 8.27 mmol (55 %)

^1H NMR

(300 MHz, CDCl_3) δ 7.51–7.24 (m, 5H), 5.31 (d, J = 1.7 Hz, 1H), 5.09 (m, 1H), 2.60–2.46 (m, 2H), 1.52 (m, 2H), 0.96 (t, J = 7.3 Hz, 3H).

$^{13}\text{C}\{^1\text{H}\}$ NMR

(75 MHz, CDCl_3) δ 148.52, 141.47, 128.25, 127.27, 126.16, 112.24, 37.48, 21.38, 13.83.

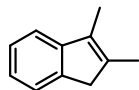
GC-MS

t_R = 5.87 min, (EI, 70 eV): m/z = 146 [M]⁺, 131, 118, 103, 91, 77, 65, 51.

Analytical data were in full agreement with M. W. Justik, G. F. Koser, *Tetrahedron Lett.* **2004**, 45, 6159-6163.

2,3-dimethyl-1H-indene

Synthesis following the procedure by H.-Q. Luo, T.-P. Loh, *Tetrahedron Lett.* **2009**, 50, 1554–1556.



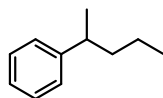
C₁₁H₁₂
144.2 g/mol

Appearance colorless oil
Yield 1.49 g, 10.3 mmol (21 %)
¹H NMR (300 MHz, CDCl₃) δ 7.40–7.08 (m, 4H), 3.27 (m, 2H), 2.07 (m, 3H), 2.04 (m, 3H).
¹³C{¹H} NMR (75 MHz, CDCl₃) δ 147.55, 142.32, 138.05, 132.51, 126.05, 123.55, 122.97, 117.91, 42.46, 13.95, 10.17.
GC-MS *t*_R = 6.74 min, (EI, 70 eV): *m/z* = 144 [*M*]⁺, 128, 115, 102, 89, 77, 71, 63, 51.

Analytical data were in full agreement with M. W. Justik, G. F. Koser, *Tetrahedron Lett.* **2004**, *45*, 6159–6163 and M. G. Schrems, E. Neumann, A. Pfaltz, *Angew. Chem. Int. Ed.* **2007**, *46*, 8274–8276.

4.3.9 Hydrogenation products

2-phenylpentane

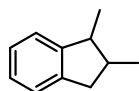


C₁₁H₁₆
148.2 g/mol

Appearance colorless liquid
¹H NMR (300 MHz, CDCl₃) δ 7.40–7.18 (m, 5H), 2.75 (m, 1H), 1.69–1.50 (m, 2H), 1.40–1.17 (m, 5H), 0.93 (t, *J* = 7.3 Hz, 3H).
¹³C{¹H} NMR (75 MHz, CDCl₃) δ 147.96, 128.30, 127.05, 125.79, 40.78, 39.74, 22.37, 20.89, 14.22.
GC-MS *t*_R = 5.56 min, (EI, 70 eV): *m/z* = 148 [*M*]⁺, 105, 91, 77, 65, 51.

Analytical data were in full agreement with R. B. Bedford, P. B. Brenner, E. Carter, T. W. Carvell, P. M. Cogswell, T. Gallagher, J. N. Harvey, D. M. Murphy, E. C. Neeve, J. Nunn, D. R. Pye, *Chem. Eur. J.* **2014**, *20*, 7935–7938.

2,3-dimethyl-1H-indane



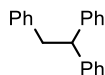
C₁₁H₁₄
146.2 g/mol

Appearance colorless liquid

¹H NMR	(300 MHz, CDCl ₃) δ 7.35–7.17 (m, 4H), 3.23 (m, 1H), 3.11–2.98 (m, 1H), 2.73–2.59 (m, 2H), 1.21 (d, <i>J</i> = 7.2 Hz, 3H), 1.05 (d, <i>J</i> = 6.8 Hz, 3H).
¹³C{¹H} NMR	(75 MHz, CDCl ₃) δ 148.78, 142.92, 126.15, 126.09, 124.50, 123.60, 42.47, 39.45, 37.92, 15.21, 14.68.
GC-MS	<i>t</i> _R = 6.02 min, (EI, 70 eV): <i>m/z</i> = 146 [<i>M</i>] ⁺ , 131, 115, 91, 77, 65, 51.

Analytical data were in full agreement with M. G. Schrems, E. Neumann, A. Pfaltz, *Angew. Chem. Int. Ed.* **2007**, *46*, 8274–8276.

Ethane-1,1,2-triyltribenzene



C₂₀H₁₈
258.4 g/mol

Appearance	pale yellow solid
¹H NMR	(300 MHz, CDCl ₃) δ 7.31–6.97 (m, 15H), 4.24 (t, <i>J</i> = 7.8 Hz, 1H), 3.37 (d, <i>J</i> = 7.8 Hz, 2H).
¹³C{¹H} NMR	(75 MHz, CDCl ₃) δ 144.45, 140.26, 129.08, 128.34, 128.05, 126.19, 125.88, 53.11, 42.11.
GC-MS	<i>t</i> _R = 10.68 min, (EI, 70 eV): <i>m/z</i> = 258 [<i>M</i>] ⁺ , 167, 152, 139, 128, 115, 91, 77, 65, 51.

Analytical data were in full agreement with K. Semba, K. Ariyama, H. Zheng, R. Kameyama, S. Sakaki, Y. Nakao, *Angew. Chem. Int. Ed.* **2016**, *55*, 6275–6279.

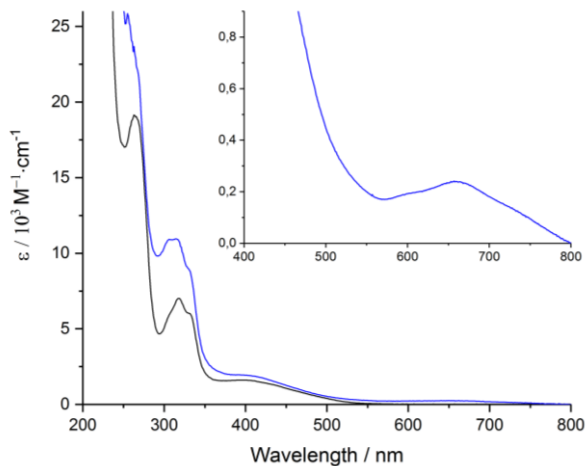


Figure 4-S1 - UV/Vis spectra of **1b** (black) and its Fe (**2b**, blue) complex in acetonitrile solution at 10^{-4} M (small graph: **2b** at 10^{-3} M).

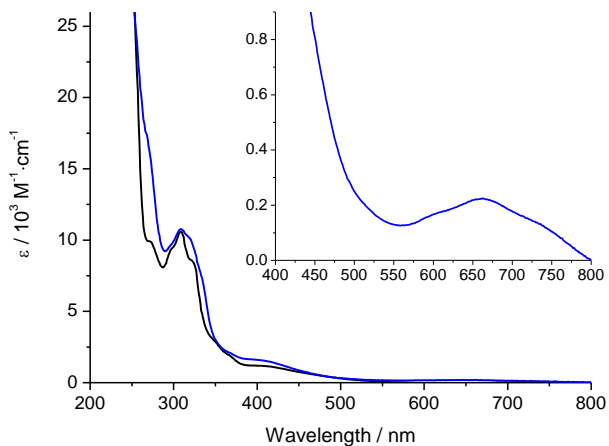


Figure 4-S2 - UV/Vis spectra of **1c** (black) and its Fe (**2c**, blue) complex in acetonitrile solution at 10^{-4} M (small graph: **2c** at 10^{-3} M).

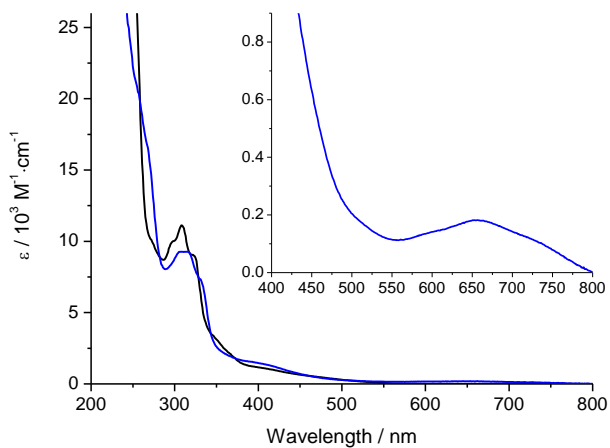


Figure 4-S3 - UV/Vis spectra of **1d** (black) and its Fe (**2d**, blue) complex in acetonitrile solution at 10^{-4} M (small graph: **2d** at 10^{-3} M).

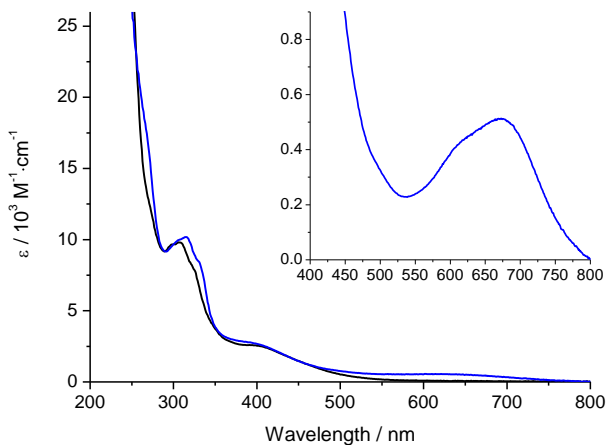


Figure 4-S4 - UV/Vis spectra of **1e** (black) and its Fe (**2e**, blue) complex in acetonitrile solution at 10^{-4} M (small graph: **2e** at 10^{-3} M).

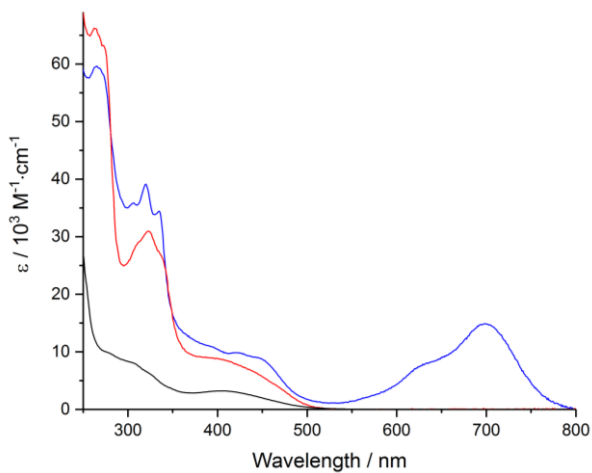
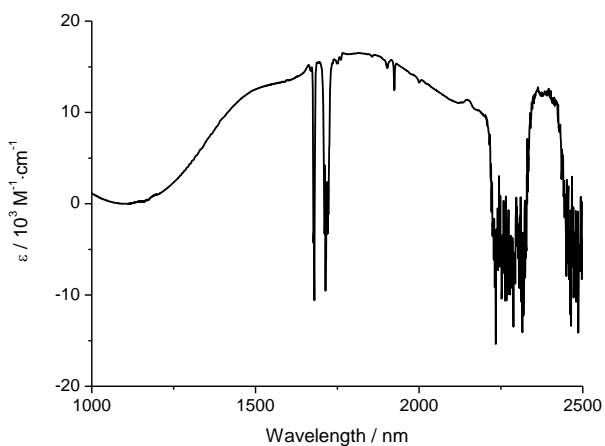


Figure 4-S5 - UV/Vis spectra of **1g** (black) and its Fe (**4g**, blue) and Zn (**5g**, red) complex in acetonitrile solution at 10^{-5} – 10^{-4} M.



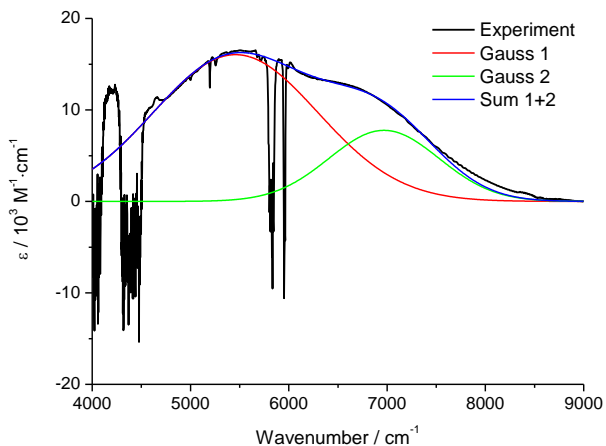


Figure 4-S6 - NIR spectrum of **2a** in acetonitrile solution at $5 \cdot 10^{-3}$ M; deconvolution of the experimental spectrum by two overlapping Gaussian shaped bands (Gauss 1: $\tilde{\nu} = 5460 \text{ cm}^{-1}$, $\Delta\tilde{\nu}_{1/2} = 1970 \text{ cm}^{-1}$, $\epsilon_{\text{max}} = 16 \text{ M}^{-1}\text{cm}^{-1}$; Gauss 2: $\tilde{\nu} = 6970 \text{ cm}^{-1}$, $\Delta\tilde{\nu}_{1/2} = 1320 \text{ cm}^{-1}$, $\epsilon_{\text{max}} = 8 \text{ M}^{-1}\text{cm}^{-1}$).

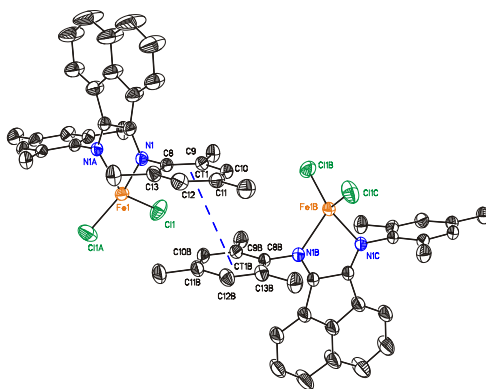


Figure 4-S7 - ORTEP diagram (50 % probability level) of $\pi \cdots \pi$ -interactions in the solid-state structure of **2b**. All hydrogen atoms and solvent molecules were omitted for clarity. Symmetry code: A: $-x, y, -z+0.5$; B: $-x+0.5, -y+1, z$; C: $x+0.5, -y+1, -z+0.5$; CT1 denotes the centroid of C8–C13. Geometrical details: CT1–CT1B $3.8635(13) \text{ \AA}$, angle between plane of C8–C13 and C8B–C13B $1.62(11)^\circ$, perpendicular distance of CT1 onto plane of C8B–C13B $3.4893(9) \text{ \AA}$.

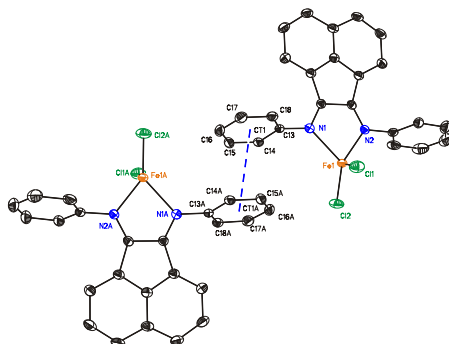


Figure 4-S8 - ORTEP diagram (50 % probability level) of $\pi\cdots\pi$ -interactions in the solid-state structure of **2c**. All hydrogen atoms, the ethyl substituents and solvent molecules were omitted for clarity. Symmetry code: A: $-x, -y, -z+1$; CT1 denotes the centroid of C13–C18. Geometrical details: CT1–CT1A 3.6486(9) Å, angle between plane of C13–C18 and C13A–C18A 0.03(8)°, perpendicular distance of CT1 onto plane of C13A–C18A 3.3747(7) Å.

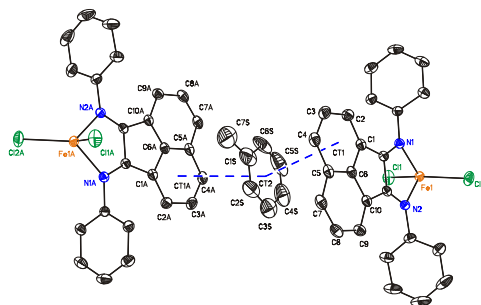


Figure 4-S9 - ORTEP diagram (50 % probability level) of $\pi\cdots\pi$ -interactions in the solid-state structure of **2c**. All hydrogen atoms and the ethyl substituents were omitted for clarity. Symmetry code: A: $-x+1, -y, -z$; CT1 denotes the centroid of C1–C6, CT2 denotes the centroid of C1S–C6S. Geometrical details: CT1–CT2 3.8269(18), CT2–CT1A 3.9783(17) Å, CT1–CT2–CT1A 152.64°, angle between plane of C1–C6 and C1S–C6S 13.46(14)°, perpendicular distance of CT1/CT1A onto plane of C1S–C6S 3.7664(7)/3.7324(7) Å.

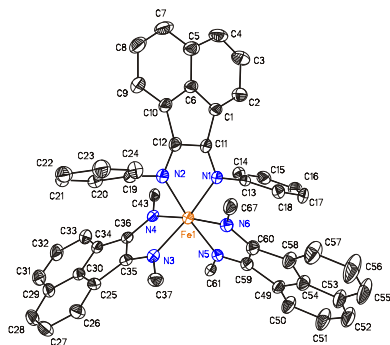


Figure 4-S10 - ORTEP diagram (50 % probability level) of the molecular structure of **3f** with the atom-numbering scheme. All hydrogen atoms, four phenyl substituents and all $[\text{FeCl}_4]^-$ counterions were omitted for clarity. Average bond distances (\AA), angles ($^\circ$): C–C of N=C–C=N 1.48, C–N 1.44, C=N 1.29, Fe–N 1.99, Fe–Cl 2.18; N–Fe–N 173.9, 90.1, sum of angles around N 359.9.

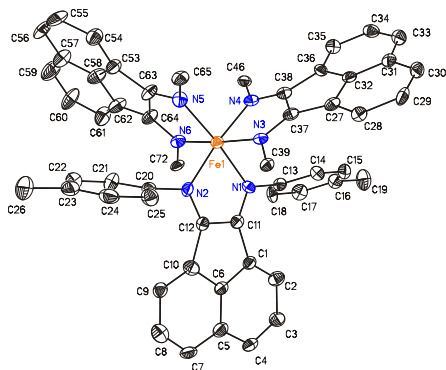


Figure 4-S11 - ORTEP diagram (50% probability level) of the molecular structure of **3g** with the atom-numbering scheme. All H atoms, four 4-tolyl substituents, all $[\text{FeCl}_4]^-$ counterions and solvent molecules are omitted for clarity. Average bond lengths (\AA), angles ($^\circ$): C–C of N=C–C=N 1.48, C–N 1.44, C=N 1.29, Fe–N 2.00, Fe–Cl 2.18; N–Fe–N 173.9, 90.1, sum of angles around N 359.8.

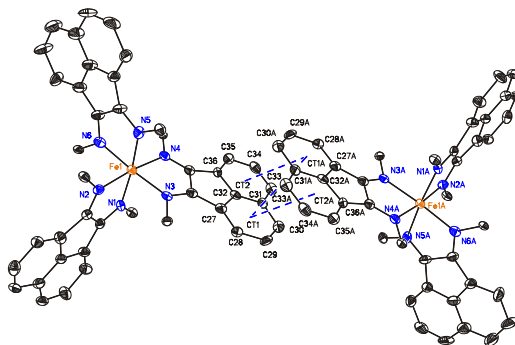


Figure 4-S12 - ORTEP diagram (50 % probability level) of $\pi\cdots\pi$ -interactions in the solid-state structure of **3g**. All hydrogen atoms, 4-tolyl substituents, $[\text{FeCl}_4]^-$ counterions and solvent molecules were omitted for clarity. Symmetry code: A: $-x+2, -y, -z+1$; CT1 denotes the centroid of C27–C32, CT2 denotes the centroid of C31–C36. Geometrical details: CT1–CT1A 3.676(4), CT1–CT2A 3.714(4) Å, angle between plane of C27–C32 and C27A–C32A 0.0(3)°, angle between plane of C27–C32 and C31A–C36A 0.9(3)°, perpendicular distance of CT1 onto plane of C27A–C32A/C31A–C36A 3.250(3)/3.272(3) Å.

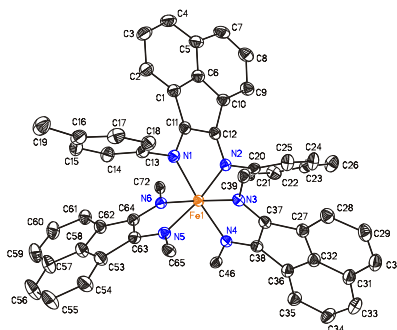


Figure 4-S13 - ORTEP diagram (50% probability level) of the molecular structure of **4g** with the atom-numbering scheme. All H atoms, four 4-tolyl substituents, all $[\text{BF}_4]^-$ counterions and solvent molecules are omitted for clarity. Average bond lengths (Å), angles (°): C–C of N=C–C=N 1.48, C–N 1.44, C=N 1.29, Fe–N 1.99; N–Fe–N 175.0, 90.0, sum of angles around N 359.9.

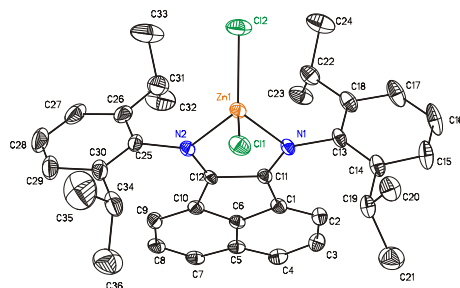


Figure 4-S14 - ORTEP diagram (50 % probability level) of the molecular structure of **5a** with the atom-numbering scheme. All hydrogen atoms were omitted for clarity. Selected bond distances (Å), angles (°): C11–C12 1.509(3), C11–N1 1.279(3), C12–N2 1.277(3), C13–N1 1.446(3), C25–N2 1.447(3), Zn1–N1 2.111(2), Zn1–N2 2.110(2), Zn1–Cl1 2.2073(7), Zn1–Cl2 2.1810(7); C11–N1–C13 119.6(2), C11–N1–Zn1 111.08(17), C13–N1–Zn1 129.02(16), C12–N2–C25 117.0(2), C12–N2–Zn1 111.04(17), C25–N2–Zn1 131.70(17), N1–Zn1–N2 80.31(8), N1–Zn1–Cl1 111.50(6), N1–Zn1–Cl2 113.18(6), N2–Zn1–Cl1 111.22(6), N2–Zn1–Cl2 115.36(6), Cl1–Zn1–Cl2 118.99(3).

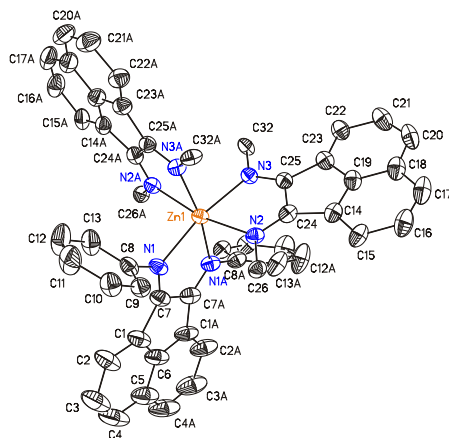


Figure 4-S15 - ORTEP diagram (50 % probability level) of the molecular structure of **5f** with the atom-numbering scheme. All hydrogen atoms, four phenyl substituents, all [BF₄]⁻ counterions and solvent molecules were omitted for clarity. Symmetry code: A: $-x+1.5, y, -z+1$. Average bond distances (Å), angles (°): C–C of N=C–C=N 1.52, C–N 1.43, C=N 1.27, Zn–N 2.18; N–Zn–N 169.4, 90.2, sum of angles around N 360.0.

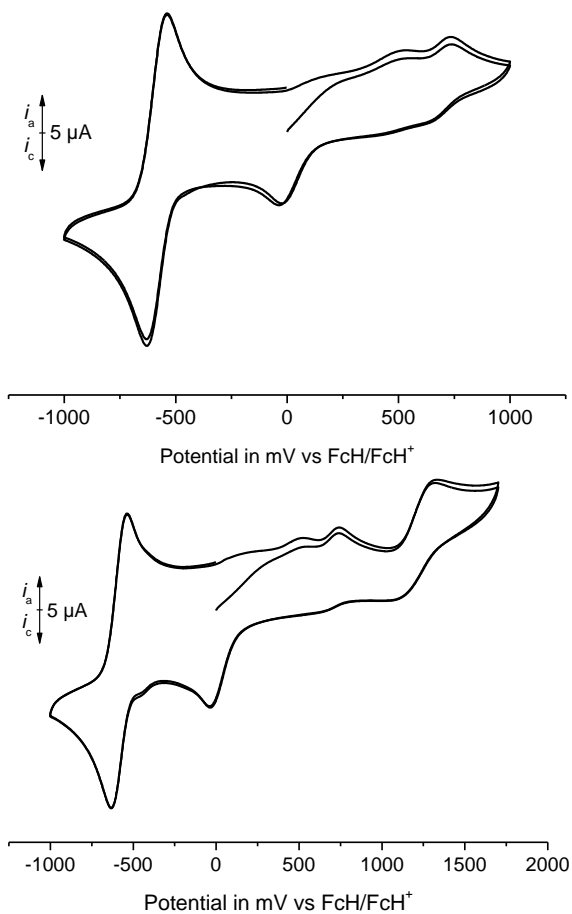


Figure 4-S16 - Cyclic voltammograms of **2a** (scan rate 200 mV·s⁻¹, concentration 10⁻³ M, first two cycles are shown).

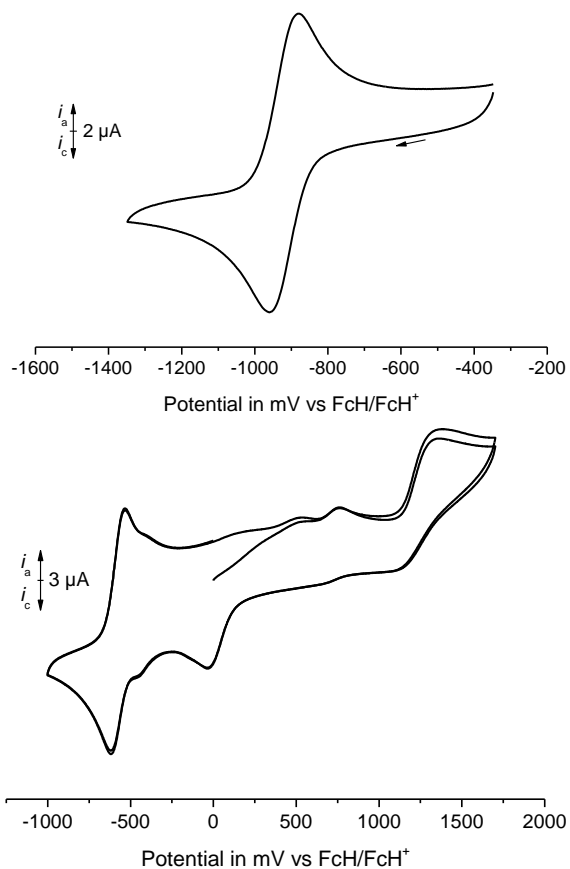


Figure 4-S17 - Cyclic voltammograms of **2c** (scan rate 200 mV·s⁻¹, concentration 10⁻³ M, first two cycles are shown in the right voltammogram).

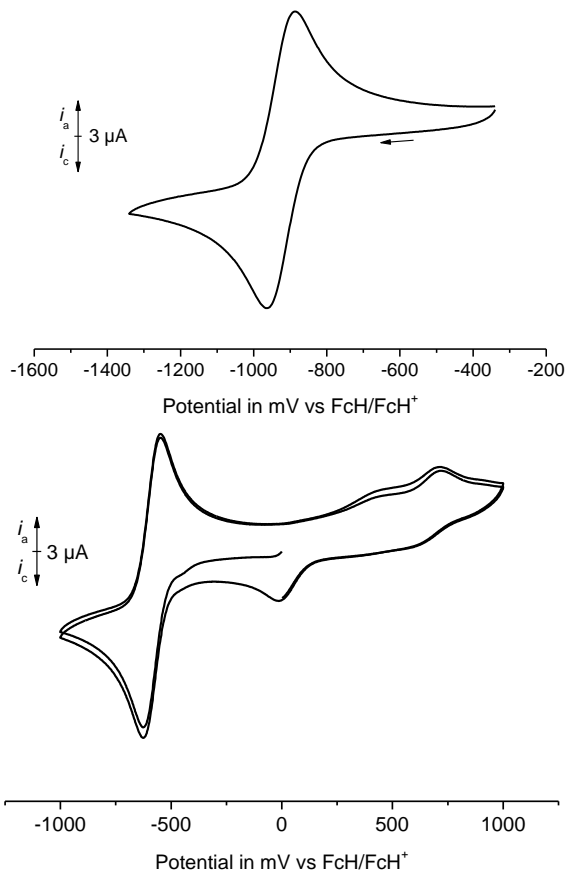


Figure 4-S18 - Cyclic voltammograms of **2d** (scan rate $200 \text{ mV}\cdot\text{s}^{-1}$, concentration 10^{-3} M , first two cycles are shown in the right voltammogram).

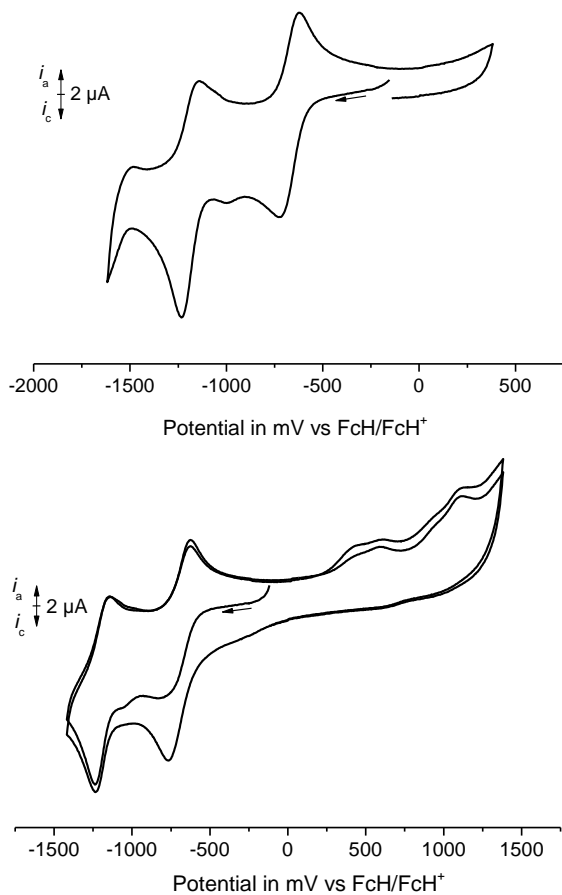


Figure 4-S19 - Cyclic voltammograms of **4f** (scan rate $200 \text{ mV}\cdot\text{s}^{-1}$, concentration $0.5\cdot 10^{-3} \text{ M}$, first two cycles are shown in the right voltammogram).

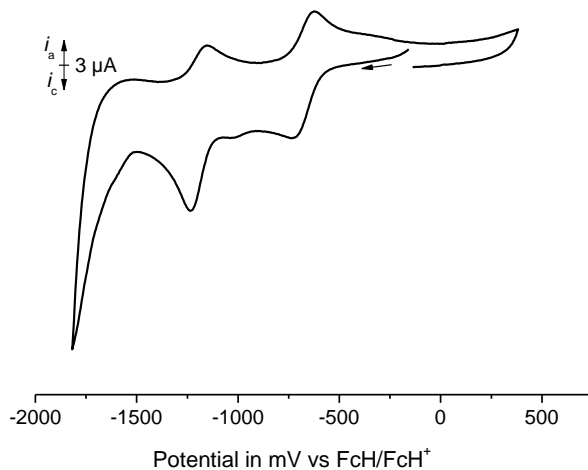


Figure 4-S20 - Cyclic voltammogram of **4f** (scan rate 200 mV·s⁻¹, concentration 0.5·10⁻³ M).

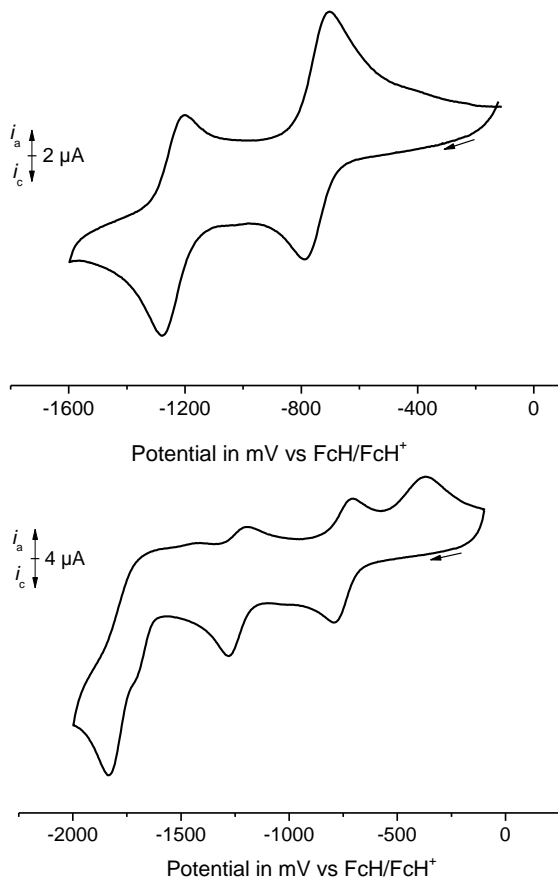


Figure 4-S21 - Cyclic voltammograms of **4g** (scan rate $200 \text{ mV}\cdot\text{s}^{-1}$, concentration $2.5\cdot 10^{-4} \text{ M}$).

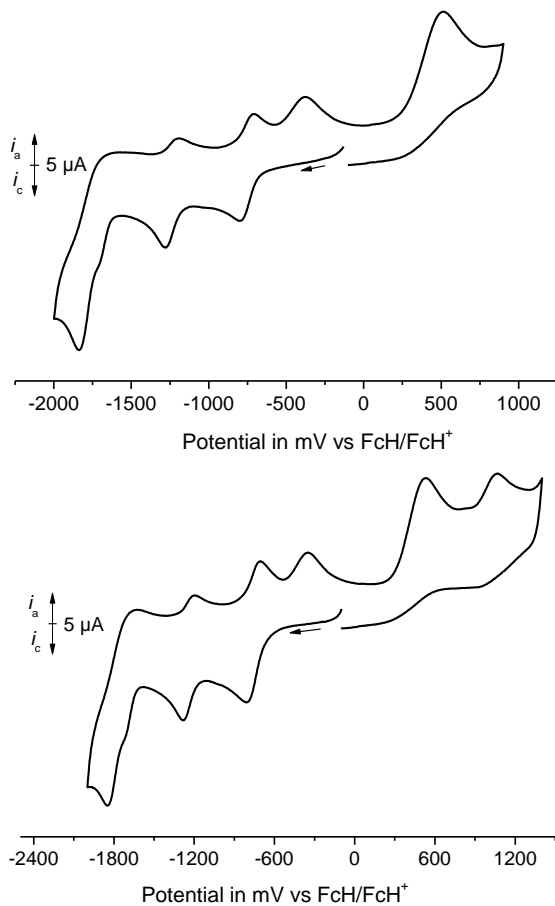


Figure 4-S22 - Cyclic voltammograms of **4g** (scan rate $200 \text{ mV}\cdot\text{s}^{-1}$, concentration $2.5\cdot 10^{-4} \text{ M}$).

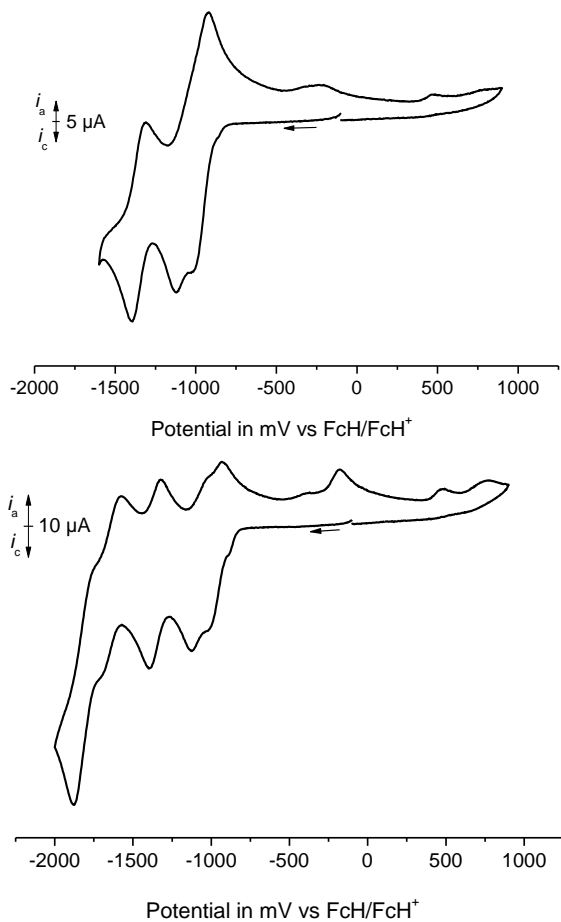


Figure 4-S23 - Cyclic voltammograms of **5g** (scan rate $200 \text{ mV}\cdot\text{s}^{-1}$, concentration 10^{-3} M).

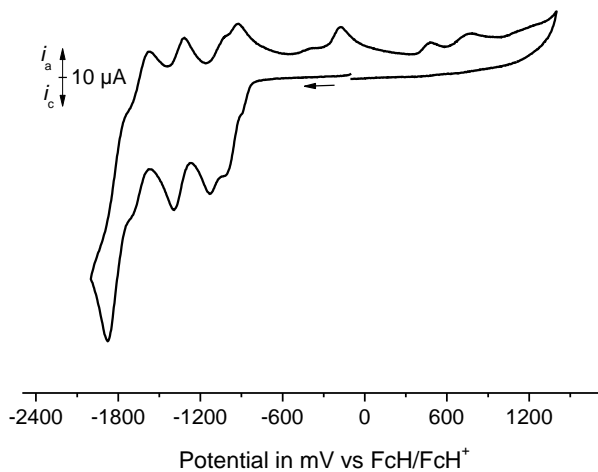


Figure 4-S24 - Cyclic voltammograms of **5g** (scan rate 200 mV·s⁻¹, concentration 10⁻³ M).

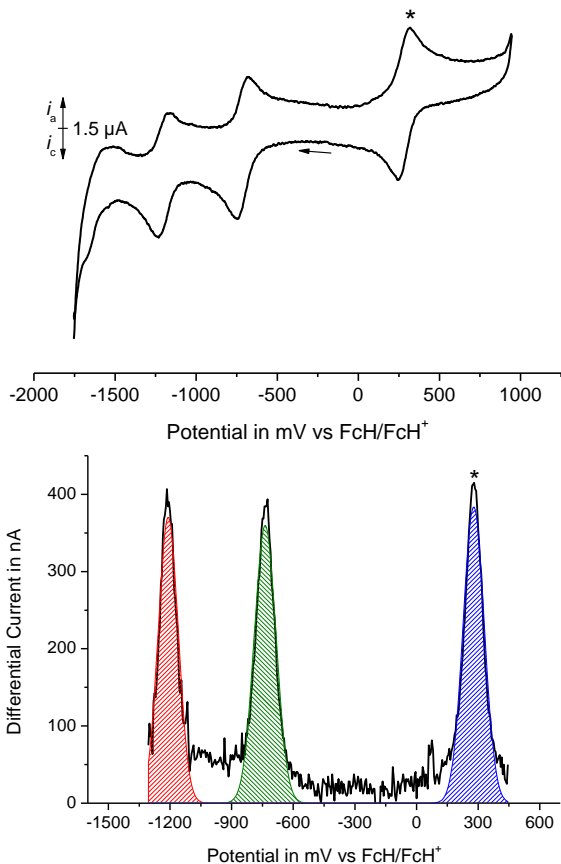


Figure 4-S25 - Cyclic voltammogram (left, scan rate $200 \text{ mV}\cdot\text{s}^{-1}$) and square wave voltammogram (right; area red:green:blue = 1.00:1.05:1.09) of **4g** (concentration $2.5\cdot 10^{-4} \text{ M}$) containing one equivalent acetylferrocene (*, $E^{\circ\prime} = 280 \text{ mV}$, $\Delta E_p = 68 \text{ mV}$).

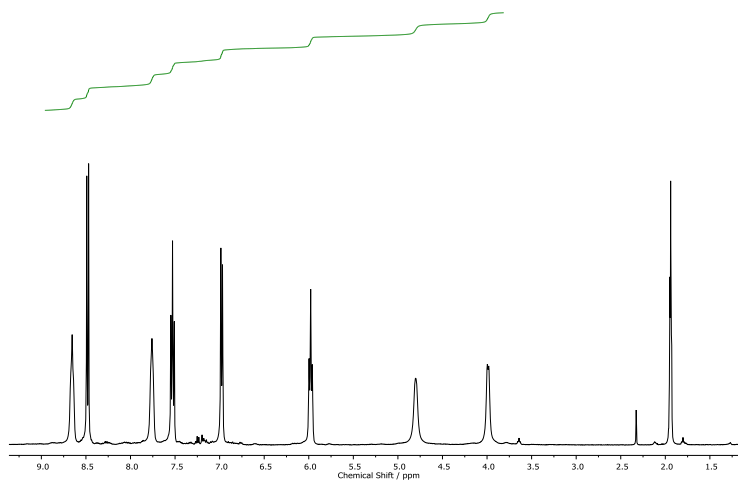


Figure 4-S26 - ^1H NMR spectrum of **4f** (CD_3CN , 400 MHz).

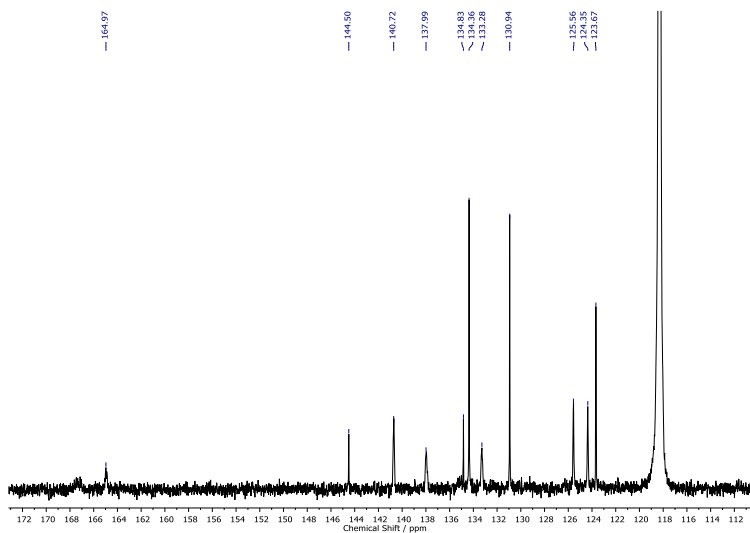


Figure 4-S27 - $^{13}\text{C}\{^1\text{H}\}$ NMR spectrum of **4f** (CD_3CN , 101 MHz).

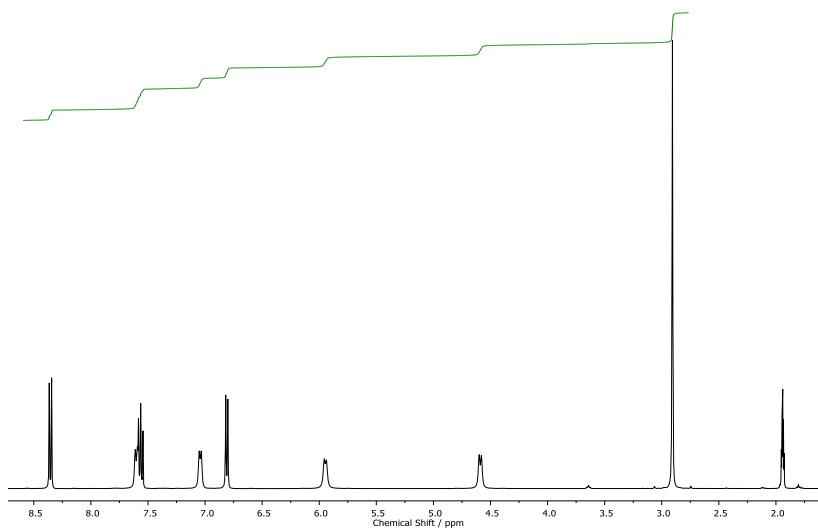


Figure 4-S28 - ^1H NMR spectrum of **4g** (CD_3CN , 400 MHz).

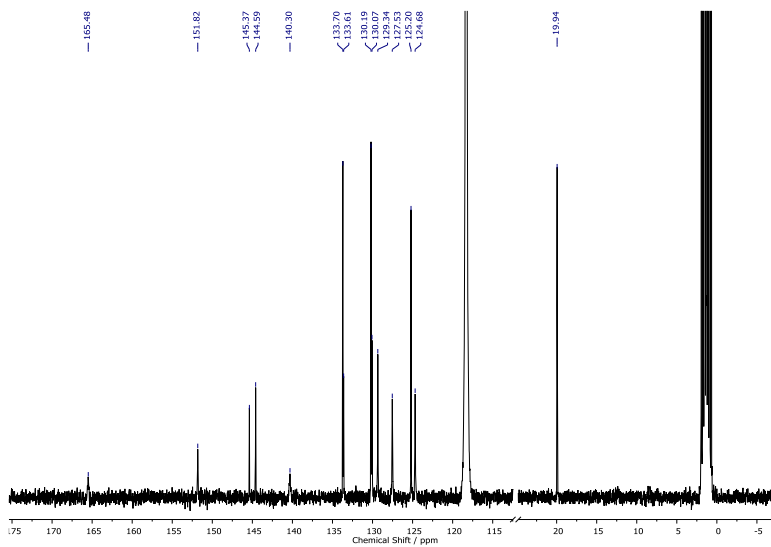


Figure 4-S29 - $^{13}\text{C}\{^1\text{H}\}$ NMR spectrum of **4g** (CD_3CN , 101 MHz).

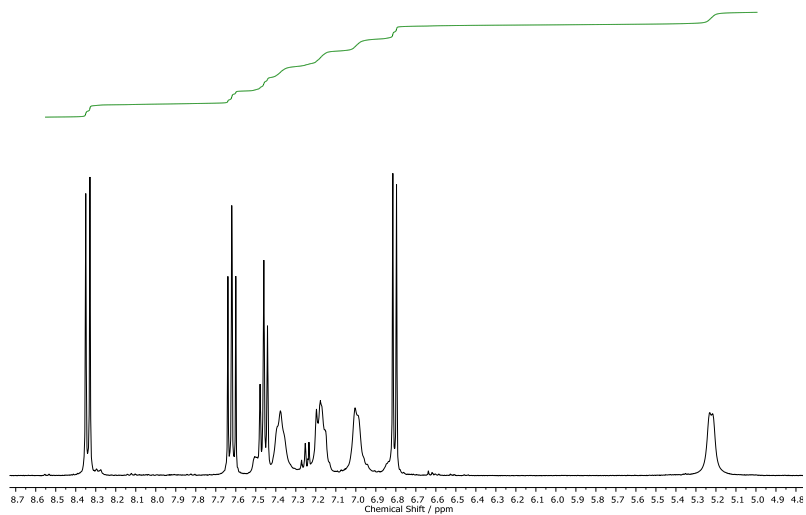


Figure 4-S30 - ^1H NMR spectrum of **5f** (CD_3CN , 400 MHz).

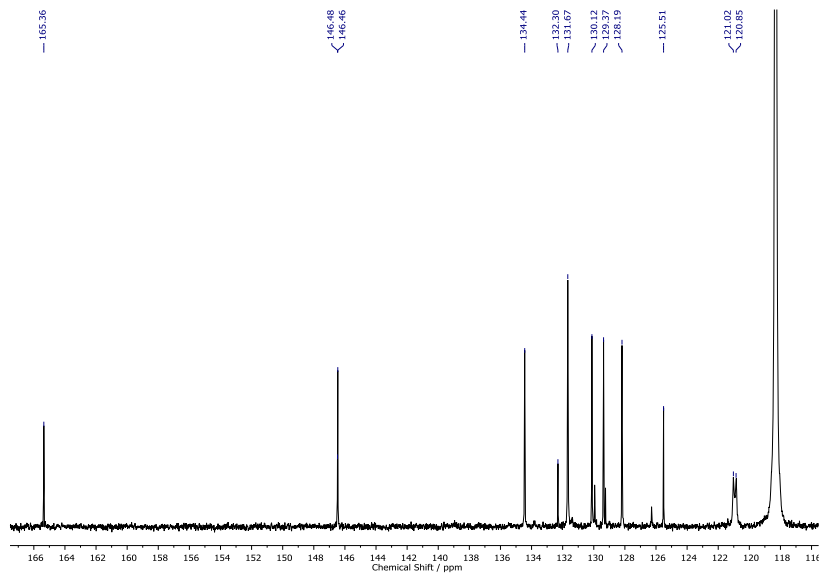


Figure 4-S31 - $^{13}\text{C}\{^1\text{H}\}$ NMR spectrum of **5f** (CD_3CN , 101 MHz).

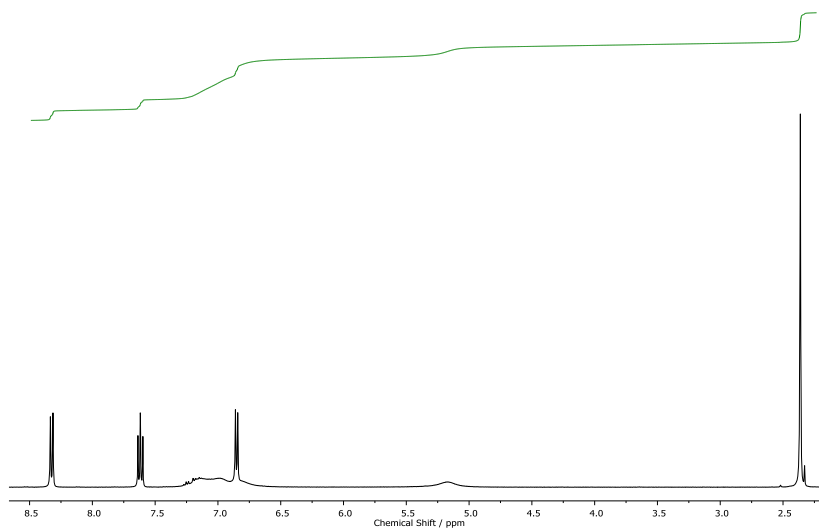


Figure 4-S32 - ^1H NMR spectrum of **5g** (CD_3CN , 400 MHz).

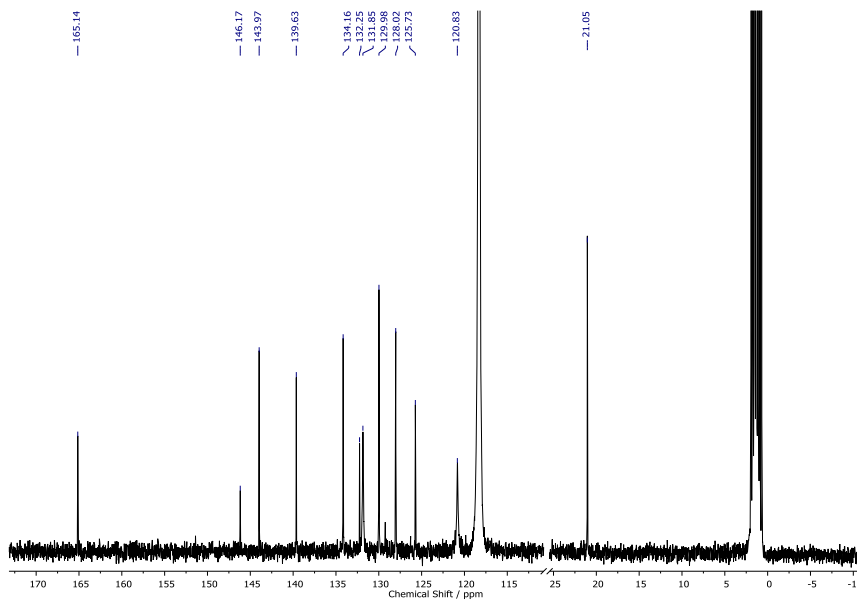


Figure 4-S33 - $^{13}\text{C}\{^1\text{H}\}$ NMR spectrum of **5g** (CD_3CN , 101 MHz).

Table 4-S1 - UV/Vis spectroscopic data of ligands **1** and complexes **2-5**.

Compound	λ_{\max} / nm (ϵ / $10^3 \text{ M}^{-1}\cdot\text{cm}^{-1}$)
1a	310 (8.07), 412 (0.96)
1b	318 (7.01), 395 (1.61)
1c	308 (10.6), 420 (1.08)
1d	308 (11.1)
1e	306 (9.81), 398 (2.57)
1f	305 (6.78), 407 (2.06)
1g	309 (9.14), 404 (3.88)
2a	310 (9.25), 410 (1.25), 663 (0.26)
2b	315 (10.9), 399 (1.94), 661 (0.24)
2c	309 (10.8), 397 (1.62), 663 (0.22)
2d	316 (9.27), 392 (1.55), 656 (0.18)
2e	315 (10.2), 398 (2.70), 673 (0.51)
4f	319 (37.5), 420 (8.53), 692 (11.6)
4g	320 (39.1), 420 (9.85), 699 (14.9)
5a	323 (8.74), 408 (1.42)
5f	323 (29.4), 414 (5.81)
5g	323 (31.0), 400 (8.85)

Table 4-S2 - Cyclic voltammetry data of **4f,g** and **5g** (all values in mV).

	E_{pc}	$E^{o_1'}$ (ΔE_p)	$E^{o_2'}$ (ΔE_p)	$E^{o_3'}$ (ΔE_p)	E_{pa1}	E_{pa2}	E_{pa3}
4f	n.d.	–	–1190 (96)	–695 (136)	–	585	1120
4g	–1850	–	–1240 (80)	–745 (88)	–345	530	1075
5g	–1885	–1355 (76)	–1080 (108)	–965 (68)	–165	–	–

n.d.: not determined. E_{pa} : anodic peak potential. E_{pc} : cathodic peak potential.

Table 4-S3 - Crystal and intensity collection data for **2b** and **2c**.

	2b × C₅H₁₂	2c × ½ C₇H₈
Chemical formula	C ₃₅ H ₄₀ Cl ₂ FeN ₂	C _{35.5} H ₃₆ Cl ₂ FeN ₂
Formula weight	615.44	617.41
Temperature / K	122.99(10)	123(2)
Wavelength / Å	0.71073	1.54184
Crystal system, space group	orthorhombic, <i>Pcca</i>	monoclinic, <i>P2₁/n</i>
<i>a</i> / Å	16.6636(4)	11.3123(2)
<i>b</i> / Å	11.3360(2)	23.2788(4)
<i>c</i> / Å	17.2866(3)	12.0628(2)
α / Å	90	90
β / Å	90	98.531(2)
γ / Å	90	90
<i>V</i> / Å ³	3265.41(11)	3141.43(9)
ρ_{calcd} / g·cm ⁻³	1.252	1.305
<i>F</i> (000)	1296	1292
Crystal size / mm	0.40 × 0.35 × 0.23	0.39 × 0.16 × 0.11
<i>Z</i>	4	4
Max. and min. transmission	0.977, 0.967	0.906, 0.778
μ / mm ⁻¹	0.651	5.608
θ / °	3.84–28.57	3.80–73.50
	–20 ≤ <i>h</i> ≤ 13	–10 ≤ <i>h</i> ≤ 14
Index ranges	–15 ≤ <i>k</i> ≤ 11	–28 ≤ <i>k</i> ≤ 26
	–23 ≤ <i>l</i> ≤ 22	–14 ≤ <i>l</i> ≤ 14
Total / unique reflections	10389 / 3614	17720 / 6164
Data / restraints / parameters	3614 / 0 / 186	6164 / 46 / 386
<i>R</i> _{int}	0.0311	0.0267
<i>R</i> ₁ , <i>wR</i> ₂ [<i>I</i> ≥ 2σ(<i>I</i>)]	0.0492, 0.1324	0.0303, 0.0746
<i>R</i> ₁ , <i>wR</i> ₂ (all data)	0.0632, 0.1440	0.0350, 0.0775
Goodness-of-fit <i>S</i> on <i>F</i> ²	1.034	1.045
Largest diff. peak and hole / eÅ ⁻³	0.937, –0.685	0.315, –0.327

Table 4-S4 - Crystal and intensity collection data for **3f** and **3g**

	3f	3g × 1.5 CH₂Cl₂
Chemical formula	C ₇₂ H ₄₈ Cl ₈ Fe ₃ N ₆	C _{79.5} H ₆₃ Cl ₁₁ Fe ₃ N ₆
Formula weight	1448.31	1659.86
Temperature / K	123.00(10)	122.98(10)
Wavelength / Å	0.71073	0.71073
Crystal system, space group	monoclinic, <i>P</i> 2 ₁ / <i>c</i>	triclinic, <i>P</i> -1
<i>a</i> / Å	18.6162(3)	16.7765(5)
<i>b</i> / Å	12.8986(3)	19.9175(6)
<i>c</i> / Å	26.4424(6)	23.9950(10)
α / Å	90	86.063(3)
β / Å	92.151(2)	85.007(3)
γ / Å	90	72.857(3)
<i>V</i> / Å ³	6345.0(2)	7624.8(5)
ρ_{calcd} / g·cm ⁻³	1.516	1.446
<i>F</i> (000)	2944	3388
Crystal size / mm	0.18 × 0.11 × 0.08	0.20 × 0.10 × 0.07
<i>Z</i>	4	4
Max. and min. transmission	0.994, 0.990	1.000, 0.485
μ / mm ⁻¹	1.063	0.997
θ / °	3.25–28.63	3.19–27.37
	-22 ≤ <i>h</i> ≤ 24	-21 ≤ <i>h</i> ≤ 21
Index ranges		
	-16 ≤ <i>k</i> ≤ 10	-24 ≤ <i>k</i> ≤ 24
	-28 ≤ <i>l</i> ≤ 35	-30 ≤ <i>l</i> ≤ 30
Total / unique reflections	31947 / 13741	36817 / 36817
Data / restraints / parameters	13741 / 277 / 889	7510 / 150 / 1853
<i>R</i> _{int}	0.0399	–
<i>R</i> ₁ , <i>wR</i> ₂ [<i>I</i> ≥ 2σ(<i>I</i>)]	0.0599, 0.1244	0.0758, 0.1993
<i>R</i> ₁ , <i>wR</i> ₂ (all data)	0.0918, 0.1406	0.0968, 0.2097
Goodness-of-fit <i>S</i> on <i>F</i> ²	1.059	1.041
Largest diff. peak and hole / eÅ ⁻³	0.788, -0.574	1.679, -1.405

Table 4-S5 - Crystal and intensity collection data for **4g**.

	4g × CH ₃ CN
Chemical formula	C ₈₀ H ₆₃ B ₂ F ₈ FeN ₇
Formula weight	1351.84
Temperature / K	123.00(10)
Wavelength / Å	1.54184
Crystal system, space group	monoclinic, <i>P2₁/n</i>
<i>a</i> / Å	14.03750(10)
<i>b</i> / Å	25.8185(2)
<i>c</i> / Å	18.49580(10)
<i>α</i> / °	90
<i>β</i> / °	93.0800(10)
<i>γ</i> / °	90
<i>V</i> / Å ³	6693.70(8)
ρ_{calcd} / g·cm ⁻³	1.341
<i>F</i> (000)	2800
Crystal size / mm	0.26 × 0.16 × 0.14
<i>Z</i>	4
Max. and min. transmission	0.941, 0.898
μ / mm ⁻¹	2.421
θ / °	3.42–73.56
	–12 ≤ <i>h</i> ≤ 17
Index ranges	
	–31 ≤ <i>k</i> ≤ 32
	–23 ≤ <i>l</i> ≤ 22
Total / unique reflections	73152 / 13314
Data / restraints / parameters	13314 / 124 / 984
<i>R</i> _{int}	0.0365
<i>R</i> ₁ , <i>wR</i> ₂ [<i>I</i> ≥ 2σ(<i>I</i>)]	0.0391, 0.1074
<i>R</i> ₁ , <i>wR</i> ₂ (all data)	0.0428, 0.1109
Goodness-of-fit <i>S</i> on <i>F</i> ²	1.034
Largest diff. peak and hole / eÅ ⁻³	0.938, –0.257

Table 4-S6 - Crystal and intensity collection data for **5a** and **5f**.

	5a	5f × 4 CH ₂ Cl ₂
Chemical formula	C ₃₆ H ₄₀ Cl ₂ N ₂ Zn	C ₇₆ H ₅₆ B ₂ Cl ₈ F ₈ N ₆ Zn
Formula weight	636.97	1575.85
Temperature / K	123.00(10)	123.00(10)
Wavelength / Å	1.54184	1.54184
Crystal system, space group	monoclinic, <i>P</i> 2 ₁ / <i>a</i>	monoclinic, <i>I</i> 2/ <i>a</i>
<i>a</i> / Å	22.4045(4)	25.4820(6)
<i>b</i> / Å	11.8055(2)	13.8227(3)
<i>c</i> / Å	26.9815(6)	20.2661(4)
α / Å	90	90
β / Å	111.522(2)	96.700(2)
γ / Å	90	90
<i>V</i> / Å ³	6638.9(2)	7089.6(3)
ρ_{calcd} / g·cm ⁻³	1.275	1.476
<i>F</i> (000)	2672	3208
Crystal size / mm	0.31 × 0.13 × 0.03	0.36 × 0.29 × 0.06
<i>Z</i>	8	4
Max. and min. transmission	0.939, 0.608	0.987, 0.945
μ / mm ⁻¹	2.697	3.847
θ / °	3.52–73.52	3.49–73.61
	–25 ≤ <i>h</i> ≤ 27	–27 ≤ <i>h</i> ≤ 31
Index ranges	–14 ≤ <i>k</i> ≤ 14	–17 ≤ <i>k</i> ≤ 16
	–33 ≤ <i>l</i> ≤ 33	–24 ≤ <i>l</i> ≤ 24
Total / unique reflections	20577 / 20577	19701 / 6909
Data / restraints / parameters	20577 / 0 / 740	6909 / 500 / 591
<i>R</i> _{int}	–	0.0221
<i>R</i> ₁ , <i>wR</i> ₂ [<i>I</i> ≥ 2σ(<i>I</i>)]	0.0351, 0.1099	0.0832, 0.1885
<i>R</i> ₁ , <i>wR</i> ₂ (all data)	0.0415, 0.1151	0.0855, 0.1896
Goodness-of-fit <i>S</i> on <i>F</i> ²	1.056	1.164
Largest diff. peak and hole / eÅ ⁻³	0.439, –0.524	0.894, –0.670

4.4 References

- [1] a) S. Enthaler, K. Junge, M. Beller, *Angew. Chem. Int. Ed.* **2008**, *47*, 3317–3321; b) *Iron Catalysis in Organic Chemistry: Reactions and Applications* (Ed.: B. Plietker), Wiley-VCH, Weinheim, **2008**; c) W. M. Czaplik, M. Meyer, J. Cvengroš, A. Jacobi von Wangelin, *ChemSusChem* **2009**, *2*, 396–417; d) I. Bauer, H.-J. Knölker, *Chem. Rev.* **2015**, *115*, 3170–3387.
- [2] See for example: R. B. Bedford, *Acc. Chem. Res.* **2015**, *48*, 1485–1493.
- [3] For selected examples see: a) R. B. Bedford, M. Betham, D. W. Bruce, S. A. Davis, R. M. Frost, M. Hird, *Chem. Commun.* **2006**, 1398–1400; b) C. Rangheard, C. de Julián Fernández, P.-H. Phua, J. Hoorn, L. Lefort, J. G. de Vries, *Dalton Trans.* **2010**, *39*, 8464–8471; c) A. Welther, M. Bauer, M. Mayer, A. Jacobi von Wangelin, *ChemCatChem* **2012**, *4*, 1088–1093; d) V. Kelsen, B. Wendt, S. Werkmeister, K. Junge, M. Beller, B. Chaudret, *Chem. Commun.* **2013**, *49*, 3416–3418; e) R. Hudson, Y. Feng, R. S. Varma, A. Moores, *Green. Chem.* **2014**, *16*, 4493–4505.
- [4] For selected examples see: a) K. G. Dongol, H. Koh, M. Sau, C. L. L. Chai, *Adv. Synth. Catal.* **2007**, *349*, 1015–1018; b) T. Hashimoto, T. Hatakeyama, M. Nakamura, *J. Org. Chem.* **2012**, *77*, 1168–1173; c) R. B. Bedford, P. B. Brenner, E. Carter, T. W. Carvell, P. M. Cogswell, T. Gallagher, J. N. Harvey, D. M. Murphy, E. C. Neeve, J. Nunn, D. R. Pye, *Chem. Eur. J.* **2014**, *20*, 7935–7938; d) L. C. Misal Castro, H. Li, J.-B. Sortais, C. Darcel, *Green Chem.* **2015**, *17*, 2283–2303.
- [5] a) M. J. Ingleson, R. A. Layfield, *Chem. Commun.* **2012**, *48*, 3579–3589; b) D. Bézier, J.-P. Sortais, C. Darcel, *Adv. Synth. Catal.* **2013**, *355*, 19–33.
- [6] a) V. Lyaskovskyy, B. de Bruin, *ACS Catal.* **2012**, *2*, 270–279; b) S. Blanchard, E. Derat, M. Desage-El Murr, L. Fensterbank, M. Malacria, V. Mourières-Mansuy, *Eur. J. Inorg. Chem.* **2012**, 376–389.
- [7] a) H. tom Dieck, A. Orlopp, *Angew. Chem. Int. Ed.* **1975**, *14*, 251–252; b) H. tom Dieck, H. Bruder, *J. Chem. Soc., Chem. Commun.* **1977**, 24–25; c) H. W. Frühauf, A. Landers, R. Goddard, C. Krüger, *Angew. Chem. Int. Ed. Engl.* **1978**, *17*, 64–65.
- [8] a) B. L. Small, M. Brookhart, A. M. A. Bennett, *J. Am. Chem. Soc.* **1998**, *120*, 4049–4050; b) G. J. P. Britovsek, V. C. Gibson, B. S. Kimberley, P. J. Maddox, S. J. McTavish, G. A. Solan, A. J. P. White, D. J. Williams, *Chem. Commun.* **1998**, 849–850; c) G. J. P. Britovsek, M. Bruce, V. C. Gibson, B. S. Kimberley, P. J. Maddox, S. Mastroianni, S. J. McTavish, C. Redshaw, G. A. Solan, S. Strömberg, A. J. P. White, D. J. Williams, *J. Am. Chem. Soc.* **1999**, *121*, 8728–8740; d) B. L. Small, M. Brookhart, *Macromolecules* **1999**, *32*, 2120–2130; e) C. Bianchini, G. Giambastiani, I. G. Rios, G. Mantovani, A. Meli, A. M. Segarra, *Coord. Chem. Rev.* **2006**, *250*, 1391–1418; f) V. C. Gibson, C. Redshaw, G. A. Solan, *Chem. Rev.* **2007**, *107*, 1745–1776; g) B. L. Small, *Acc. Chem. Res.* **2015**, *48*, 2599–2611.
- [9] a) R. van Asselt, C. J. Elsevier, *J. Mol. Catal.* **1991**, *65*, L13–L19; b) R. van Asselt, C. J. Elsevier, *Organometallics* **1992**, *11*, 1999–2001; c) R. van Asselt, C. J.

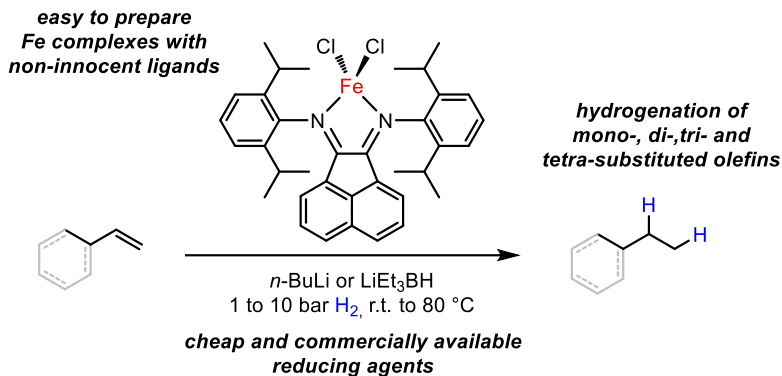
- Elsevier, W. J. J. Smeets, A. L. Spek, R. Benedix, *Recl. Trav. Chim. Pays-Bas* **1994**, *113*, 88–98.
- [10] N. J. Hill, I. Vargas-Baca, A. H. Cowley, *Dalton Trans.* **2009**, 240–253.
- [11] For selected examples see: a) V. Rosa, C. I. M. Santos, R. Welter, G. Aullón, C. Lodeiro, T. Avilés, *Inorg. Chem.* **2010**, *49*, 8699–8708; b) M. J. Sgro, D. W. Stephan, *Dalton Trans.* **2010**, *39*, 5786–5794; c) P. de Frémont, H. Clavier, V. Rosa, T. Avilés, P. Braunstein, *Organometallics* **2011**, *30*, 2241–2251; d) B. Gao, W. Gao, Q. Wu, X. Luo, J. Zhang, Q. Su, Y. Mu, *Organometallics* **2011**, *30*, 5480–5486; e) T. L. Lohr, W. E. Piers, M. Parvez, *Inorg. Chem.* **2012**, *51*, 4900–4902; f) P. Papanikolaou, P. D. Akrios, A. Czapik, B. Wicher, M. Gdaniec, N. Tkachenko, *Eur. J. Inorg. Chem.* **2013**, 2418–2431; g) K. Hasan, E. Zysman-Colman, *Eur. J. Inorg. Chem.* **2013**, 4421–4429; h) H. Tsurugi, H. Tanahashi, H. Nishiyama, W. Fegler, T. Saito, A. Sauer, J. Okuda, K. Mashima, *J. Am. Chem. Soc.* **2013**, *135*, 5986–5989; i) J. Tory, G. Gobaille-Shaw, A. M. Chippindale, F. Hartl, *J. Organomet. Chem.* **2014**, *760*, 30–41; j) S. J. Carrington, I. Chakraborty, P. K. Mascharak, *Dalton Trans.* **2015**, *44*, 13828–13834; k) K. M. Clark, *Inorg. Chem.* **2016**, *55*, 6443–6448.
- [12] a) L. K. Johnson, C. M. Killian, M. Brookhart, *J. Am. Chem. Soc.* **1995**, *117*, 6414–6415; b) B. S. Williams, M. D. Leatherman, P. S. White, M. Brookhart, *J. Am. Chem. Soc.* **2005**, *127*, 5132–5146; c) C. Romain, V. Rosa, C. Fliedel, F. Bier, F. Hild, R. Welter, S. Dagorne, T. Aviles, *Dalton Trans.* **2012**, *41*, 3377–3379; d) F. Amoroso, E. Zangrando, C. Carfagna, C. Mueller, D. Vogt, M. Hagar, F. Ragaini, B. Milani, *Dalton Trans.* **2013**, *42*, 14583–14602; e) C. A. Figueira, A. F. G. Ribeiro, C. S. B. Gomes, A. C. Fernandes, L. H. Doerrer, P. T. Gomes, *J. Braz. Chem. Soc.* **2014**, *25*, 2295–2303.
- [13] a) R. van Asselt, C. J. Elsevier, *Organometallics* **1994**, *13*, 1972–1980; b) M. W. van Laren, C. J. Elsevier, *Angew. Chem. Int. Ed.* **1999**, *38*, 3715–3717; c) D. B. Llewellyn, D. Adamson, B. A. Arndtsen, *Org. Lett.* **2000**, *2*, 4165–4168; d) F. Ragaini, S. Cenini, M. Gasperini, *J. Mol. Catal. A* **2001**, *174*, 51–57; e) L. Li, P. S. Lopes, C. A. Figueira, C. S. B. Gomes, M. T. Duarte, V. Rosa, C. Fliedel, T. Aviles, P. T. Gomes, *Eur. J. Inorg. Chem.* **2013**, 1404–1417; f) M. Gholinejad, V. Karimkhani, I. Kim, *Appl. Organomet. Chem.* **2014**, *28*, 221–224; g) C. D. Nunes, P. D. Vaz, V. Felix, L. F. Veiros, T. Moniz, M. Rangel, S. Realista, A. C. Mourato, M. J. Calhorda, *Dalton Trans.* **2015**, *44*, 5125–5138.
- [14] a) A. Paulovicova, U. El-Ayaan, K. Umezawa, C. Vithana, Y. Ohashi, Y. Fukuda, *Inorg. Chim. Acta* **2002**, *339*, 209–214; b) D. A. Piryazev, M. A. Ogienko, A. V Virovets, N. A. Pushkarevsky, S. N. Konchenko, *Acta Crystallogr. Sect. C* **2012**, *68*, m320–m322; c) I. L. Fedushkin, A. A. Skatova, N. M. Khvoinova, A. N. Lukoyanov, G. K. Fukin, S. Y. Ketkov, M. O. Maslov, A. S. Bogomyakov, V. M. Makarov, *Russ. Chem. Bull.* **2013**, *62*, 2122–2131; d) M. Schmitz, M. Seibel, H.

- Kelm, S. Demeshko, F. Meyer, H.-J. Krüger, *Angew. Chem. Int. Ed.* **2014**, *53*, 5988–5992.
- [15] a) B. L. Small, R. Rios, E. R. Fernandez, M. J. Carney, *Organometallics* **2007**, *26*, 1744–1749; b) B. M. Schmiede, M. J. Carney, B. L. Small, D. L. Gerlach, J. A. Halfen, *Dalton Trans.* **2007**, 2547–2562; c) B. L. Small, R. Rios, E. R. Fernandez, D. L. Gerlach, J. A. Halfen, M. J. Carney, *Organometallics* **2010**, *29*, 6723–6731.
- [16] F. S. Wekesa, R. Arias-Ugarte, L. Kong, Z. Sumner, G. P. McGovern, M. Findlater, *Organometallics* **2015**, *34*, 5051–5056.
- [17] M. J. Supej, A. Volkov, L. Darko, R. A. West, J. M. Darmon, C. E. Schulz, K. A. Wheeler, H. M. Hoyt, *Polyhedron* **2016**, *114*, 403–414.
- [18] During a synthesis of **2a**, when oxygen was not strictly excluded from the reaction mixture, the product was contaminated with 10 % of the respective Fe(III) complex.
- [19] a) M. M. Khusniyarov, K. Harms, O. Burghaus, J. Sundermeyer, *Eur. J. Inorg. Chem.* **2006**, 2985–2996; b) K. M. Clark, J. Bendix, A. F. Heyduk, J. W. Ziller, *Inorg. Chem.* **2012**, *51*, 7457–7459; c) J. Bendix, K. M. Clark, *Angew. Chem. Int. Ed.* **2016**, *55*, 2748–2752; d) R. A. Zarkesh, A. S. Ichimura, T. C. Monson, N. C. Tomson, M. R. Anstey, *Dalton Trans.* **2016**, *45*, 9962–9969.
- [20] D. N. Coventry, A. S. Batsanov, A. E. Goeta, J. A. K. Howard, T. B. Marder, *Polyhedron* **2004**, *23*, 2789–2795.
- [21] a) V. Rosa, C. I. M. Santos, R. Welter, G. Aullón, C. Lodeiro, T. Avilés, *Inorg. Chem.* **2010**, *49*, 8699–8708; b) K. Hasan, E. Zysman-Colman, *J. Phys. Org. Chem.* **2013**, *26*, 274–279; c) D. A. Evans, L. M. Lee, I. Vargas-Baca, A. H. Cowley, *Organometallics* **2015**, *34*, 2422–2428.
- [22] D. Nicholls, *The Chemistry of Iron, Cobalt and Nickel*, Pergamon, Oxford, **1973**, p. 1049.
- [23] Mean Fe–Cl distance in $[\text{FeCl}_4]^-$: 2.18 and in $[\text{FeCl}_4]^{2-}$: 2.29 Å (CSD version 5.37).
- [24] N. Muresan, C. C. Lu, M. Ghosh, J. C. Peters, M. Abe, L. M. Henling, T. Weyhermüller, E. Bill, K. Wieghardt, *Inorg. Chem.* **2008**, *47*, 4579–4590.
- [25] M. Viganò, F. Ferretti, A. Caselli, F. Ragaini, M. Rossi, P. Mussini, P. Macchi, *Chem. Eur. J.* **2014**, *20*, 14451–14464.
- [26] V. Rosa, S. A. Carabineiro, T. Avilés, P. T. Gomes, R. Welter, J. M. Campos, M. R. Ribeiro, *J. Organomet. Chem.* **2008**, *693*, 769–775.
- [27] I. L. Fedushkin, A. A. Skatova, V. A. Chudakova, G. K. Fukin, *Angew. Chem. Int. Ed.* **2003**, *42*, 3294–3298.
- [28] For an example of the formation of dimeric metal complexes with reduced BIAN ligands, see: I. L. Fedushkin, A. A. Skatova, S. Y. Ketkov, O. V. Eremenko, A. V. Piskunov, G. K. Fukin, *Angew. Chem. Int. Ed.* **2007**, *46*, 4302–4305.
- [29] a) K. Junge, K. Schröder, M. Beller, *Chem. Commun.* **2011**, *47*, 4849–4859; b) B. A. F. Le Bailly, S. P. Thomas, *RSC Adv.* **2011**, *1*, 1435–1445.
- [30] Selected examples of iron-catalyzed hydrogenations with molecular catalysts: S. C. Bart, E. Lobkovsky, P. J. Chirik, *J. Am. Chem. Soc.* **2004**, *126*, 13794–13807; b) S.

- C. Bart, E. J. Hawrelak, E. Lobkovsky, P. J. Chirik, *Organometallics* **2005**, *24*, 5518–5527; c) R. J. Trovitch, E. Lobkovsky, E. Bill, P. J. Chirik, *Organometallics* **2008**, *27*, 1470–1478; d) S. K. Russell, J. M. Darmon, E. Lobkovsky, P. J. Chirik, *Inorg. Chem.* **2010**, *49*, 2782–2792; e) P. J. Chirik, *Acc. Chem. Res.* **2015**, *48*, 1687–1695; f) D. Srimani, Y. Diskin-Posner, Y. Ben-David, D. Milstein, *Angew. Chem. Int. Ed.* **2013**, *52*, 14131–14134; g) E. Alberico, P. Sponholz, C. Cordes, M. Nielsen, H.-J. Drexler, W. Baumann, H. Junge, M. Beller, *Angew. Chem. Int. Ed.* **2013**, *52*, 14162–14166.
- [31] Selected examples for the use of other reducing agents in iron-catalyzed hydrogenations: a) T. S. Carter, L. Guiet, D. J. Frank, J. West, S. P. Thomas, *Adv. Synth. Catal.* **2013**, *355*, 880–884; b) A. J. MacNair, M.-M. Tran, J. E. Nelson, G. U. Sloan, A. Ironmonger, S. P. Thomas, *Org. Biomol. Chem.* **2014**, *12*, 5082–5088; c) T. N. Gieshoff, M. Villa, A. Welther, M. Plois, U. Chakraborty, R. Wolf, A. Jacobi von Wangelin, *Green Chem.* **2015**, *17*, 1408–1413.
- [32] a) H. Lee, M. G. Campbell, R. Hernández Sánchez, J. Börgel, J. Raynaud, S. E. Parker, T. Ritter, *Organometallics* **2016**, *35*, 2923–2929; b) C. Lichtenberg, L. Viciu, M. Adelhardt, J. Sutter, K. Meyer, B. de Bruin, H. Grützmacher, *Angew. Chem. Int. Ed.* **2015**, *54*, 5766–5771.
- [33] Owing to the low solubility of $\text{FeCl}_2(\text{thf})_{1.5}$ in toluene the respective hydrogen experiments were conducted in toluene:thf=1.5:1 to ensure complete solubility of the iron salt.
- [34] M. Gasperini, F. Ragaini, S. Cenini, *Organometallics* **2002**, *21*, 2950–2957.
- [35] D. N. Coventry, A. S. Batsanov, A. E. Goeta, J. A. K. Howard, T. B. Marder, *Polyhedron* **2004**, *23*, 2789–2795
- [36] a) D. Schaarschmidt, A. Hildebrandt, S. Bock, H. Lang, *J. Organomet. Chem.* **2014**, *751*, 742–753; b) D. Miesel, A. Hildebrandt, M. Korb, D. Schaarschmidt, *Organometallics* **2015**, *34*, 4293–4304; c) D. Miesel, A. Hildebrandt, M. Korb, D. A. Wild, P. J. Low, H. Lang, *Chem. Eur. J.* **2015**, *21*, 11545–11559; d) C. Gäbler, J. M. Speck, M. Korb, D. Schaarschmidt, H. Lang, *J. Organomet. Chem.* **2016**, *813*, 26–35; e) A. Hildebrandt, K. Al Khalyfeh, D. Schaarschmidt, M. Korb, *J. Organomet. Chem.* **2016**, *804*, 87–94.
- [37] G. Gritzner, J. Kuta, *Pure Appl. Chem.* **1984**, *56*, 461–466.
- [38] The number of electrons transferred in the reductions was determined by using acetylferrocene as internal reference (Figure S25).
- [39] a) K. M. Clark, J. Bendix, A. F. Heyduk, J. W. Ziller, *Inorg. Chem.* **2012**, *51*, 7457–7459; c) J. Bendix, K. M. Clark, *Angew. Chem. Int. Ed.* **2016**, *55*, 2748–2752; c) R. A. Zarkesh, A. S. Ichimura, T. C. Monson, N. C. Tomson, M. R. Anstey, *Dalton Trans.* **2016**, *45*, 9962–9969.
- [40] For examples on metal complexes with two or three BIAN ligands in different oxidation states, see: a) I. L. Fedushkin, V. M. Makarov, V. G. Sokolov, G. K. Fukin, *Dalton Trans.* **2009**, 8047–8053; b) I. L. Fedushkin, O. V. Maslova, A. N.

- Lukoyanov, G. K. Fukin, *Compt. Rend. Chimie* **2010**, *13*, 584–592; c) E. J. Schelter, R. Wu, B. L. Scott, J. D. Thompson, T. Cantat, K. D. John, E. R. Batista, D. E. Morris, J. L. Kiplinger, *Inorg. Chem.* **2010**, *49*, 924–933; d) M. M. Khusniyarov, K. Harms, O. Burghaus, J. Sundermeyer, *Eur. J. Inorg. Chem.* **2006**, 2985–2996
- [41] G. M. Sheldrick, *Acta Crystallogr. Sect. A* **2008**, *64*, 112–122.
- [42] A. L. Spek, *Acta Crystallogr. Sect. D* **2009**, *65*, 148–155.
- [43] The general procedure for the synthesis of (Ar₂BIAN)FeCl₂ afforded with ligand **1b** (mes₂BIAN)FeCl₂·C₇H₈ as a brown solid. We believe that the toluene molecule interacts strongly with the aromatic moieties of the mes₂BIAN ligand as observed in the solid-state structure of **2c**. The toluene could not be removed by heating the complex in vacuo. However, dissolving **2b**·C₇H₈ in acetonitrile and removing the solvent under reduced pressure gave solvent-free **2b** as a green solid.

5 Hydrogenations catalyzed by Redox-active Bis(imino)acenaphthene (BIAN) Iron Complexes^{i,ii}



A novel hydrogenation catalyst based on the newly synthesized tetrahedral (BIAN)FeCl₂ complex family was developed. These iron precursors, upon activation with different reducing agents, such as *n*-butyllithium or lithium triethylborohydride, proved to be active in the catalytic hydrogenation of mono-, di and tri-substituted olefins, even challenging tetra-substituted alkenes have shown partial conversion. Aiming at the identification of the active species operating in this transformation, initial mechanistic investigations were performed. The evidences obtained pointed at a reduced ferrate as key intermediate for this reaction.

ⁱ unpublished results.

ⁱⁱ substrate scope (Scheme 5-2) and mass spectroscopy analysis were performed in collaboration with M.Sc. Sebastian Sandl.

5.1 Introduction

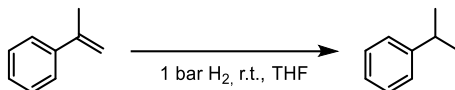
The field of iron-catalyzed transformations received an incredible boost in the last decades thanks to the remarkable achievements obtained in the rational synthesis of iron complexes bearing non-innocent iron ligands. These redox active molecules proved to be the right structure element to provide a certain level of “nobility” to the iron chemistry. Non-innocent ligand-based electrons reservoir can on one hand allow the metal center to maintain a suitable oxidation state throughout the entire process, and on the other hand unlocks the two-electrons redox steps typical of noble metals.^[1] In chapter 1, a few examples of the most representative iron-based catalytic systems involving such ligands have been described. Diiminopyridine scaffolds^[2] and similar tri- and tetradentate pincer ligands^[3] constitute the essential element for the great results obtained by these catalysts in hydrogenation of various substrates. These ligands proved to be efficient also for other kind of transformations such as hydroboration, hydrosilylation, cycloaddition and so on.^[4]

A hydrogenation catalyst composed by a ligand-free reduced iron species has been described in chapter 2, with cheap and available iron trichloride activated by similarly convenient lithium aluminum hydride resulted in an active system without the need of additional additives. Despite the eco-friendliness of this *in situ* prepared catalyst, tri- and tetra-substituted olefins proved to be challenging substrates and required higher dihydrogen pressures, and the lack of a stabilizing ligand led to the formation of less active iron-nanoparticles within short reaction times by ageing of the catalyst. Notwithstanding the non-innocent nature of ligands containing bis(imino)acenaphthene moieties only a couple of examples on Iron-BIAN complexes are known in the literature^[5] and even less have been applied as catalysts. In chapter 4 two simple methodologies for the synthesis of tetrahedral and octahedral Fe-BIAN complexes have been described. Being intrigued by the redox properties of bis(imino)acenaphthenes, combined with our results in the development of hydrogenation catalysts based on reduced iron-species herein and previously^[6] described, we envisioned the application of the recently synthesized tetrahedral Fe-BIAN complexes as precursors for the synthesis of active hydrogenation catalysts. In chapter 4 few preliminary results have been reported, herein we described early stage developments of this catalytic system and further optimizations.

5.2 Results and Discussion

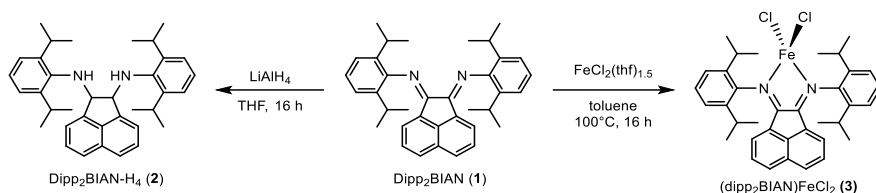
Initial investigations aiming at the identification of possible reactivity of Fe-BIAN species towards hydrogenation involved the screening of different reductants, directed at the recognition of active iron species in low oxidation state. Different combinations of dipp₂BIAN (1,2-bis[(2,6-diisopropylphenyl)imino]acenaphthene), reducing agents/bases and metal salts, were mixed and the resulting mixture was subsequently tested as catalyst for the hydrogenation of α -methylstyrene. The initial iron loading was kept constant to 10 mol% and the ratio between ligands and metals 1:1 (Table 5-1). Sodium is known to efficiently reduce BIAN ligands^[7], therefore it was tested for initial reduction of the ligand followed by *in situ* complexation with iron dichloride. Equimolar amount proved to be ineffective, while 20 mol% led to complete hydrogenation of the test substrate (Table 5-1, entries 1 and 2). Substitution of iron dichloride with zinc dichloride (Table 5-1, entries 3 and 4) afforded an inactive catalytic system, proving the essential role of iron. To investigate the reduction extent of the ligand during these hydrogenations, completely hydrogenated dipp₂BIAN (dipp₂BIAN-H₄, **2**) was synthesized according to reported procedure^[8].

Table 5-1 - Initial hydrogenation screenings with BIAN as ligand.



Entry	Ligand	Reducing agent / base	Metal	Yield (%) ^a
1	1 (10 mol%)	Na (10 mol%)	FeCl ₂ (thf) _{1.5} (10 mol%)	0
2	1 (10 mol%)	Na (20 mol%)	FeCl ₂ (thf) _{1.5} (10 mol%)	95
3	1 (10 mol%)	Na (10 mol%)	ZnCl ₂ (10 mol%)	0
4	1 (10 mol%)	Na (20 mol%)	ZnCl ₂ (10 mol%)	0
5	2 (10 mol%)	-	FeCl ₂ (thf) _{1.5} (10 mol%)	0
6	2 (10 mol%)	<i>n</i> -BuLi (20 mol%)	FeCl ₂ (thf) _{1.5} (10 mol%)	83
7	2 (10 mol%)	NaH (20 mol%)	FeCl ₂ (thf) _{1.5} (10 mol%)	0
8	2 (10 mol%)	KHMDS (20 mol%)	FeCl ₂ (thf) _{1.5} (10 mol%)	0

reducing agent/base was added to a solution of the ligand, after stirring for 30 minutes the metal salt was added ^a quantitative GC-FID vs. *n*-pentadecane as internal reference, conversion in % in parentheses if < 95 %

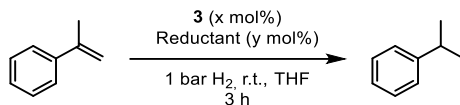


Scheme 5-1 - Ligands tested during the initial screening.

Deprotonation of ligand **2** was attempted with several different bases, $\text{FeCl}_2(\text{thf})_{1.5}$ was then added and the resulting mixture was applied for catalytic hydrogenation of the test substrate. Treatment of ligand **2** with butyllithium and the iron salt led to the formation of a black particles suspension, active in hydrogenation (Table 5-1, entry 6). On the other and the application of other bases such as NaH and KHMDS (Table 5-1, entries 7 and 8) resulted in inactive systems. These results indicate that organolithium reagent, in this case, acts as reducing agent for the formation of iron nanoparticles.

Further investigations were performed on the $(\text{dipp}_2\text{BIAN})\text{FeCl}_2$ (**3**), the synthesis of which is described in chapter 4 (Scheme 5-1). Treatment of the pre-catalyst with 20 mol% of sodium resulted in only poor conversion, with 40 mol% of reductant the yield slightly increased but the formation of undesired side product was observed. Organometallic reducing agents such as butyllithium showed to be very effective in the generation of an active hydrogenation species (Table 5-2, entry 3), and a fast optimization allowed to decrease the loading of the catalyst down to 3 mol% without losing catalytic activity (Table 5-2, entry 4).

Table 5-2 - Hydrogenation screening with preformed complex **3**.



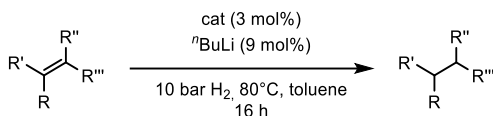
Entry	catalyst	Reductant	Modification to the system	Yield (%) ^a
1	3 (10 mol%)	Na (20 mol%)	-	19 (41)
2	3 (10 mol%)	Na (40 mol%)	-	36 (100)
3	3 (10 mol%)	<i>n</i> -BuLi (10 mol%)	-	100
4	3 (3 mol%)	<i>n</i> -BuLi (9 mol%)	-	100
5	3 (3 mol%)	-	Without reductant	0 (0)
6	1 (3 mol%)	<i>n</i> -BuLi (9 mol%)	Without Fe	0 (0)

7	FeCl ₂ (thf) _{1.5} (3 mol%)	<i>n</i> -BuLi (9 mol%)	Without ligand	100
---	--	-------------------------	----------------	-----

^a quantitative GC-FID vs. *n*-pentadecane as internal reference, conversion in % in parentheses if < 95 %

Blank experiments confirmed that unreduced complex **3** does not catalyze this transformation (Table 5-2, entry 5). In the absence of iron, dipp₂BIAN ligand was treated with *n*-BuLi, the resulting mixture was not active in hydrogenation and decomposition of **2** was observed. As previously observed (Table 5-1, entry 6), reduction of iron dichloride with butyllithium formed a competent catalyst for the hydrogenation of α -methylstyrene (Table 5-2, entry 7), nevertheless the physical appearance of the two catalyst solutions, with and without ligand, was completely different. A deep red solution is formed when a green solution of pre-catalyst **3** is treated with strong reductants, on the other hand after addition of *n*-BuLi to a solution of FeCl₂(thf)_{1.5} the formation of a heterogeneous system, with small black particles floating in the solvent, was detected. The catalytic activity of low valent iron species formed by reduction of common iron salt with organometallic reducing agents is described in many reports. In order to investigate the role of ligand **2** and its effect on the catalytic system a new series of hydrogenation were performed on more substituted and challenging olefins.^[2f]

Table 5-3 - Catalytic activity comparison between **3** and FeCl₂(thf)_{1.5}.



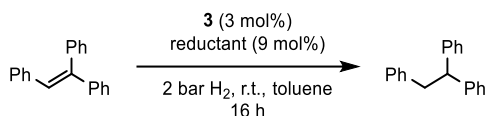
Entry	catalyst	Substrate	Yield (%) ^a
1	FeCl ₂ (thf) _{1.5} ^b		40 (40)
2	3		100
3	FeCl ₂ (thf) _{1.5} ^b		4 (4)
4	3		91

^a quantitative GC-FID vs. *n*-pentadecane as internal reference, conversion in % in parentheses if <95 %; ^b THF as co-solvent to ensure complete solubility of the iron salt.

The results of this comparison are summarized in Table 5-3, 1,2-diphenylethenylbenzene and 2,3-dimethyl-1*H*-indene were selected as substrates and harsher conditions were applied. These initial data show that reduction of the pre-catalyst **3** culminated in a catalytic species (Table 5-3, entries 2 and 4) more active respect to the one arose from FeCl₂(thf)_{1.5} (Table 5-3, entries 1 and 3). In light of these observations, the optimizations of system conditions were pursued.

Other reductants were tested for the activation of complex **3**. Considering the high activity showed by the catalyst, challenging 1,2-diphenylethenylbenzene was applied as test substrate.

Table 5-4 - Further screening of reducing agents.

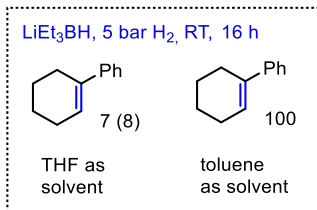
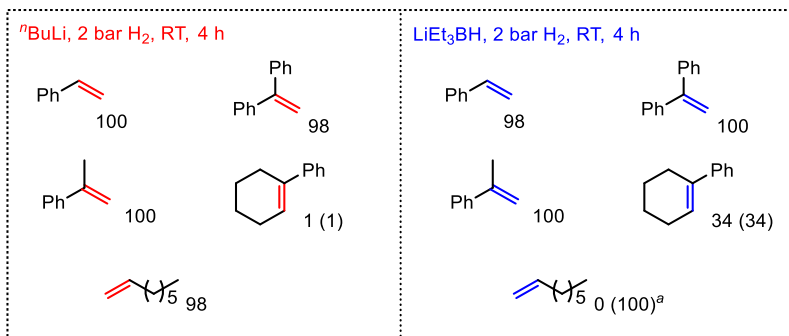
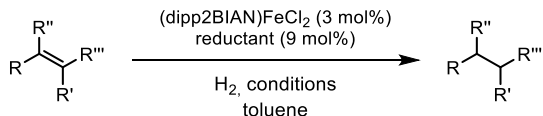


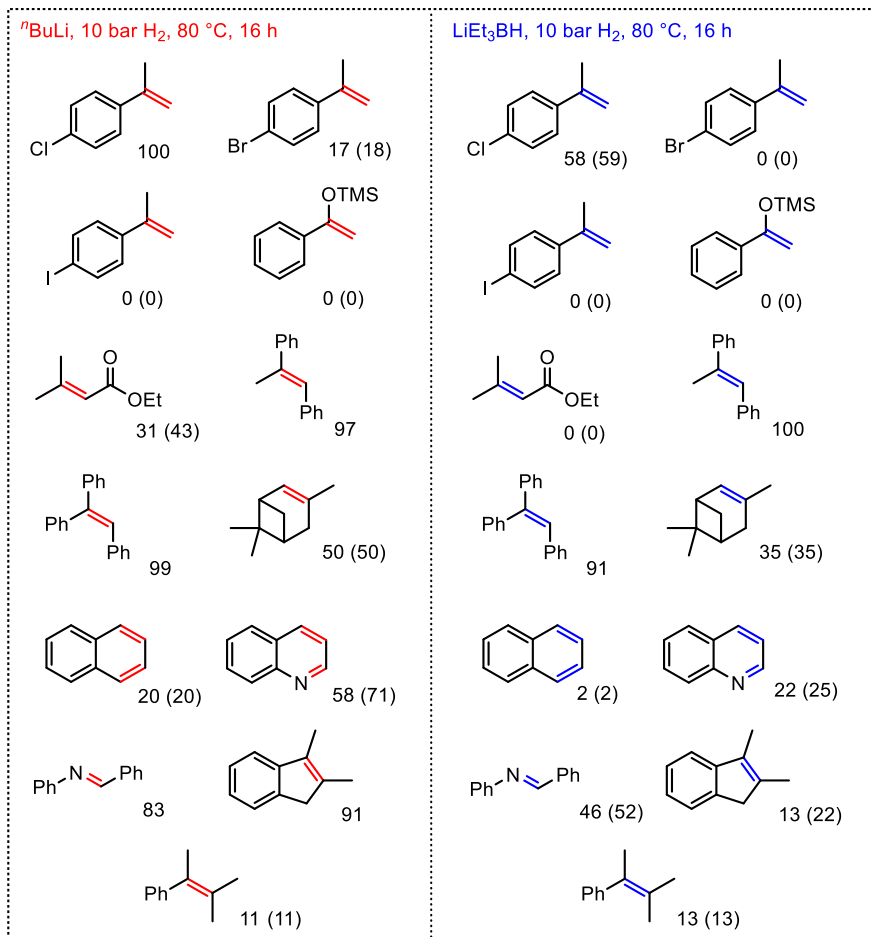
Entry	Reductant	Yield (%) ^a
1	<i>n</i> -BuLi	31 (31)
2	<i>i</i> -PrMgCl	51 (51)
3	LiEt ₃ BH	77 (79)
4	NaEt ₃ BH	3 (3)
5	L-selectride	62 (62)
6	N-selectride	1 (1)
7	DiBAL-H	25 (25)
8	HBPIn + KO <i>t</i> -Bu ^b	3 (3)

^a quantitative GC-FID vs. *n*-pentadecane as internal reference, conversion in % in parentheses; ^b THF as solvent.

Classic organometallic reducing agents, Grignard reagents and organolithium species, proved to have similar effect on the catalytic system, 1,2-diphenylethenylbenzene was hydrogenated with modest yield under mild condition. Organoboron activated reductants such as Super-Hydride and selectride showed interesting results, the formation of a competent hydrogenation catalyst was observed only with lithium as counter-cation (Table 5-4, entries 3 and 4). Yield of 77% was achieved by treatment of **3** with 9 mol% of LiEt₃BH. Organoaluminium species, such as diisobutylaluminum hydride, were also tested but the activity of the catalyst generated by it was lower compared to the previous results. In a recent report by Thomas *et al.*,^[9] very reactive organoboron-based reductants were formed *in situ* mixing the mildly reactive 4,4,5,5-tetramethyl-1,3,2-dioxaborolane

with bases, such as sodium *tert*-butoxide. The resulting borate was efficiently applied for the reduction of a broad range of iron pincer complex, subsequently tested as catalysts for hydroboration and hydrosilylation reactions. Similar approach was applied for the activation of complex **3**, unfortunately with poor results (Table 5-4, entry 8).





Scheme 5-2 - Substrate scope of iron-catalyzed hydrogenations of alkenes. Bonds in red/blue indicate the site of π -bond hydrogenation. Yields were determined by quantitative GC-FID vs. *n*-pentadecane. Conversions are given in parentheses if < 95 %; ^a complete isomerization of starting material.

With these optimized reaction conditions, the scope of the reaction was investigated, and the results are summarized in Scheme 5-2. Using LiTEBH as reducing agent primary and secondary alkenes such as styrene, α -methylstyrene, and 1,1-diphenylethylene were hydrogenated under mild reaction conditions (2 bar H_2 , r.t., 4 h) accordingly to the results obtained employing *n*-butyllithium as reducing agent (chapter 4). On the other hand

octene, which was fully hydrogenated with *n*-BuLi protocol, underwent isomerization reaction applying Super-Hydride. Tri-substituted olefins such as triphenylethylene and *E*- α -methylstilbene displayed only partial hydrogenation under these mild conditions. However, increasing reaction time and hydrogen pressure resulted in excellent yields. Sterically demanding α -pinene was only partially converted and interestingly 1-phenylcyclohexene was hydrogenated exclusively employing LiEt₃BH as reductant, *n*-BuLi proved to be ineffective. Hydrogenation of 1-phenylcyclohexene was attempted with different solvents and completely opposite results were obtained, indicating a prominent solvent effect on this catalytic system. Under 5 bar of dihydrogen full conversion was observed in toluene and only 7% of yield was detectable employing THF. These results could be rationalized in sight of a possible π -stabilization operated by toluene, which is lacking with ethereal solvents, during the reduction of (dipp₂BIAN)FeCl₂. This aspect will be deeply discussed in the next chapter. 2,3-dimethyl-1*H*-indene, completely converted with *n*-BuLi as reductant, was less reactive under the triethylborohydride protocol resulting in only 13% yield, naphthalene followed the same pattern. The hydrogenation of (3-methylbut-2-en-2-yl)benzene resulted in only traces of product.

Stability of this catalytic system towards some of the most widespread functional groups was tested employing FGs-containing substrates. 4-chloro- α -methylstyrene gave good results, 4-bromo- α -methylstyrene showed only partial conversion while 4-iodo- α -methylstyrene was entirely recovered at the end of the reaction. This reactivity pattern for halogenated olefins reflects the strength of the corresponding C-X bond. Indeed, in all these cases traces of dehalogenated product were detected and halogen cleavage, already described in other iron-catalyzed hydrogenation systems^[10], leads to a metal center oxidation and subsequent catalyst deactivation. Ethyl 3,3-dimethylacrylate showed reactivity only with *n*-buthyllithium as reducing agent while silyl enol ethers were not tolerated by the system. Nitrogen containing quinoline and *N*,1-diphenylmethanimine were hydrogenated with good yields employing *n*-buthyllithium as reductant. Overall from these results is possible to conclude that the catalyst obtained by treatment of **3** with *n*-BuLi as reducing agent, compared with the super hydride protocol, is more stable respect to the functional groups tested.

5.3 Mechanistic experiments

This catalyst showed interesting reactivity towards hydrogenation of olefins, initial comparison of iron reduced species in presence and in absence of the ligand indicated a strong positive influence of the BIAN ligand. In order to identify the nature of the system a series of mechanistic investigations were performed. At first, as mentioned in chapter 4, different isolation attempts of the active species were carried out. The reduction in toluene of 150 mg of $(\text{dipp}_2\text{BIAN})\text{FeCl}_2$ with 3 equivalents of butyllithium led to a dark-red solution. After evaporation of the solvent and subsequent steps of extraction and washing with hexane, toluene, and THF, isolation of two distinct fractions was possible. The first, non-polar and major fraction ($\sim 70\%$), proved to be composed of an iron(0) complex η^6 -toluene-coordinated bearing a neutral dipp_2BIAN fragment, recently described by Findlater *et al.*^[5c] Tests of this complex in catalytic hydrogenation of α -methylstyrene proved its inefficiency. On the other hand, applying the second fraction previously obtained, as catalyst, a successful hydrogenation reaction with a very similar kinetic was observed (Figure 5-1). These results indicated that the second fraction consists in the active hydrogenation catalyst.

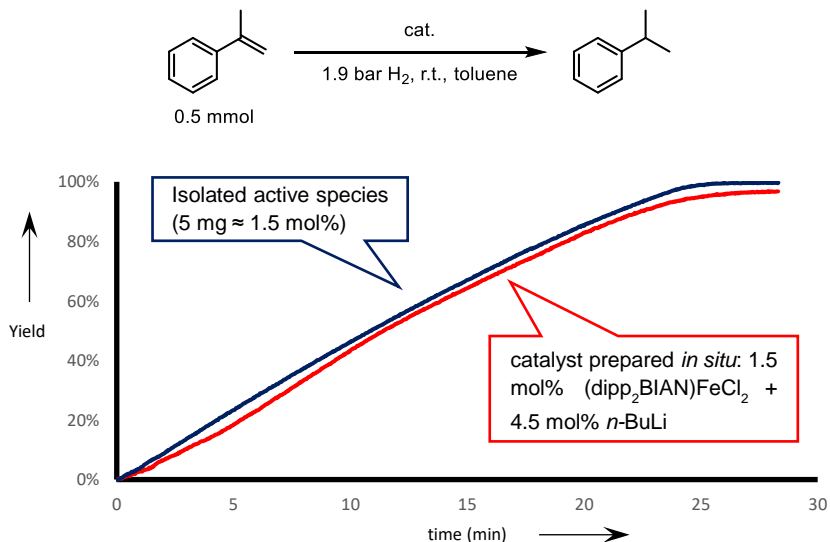


Figure 5-1 – Reactivity comparison between *in situ* generated and isolated catalyst.

Unfortunately, all attempts of crystallization of this active species failed. Investigations of the nature of this fraction by NMR were pursued, but due to the high sensitivity of this compound towards moisture, during the preparation of the sample the decomposition of

the species was observed, revealed by a change of the sample color. The NMR spectrum obtained (Figure 5-S2) showed a set of signals indicating the presence in the sample of the reduced BIAN species **4**. Considering the stoichiometry of the reduction reaction is clear that the amount of reductant exceed the values necessary for the synthesis of an iron(0) species, very likely the non-innocent ligand is also reduced and acts as an electron reservoir, yielding to the formation of an anionic species. The presence of **4**, therefore, could be derived from the hydrolysis, detected during the sample preparation, of an iron complex coordinated to the dianionic **5**.

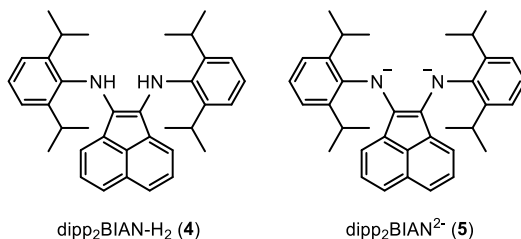


Figure 5-2 – $2 e^-$ reduced dipp₂BIAN in its neutral (**4**) and dianionic form (**5**).

Analysis of the isolated active species via mass-spectrometry led to inconclusive results. A second attempt was performed without isolation, preparing the sample *in situ*, (dipp₂BIAN)FeCl₂ was treated with 3 equivalents of Li(Et₃BH) in toluene and the resulting mixture was analyzed *via* MS. Two major species were detected in the resulting spectrum (Figure 5-3), the presence of the Fe(0)-BIAN complex, isolated and reported by Findlater^[5c] was confirmed by a peak with mass of 648 *m/z*. The second intense signal with a mass of 655 *m/z* possibly indicate the presence of a further reduced iron species, a ferrate coupled with lithium as counter-cation, [(η⁶-toluene)Fe(dipp₂BIAN)]⁻[Li]⁺. All these analytic results, albeit preliminary, suggests an Fe-BIAN complex with a structure similar to **7** as active catalytic species operating in this catalytic hydrogenation.

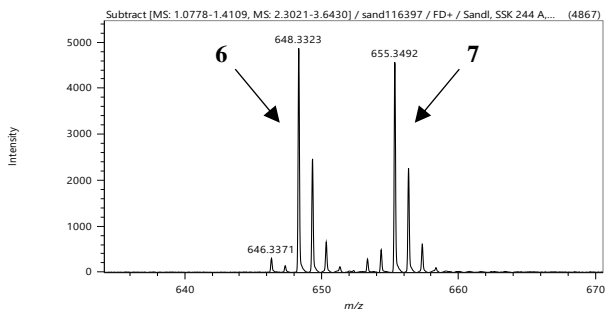
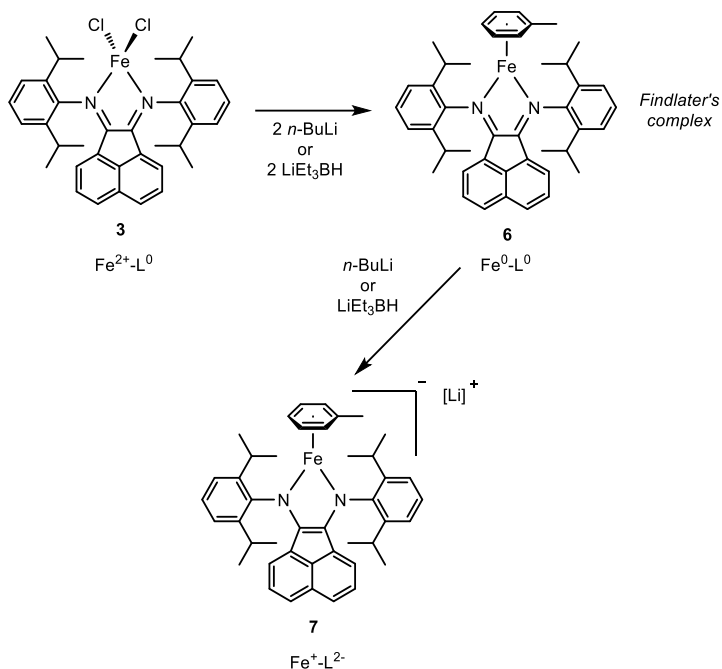


Figure 5-3 – LIFDI-MS spectrum of reduced Fe-BIAN species.



Scheme 5-3 – Proposed active hydrogenation catalyst **7**.

5.4 Conclusions

In summary we have developed an active hydrogenation catalyst based on the tetrahedral (BIAN) FeCl_2 complexes described and characterized in chapter 4. These precursors activated by different reducing agents such as *n*-butyllithium or lithium triethylborohydride resulted in the formation of active species able to efficiently catalytically hydrogenate mono-, di-, and trisubstituted olefins, even challenging tetra-substituted alkenes are partially converted. Considering the preliminary mechanistic investigations performed, we postulate a ferrate, coordinated to a reduced non-innocent bis(imino)acenaphthene ligand, as active catalytic species.

5.5 Experimental part

5.4.1 General

Chemicals and Solvents: Commercially available olefins were distilled under reduced pressure prior use. Commercially available reductant (*n*-BuLi, *i*-PrMgCl, LiEt₃BH, NaEt₃BH, L-selectride, N-selectride and DiBAIH) were used as received from Sigma Aldrich or diluted before use. Solvents (THF, toluene) were distilled over sodium and benzophenone and stored over molecular sieves (4 Å). BIAN ligands were synthesized according to literature procedures^[11]. Solvents used for column chromatography were distilled under reduced pressure prior use (ethyl acetate).

Analytical Thin-Layer Chromatography: TLC was performed using aluminium plates with silica gel and fluorescent indicator (*Merck*, 60, F254). Thin layer chromatography plates were visualized by exposure to ultraviolet light (366 or 254 nm) or by immersion in a staining solution of molybdotophosphoric acid in ethanol or potassium permanganate in water.

Column Chromatography: Flash column chromatography with silica gel 60 from *KMF* (0.040-0.063 mm). Mixtures of solvents used are noted in brackets.

High Pressure Reactor: Hydrogenation reactions were carried out in 160 and 300 mL high pressure reactors (*Parr*TM) in 4 mL glass vials. The reactors were loaded under argon, purged with H₂ (1 min), sealed and the internal pressure was adjusted. Hydrogen (99.9992%) was purchased from *Linde*.

¹H- und ¹³C-NMR-Spectroscopy: Nuclear magnetic resonance spectra were recorded on a *Bruker* Avance 300 (300 MHz) and *Bruker* Avance 400 (400 MHz). ¹H-NMR: The following abbreviations are used to indicate multiplicities: s = singlet; d = doublet; t = triplet, q = quartet; m = multiplet, dd = doublet of doublet, dt = doublet of triplet, dq = doublet of quartet, ddt = doublet of doublet of quartet. Chemical shift δ is given in ppm to tetramethylsilane.

Gas chromatography with FID (GC-FID): HP6890 GC-System with injector 7683B and *Agilent* 7820A System. Column: HP-5, 19091J-413 (30 m \times 0.32 mm \times 0.25 μ m), carrier gas: N₂. GC-FID was used for reaction control and catalyst screening (Calibration with internal standard *n*-pentadecane and analytically pure samples).

Gas chromatography with mass-selective detector (GC-MS): *Agilent* 6890N Network GC-System, mass detector 5975 MS. Column: HP-5MS (30 m \times 0.25 mm \times 0.25 μ m, 5% phenylmethylsiloxane, carrier gas: H₂. Standard heating procedure: 50 °C (2 min), 25 °C/min -> 300 °C (5 min).

Mass Spectrometry: Mass spectra were recorded on a Joel AccuTOF GCX in liquid injection field desorption ionization (LIFDI) mode.

Gas-uptake reaction monitoring: Gas-uptake was monitored with a *Man On the Moon X201* kinetic system to maintain a constant reaction pressure. The system was purged with hydrogen prior use. Reservoir pressure was set to about 9 bar H₂. Calibration of the reservoir pressure drop in relation to H₂ consumption was performed by quantitative hydrogenation of various amounts of α -methylstyrene with a Pd/C catalyst in 1 mL of THF.

5.4.2 General procedure for catalytic hydrogenations

A 4 mL vial was charged with a freshly prepared solution of (dipp₂BIAN)FeCl₂ in toluene (2.50 mL, 0.003 M) and an aliquot of a solution of *n*-BuLi in toluene (90 μ L, 0.25 M) was added under an argon atmosphere. The alkene (0.25 mmol) was added and the vial transferred to a high pressure reactor. The reactor was purged with H₂ (1 min), sealed, and the internal temperature and pressure adjusted. After the desired reaction time, the autoclave was purged and the vial was retrieved. The reaction was quenched with saturated aqueous NaHCO₃ (0.5 mL) and extracted with ethyl acetate (1 mL). The organic phases were filtered through a plug of silica (ethyl acetate as eluent) and analyzed by quantitative GC-FID analysis vs. *n*-pentadecane as internal reference.

5.4.3 Synthesis (dipp₂BIAN)FeCl₂

In a Schlenk flask FeCl₂(thf)_{1.5} (1 mmol, 1 equiv.) and dipp₂BIAN (1.1 mmol, 1.1 equiv.) were suspended in toluene (20 mL). The mixture was heated to 100 °C and stirred for 16 h during which the formation of a precipitate was observed. After cooling to r.t. the suspension was concentrated in vacuo and filtered. The solid residue was washed with toluene (3×5 mL) and dried to afford the desired complex as a green solid, 86 % yield. mp >240 °C (decomp); Anal. calcd (%) for C₃₆H₄₀Cl₂FeN₂: C, 68.91; H, 6.43; N, 4.46. Found: C, 69.99; H, 6.15; N, 4.33; IR: $\tilde{\nu}$ = 2957, 2926, 2866, 1647, 1614, 1597, 1577, 1463, 1433, 1417, 1286, 836, 802, 783, 760 cm⁻¹; LIFDI-MS (*m/z*) calcd for C₃₆H₄₀Cl₂FeN₂: 626.1914, found: 626.1756 [*M*]⁺.

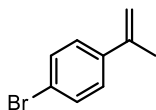
5.4.4 Synthesis of starting material

General procedure for styrene synthesis in a Wittig reaction

A 50 mL flask was charged with a suspension of methyltriphenylphosphonium bromide (1 equiv.) in THF (0.7 M). Then, NaH-suspension in paraffine (60%, 1 equiv.) was added in small portions. The reaction mixture was stirred at room temperature for 20 h followed by a dropwise addition of a solution of a ketone/aldehyde derivative (1 equiv.) in THF (0.7 M). The reaction mixture was stirred for 2 d at room temperature, quenched with H₂O (15 mL) and extracted with Et₂O (3 × 15 mL). The combined organic layers were dried (Na₂SO₄), concentrated and subjected to silica gel flash chromatography (*n*-pentane).

4-Bromo- α -methylstyrene

Synthesis following the general procedure for styrene synthesis in a Wittig reaction.



C₉H₉Br

197.08 g/mol

Appearance

colorless oil

Yield

1.06 g, 5.39 mmol (77%)

TLC

R_f = 0.59 (SiO₂, *n*-pentane)

¹H-NMR

(400 MHz, CDCl₃) δ 7.50-7.35 (m, 2H), 7.42-7.29 (m, 2H), 5.36 (s, 1H), 5.10 (s, 1H), 2.12 (s, 3H).

¹³C-NMR

(101 MHz, CDCl₃) δ 142.2, 140.1, 131.3, 127.2, 121.4, 113.1, 21.7.

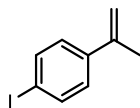
GC-MS

t_R = 6.51 min, (EI, 70 eV): m/z = 197 [M⁺], 183, 171, 156, 115, 102, 91, 75, 63, 51.

Analytical data were in full agreement with T. Taniguchi, A. Yajima, H. Ishibashi, *Adv. Synth. Catal.* **2011**, 353, 2643–2647.

4-Iodo- α -methylstyrene

Synthesis following the general procedure for styrene synthesis in a Wittig reaction.



C₉H₉I

244.08 g/mol

Appearance

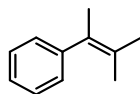
colorless solid

Yield	1.21 g, 4.96 mmol (71%)
TLC	$R_f = 0.84$ (SiO ₂ , <i>n</i> -pentane)
¹H-NMR	(300 MHz, CDCl ₃) δ 7.70 – 7.59 (m, 2H), 7.24 – 7.15 (m, 2H), 5.40 – 5.33 (m, 1H), 5.12 – 5.07 (m, 1H), 2.14 – 2.09 (m, 3H).
¹³C-NMR	(75 MHz, CDCl ₃) δ 142.28, 140.70, 137.27, 134.97, 127.41, 113.15, 92.88, 21.62.
GC-MS	$t_R = 7.14$ min, (EI, 70 eV): $m/z = 244$ [M ⁺], 127, 115, 102, 91, 75, 63, 50.

Analytical data were in full agreement with G. B. Bachman, C. L. Carlson, M. Robinson, *J. Am. Chem. Soc.* **1951**, 73, 1964–1965.

(3-methylbut-2-en-2-yl)benzene

Synthesis following the procedure by W. Adam, M. A. Arnold, M. Grüne, W. M. Nau, U. Pischel, C. R. Saha-Möller, *Organic Letters* **2002**, 4, 537-540.



C₁₁H₁₄

146,23 g/mol

Appearance colorless liquid

Yield 850 mg, 5.8 mmol (39%)

¹H-NMR (300 MHz, CDCl₃) δ 7.36 – 7.13 (m, 5H), 1.99 (s, 3H), 1.84 (s, 3H), 1.62 (s, 3H).

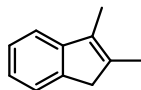
¹³C-NMR (75 MHz, CDCl₃) δ 145.35, 130.00, 128.44, 127.94, 127.23, 125.73, 22.11, 20.85, 20.59.

GC-MS $t_R = 5.62$ min, (EI, 70 eV): $m/z = 146$ [M⁺], 131, 115, 103, 91, 77, 65, 51.

Analytical data were in full agreement with W. Adam, M. A. Arnold, M. Grüne, W. M. Nau, U. Pischel, C. R. Saha-Möller, *Org. Lett.* **2002**, 4, 537-540.

2,3-dimethyl-1*H*-indene

Synthesis following the procedure by H.-Q. Luo, T.-P. Loh, *Tetrahedron Lett.* **2009**, 50, 1554–1556.



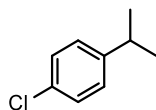
C₁₁H₁₂
144.2 g/mol

Appearance	colorless oil
Yield	1.49 g, 10.3 mmol (21 %)
¹H NMR	(300 MHz, CDCl ₃) δ 7.40–7.08 (m, 4H), 3.27 (m, 2H), 2.07 (m, 3H), 2.04 (m, 3H).
¹³C{¹H} NMR	(75 MHz, CDCl ₃) δ 147.55, 142.32, 138.05, 132.51, 126.05, 123.55, 122.97, 117.91, 42.46, 13.95, 10.17.
GC-MS	<i>t</i> _R = 6.74 min, (EI, 70 eV): <i>m/z</i> = 144 [M] ⁺ , 128, 115, 102, 89, 77, 71, 63, 51.

Analytical data were in full agreement with M. W. Justik, G. F. Koser, *Tetrahedron Lett.* **2004**, *45*, 6159–6163 and M. G. Schrems, E. Neumann, A. Pfaltz, *Angew. Chem. Int. Ed.* **2007**, *46*, 8274–8276.

5.4.5 Hydrogenation products

1-Chloro-4-isopropylbenzene

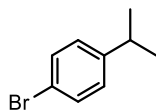


C₉H₁₁Cl
154.64 g/mol

¹H-NMR	(300 MHz, CDCl ₃) δ 7.25 (m, 2H), 7.21–7.09 (m, 2H), 2.89 (m, 1H), 1.23 (d, <i>J</i> = 6.9 Hz, 6H).
¹³C-NMR	(75 MHz, CDCl ₃) δ 142.3, 131.3, 128.4, 127.8, 33.6, 23.9.
GC-MS	<i>t</i> _R = 5.37 min, (EI, 70 eV): <i>m/z</i> = 154 [M] ⁺ , 139, 125, 119, 105, 89, 77, 63, 51.

Analytical data were in full agreement with S. S. Kim, C. S. Kim, *J. Org. Chem.* **1999**, *64*, 9261–9264.

1-Bromo-4-isopropylbenzene

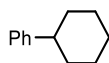


C₉H₁₁Br
199.09 g/mol

¹H-NMR	(300 MHz, CDCl ₃) δ 7.47 – 7.36 (m, 2H), 7.15 – 7.04 (m, 2H), 2.87 (hept, <i>J</i> = 6.9 Hz, 1H), 1.23 (d, <i>J</i> = 6.9 Hz, 6H).
¹³C-NMR	(101 MHz, CDCl ₃) δ 147.8, 131.3, 128.2, 119.3, 33.7, 30.9, 23.8.
GC-MS	<i>t_R</i> = 6.16 min, (EI, 70 eV): <i>m/z</i> = 198 [M ⁺], 185, 169, 158, 143, 119, 104, 91, 77, 63, 51.

Analytical data were in full agreement with M. A. Hall, J. Xi, C. Lor, S. Dai, R. Pearce, W. P. Dailey, R. G. Eckenhoff, *J. Med. Chem.* **2010**, *53*, 5667–5675.

Phenylcyclohexane



C₁₂H₁₆

160.26 g/mol

¹H-NMR	(300 MHz, CDCl ₃) δ 7.34 – 7.25 (m, 2H), 7.24 – 7.14 (m, 3H), 2.60 – 2.39 (m, 1H), 2.00 – 1.79 (m, 4H), 1.80 – 1.73 (m, 1H), 1.51 – 1.19 (m, 5H).
¹³C-NMR	(75 MHz, CDCl ₃) δ 148.1, 128.3, 126.5, 125.8, 44.7, 34.52, 27.0, 26.2.
GC-MS	<i>t_R</i> = 7.30 min, (EI, 70 eV): <i>m/z</i> = 160 [M ⁺], 143, 129, 115, 102, 91, 77, 63, 51.

Analytical data were in full agreement with W. M. Czaplik, M. Mayer, A. Jacobi von Wangelin, *Angew. Chem. Int. Ed.* **2009**, *48*, 607–610.

1,1-Diphenylethane



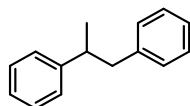
C₁₄H₁₄

182.27 g/mol

¹H-NMR	(300 MHz, CDCl ₃) δ 7.35 – 7.11 (m, 10H), 4.15 (q, <i>J</i> = 7.2, 1H), 1.63 (d, <i>J</i> = 7.2, 3H).
GC-MS	<i>t_R</i> = 7.97 min, (EI, 70 eV): <i>m/z</i> = 182 [M ⁺], 167, 152, 139, 128, 115, 103, 89, 77, 63, 51.

Analytical data were in full agreement with F. Schoenebeck, J. A. Murphy, S.-z. Zhou, Y. Uenoyama, Y. Miclo, T. Tuttle, *J. Am. Chem. Soc.* **2007**, *129*, 13368–13369.

Propane-1,2-diyl dibenzene



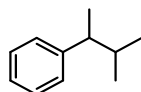
C₁₅H₁₆

196,29 g/mol

- ¹H-NMR** (300 MHz, CDCl₃) δ 7.44 – 7.10 (m, 10H), 3.17 – 2.95 (m, 2H), 2.91 – 2.78 (m, 1H), 1.31 (d, *J* = 6.8 Hz, 3H).
- ¹³C-NMR** (75 MHz, CDCl₃) δ 147.05, 140.88, 129.23, 128.37, 128.17, 127.11, 126.09, 125.91, 45.13, 41.96, 21.23.
- GC-MS** *t*_R = 8,24 min, (EI, 70 eV): *m/z* = 196 [M⁺], 178, 165, 152, 139, 128, 115, 105, 91, 77, 65, 51.

Analytical data were in full agreement with C. Metallinos, J. Zaifman, L. Van Belle, L. Dodge, M. Pilkington, *Organometallics* **2009**, 28, 4534-4543.

(3-methylbutan-2-yl)benzene



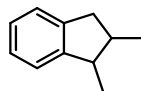
C₁₁H₁₆

148,28 g/mol

- ¹H-NMR** (300 MHz, CDCl₃) δ 7.35 – 7.14 (m, 5H), 2.42 (m, 1H), 1.77 (m, 1H), 1.24 (d, *J* = 7.0 Hz, 3H), 0.94 (d, *J* = 6.7 Hz, 3H), 0.76 (d, *J* = 6.7 Hz, 3H).
- ¹³C-NMR** (75 MHz, CDCl₃) δ 147.10, 128.02, 127.65, 125.68, 46.88, 34.45, 21.20, 20.20, 18.78.
- GC-MS** *t*_R = 5,41 min, (EI, 70 eV): *m/z* = 148 [M⁺], 131, 115, 105, 77, 65, 51.

Analytical data were in full agreement with V. Jurčik, S. P. Nolan, C. S. J. Cazin, *Chemistry – A European Journal* **2009**, 15, 2509-2511.

1,2-dimethyl-2,3-dihydro-1H-indene



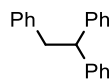
C₁₁H₁₄

146.23 g/mol

- ¹H-NMR** (400 MHz, CDCl₃) δ 7.23 – 7.10 (m, 4H), 3.17 (m, 1H), 3.04 – 2.92 (m, 1H), 2.63 – 2.53 (m, 2H), 1.15 (d, *J* = 7.2 Hz, 3H), 0.99 (d, *J* = 6.8 Hz, 3H).
- ¹³C-NMR** (75 MHz, CDCl₃) δ 148.81, 142.95, 126.10, 126.04, 124.48, 123.59, 42.39, 39.39, 37.84, 15.20, 14.67.
- GC-MS** *t*_R = 6.03 min, (EI, 70 eV): *m/z* = 146 [M⁺], 131, 115, 103, 91, 77, 63, 51.

Analytical data were in full agreement with R. P. Yu, J. M. Darmon, J. M. Hoyt, G. W. Margulieux, Z. R. Turner, P. J. Chirik, *ACS Catal.* **2012**, 2, 1760–1764.

Ethane-1,1,2-triyltribenzene



$C_{20}H_{18}$

258.36 g/mol

1H -NMR (300 MHz, $CDCl_3$) δ 7.30 – 6.95 (m, 15H), 4.24 (t, $J = 7.8$ Hz, 1H), 3.37 (d, $J = 7.8$ Hz, 2H).

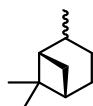
^{13}C -NMR (75 MHz, $CDCl_3$) δ 144.45, 140.26, 129.08, 128.34, 128.05, 126.19, 125.88, 53.11, 42.11.

GC-MS $t_R = 10.67$ min, (EI, 70 eV): $m/z = 258 [M^+]$, 167, 152, 139, 128, 115, 102, 91, 77, 65, 51.

Analytical data were in full agreement with T. C. Fessard, H. Motoyoshi, E. M. Carreira, *Angew. Chem. Int. Ed.* **2007**, 46, 2078–2081.

Pinane

Mixture of diastereomers.



$C_{10}H_{18}$

138.25 g/mol

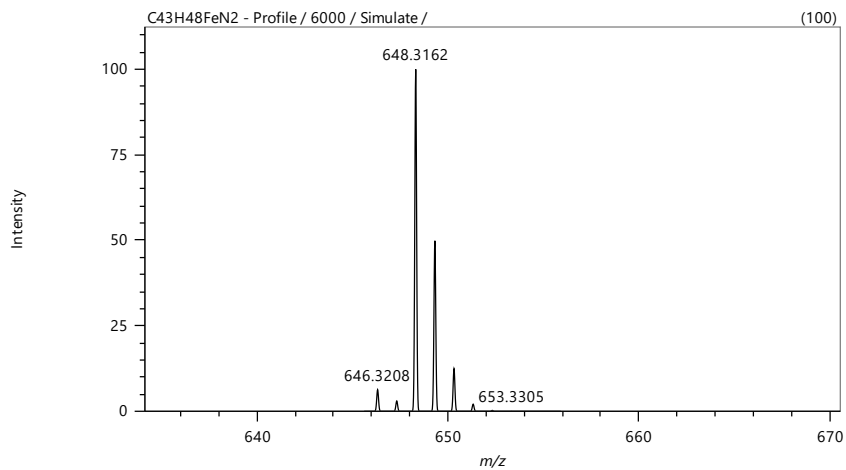
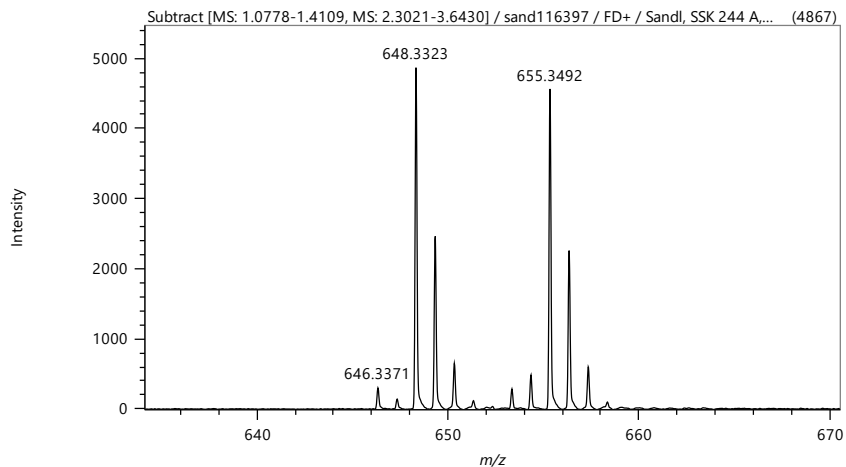
1H -NMR mixture of isomers

^{13}C -NMR (75 MHz, $CDCl_3$) δ 67.98, 65.88, 48.07, 47.62, 41.35, 40.88, 39.49, 38.82, 35.95, 33.96, 29.35, 28.30, 26.84, 26.54, 25.63, 24.61, 23.93, 23.83, 23.22, 23.04, 22.90, 21.61, 20.09, 15.29.

GC-MS $t_R = 4.67$ min, (EI, 70 eV): $m/z = 138 [M^+]$, 123, 95, 81, 67, 55.

Analytical data were in full agreement with A. Stolle, B. Ondruschka, W. Bonrath, T. Netscher, M. Findeisen, M. M. Hoffmann, *Chemistry* **2008**, 14, 6805–6814.

Chapter 5 - Hydrogenations catalyzed by Redox-active Bis(imino)acenaphthene (BIAN) Iron Complexes



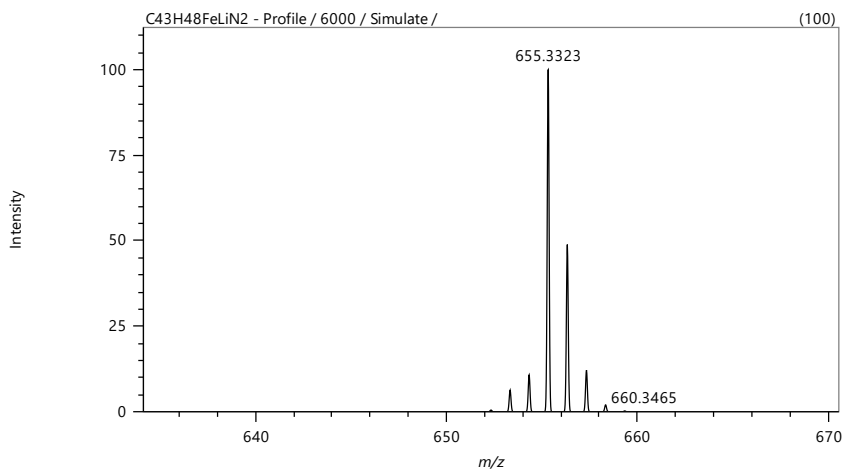


Figure 5-S1 - LIFDI-MS spectrum of $(\eta^6\text{-toluene})\text{Fe}(\text{dipp}_2\text{BIAN})$ and $[(\eta^6\text{-toluene})\text{Fe}(\text{dipp}_2\text{BIAN})]^+[\text{Li}]^+$ (**6**) in toluene.

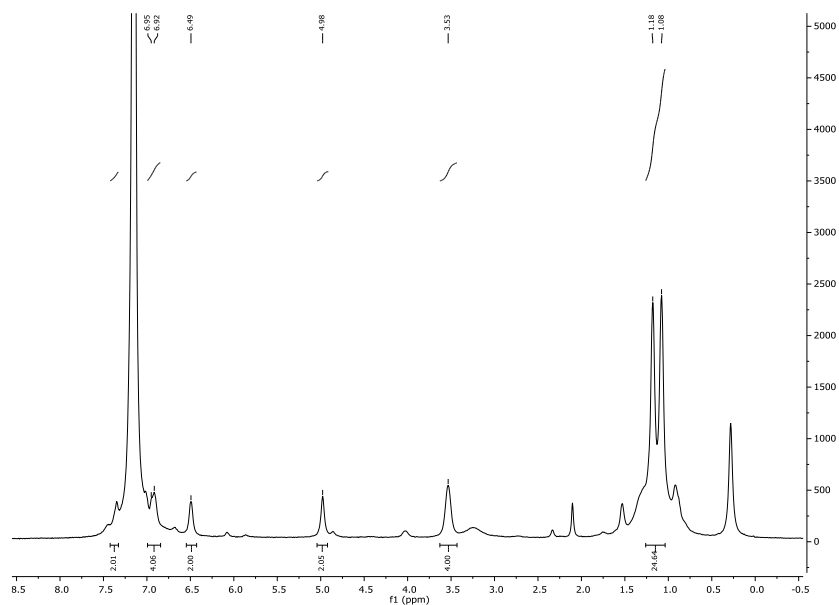


Figure 5-S2 – NMR spectra of the isolated active species.

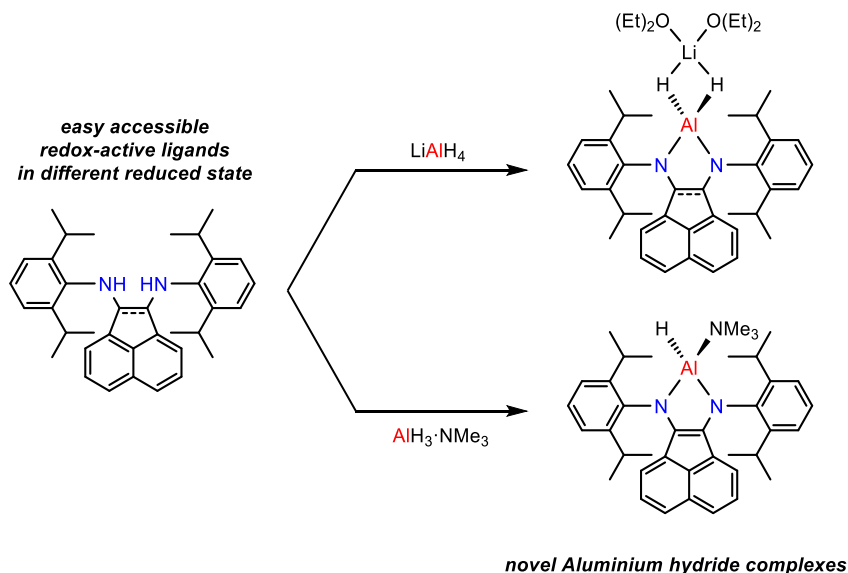
5.6 References

- [1] A. Fuerstner, *ACS Cent. Sci.* **2016**, *2*, 778-789.
- [2] a) A. M. Archer, M. W. Bouwkamp, M.-P. Cortez, E. Lobkovsky, P. J. Chirik, *Organometallics* **2006**, *25*, 4269-4278; b) S. C. Bart, E. Lobkovsky, E. Bill, K. Wiegardt, P. J. Chirik, *Inorg. Chem.* **2007**, *46*, 7055-7063; c) P. J. Chirik, *Acc. Chem. Res.* **2015**, *48*, 1687-1695; d) S. K. Russell, J. M. Darmon, E. Lobkovsky, P. J. Chirik, *Inorg. Chem.* **2010**, *49*, 2782-2792; e) S. C. E. Stieber, C. Milsmann, J. M. Hoyt, Z. R. Turner, K. D. Finkelstein, K. Wiegardt, S. DeBeer, P. J. Chirik, *Inorg. Chem.* **2012**, *51*, 3770-3785; f) R. P. Yu, J. M. Darmon, J. M. Hoyt, G. W. Margulieux, Z. R. Turner, P. J. Chirik, *ACS Catal.* **2012**, *2*, 1760-1764.
- [3] a) R. Langer, Y. Diskin-Posner, G. Leitus, L. J. Shimon, Y. Ben-David, D. Milstein, *Angew. Chem. Int. Ed.* **2011**, *50*, 9948-9952; b) R. Langer, G. Leitus, Y. Ben-David, D. Milstein, *Angew. Chem. Int. Ed.* **2011**, *50*, 2120-2124; c) J. F. Sonnenberg, R. H. Morris, *ACS Catal.* **2013**, *3*, 1092-1102; d) W. Zuo, A. J. Lough, Y. F. Li, R. H. Morris, *Science* **2013**, *342*, 1080.
- [4] a) A. M. Tondreau, C. C. H. Atienza, J. M. Darmon, C. Milsmann, H. M. Hoyt, K. J. Weller, S. A. Nye, K. M. Lewis, J. Boyer, J. G. P. Delis, E. Lobkovsky, P. J. Chirik, *Organometallics* **2012**, *31*, 4886-4893; b) A. M. Tondreau, E. Lobkovsky, P. J. Chirik, *Org. Lett.* **2008**, *10*, 2789-2792; c) S. C. Bart, E. Lobkovsky, P. J. Chirik, *J. Am. Chem. Soc.* **2004**, *126*, 13794-13807; d) B. L. Small, M. Brookhart, *J. Am. Chem. Soc.* **1998**, *120*, 7143-7144; e) B. L. Small, M. Brookhart, A. M. A. Bennett, *J. Am. Chem. Soc.* **1998**, *120*, 4049-4050; f) G. J. P. Britovsek, M. Bruce, V. C. Gibson, B. S. Kimberley, P. J. Maddox, S. Mastroianni, S. J. McTavish, C. Redshaw, G. A. Solan, S. Stroemberg, A. J. P. White, D. J. Williams, *J. Am. Chem. Soc.* **1999**, *121*, 8728-8740; g) G. J. P. Britovsek, V. C. Gibson, B. S. Kimberley, P. J. Maddox, S. J. McTavish, G. A. Solan, A. J. P. White, D. J. Williams, *Chem. Commun.* **1998**, 849-850; h) K. T. Sylvester, P. J. Chirik, *J. Am. Chem. Soc.* **2009**, *131*, 8772-8774.
- [5] a) I. L. Fedushkin, A. A. Skatova, N. M. Khvoinova, A. N. Lukoyanov, G. K. Fukin, S. Y. Ketkov, M. O. Maslov, A. S. Bogomyakov, V. M. Makarov, *Russ. Chem. Bull.* **2013**, *62*, 2122-2131; b) M. J. Supej, A. Volkov, L. Darko, R. A. West, J. M. Darmon, C. E. Schulz, K. A. Wheeler, H. M. Hoyt, *Polyhedron* **2016**, *114*, 403-414; c) F. S. Wekesa, R. Arias-Ugarte, L. Kong, Z. Sumner, G. P. McGovern, M. Findlater, *Organometallics* **2015**, *34*, 5051-5056.
- [6] a) P. Buschelberger, D. Gartner, E. Reyes-Rodriguez, F. Kreyenschmidt, K. Koszinowski, A. Jacobi von Wangelin, R. Wolf, *Chem. Eur. J.* **2016**; b) D. Gaertner, A. Welther, B. R. Rad, R. Wolf, A. Jacobi Von Wangelin, *Angew. Chem. Int. Ed.* **2014**, *53*, 3722-3726; c) T. N. Gieshoff, U. Chakraborty, M. Villa, A. Jacobi von Wangelin, *Angew. Chem. Int. Ed.* **2017**; d) T. N. Gieshoff, M. Villa, A. Welther, M. Plois, U. Chakraborty, R. Wolf, A. Jacobi von Wangelin, *Green Chem.* **2015**; e) T. N. Gieshoff, A. Welther, M. T. Kessler, M. H. G. Prechtel, A. Jacobi von Wangelin, *Chem. Commun.* **2014**, *50*, 2261-2264; f) A. Welther, M. Bauer, M. Mayer, A. Jacobi von Wangelin, *ChemCatChem* **2012**, *4*, 1088-1093.
- [7] I. L. Fedushkin, A. A. Skatova, V. A. Chudakova, G. K. Fukin, *Angew. Chem. Int. Ed.* **2003**, *42*, 3294-3298.

- [8] S. Dastgir, K. S. Coleman, A. R. Cowley, M. L. H. Green, *Organometallics* **2010**, *29*, 4858-4870.
- [9] J. H. Docherty, J. Peng, A. P. Dominey, S. P. Thomas, *Nat. Chem.* **2017**, *advance online publication*.
- [10] a) F. Alonso, I. P. Beletskaya, M. Yus, *Chem. Rev.* **2002**, *102*, 4009-4092; b) W. M. Czaplik, S. Grupe, M. Mayer, A. Jacobi von Wangelin, *Chem. Commun.* **2010**, *46*, 6350-6352.
- [11] M. Gasperini, F. Ragaini, S. Cenini, *Organometallics* **2002**, *21*, 2950-2957.

6 Synthesis of Reduced Bis(imino)acenaphthene (BIAN)

Aluminium Complexes^{i,ii}



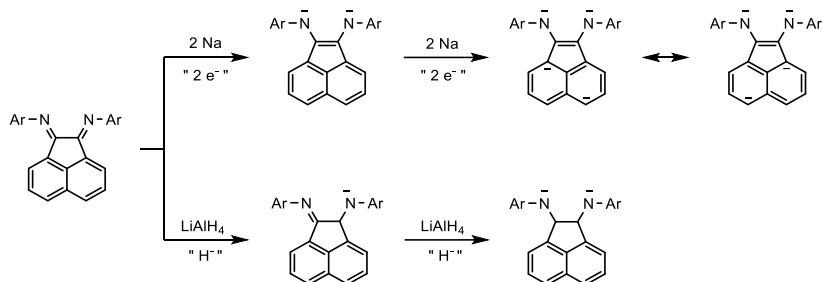
Bis(imino)acenaphthene ligands possess pronounced redox properties. Fascinated by the potential applications of these structure motifs, the synthesis of aluminium hydride complexes coordinated to BIAN ligands in different reduction states was investigated. A set of novel tetrahedral Al-bis(imino)acenaphthene complexes, efficiently synthesized in a single-step procedure, were isolated and herein described.

ⁱ unpublished results.

ⁱⁱ complex synthesis was performed in collaboration with Dr. Dieter Schaarschmidt. Reproducibility problems were observed and further investigations will be carried out in the research group.

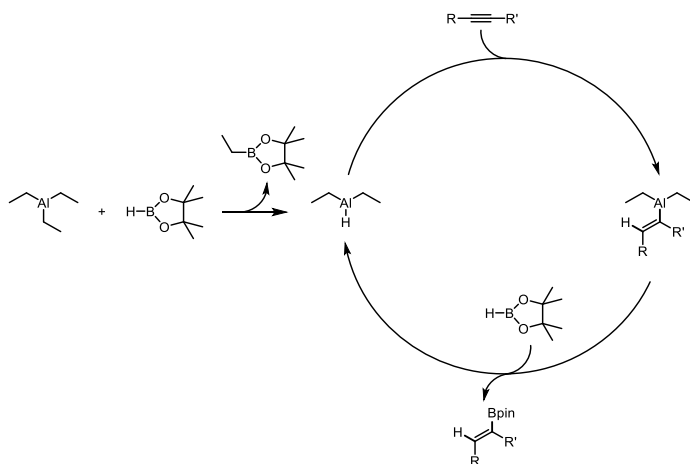
6.1 Introduction

Reports by the group of Fedushkin^[1] in the early two thousands showed the ability of bis(imino)acenaphthene molecules (BIANs) to accept up to 4 electrons without chemical decomposition (Scheme 6-1). Initially, alkali metals and alkaline earth metals have been applied as reductants (sodium, magnesium, and calcium) but recent studies by other groups extended the range of feasible reducing agents.^[2]



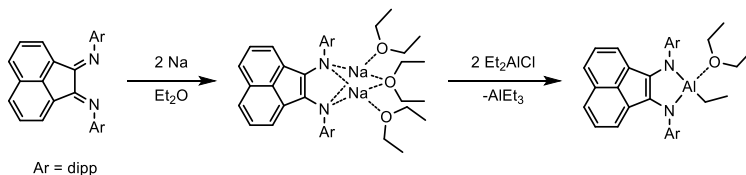
Scheme 6-1 - Simplified scheme of BIAN reduction.

Different BIANs have been efficiently isolated in their corresponding reduced form, voltammographic studies and comparison with more famous organic redox couples (quinones/hydroquinones) demonstrated that BIANH₂ are stronger reductants, moreover varying the substitution pattern of bis(imino)acenaphthenes is possible to tune also their redox potential disclosing the way to an application of such compounds as reducing agents.^[2]



Scheme 6-2 - Hydroboration catalytic cycle proposed by Thomas *et al.*

Similarly to their oxidized counterpart also reduced bis(imino)acenaphthenes were tested as ligands for different metals. The classical approach to complexations is merely a transmetallation between the reduced anionic BIAN and the desired metal salt, not many reports however have been published so far. Fedushkin described a few years ago^[3] the synthesis and characterization of a series of alkyl aluminum complexes coordinated to a two-electrons reduced di*iso*-propylphenyl-BIAN (scheme 6-3) and more recently the same group investigated their reactivity towards simple molecules such as alcohols, amines, and alkynes.^[4]



Scheme 6-3 - Synthesis of Al-BIAN complexes proposed by Fedushkin *et al.*

Besides its historical application as Lewis acid, aluminum has recently attracted attention thanks to its “green” properties, and different catalytic applications have been published in the last couple of years. The groups of Thomas^[5] and Tobisch^[6] developed catalytic hydroboration and hydroamination processes (Scheme 6-2) in which an initial hydroalumination step occurs, subsequently a hydride source allows the regeneration of the active catalyst.

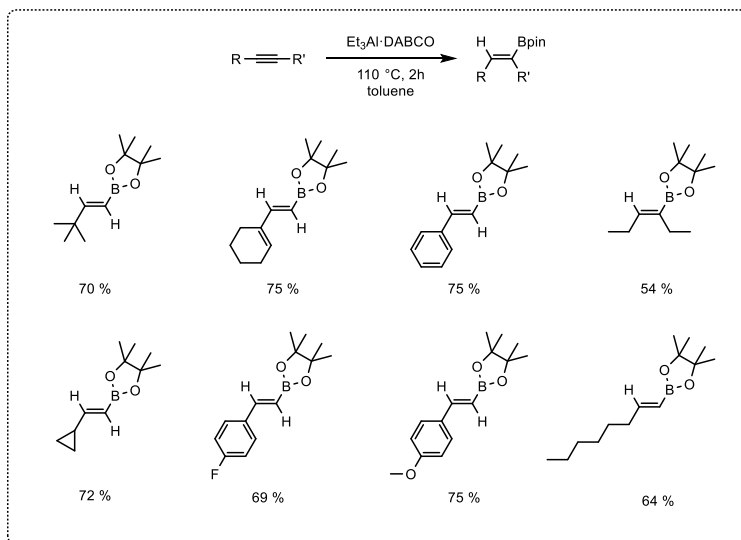
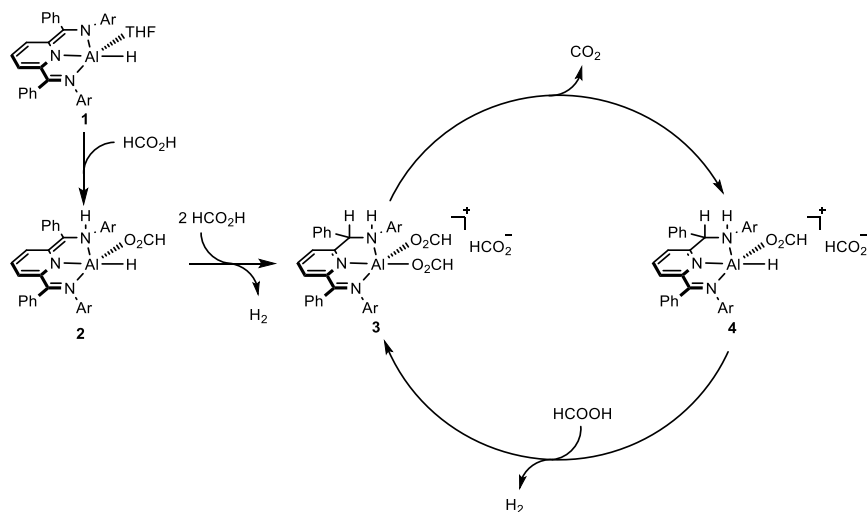


Figure 6-1 – Hydroboration scope reported by Thomas *et al.*

These catalytic variants of hydroalumination constitute a very powerful tool compared to their hazardous and wasteful stoichiometric counterpart. Examples of aluminum complexes with non-innocent ligands are known in literature, especially bis(imino)pyridine motives have been investigated for different catalytic applications such as dehydrogenation of formic acid^[7] and dehydrogenative coupling.^[8] An example is shown in Scheme 6-4, the ligand, similarly to the cases described in chapter 1, actively interact with the substrates, act as base deprotonating one equivalent of formic acid transforming **1** to **2**, treatment with other 2 equivalents of the acid results in the formation of complex **3**. In these steps, thanks to the redox activity of the ligand the aluminum stayed in its more common oxidation state (+3). **3** can then undergoes decarboxylation yielding free carbon monoxide and **4**. Upon interaction with another equivalent of formic acid complex **3** is regenerated, closing the catalytic cycle.



Scheme 6-4 - Dehydrogenation of formic acid to H_2 and CO_2 proposed by Berben *et al.*

Very recently Nembenna *et al.* described^[9] another hydroboration catalyst based on an aluminum hydride complex bearing an alpha-diamine as ligand (**5**). The interesting feature of this catalyst is its chemoselectivity, by choosing the appropriate conditions aldehydes can be completely reduced while ketones remain untouched.

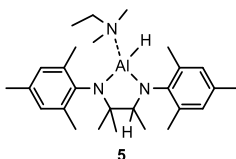
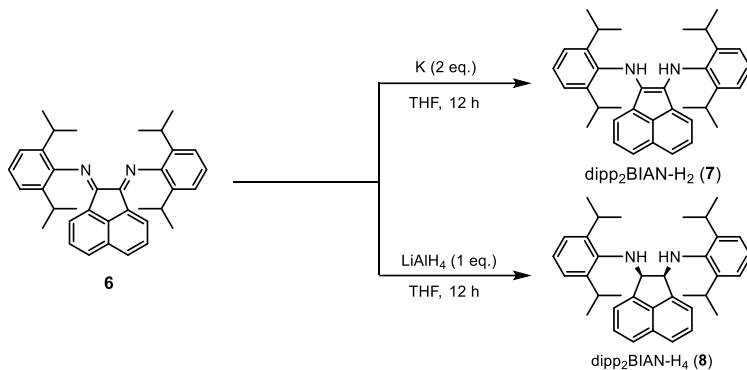


Figure 6-2 - Hydroboration catalyst reported by Nembenna *et al.*

Intrigued by the redox properties of bis(imino)acenaphthenes and by the possible applications of aluminum hydride complexes a series of studies were performed aiming at the synthesis of novel Al-H complexes bearing reduced BIAN species (BIANH₂ and BIANH₄) and herein we report the results.

6.2 Results and Discussion

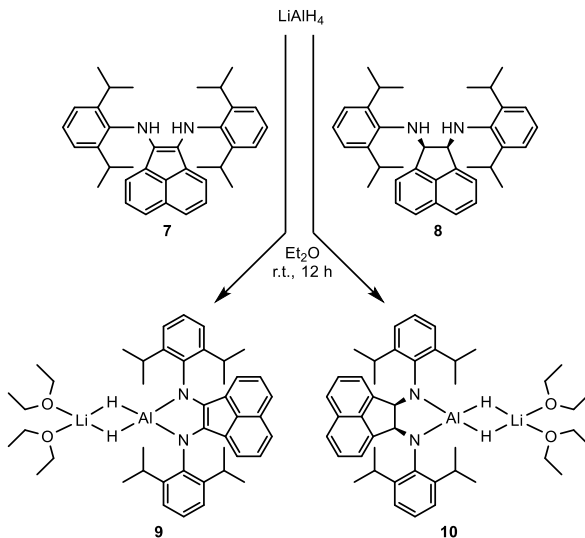
Initial investigations in the field of aluminum-BIAN complexes started with the synthesis of the two electrons (**7**) and four electrons (**8**) reduced dipp₂BIAN ligands (Scheme 6-5). According to literature procedures, treatment of **6** with different reducing agents resulted in the synthesis of the desired ligand **7**^[10] and **8**^[11] in almost quantitative yields.



Scheme 6-5 – Synthesis of reduced dipp₂BIAN.

As previously reported the synthesis of the few aluminum-BIAN complexes described in literature involved the coordination of *in situ* generated anionic ligands with alkylaluminum halides^[3a]. Aiming at the synthesis of hydrido complexes we envisioned a different synthetic procedure in which the cheap and available lithium aluminumhydride acts initially as base, deprotonating the ligand, and subsequently upon coordination with **7/8** yield the desired complexes. This approach resulted to be successful, isolation of aluminum hydride complexes **9** and **10** (Scheme 6-6) was possible blending together equimolar amount of LiAlH₄ and the desired ligand in diethyl ether, and stirring the resulting mixture at room temperature for 12 hours. These reactions proceeded with excellent yields and proved to be clean and selective, simple removal of the volatiles afforded pure [(dipp₂BIAN²⁻)AlH][HLi(OEt₂)₂] (**10**, 92 % yield), while a single washing step with heptane resulted in the isolation of **9** (81 % yield). NMR, elemental analysis and mass spectroscopy confirmed the nature of these complexes. Single crystals of these compounds were obtained by recrystallization from diethyl ether at -20°C, the structures obtained from the X-Ray diffraction analysis are reported in Figure 6-4 and 6-5. In both of these complexes the central aluminum atom, in (+3) oxidation state, is coordinated with one equivalent of the ligand and with one lithium atom *via* two bridging hydrides. The metal ions are coordinated in a distorted tetrahedral N₂H₂ geometry probably due to the rigidity of the ligand structure. The BIAN backbone in **10** is essentially planar while in **9** from the saturation of the C=C double bond arose a certain degree of flexibility. The bond

lengths of the moieties N-C-C-N (**9**) and N-C=C-N (**10**) match the values reported in literature for similar compounds.^[3]



Scheme 6-6 – Synthesis of complex **9** and **10**.

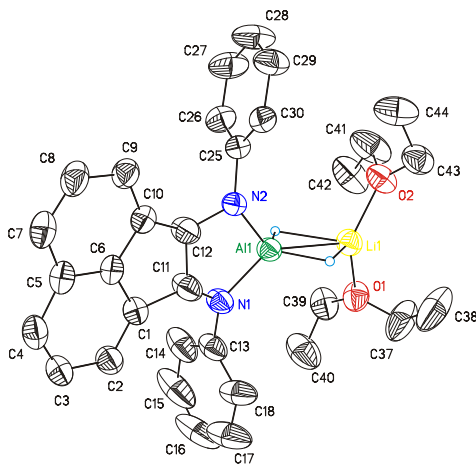


Figure 6-3 - ORTEP diagram (50% probability level) of the molecular structure of **9** with the atom-numbering scheme. Isopropyl substituents, H atoms of the ligand backbone and of diethylether omitted for clarity. Selected bond lengths (Å), angles (°): C(11)-C(12)

1.429(4), C(11)-N(1) 1.397(3), C(13)-N(1) 1.418(3) N(1)-Al(1) 1.842(2), Al(1)-H(1AL) 1.56(3), Li(1)-H(1AL) 2.01(3), Li(1)-Al(1) 2.608(5), O(1)-Li(1) 1.898(5); C(11)-N(1)-C(13) 122.3(2), C(11)-N(1)-Al(1) 105.73(16), N(1)-Al(1)-N(2) 92.61(9), N(1)-Al(1)-H(1AL) 113.7(10), N(1)-Al(1)-Li(1) 132.70(12), H(1AL)-Al(1)-H(2AL) 98.7(14), O(1)-Li(1)-H(1AL) 104.4(8), O(1)-Li(1)-O(2) 129.3(3).

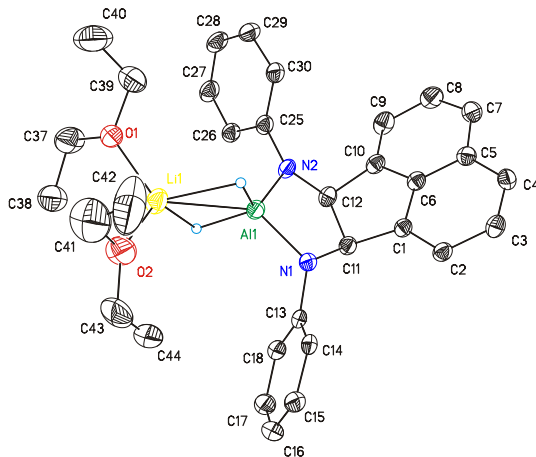
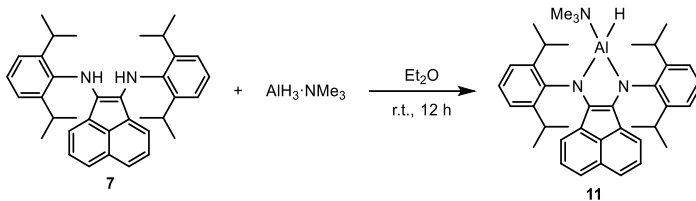


Figure 6-4 - ORTEP diagram (50% probability level) of the molecular structure of **10** with the atom-numbering scheme. Isopropyl substituents, H atoms of the ligand backbone and of diethylether omitted for clarity. Selected bond lengths (Å), angles (°): C(11)-C(12) 1.590(3), C(11)-N(1) 1.469(3), C(13)-N(1) 1.425(3), N(1)-Al(1) 1.827(2), Al(1)-H(1AL) 1.57(2), Li(1)-Al(1) 2.649(4), Li(1)-H(1AL) 2.04(2), Li(1)-O(1) 1.940(5); C(13)-N(1)-C(11) 118.27(18), C(11)-N(1)-Al(1) 111.51(14), N(2)-Al(1)-N(1) 92.38(9), N(1)-Al(1)-H(1AL) 120.8(9), N(1)-Al(1)-Li(1) 135.33(12), H(1AL)-Al(1)-H(2AL) 93.7(12), O(1)-Li(1)-H(1AL) 113.4(7), O(2)-Li(1)-O(1) 113.0(2).

Another approach has been investigated in order to obtain BIAN-aluminum hydride complexes. Treatment of ligand **7** with equimolar amount of $\text{AlH}_3 \cdot \text{NMe}_3$ results in the formation of a similar complex, **11**, as a blue solid. Despite an identical work-up procedure lower yield was achieved in this case (62 %). X-Ray structure of the complex is shown in Figure 6-5, the aluminum atom adopts an analogous distorted tetrahedral geometry, in which one of the bridging hydrides is replaced by a trimethylamine molecule. The bond lengths and angles match pretty closely the values of complex **9**.



Scheme 6-7 – synthesis of compound **11**.

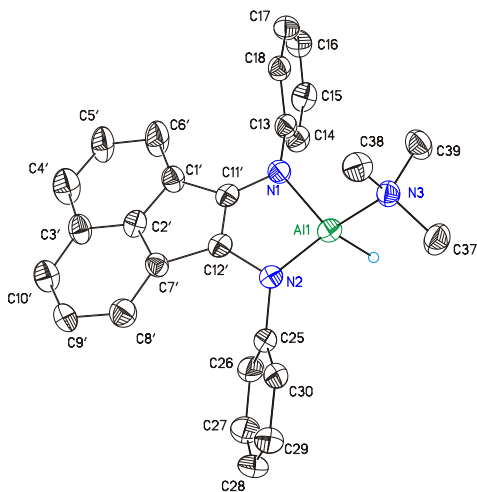


Figure 6-5 - ORTEP diagram (50% probability level) of the molecular structure of **11** with the atom-numbering scheme. Isopropyl substituents, H atoms of the ligand backbone and of trimethylamine omitted for clarity. Selected bond lengths (Å), angles (°): C(11')-C(12') 1.410(10), C(11')-N(1) 1.317(8), C(13)-N(1) 1.431(3), N(1)-Al(1) 1.8368(18), Al(1)-H(1AL) 1.52(3), N(3)-Al(1) 2.0168(18); C(11')-N(1)-C(13) 114.8(4), C(11')-N(1)-Al(1) 105.3(3), N(2)-Al(1)-N(1) 93.66(8), N(1)-Al(1)-N(3) 105.60(8), N(1)-Al(1)-H(1AL) 125.5(9), N(3)-Al(1)-H(1AL) 98.6(9).

6.3 Conclusion

In summary a series of novel aluminium hydride complexes coordinated to BIAN ligands with partially (**9**, **11**), and fully reduced backbones (**10**) were synthesized with a simple and clean procedure. Initial catalytic investigations on these complexes indicated these complexes as competent catalysts for hydrofunctionalization of aldehydes, ketones and nitriles. Further studies of the catalytic properties of these complexes are currently being preformed in our group.

6.4 Experimental part

6.4.1 General

Chemicals and Solvents: All experiments involving air- and moisture-sensitive compounds were performed under an atmosphere of dry argon or nitrogen using standard Schlenk and glovebox techniques. Solvents (diethyl ether, THF) were distilled over sodium and benzophenone and stored over molecular sieves (4 Å). Commercial lithium aluminium hydride was purified by extraction with diethyl ether and subsequent removal of the solvent under high vacuum. Starting BIAN^[12] ligands and reduced **7**^[10] and **8**^[11] were synthesized according to literature procedures. Solvents used for column chromatography were distilled under reduced pressure prior use (ethyl acetate).

Analytical Thin-Layer Chromatography: TLC was performed using aluminium plates with silica gel and fluorescent indicator (*Merck*, 60, F254). Thin layer chromatography plates were visualized by exposure to ultraviolet light (366 or 254 nm) or by immersion in a staining solution of molybdato-phosphoric acid in ethanol or potassium permanganate in water.

Column Chromatography: Flash column chromatography with silica gel 60 from *KMF* (0.040-0.063 mm). Mixtures of solvents used are noted in brackets.

¹H- und ¹³C-NMR-Spectroscopy: Nuclear magnetic resonance spectra were recorded on a *Bruker* Avance 300 (300 MHz) and *Bruker* Avance 400 (400 MHz). ¹H-NMR: The following abbreviations are used to indicate multiplicities: s = singlet; d = doublet; t = triplet, q = quartet; m = multiplet, dd = doublet of doublet, dt = doublet of triplet, dq = doublet of quartet, ddt = doublet of doublet of quartet. Chemical shift δ is given in ppm to tetramethylsilane.

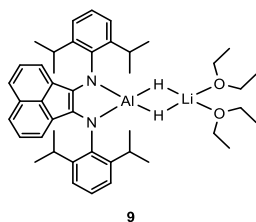
Elemental Analyses (CHN): Elemental analyses (CHN) were performed with a Vario micro cube elemental analyzer.

Mass Spectrometry: Mass spectra were recorded on a Joel AccuTOF GCX in liquid injection field desorption ionization (LIFDI) mode.

X-Ray Diffraction: Data were collected with an Agilent Technologies SuperNova Atlas CCD diffractometer with microfocus Cu K α radiation ($\lambda = 1.54184$ Å) and a SuperNova Eos CCD diffractometer with microfocus Mo K α radiation ($\lambda = 0.71073$ Å).

6.4.2 Synthesis of Aluminum-Complexes

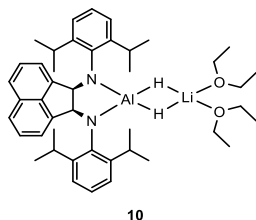
Synthesis of Complex 9:



To the solution of **7** (0.50 g, 0.99 mmol) in diethyl ether (15 mL) was added LiAlH_4 (38 mg, 1.00 mmol). The reaction mixture was stirred at room temperature for 12 h. All volatiles were removed under reduced pressure and the solid residue was washed with heptane (20 mL). The title compound was obtained as a green solid material (555 mg, 0.81 mmol, 81 %). Single crystals of the title compound were obtained by recrystallization from diethyl ether at $-20\text{ }^\circ\text{C}$.

Anal. calcd (%) for $\text{C}_{44}\text{H}_{62}\text{AlLiN}_2\text{O}_2$: C, 77.16; H, 9.12; N, 4.09. Found: C, 77.13; H, 8.75; N, 4.06; **LIFDI-MS** (m/z) calcd for $\text{C}_{36}\text{H}_{42}\text{AlLiN}_2$ [**9** - $(\text{OEt}_2)_2$]: 536.33, found: 536.41 [M]⁺.

Synthesis of Complex 10:

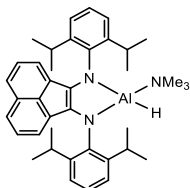


To the solution of **8** (0.38 g, 0.75 mmol) in diethyl ether (15 mL) was added LiAlH_4 (29 mg, 0.75 mmol). The reaction mixture was stirred at room temperature for 12 h. Evaporation of the solvent gave the title compound as a colourless solid material (475 mg, 0.69 mmol, 92 %). Single crystals of the title compound were obtained by recrystallization from diethyl ether at $-20\text{ }^\circ\text{C}$.

¹H NMR (400 MHz, C_6D_6) δ = 7.51 (d, J = 8.1 Hz, 2H), 7.33 (dd, J = 7.1, 2.0 Hz, 2H), 7.18–7.29 (m, 6H), 6.98 (d, J = 6.8 Hz, 2H), 5.70 (s, 2H; N–CH), 4.26–4.38 (m, 2H; $\text{CH}(\text{CH}_3)_2$), 3.89 (br, 2H; Al–H), 3.77–3.89 (m, 2H; $\text{CH}(\text{CH}_3)_2$), 2.81 (q, J = 7.1 Hz, 8H; $\text{O}(\text{CH}_2\text{CH}_3)_2$), 1.61 (d, J = 6.9 Hz, 6H; $\text{CH}(\text{CH}_3)_2$), 1.50 (d, J = 6.7 Hz, 6H; $\text{CH}(\text{CH}_3)_2$),

1.08 (d, $J = 6.9$ Hz, 6H; $\text{CH}(\text{CH}_3)_2$), 1.04 (d, $J = 6.8$ Hz, 6H; $\text{CH}(\text{CH}_3)_2$), 0.59 ppm (t, $J = 7.1$ Hz, 12H; $\text{O}(\text{CH}_2\text{CH}_3)_2$); $^{13}\text{C}\{^1\text{H}\}$ NMR (101 MHz, C_6D_6) $\delta = 148.9$ (quart. C), 148.8 (quart. C), 148.3 (quart. C), 148.0 (quart. C), 136.8 (quart. C), 132.5 (quart. C), 127.8, 124.6, 123.6, 123.3, 123.1, 120.5, 71.1 (N-CH), 65.6 ($\text{O}(\text{CH}_2\text{CH}_3)_2$), 28.8 ($\text{CH}(\text{CH}_3)_2$), 27.7 ($\text{CH}(\text{CH}_3)_2$), 27.3 ($\text{CH}(\text{CH}_3)_2$), 26.3 ($\text{CH}(\text{CH}_3)_2$), 25.4 ($\text{CH}(\text{CH}_3)_2$), 23.3 ($\text{CH}(\text{CH}_3)_2$), 14.2 ppm ($\text{O}(\text{CH}_2\text{CH}_3)_2$). **Anal. calcd (%)** for $\text{C}_{44}\text{H}_{64}\text{AlLiN}_2\text{O}_2$: C, 76.93; H, 9.39; N, 4.08. Found: C, 77.76; H, 9.17; N, 4.10; ; **LIFDI-MS** (m/z) calcd for $\text{C}_{72}\text{H}_{88}\text{Al}_2\text{Li}_4\text{N}_4$ [(**10**)₂ - (OEt_2)₂ + 2Li]: 1090.73, found: 1090.84 [M]⁺.

Synthesis of Complex 11:



11

To the solution of **7** (0.50 g, 0.99 mmol) in diethyl ether (15 mL) was added a solution of $\text{AlH}_3 \times \text{NMe}_3$ (0.7 M in toluene, 1.56 mL, 1.09 mmol). The reaction mixture was stirred at room temperature for 12 h. All volatiles were removed under reduced pressure and the solid residue was washed with hexane (20 mL). The title compound was obtained as a blue solid material (363 mg, 0.62 mmol, 62 % based on **7**). Single crystals of the title compound were obtained by cooling the filtrate to -20 °C.

^1H NMR (400 MHz, C_6D_6) $\delta = 7.24$ – 7.31 (m, 6H), 7.07 (d, $J = 8.2$ Hz, 2H), 6.85 (dd, $J = 8.2, 7.0$ Hz, 2H), 6.17 (d, $J = 7.0$ Hz, 2H), 4.48 (br, 1H; Al-H), 3.87–4.08 (m, 4H; $\text{CH}(\text{CH}_3)_2$), 1.78 (s, 9H; $\text{N}(\text{CH}_3)_3$), 1.48 (d, $J = 6.9$ Hz, 6H; $\text{CH}(\text{CH}_3)_2$), 1.27 (d, $J = 6.7$ Hz, 6H; $\text{CH}(\text{CH}_3)_2$), 1.20 (d, $J = 7.0$ Hz, 6H; $\text{CH}(\text{CH}_3)_2$), 1.14 ppm (d, $J = 6.8$ Hz, 6H; $\text{CH}(\text{CH}_3)_2$); $^{13}\text{C}\{^1\text{H}\}$ NMR (101 MHz, C_6D_6) $\delta = 147.2$ (quart. C), 146.7 (quart. C), 144.0 (quart. C), 136.2 (quart. C), 134.1 (quart. C), 127.6 (quart. C), 127.14 (quart. C), 127.05, 125.6, 124.4, 124.2, 123.8, 118.4, 45.5 ($\text{N}(\text{CH}_3)_3$), 29.2 ($\text{CH}(\text{CH}_3)_2$), 28.1 ($\text{CH}(\text{CH}_3)_2$), 25.6 ($\text{CH}(\text{CH}_3)_2$), 25.5 ($\text{CH}(\text{CH}_3)_2$), 25.3 ($\text{CH}(\text{CH}_3)_2$), 24.5 ppm ($\text{CH}(\text{CH}_3)_2$); **Anal. calcd (%)** for $\text{C}_{39}\text{H}_{50}\text{AlN}_3$: C, 79.69; H, 8.57; N, 7.15. Found: C, 79.70; H, 8.20; N, 6.83; **LIFDI-MS** (m/z) calcd for $\text{C}_{39}\text{H}_{50}\text{AlN}_3$: 587.3820, found: 587.4813 [M]⁺.

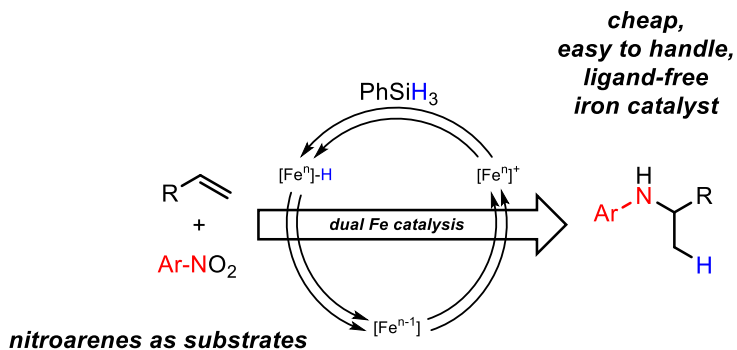
Table S-1 - Crystal and intensity collection data for **9**, **10** and **11**.

	9	10	11
Chemical formula	C ₄₄ H ₆₂ AlLiN ₂ O ₂	C ₄₄ H ₆₄ AlLiN ₂ O ₂	C ₃₉ H _{51.25} AlN ₃
Formula weight	684.87	686.89	589.06
Temperature / K	123.00	122.99	123.01
Wavelength / Å	1.54184	0.71073	1.54184
Crystal system, space group	monoclinic, P2 ₁ /n	monoclinic, P2 ₁ /n	monoclinic, P2 ₁ /n
<i>a</i> / Å	11.0627(5)	12.0961(4)	16.3708(5)
<i>b</i> / Å	17.8984(11)	20.0272(7)	12.5692(3)
<i>c</i> / Å	21.6065(10)	18.2501(7)	17.1359(5)
α / Å	90	90	90
β / Å	95.684(4)	106.957(4)	104.541(3)
γ / Å	90	90	90
<i>V</i> / Å ³	4257.2(4)	4228.9(3)	3413.07
ρ_{calcd} / g·cm ⁻³	1.069	1.079	1.146
<i>F</i> (000)	1488	1496	1277
Crystal size / mm	0.24 x 0.19 x 0.05	0.26 x 0.16 x 0.04	0.22 x 0.11 x 0.08
<i>Z</i>	4	4	4
Max. and min. transmission	0.994, 0.970	0.997, 0.988	0.988, 0.973
μ / mm ⁻¹	0.674	0.083	0.736
θ / °	4.112-73.599	3.267-27.996	4.315-73.509
Index ranges	-13 ≤ <i>h</i> ≤ 13	-15 ≤ <i>h</i> ≤ 14	-13 ≤ <i>h</i> ≤ 20
	-22 ≤ <i>k</i> ≤ 19	-23 ≤ <i>k</i> ≤ 24	-15 ≤ <i>k</i> ≤ 14
	-26 ≤ <i>l</i> ≤ 18	-23 ≤ <i>l</i> ≤ 21	-21 ≤ <i>l</i> ≤ 18
Total / unique reflections	22786 / 8357	25660 / 9049	19222 / 6691
Data / restraints / parameters	8357 / 84 / 477	9049 / 0 / 468	6691 / 221 / 497
<i>R</i> _{int}	0.0409	0.0575	0.0311
<i>R</i> ₁ , <i>wR</i> ₂ [<i>I</i> ≥ 2σ(<i>I</i>)]	0.0659, 0.1645	0.0663, 0.1563	0.0578, 0.1276
<i>R</i> ₁ , <i>wR</i> ₂ (all data)	0.1023, 0.1928	0.1067, 0.1810	0.0704, 0.1337
Goodness-of-fit <i>S</i> on <i>F</i> ²	1.018	1.035	1.129
Largest diff. peak and hole / eÅ ⁻³	0.413, -0.276	0.636, -0.482	0.235, -0.251

6.5 References

- [1] a) I. L. Fedushkin, A. A. Skatova, V. A. Chudakova, G. K. Fukin, *Angew. Chem. Int. Ed.*, **2003**, *42*, 3294-3298; b) I. L. Fedushkin, A. A. Skatova, V. A. Chudakova, G. K. Fukin, S. Dechert, H. Schumann, *Eur. J. Inorg. Chem.* **2003**, *2003*, 3336-3346.
- [2] M. Vigano, F. Ferretti, A. Caselli, F. Ragaini, M. Rossi, P. Mussini, P. Macchi, *Chem. Eur. J.* **2014**, *20*, 14451-14464.
- [3] a) A. N. Lukoyanov, I. L. Fedushkin, M. Hummert, H. Schumann, *Russ. Chem. Bull.* **2006**, *55*, 422-428; b) A. N. Lukoyanov, I. L. Fedushkin, H. Schumann, M. Hummert, *Z. Anorg. Allg. Chem.* **2006**, *632*, 1471-1476.
- [4] a) I. L. Fedushkin, M. V. Moskalev, A. N. Lukoyanov, A. N. Tishkina, E. V. Baranov, G. A. Abakumov, *Chem. Eur. J.* **2012**, *18*, 11264-11276; b) M. V. Moskalev, A. N. Lukoyanov, E. V. Baranov, I. L. Fedushkin, *Dalton Trans.* **2016**, *45*, 15872-15878.
- [5] A. Bismuto, S. P. Thomas, M. J. Cowley, *Angew. Chem. Int. Ed.* **2016**, *55*, 15356-15359.
- [6] S. Tobisch, *Dalton Trans.* **2015**, *44*, 12169-12179.
- [7] T. W. Myers, L. A. Berben, *Chem. Sci.* **2014**, *5*, 2771.
- [8] T. W. Myers, L. A. Berben, *J. Am. Chem. Soc.* **2013**, *135*, 9988-9990.
- [9] V. K. Jakhar, M. K. Barman, S. Nembenna, *Org. Lett.* **2016**, *18*, 4710-4713.
- [10] I. L. Fedushkin, V. A. Chudakova, G. K. Fukin, S. Dechert, M. Hummert, H. Schumann, *Russ. Chem. Bull.* **2004**, *53*, 2744-2750.
- [11] S. Dastgir, K. S. Coleman, A. R. Cowley, M. L. H. Green, *Organometallics* **2010**, *29*, 4858-4870.
- [12] M. Gasperini, F. Ragaini, S. Cenini, *Organometallics* **2002**, *21*, 2950-2957.

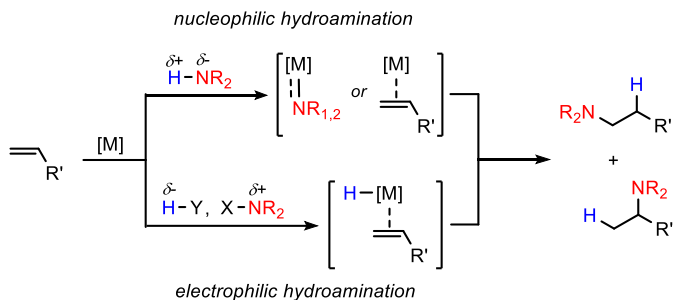
7 Hydroaminations of Alkenes: A Radical, Revised, and Expanded Editionⁱ



Hydroaminations of alkenes constitute a key synthetic strategy in fine chemicals synthesis and drug discovery. The arsenal of available metal-catalyzed methods has been significantly expanded by the advent of radical mechanisms involving initial hydrogen atom transfer to the alkene. This article assesses the current state of the art and highlights a most recent Fe-catalyzed protocol which utilizes stable nitrobenzenes as electrophilic *N*-component and operates via dual catalytic activation of both starting materials.

ⁱ Reproduced from M. Villa, A. Jacobi von Wangelin, *Angew. Chem. Int. Ed.* **2015**, *54*, 11906-11908, with permission from Wiley-VCH. Schemes, tables and text may differ from published version.

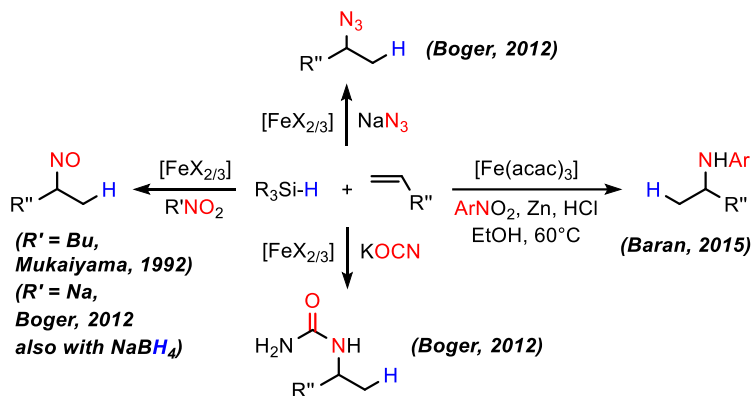
The preparation of *N*-containing molecules is of utmost importance to all fields of organic chemistry and the prevalence of C-N bond motifs in natural products, drugs, fine chemicals, agrochemicals, and materials a constant driver for innovation of synthetic methods.^[1] Among the numerous concepts of forging a C-N bond, the hydro-amination of olefins constitutes an especially attractive strategy which relies upon olefins and amines as most basic, widely available, yet diverse families of starting materials.^[2] Today, a vast arsenal of metal-catalyzed hydroamination protocols is available (Scheme 7-1). Depending on the nature of the employed metal catalyst and substrates, the reaction mechanisms can involve two general activation modes: The formation of active amido or imido complexes is mostly observed with Lewis acidic catalysts (alkaline earth, rare earth, early transition metals).^[2] Late transition metals and group 11 and 12 metals mostly undergo coordinative π -activation of the alkene.^[2] Contrary to this, electrophilic aminations have been reported with hydroxylamine derivatives.^[3] These strategies require the employment of a hydride reagent (hydrosilane, alkylmagnesium halide). The low price and low toxicity of iron has recently stimulated great interest in the development of Fe-catalyzed hydroamination procedures based on either mechanistic scenario.^[4] However, the substrate scope is still very limited (styrenes with weakly nucleophilic tosylamines,^[4a] intramolecular reactions of *gem*-dialkyl aminoalkenes,^[4b-4d] low functional group tolerance due to Grignard reagent^[4e]).



Scheme 7-1 - Common modes of substrate activation in metal-catalyzed nucleophilic (top) and electrophilic (bottom) hydroamination.^[2-4]

A conceptually different radical addition with nitrobenzenes was very recently added to the manifold of net hydroamination processes.^[5] Baran *et al.* reported the sequential combination of an Fe-catalyzed hydrogen atom transfer (HAT)^[6] and an Fe-catalyzed reductive deoxygenation in a one-pot operation which allows the facile preparation of *tert*- and *sec*-alkyl arylamines. Based on some literature precedents,^[7,8] a highly practical procedure was developed which uses various alkenes, aromatic nitro compounds as *N*-electrophiles, phenylsilane as HAT reagent, and iron(III) acetylacetonate as pre-catalyst under thermal conditions (ethanol, 60°C, Scheme 7-2). Isolated examples of Fe-catalyzed

HAT to alkenes and subsequent reaction of the alkyl radicals with 1-butylnitrite to give nitrosoalkanes under similar conditions was reported by Mukaiyama in 1992.^[7a] Boger extended this formal hydroamination method to include other *N*-based radical traps (NaN_3 , KOCN , NaNO_2).^[7b] Cobalt-catalyzed oxidative hydroaminations were reported by Carreira *et al.* and Shigehisa and co-workers.^[8]

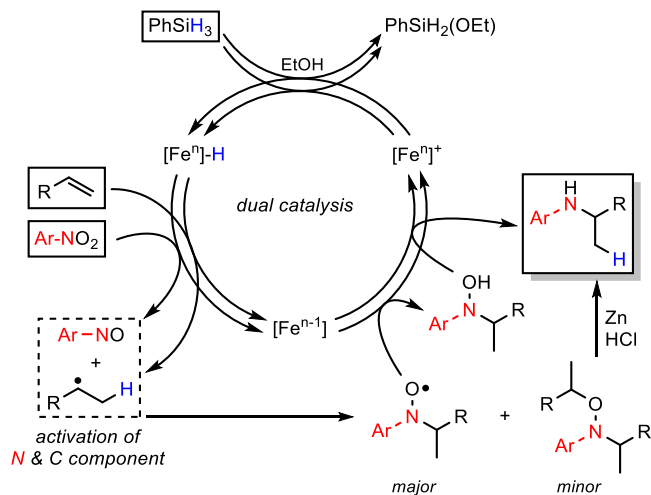


Scheme 7-2 - Evolution of Fe-mediated radical hydroaminations.^{[5],[7]}

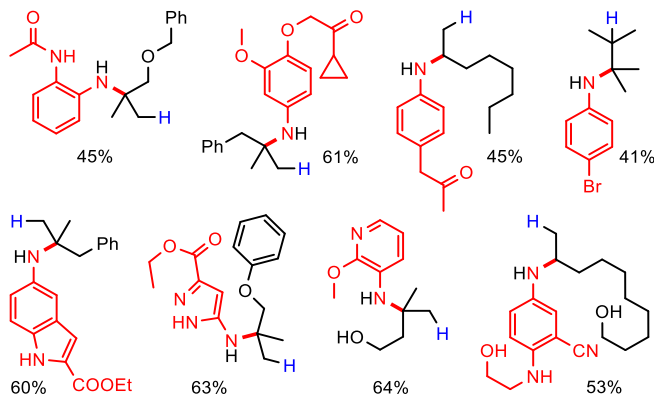
The new Fe-catalyzed hydroamination is believed to proceed via dual substrate activation through initial HAT from an *in situ* prepared hydridoiron complex^[9] to both the alkene and nitrobenzene (Scheme 7-3). The resultant alkyl radical and nitrosobenzene combine to an aminyloxyl radical^[10] which engages in sequential re-oxidation of two equivalents of iron catalyst upon generation of a hydroxylamine intermediate which ultimately leads to the amine product. It is especially noteworthy that the reduction of the *N*-electrophile (nitroarene) is embedded within the overall catalytic cycle, which obviates the need for a separate reductive operation. The mechanistic design of Baran and co-workers elegantly draws on two closed catalytic one-electron redox cycles. These effect two H atom transfers to the alkene and the nitroarene, which are both formal oneelectron reductions of Fe^{III} to Fe^{II} , and two sequential oneelectron oxidations of Fe^{II} to Fe^{III} by the intermediate alkyl aminyloxyl species. This mechanistic layout in combination with the use of simple starting materials renders the method utmost industrial relevance. The double alkylation of the nitrosoarene to give the *N,O*-dialkyl hydroxylamine as a side product could be suppressed by addition of Zn/HCl to the reaction mixture. Some of the nitrosoarene undergoes further reduction to give the corresponding aniline, which is unreactive under these reaction conditions (Scheme 7-3, bottom right)

The reaction tolerates various functional groups including thioethers, amides, ketones, amines, halides, triflates, alcohols, nitriles, heterocycles, and boronic acids. The covered

chemical space is much wider and diverse than that achieved with common hydroamination reactions, and includes the synthesis of many highly substituted and functionalized amines for the first time. Sterically congested amines can easily be obtained from the tri- and tetra-substituted olefins in a single catalytic operation (Scheme 7-4). However, the general procedure is limited to aromatic nitro compounds and cannot be applied to the synthesis of tertiary amines.



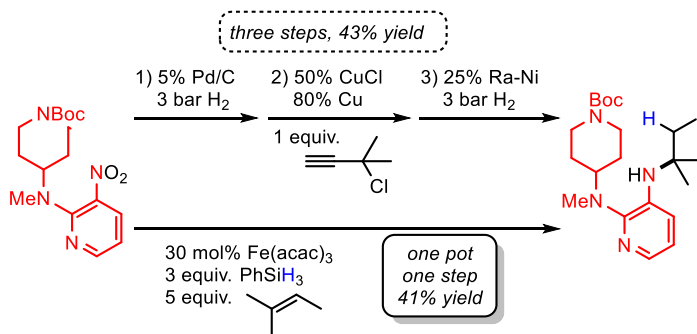
Scheme 7-3 - Proposed mechanism involving dual catalytic activation.



Scheme 7-4 - Selected substrate scope.

This strategy bears great potential to significantly shorten and streamline the synthesis of bioactive molecules as exemplarily shown by vinblastine functionalizations^[7b] and the preparation of an HIV-1 reverse transcriptase inhibitor which so far required three synthetic steps with noble metal catalysts (Scheme 7-5).^[11]

A key challenge of common hydroamination endeavours is the strict control of regioselectivity. Significant effort has been devoted to the development of anti-Markovnikov reactions due to the immediate relevance of linear alkylamines as biologically active building blocks. On the contrary, the radical nature of the underlying mechanism stipulates Markovnikov selectivity of Baran's protocol. Technical applications will certainly benefit from the cheap, stable, easy-to-handle, and "ligand-free" pre-catalyst $\text{Fe}(\text{acac})_3$ in comparison with common rare-earth or transition metal catalyst systems. However, the addition of 2-3 equiv. phenylsilane (PhSiH_3 , 830 €/mol) as H atom donor and excess amounts of Zn (20 equiv.) as reductant of the undesired double alkylation product diminish the overall efficiency. Altogether, this Fe-catalyzed reductive hydro-amination of alkenes with nitrobenzenes is an important addition to the arsenal of available amine syntheses which is based on a different mechanistic paradigm than the common hydroamination reactions of rareearth, alkaline-earth, and transition-metal catalysts. Highly functionalized, sterically encumbered alkyl aryl amines could thus be prepared, and the method exhibits an orthogonal scope to Buchwald–Hartwig and reductive amination reactions. Its incipient exploitation in syntheses of important bioactive molecules by Baran and co-workers is surely only the beginning of an era to come during which such strategies will be gaining a strong foothold among modern amination methods.



Scheme 7-5 - Exemplary synthesis of an HIV-1 reverse transcriptase inhibitor by conventional noble metal and new Fe catalysis.

7.1 References

- [1] a) *Science of Synthesis*, Vol. 40 (Eds.: D. Enders, E. Schaumann), Thieme, Stuttgart, **2009**; b) *Amino Group Chemistry* (Ed.: A. Ricci), Wiley-VCH, Weinheim, **2008**; c) D. J. C. Constable, P. J. Dunn, J. D. Hayler, G. R. Humphrey, J. L. Leazer, Jr., R. J. Linderman, K. Lorenz, J. Manley, B. A. Pearlman, A. Wells, A. Zaks, T. Y. Zhang, *Green Chem.* **2007**, *9*, 411-420.
- [2] a) T. E. Mueller, K. C. Hultzsich, M. Yus, F. Foubelo, M. Tada, *Chem. Rev.* **2008**, *108*, 3795-3892; b) L. Huang, M. Arndt, K. Goossen, H. Heydt, L. J. Goossen, *Chem. Rev.* **2015**, *115*, 2596-2697. Radical transfer hydroamination involving single-electron redox activation of either reagent was also achieved by metal-free protocols: c) E. Bernoud, C. Lepori, M. Mellah, E. Schulz, J. Hannedouche, *Catal. Sci. Technol.* **2015**, *5*, 2017-2037.
- [3] X. Yan, X. Yang, C. Xi, *Catal. Sci. Technol.* **2014**, *4*, 4169-4177.
- [4] a) J. Michaux, V. Terrasson, S. Marque, J. Wehbe, D. Prim, J.-M. Campagne, *Eur. J. Org. Chem.* **2007**, 2601-2603; b) K. Komeyama, T. Morimoto, K. Takaki, *Angew. Chem. Int. Ed.* **2006**, *45*, 2938-2941; c) M. S. Jung, W. S. Kim, Y. H. Shin, H. J. Jin, Y. S. Kim, E. J. Kang, *Org. Lett.* **2012**, *14*, 6262-6265; d) E. Bernoud, P. Oulie, R. Guillot, M. Mellah, J. Hannedouche, *Angew. Chem. Int. Ed.* **2014**, *53*, 4930-4934; e) B. Huehls, A. Lin, J. Yang, *Org. Lett.* **2014**, *16*, 3620-3623.
- [5] J. Gui, C.-M. Pan, Y. Jin, T. Qin, J. C. Lo, B. J. Lee, S. H. Spergel, M. E. Mertzman, W. J. Pitts, T. E. La Cruz, M. A. Schmidt, N. Darvatkar, S. R. Natarajan, P. S. Baran, *Science* **2015**, *348*, 886-891.
- [6] For related hydrofunctionalizations of alkenes initiated by HAT, see: a) M. D. Greenhalgh, A. S. Jones, S. P. Thomas, *ChemCatChem* **2015**, *7*, 190-222; b) J. C. Lo, J. Gui, Y. Yabe, C.-M. Pan, P. S. Baran, *Nature* **2014**, *516*, 343-348; c) J. C. Lo, Y. Yabe, P. S. Baran, *J. Am. Chem. Soc.* **2014**, *136*, 1304-1307.
- [7] a) K. Kato, T. Mukaiyama, *Chem. Lett.* **1992**, 1137-1140; b) E. K. Leggans, T. J. Barker, K. K. Duncan, D. L. Boger, *Org. Lett.* **2012**, *14*, 1428-1431.
- [8] a) J. Waser, B. Gaspar, H. Nambu, E. M. Carreira, *J. Am. Chem. Soc.* **2006**, *128*, 11693-11712; b) H. Shigehisa, N. Koseki, N. Shimizu, M. Fujisawa, M. Niitsu, K. Hiroya, *J. Am. Chem. Soc.* **2014**, *136*, 13534-13537.
- [9] H. Nakazawa, M. Itazaki, *Top. Organomet. Chem.* **2011**, *33*, 27-81.
- [10] G. A. Russell, C. F. Yao, *Heteroatom Chem.* **1993**, *4*, 433-434.
- [11] D. L. Romero, R. A. Olmsted, T. J. Poel, R. A. Morge, C. Biles, B. J. Keiser, L. A. Kopta, J. M. Friis, J. D. Hosley, K. J. Stefanski, D. G. Wishka, D. B. Evans, J. Morris, R. G. Stehle, S. K. Sharma, Y. Yagi, R. L. Voorman, W. J. Adams, W. G. Tarpley, R. C. Thomas, *J. Med. Chem.* **1996**, *39*, 3769-3789.

8 Appendix

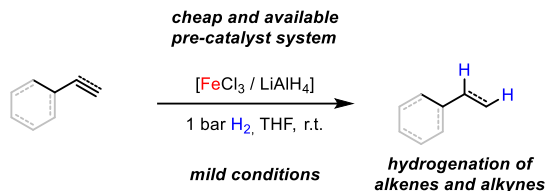
8.1 List of abbreviations

Ac	acetyl	LIFDI	liquid injection field desorption ionization
acac	acetylacetonate	LiTEBH	lithium triethylborohydride
ATR	attenuated total reflection	Me	methyl
BDSB	Bis(dimethylsilyl)benzene	Mes	mesityl
BIAN	Bis(imino)acenaphthene	min	minute
Bn	benzyl	MS	mass spectrometry
Bu	butyl	NMR	nuclear magnetic resonance
CV	Cyclic voltammetry	NPs	nanoparticles
d	day	Ot-Bu	<i>tert</i> -butoxide
DAB	diazabutadiene	PDI	diiminopyridine
dct	dibenzo[<i>a,e</i>]cyclooctatetraene	Ph	phenyl
DiBAIH	diisobutylaluminiumhydride	Pr	propyl
dipp	2,6-diisopropylphenyl	py	pyridine
ESI	electron spray ionization	R_f	retention factor
Et	ethyl	rt	room temperature
Fc	ferrocene	SET	Single electron transfer
FID	flame ionization	TCD	thermal conductivity detector
FT-IR	Fourier-Transform-Infrared spectroscopy	thf	tetrahydrofuran
GC	gas chromatography	TLC	thin layer chromatography
h	hour	TMS	trimethylsilyl
HAT	hydrogen atom transfer	TOF	turnover frequency
hmds	1,1,1,3,3,3-hexamethyl-disilazan-2-ide	TON	turnover number
HR	high resolution	UV	ultraviolet radiation
IL	ionic liquid	Vis	visible radiation

8.2 Summary

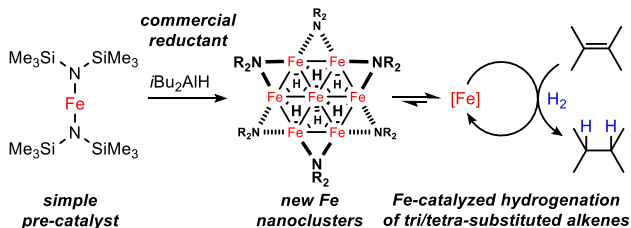
The aim of this thesis was the investigation of different approaches towards the development of hydrogenation catalytic systems based on iron as cheap and environmentally friendly metal.

The first chapter offers an overview of the last developments in the field of iron-catalyzed hydrogenation systems, special attention has been devoted on catalysts based on non-innocent ligand containing iron complexes, with the description of selected examples. The implementation of this redox active moieties granted to these complexes unseen properties resulting in astonishing results.



Scheme 8-1 – Abstract scheme of chapter 2

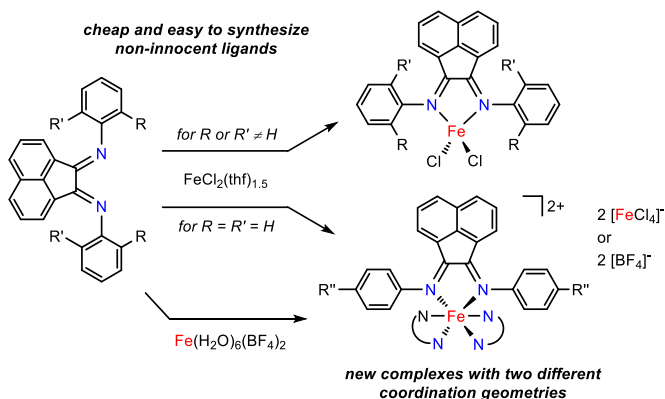
In the second chapter (Scheme 8-1) a practical and simple hydrogenation system was described, the use of widespread available iron trichloride and lithium aluminumhydride as precursors allow facile implementation of this methodology in synthetic laboratories. Mono- and di-substituted olefins were converted under mild reaction conditions. Different functional groups were tolerated and mechanistic investigations indicated the presence of a homogeneous catalyst in the early stage of the reaction, less reactive nanoparticles are subsequently formed as result of aggregation.



Scheme 8-2 – Abstract scheme of chapter 3

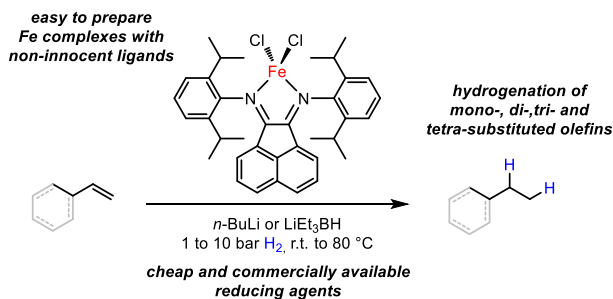
A different hydrogenation protocol was described in chapter 3 (Scheme 8-2). This catalyst, based on iron(II) bis(1,1,1,3,3,3-hexamethyl-disilazan-2-ylidene) or on a most friendly *in situ* generated iron amide, upon activation with diisobutylaluminum hydride,

resulted in an unprecedented active system. Tri- and tetra-substituted alkenes were efficiently hydrogenated under mild reaction conditions. Novel low-valent nanoclusters with planar Fe_4 , Fe_6 , and Fe_7 geometries were isolated during the study. These structures standing on the border between homogeneous and heterogeneous catalysts furnish new insights about the growth of metal nanoparticles.



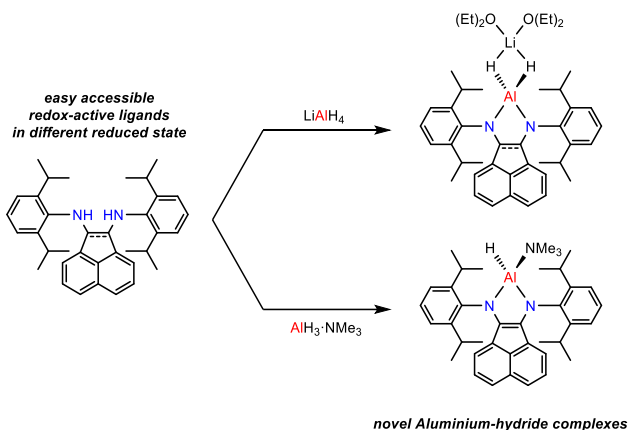
Scheme 8-3 – Abstract scheme of chapter 4

In the fourth chapter the easy synthesis of novel iron complexes coordinated to non-innocent bis(imino)acenaphthene ligands was described (Scheme 8-3). The morphology of the resulting complex can be predicted on the basis of the sterical hinderance of the selected BIAN ligand. Sterically demanding backbones led to the formation of high-spin tetrahedral complexes while less bulky ligands resulted in the creation of low-spin octahedral complexes. The electrochemical properties of both the set of iron species were investigated, showing interesting ligand centered reduction events.



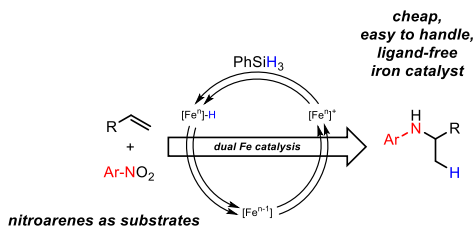
Scheme 8-4 – Abstract scheme of chapter 5

The potential catalytic application of these Fe complexes coordinated to redox-active BIAN scaffolds was investigated and described in the fifth chapter (Scheme 8-4). Tetrahedral iron(II) species did not show any hydrogenation capacity, nevertheless, activation of these complexes with different reducing agents led to an active species able to catalyze olefins hydrogenation. Different reductants have been screened and hydrogenation of mono-, di-, tri- and even tetra-substituted olefins was observed employing the optimized conditions. Preliminary mechanistic studies indicated in a reduced anionic iron complex, a ferrate, the competent active catalyst operating in these transformations.



Scheme 8-5 – Abstract scheme of chapter 6

Intrigued by the redox properties of bis(imino)acenaphthene moieties further studies were carried on aiming at the isolation of aluminum hydride complexes coordinated to pre-reduced BIAN ligand. The results were described in chapter 6 (Scheme 8-5). The synthesis of novel aluminum complexes was efficiently achieved in a single step, mixing the desired ligand and lithium aluminumhydride.



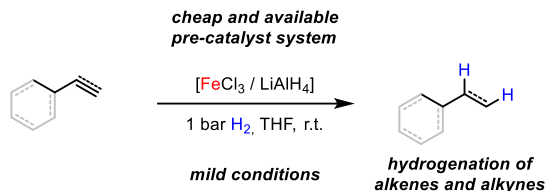
Scheme 8-6 – Abstract scheme of chapter 7

In the last chapter (Scheme 8-6) an analysis of the different hydroamination approaches known in literature was proposed. The remarkable results obtained in this field thanks to iron-catalyzed hydrogen atom transfer were then discussed.

8.3 Zusammenfassung

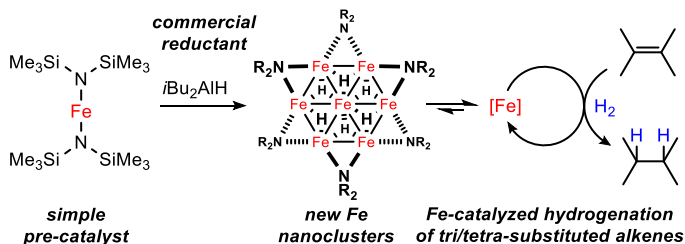
Das Ziel dieser Arbeit war die Untersuchung verschiedener Ansätze zur Entwicklung von Hydrierungs-Katalysatorsystemen basierend auf Eisen als billiges und umweltfreundliches Übergangsmetall.

Das erste Kapitel bietet eine Übersicht der neuesten Entwicklungen auf dem Gebiet der Eisen-katalysierten Hydrierungssystemen. Dabei wurde besondere Aufmerksamkeit Eisenkomplexen, die redoxaktive Liganden tragen, gewidmet. Die Verwendung solch redoxaktiver Gruppen in diesen Komplexen führte zu ungekannten Eigenschaften und herausragenden Ergebnissen.



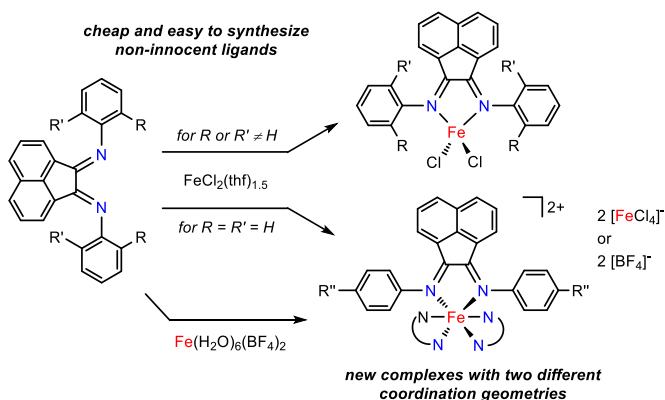
Scheme 8-7 - Allgemeines Schema für Kapitel 2

Im zweiten Kapitel (Scheme 8-7) wurde ein praktikables und einfaches Hydrierungssystem beschrieben. Die Verwendung von allseits verfügbarem Eisenchlorid und Lithiumaluminiumhydrid als Vorstufen, ermöglicht die leichte Einführung dieser Methode in synthetischen Laboratorien. Einfach- und zweifach-substituierte Olefine wurden unter milden Reaktionsbedingungen hydriert und diverse funktionelle Gruppen toleriert. Mechanistische Untersuchungen legten die Gegenwart eines homogenen Katalysators zu Beginn der Reaktion und die Bildung von weniger reaktiven Nanopartikeln als Folge von Aggregation über den Reaktionsverlauf, nahe.



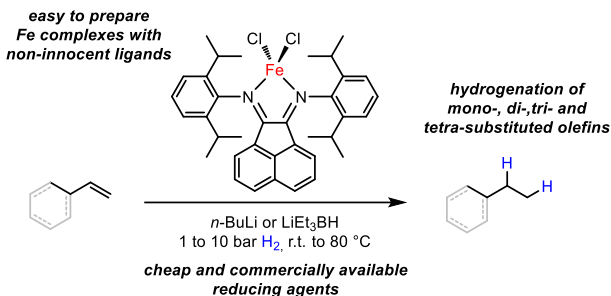
Scheme 8-8 - Allgemeines Schema für Kapitel 3

Ein anderes Hydrierungsprotokoll wurde in Kapitel drei beschrieben (Scheme 8-8). Der hierin genannte Katalysator, basierend auf Eisen(II)hexamethyldisilazid oder einem anderen *in situ* erzeugten Eisenamid, stellte nach Aktivierung mit Diisobutylaluminiumhydrid ein bislang beispielloses aktives System dar. Drei- und vierfach-substituierte Alkene wurden unter milden Reaktionsbedingungen effizient hydriert. Neue niedervalente Nanocluster mit planaren Fe₄, Fe₆ und Fe₇ Geometrien wurden dabei isoliert. Letztere Strukturen, die sich an der Grenzfläche zwischen homogenen und heterogenen Katalysatoren bewegen, lieferten neue Einblicke über das Wachstum von Metall-Nanopartikeln.



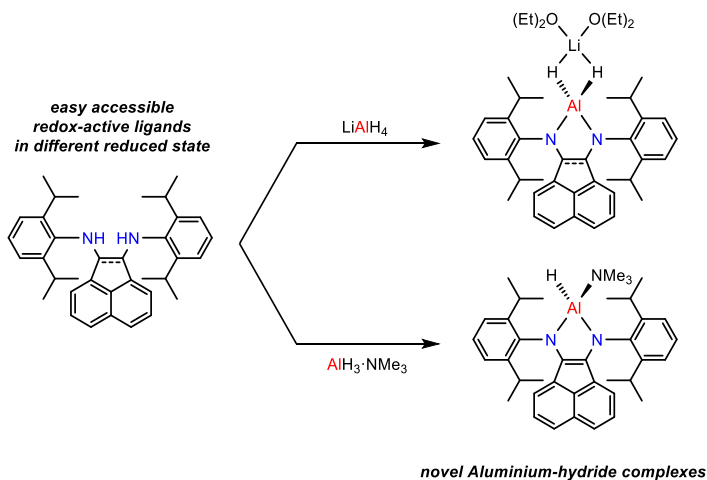
Scheme 8-9 - Allgemeines Schema für Kapitel 4

Im vierten Kapitel wurde die leichte Synthese neuer Eisenkomplexe, die non-innocente bis(imino)acenaphthene Liganden tragen, dargelegt (Scheme 8-9). Die Morphologie der jeweiligen Komplexe kann auf Basis des sterischen Anspruchs des gewählten BIAN-Liganden vorhergesagt werden. Sterisch anspruchsvolle Rückgrate führten zur Bildung von tetraedrischen high-spin Komplexen, wohingegen weniger sperrige Liganden oktaedrische low-spin Komplexe bildeten. Die elektrochemischen Eigenschaften von beiden Eisenspezies-Reihen wurden untersucht, wobei sich interessante Ligand-zentrierte Reduktionsereignisse zeigten.



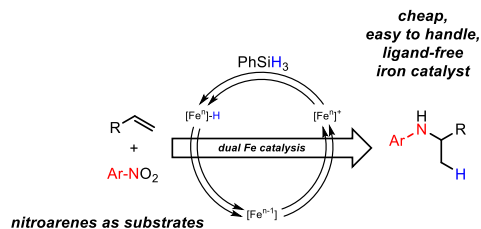
Scheme 8-10 - Allgemeines Schema für Kapitel 5

Die potenzielle katalytische Anwendung dieser Eisenkomplexe mit redoxaktivem BIAN-Gerüst wurde im fünften Kapitel beleuchtet (Scheme 8-10). Die tetraedrischen Eisen(II)-spezies zeigten keinerlei Hydrierungsvermögen. Nichtsdestotrotz führte die Aktivierung dieser Komplexe mit verschiedenen Reduktionsmitteln zu einer aktiven Spezies bei der katalytischen Hydrierung von Olefinen. Diverse Reduktionsmittel wurden geprüft und die Hydrierung von einfach-, zweifach-, dreifach- und sogar vierfach-substituierten Olefinen wurde bei Anwendung der optimierten Bedingungen beobachtet. Erste mechanistische Untersuchungen weisen auf einen reduzierten, anionischen Eisenkomplex (Ferrate) als passable aktive Spezies bei diesen Umsetzungen hin.



Scheme 8-11 - Allgemeines Schema für Kapitel 6

Inspiziert durch die Redox Eigenschaften der BIAN-Gerüste wurden weitere Studien zur Isolierung von Aluminiumhydrid-Komplexen, die durch vorher reduzierte BIAN-Liganden koordiniert werden, durchgeführt (Scheme 8-11). Diese Ergebnisse wurden in Kapitel sechs beschrieben. Die effiziente Einstufensynthese neuer Aluminiumkomplexe wurde durch das Mischen des gewünschten Liganden mit Lithiumaluminiumhydrid bewerkstelligt.



Scheme 8-12 - Allgemeines Schema für Kapitel 6

Im letzten Kapitel (Scheme 8-12) wurde eine Analyse von verschiedenen literaturbekannten Hydroaminierungsmethoden zur Verfügung gestellt. Die beeindruckenden Ergebnisse, die auf diesem Gebiet dank Eisen-katalysiertem Atomtransfer erzielt wurden, wurden anschließend diskutiert.

8.4 Curriculum Vitae

Personal Informations

Name	Matteo Villa
Date of Birth	July 1 st 1989
Place of Birth	Busto Arsizio (VA)
Nationality	Italian

Education and academic background

01.2014 - present	<p>Doctoral thesis in organic Chemistry, University Regensburg, "Iron Complexes with Nitrogen Ligands for Catalytic Hydrogenation of Olefins"</p> <p>Advisor: Prof. Dr. Axel Jacobi von Wangelin</p>
10.2011 – 12.2013	<p>Master Degree in Industrial Chemistry – Università degli Studi di Milano. Graduated on December 20th, 2013, with 110/110. Thesis internship program carried out at Department of Chemistry, on "Synthesis of Iron Complexes with Nitrogen ligands and their Use in Catalysis".</p> <p>Advisor: Prof. Fabio Attilio Cirillo Ragaini</p>
10.2008 – 10.2011	<p>Bachelor Degree in Industrial Chemistry – Università degli Studi di Milano. Graduated on October 21st, 2011, with 107/110.</p> <p>Thesis internship program carried out at Department of Inorganic, Metallorganic and Analytical Chemistry "L. Malatesta" on the "Preparation of conductive polyaniline nanofibers highly soluble".</p> <p>Advisor: Dott.ssa Cristina Della Pina.</p>
09.2003 – 06.2008	<p>Technical Institute High School Diploma in Industrial Chemistry – Istituto Tecnico Industriale Statale "C. Facchinetti" (Busto Arsizio).</p>

Scholarships

2014 - 2016	Kekulé-Stipendium (Fonds der Chemischen Industrie)
-------------	--

List of publications

- 1 F. Ragaini, M. Vigano, F. Ferretti, M. Hagar, D. Formenti, M. Villa; "Schiff bases of the BIAN family. The evolution of a ligand"; *Chimica e l'Industria (Milan, Italy)* **2013**, *95*, 133-139.
- 2 T. N. Gieshoff, M. Villa, A. Welther, M. Plois, U. Chakraborty, R. Wolf, A. Jacobi von Wangelin; "Iron-catalyzed olefin hydrogenation at 1 bar H₂ with a FeCl₃-LiAlH₄ catalyst"; *Green Chem.* **2015**, *17*, 1408-1413.
- 3 M. Villa, A. Jacobi von Wangelin; "Hydroaminations of Alkenes: A Radical, Revised, and Expanded Edition" *Angew. Chem. Int. Ed.* **2015**, *54*, 11906-11908.
- 4 T. N. Gieshoff, U. Chakraborty, M. Villa, A. Jacobi von Wangelin; "Alkene Hydrogenations by Soluble Iron Nanocluster Catalysts", *Angew. Chem. Int. Ed.* **2017**, *56*, 3585-3589.
- 5 Matteo Villa, Dominique Miesel, Alexander Hildebrandt, Fabio Ragaini, Dieter Schaarschmidt, Axel Jacobi von Wangelin; "Synthesis and Catalysis of Redox-active Bis(imino)acenaphthene (BIAN) Iron Complexes"; *ChemCatChem* **2017**, DOI: 10.1002/cctc.201700144.
- 6 Matteo Villa, Axel Jacobi von Wangelin "Hydrogenations catalyzed by Redox-active Bis(imino)acenaphthene (BIAN) Iron Complexes", *in preparation*.

Conference contributions

- 1 F. Ragaini, M. Hagar, E. Storer, F. Ferretti, D. Formenti, M. Villa; "Alkyl Formates as CO Alternatives in Nitroarene Deoxygenation to give Indoles." 20th EuCheMS Conference on Organometallic Chemistry, **2013**, St. Andrews (Scotland). (Poster)
- 2 M. Villa, A. Jacobi von Wangelin; "Synthesis and Application of Iron Catalysts derived from Defined Complexes"; Wissenschaftsforum Chemie (WiFo), **2015**, Leipzig (Germany). (Poster)
- 3 M. Villa, A. Jacobi von Wangelin; "Synthesis and Characterization of Bis(imino)acenaphthene-Iron(II) Complexes"; OrChem, **2016**, Weimar (Germany). (Poster)

8.5 Acknowledgements

In the first place my heartfelt thanks go to Axel, thank you very much for the really interesting research topics and for the support and guidance that you provide me during these three years.

My most sincere thanks to Prof. Göpferich, Prof. Garcia-Mancheño und Prof. Matysik for reading my thesis and for accepting to be part of my defense committee.

Huge thanks also to all the Jacobi group for the great atmosphere and memories collected during these years, thanks to the “old” guys, Josef, Michal and Dominik for the very warm welcome they gave me during my first days here in Germany, thanks to Raúl for the meaningful and unforgotten life lessons, great thanks to Tim for the enjoyable and fruitful collaboration throughout this period. Of course I cannot forget the “new” guys, thanks to Effi, “Bernie” (Josef), Michi, Sebastian, Patrick, Denis, “Greg” (Bernhard), Uttam and Guojiao, was a true pleasure to work with all of you and I will miss the time spent together.

All my thanks to Michaela and Veronica, our wonderful technicians, for all the essential help provided during my working period in the group.

Thanks to all the people from other research groups who helped me during my Ph.D., especially thanks to the Fleischer’s group for the always interesting seminars and to the Wolf’s group for the multiple interesting collaborations.

I would like to thank Fonds der Chemischen Industrie, namely Frau Kiefer, for the financial support and the great opportunity they have granted me.

In quanto a ringraziamenti non potr  mai ringraziare a sufficienza i miei genitori, Mariella e Danilo, e tutta la mia famiglia. Mi avete sostenuto durante tutto questo percorso, sin dalla nascita dell’idea di trasferirmi in Germania, durante tutti questi tre anni, fino alla scrittura di questa tesi. Siete sempre stati disponibili ad aiutarmi in ogni modo possibile e non potr  mai ripagarvi a sufficienza per questo, sono davvero incredibilmente fortunato ad avere una famiglia cos .

Un ringraziamento a tutti gli amici in Italia, specialmente Dario e Luca, siete come fratelli per me dopo tutti gli anni trascorsi insieme, anche a distanza. Non so come abbiate fatto ma ad ogni mio ritorno a casa siete sempre riusciti a farmi sentire come se non me ne fossi mai andato.

Un grazie di cuore anche a tutti gli amici italiani “espatriati” e conosciuti a Regensburg, Andrea, Laura, Andrea, Nadia, Polyssena, Salvo e tutti gli altri, ancora qui o dislocati per l’Europa. Un grande grazie va a Davide, amico e collega che si   unito al gruppo pochi mesi fa, per il suo aiuto durante le ultime concitate settimane del mio dottorato.

8.6 Eidesstattliche Erklärung

- I. Ich erkläre hiermit an Eides statt, dass ich die vorliegende Arbeit ohne unzulässige Hilfe Dritter und ohne Benutzung anderer als der angegebenen Hilfsmittel angefertigt habe; die aus anderen Quellen direkt oder indirekt übernommenen Daten und Konzepte sind unter Angabe des Literaturzitats gekennzeichnet.

- II. Bei der Auswahl und Auswertung haben mir die in den jeweiligen Kapiteln aufgeführten Personen in der beschriebenen Art und Weise unentgeltlich geholfen.

- III. Weitere Personen waren an der inhaltlich-materiellen Herstellung der vorliegenden Arbeit nicht beteiligt. Insbesondere habe ich hierfür nicht die entgeltliche Hilfe eines Promotionsberaters oder anderer Personen in Anspruch genommen. Niemand hat von mir weder unmittelbar noch mittelbar geldwerte Leistungen für Arbeiten erhalten, die im Zusammenhang mit dem Inhalt der vorgelegten Dissertation stehen.

- IV. Die Arbeit wurde bisher weder im In- noch im Ausland in gleicher oder ähnlicher Form einer anderen Prüfungsbehörde vorgelegt.

Regensburg, den 10.04.2017